
# ADVANCING DOUBLE STAR STUDIES IN AN AGE OF SPACE-BASED ASTROMETRIC MISSIONS

A Thesis submitted by

Roderick R. Letchford

BSc, ThL, MA, PhD,
GradCertAstron

For the award of

Doctor of Philosophy

2022

# ABSTRACT

The astrometric study of double stars is over 200 years old, and historically it has been a driver of stellar astrophysics resulting in the determination of the properties of stars, as well as formation and evolution models. Modern, space-based astronomy, from missions such as HIPPARCOS and *Gaia*, has opened a new sophisticated avenue of binary star studies. These space missions give the astrometric measures of a double star, its angular separation in arcseconds and position angle in degrees, with precisions that are 3 to 4 orders of magnitude more precise than has been available to-date from single-aperture ground observations (aside from speckle interferometry on close pairs). In this thesis, Paper 1 crossmatches the double stars from the first published catalogue of double stars in the southern hemisphere (the *Dunlop Catalogue*) with the *Gaia Data Release 2 (Gaia DR2)* from the *Gaia* space-based mission and estimates the accuracy of the measures in the *Dunlop Catalogue*. Overall position angles are within 70°”/separation”, separations within 7%, and apparent visual magnitudes are within 1 mag. Paper 2 develops an iteration-based technique for the determination of the first order orbital elements for long period and under-sampled arcs. This technique is then applied to a sample of binary stars from the *Dunlop Catalogue*. Orbital elements with a mean period and semi-major axis of ~81,000 years and ~76” respectively, were calculated displaying a mean uncertainty of ~37%. Paper 3 confirms the presence of 14 optical double stars within the *Dunlop Catalogue* and presents and applies an upgraded technique for calculating their rectilinear elements. This upgraded technique results in a minimum one order of magnitude improvement in their one sigma uncertainties over the current method.

# CERTIFICATION OF THESIS

I *Roderick Ronald Letchford* that the PhD Thesis entitled *Advancing Double Star Studies in an age of space-based astrometric missions* is not more than 100,000 words in length including quotes and exclusive of tables, figures, appendices, bibliography, references, and footnotes. The thesis contains no material that has been submitted previously, in whole or in part, for the award of any other academic degree or diploma. Except where otherwise indicated, this thesis is my own work.

Date: 21 July 2022

Endorsed by:

Carolyn J. Brown

Principal Supervisor

Graeme L. White

Associate Supervisor

Student and supervisors' signatures of endorsement are held at the University.

# STATEMENT OF CONTRIBUTION

This section details contributions by the various authors for each of the papers presented in this thesis by publication.

Paper 1:

Letchford, R. R., White, G. L., & Brown, C. J. 2022, *MNRAS*, 510, 5330-5347. https://doi.org/10.1093/mnras/stab3777.

Student contributed 80% to this paper. Collectively, G. L. White and C. J. Brown contributed the remainder.

Paper 2:

Letchford, R. R., White, G. L., & Brown, C. J. 2022, *Astron. Nachr.*, 343, 1-13. e20210113. https://doi.org/10.1002/asna.20210113.

Student contributed 80% to this paper. Collectively, G. L. White and C. J. Brown contributed the remainder.

Paper 3:

Letchford, R. R., White, G. L., & Brown, C. J. 2022, *Astron. Nachr.*, 343, 1-14, e20220018. https://doi.org/10.1002/asna.20220018.

Student contributed 80% to this paper. Collectively, G. L. White and C. J. Brown contributed the remainder.

# ACKNOWLEDGEMENTS

I wish to thank my wife, Heather, and children, particularly those still living at home during all or part of my research, Gerard, Felicity, and Dominic. I thank them for their patience and understanding.

Next, I wish to thank my two supervisors, Adjunct Professor, Dr Graeme White, and Dr Carolyn Brown of the University of Southern Queensland. To say that I could not have raised the standard of my research to publication level without them would be an understatement. I look forward to continuing our collaborative work on double stars.

I wish to thank Professor Bradley Carter, Professor of Physics and Director of the Centre for Astrophysics at the University of Southern Queensland, for taking the risk of accepting me for post-graduate research, even though my interests are not in the core area of focus of the Centre.

I also acknowledge the early assistance of Allan Ernest (Adjunct Professor, Charles Sturt University), Nick Lomb (Adjunct Professor, University of Southern Queensland) and Tim Napier-Munn (Emeritus Professor, University of Queensland), and personal correspondence from Dr Andrew Jacobs, Curator of the NSW Museum of Applied Arts and Sciences' Sydney Observatory, regarding the Banks Refractor (currently housed there) and associated micrometers (which to date have not been located).

This research has been supported by an Australian Government Research Training Program Scholarship.

# DEDICATION

## Ad majorem Dei gloriam

Ἐν ἀρχῇ ἐποίησεν ὁ θεὸς τὸν οὐρανὸν καὶ τὴν γῆν. . . . καὶ ἰδοὺ καλὰ λίαν.

In *the* beginning God created the heaven and the earth . . . and behold, *it was* very good.

Genesis 1:1,31

# TABLE OF CONTENTS

# LIST OF TABLES

# LIST OF FIGURES

# CHAPTER 1: Introduction

## 1.1 BROAD CONTEXT

Double stars are pairs of stars in abnormal astrometric proximity on the celestial sphere. They are usually divided into two classes: optical double stars where the two stars only appear close together but are in fact gravitationally unbound (i.e. their binding energy is > 0), and binary double stars (or simply binary stars) where the two stars are gravitationally bound (i.e. their binding energy is < 0) (Aarseth, Tout, & Mardling 2008; Benacquista 2012; Kouwenhoven et al. 2010; Penoyre, Belokurov, & Evans 2022; Wiley & Rica 2015).
Visual double stars are studied for a variety of reasons, including:

- *To determine the relationship between two stars*. Distinguishing between optical double stars and binary stars enables multiplicity ratios to be determined for different galactic environments (e.g., areas of the Galaxy with different gas and stellar densities). Binary and multiple stars make up more than half of all star systems and so accurate multiplicity ratios for different galactic environments and different spectral types leads to better stellar formation and evolution models (Andrews, Chanamé, & Agüeros 2017; Chanamé, Harmanec, & Guinan 2007; Guinan, Harmanec, & Hartkopf 2007; Igoshev & Perets 2019; Moe 2019).
- *To determine a fundamental parameter of stars, specifically their mass*. The main properties of a star can be defined by three fundamental parameters: mass, radius, and luminosity. Other parameters such as metallicity, magnetic field, and rotation, are known as secondary parameters (LeBlanc 2011). Combined masses can be determined via Kepler's Third Law on known binaries whose orbits are well-enough defined to

calculate good estimates of their semi-major axes and orbital periods. Likewise, more precise measurement of the mass of a star can increase the accuracy of the mass-luminosity relation. For more detailed discussion on this topic see, Andersen (1991) and Torres, Andersen, and Giménez (2010).

- *To probe the presence of (otherwise unseen) perturbers*. Fragile binaries (binaries whose binding energies are close to zero) have orbits that are easily disrupted by encounters with other objects such as other stars, molecular clouds, black holes, planetary bodies, and in the case of halo binaries, Massive Compact Halo Objects (MACHOs). Chanamé and Gould (2004) found a large number of fragile halo binaries, but Yoo, Chanamé, and Gould (2004) failed to detect a clear signature of the disrupting effect of MACHOs on the widest, and hence most weakly bound, binaries. What is needed are larger samples of confirmed fragile binaries to test the disruptive effect or otherwise of MACHOs.

More reasons can be given for the study of binary double stars than those described above. See for example, Chanamé, et al. (2007), Hartkopf, Harmanec, and Guinan (2007), and the review paper by Maceroni and Sterken (2006).

The study of optical double stars, on the other hand, apart from aiding the calculation of multiplicity ratios, also has an important role in observational astrophysics. For example, confirmed optical double stars can serve as calibrators of plate scale and rotation.

This thesis is particularly concerned with wide visual double stars, which are double stars with apparent separations greater than about 1 arcsecond (”).

## 1.2 AIMS

Modern, space-based astronomy, from missions such as HIPPARCOS (Perryman et al. 1997) and *Gaia* (Collaboration et al. 2018), has opened a new sophisticated avenue of double star studies. These space missions give the astrometric measures of a double star, its (angular) separation (ρ or Sep) measured in arcseconds (”), and position angle (θ or PA) measured in degrees (°), with precisions that are 3-4 orders of magnitude more precise than has been available to-date from single-aperture ground observations (aside from speckle interferometry on close pairs).

Unfortunately, these space-based measures are over a relatively short span of epoch in the case of wide visual double stars, and the determination of relative movement can only be determined by the combination of historic measures with space-based measures so that the epoch span of the data set can be extended up to ~200 years.

This reality suggests three questions:

- How accurate are the historic non-space-based measures?
- How can the inclusion of space-based astrometry lead to better estimates of orbits of wide slow-moving binaries?
- How can the inclusion of space-based astrometry lead to better estimates of the rectilinear motion of optical double stars?

This thesis addresses these questions by:

i. analysing the precision of the first southern double star catalogue of some 253 double stars by James Dunlop published in 1829 (hereafter the *Dunlop Catalogue*);

ii. compiling a *Working Dunlop Catalogue*, consisting of 40 double stars from the *Dunlop Catalogue* where both components have full data sets from HIPPARCOS and *Gaia Data Release 2 (Gaia DR2)* and are also currently listed in the *Washington Double Star Catalog (WDS)*; and

iii. developing power-based computational techniques for the determination of the orbital elements of long period binary systems of short observational arc, and the rectilinear elements for optical doubles, and in so doing, differentiate binaries and optical doubles within the *Working Dunlop Catalogue*. These computational techniques are applicable to general double star work and are not specific to the Dunlop pairs, which are only used in these papers to illustrate the power of the techniques.

Therefore, this work is NOT a thesis on the history of astronomy, nor an adventure into the early history of Australia. This thesis is an attempt to enhance current astronomy/astrophysics using state-of-the-art data and computational methods, and through the revaluing of historic data that is so important in this research area.

## 1.3 UNIQUENESS OF PRESENTED RESEARCH

This thesis represents the first attempt to specifically use space-based astrometry and photometry to:

a) Assess the accuracy of measures of an old *double* star catalogue. Previous work on old *single* star catalogues has been done by others using data from HIPPARCOS (Verbunt & van Gent 2010a, 2010b, 2011, 2012), but not for old *double* star catalogues.
b) Calculate first order orbital elements for wide, slow moving, binary stars which have been measured only over a short arc. Here the combination of data from HIPPARCOS with an Epoch of 1991.25 and *Gaia DR2* with an epoch of 2015.5 are used, in addition to the historic measures.
c) Calculate rectilinear elements for optical stars using data from HIPPARCOS and *Gaia DR2* with known and small uncertainties,

rather than historical data with unknown uncertainties, as was done previously.

## 1.4 OUTLINE OF THESIS

Chapter 2 presents the literature review or background to the present research, and after the preamble, is divided into three sections representing the background literature to each of chapters 3, 4 and 5, respectively.

Chapter 3 reproduces Paper 1, published in the *Monthly Notices of the Royal Astronomical Society*, and answers the first research question, "How accurate are the historic non-space-based measures", by analysing the measures in the *Dunlop Catalogue*.

Chapter 4 reproduces Paper 2, published in the *Astronomische Nachrichten*, and answers the second research question, "How can the inclusion of space-based astrometry lead to better estimates of orbits of wide slow-moving binaries", by developing and testing an iteration-based computational technique for the determination of the orbital elements for long period and under sampled arcs relying on data from HIPPARCOS and *Gaia DR2* and them applying the technique to a select sample of binary stars from the *Working Catalogue*.

Chapter 5 reproduces Paper 3, also published in the *Astronomische Nachrichten*, answers the third research question, "How can the inclusion of space-based astrometry lead to better estimates of the rectilinear motion of optical double stars?"

Chapter 6 is a discussion and conclusion to the thesis, where the results of the three papers are brought together and their implications discussed.

# CHAPTER 2: LITERATURE REVIEW: RESEARCH BACKGROUND

## 2.1 PREAMBLE

This research grew out of an initial interest in the scientific output of the Parramatta Observatory which operated between 1822 and 1839 on the grounds of Government House about 20 km west of central Sydney (Australia). This early interest resulted in seven papers in the *Journal of Double Star Observations*, a non-ranked, web-based journal (Letchford, White, & Ernest 2017, 2018a, 2018b, 2019a, 2019b, 2019c, 2019d). Further studies of the Parramatta Observatory, its research output, staff and heritage can be found in Haynes et al. (1996), Richardson (1835), Saunders (1990), Saunders (2004), Schaffer (2010), and other references listed in the Introduction to Paper 1. A succinct overview of James Dunlop and his work is available in Argyle, Swan, and James (2019), p. 21.

This review will examine some of the scholarly works forming the research background of Papers 1, 2 and 3 (Chapters 3, 4 and 5, respectively of this thesis). Section 2.2 outlines both a history and current status of double star catalogues, astrometry and magnitude estimation. Section 2.3 will then summarise the history and current status of binary orbit calculation, and Section 2.4 will review the literature on the description of rectilinear motion of optical double stars.

## 2.2 DOUBLE STAR CATALOGUES AND ASTROMETRY

Paper 1 (Chapter 3) assesses the accuracy of the measures contained in the first published catalogue of double stars in the southern hemisphere, the *Dunlop Catalogue*. An appreciation of the

background to this study requires some awareness of both double star catalogues, and the state of astrometry and visual magnitude estimation at the time of the *Dunlop Catalogue* (1829), as well as what is available today.

### 2.2.1 The *Dunlop Catalogue*

Published in the *Monthly Notices of the Royal Astronomical Society* in 1829 as *Approximate Places of Double Stars in the Southern Hemisphere, observed at Parramatta in New South Wales* by James Dunlop (Dunlop 1829), the paper represented the first dedicated southern double star catalogue. It consists of (incomplete) measures of a purported 253 double stars in the southern hemisphere south of -23° declination arranged in order of right ascension. A more complete description is given in Section 2 of Paper 1. Right ascensions and declinations of the primary star are given to the nearest sidereal second and arcminute, respectively. The smallest noted separation is 2 arcseconds and apparent visual magnitudes are estimated to the nearest half magnitude.

Many other catalogues and lists of double stars followed in the 19$^{th}$ and 20$^{th}$ centuries, most notably that of F. G. Wilhelm Struve who worked in Dorpat, Russia, now Tartu in Estonia (Struve 1822, 1827, 1837; Struve & Struve 1840). In 1964, with the support of International Astronomical Union (IAU) Commission 26, the central depository of double star measures was transferred to the *United States Naval Observatory* (USNO) and renamed the *Washington Double Star Catalog* (van de Kamp 1966). The earliest measure of a double star in the WDS is $\mu$ Draconis (STFA 35), with a first measure date of 1690. Now over 154,000 double stars are catalogued in the WDS.

The need for Visual Double Star catalogues grew originally from the race to identify optical double stars from which parallax (stellar distances) could be detected and measured. With William's Herschel's discovery of binary stars (Herschel 1803) and Savary's proof that their orbits follow Keplerian laws (Savary 1827a, 1827b), the continuous measuring and discovery of binary stars held the opportunity of directly measuring stellar distances and masses. Today, the discovery, measuring and cataloguing of double stars remains crucial for many astrophysical problems, notably stellar formation and evolution (Section 1.2).

### 2.2.3 Astrometry

Astrometric precision (and visual magnitude estimates) has increased markedly over the last two centuries since the publication of the *Dunlop Catalogue*. The foundation of double star studies is the precision measurement of their position angles and separations. These are referred to as "measures". Early measures remain crucial in determining the Orbital Elements of wide binary stars with long periods. An understanding of historic positional uncertainties can lead to tighter estimates of the orbital parameters of binary systems thus contributing to better estimates of fundamental stellar parameters.

Erik Høg's most recent work on the history of astrometry (Høg 2017), contains a plot tracing the astrometric accuracy of *single* star catalogues over the past 2000 years (Figure 1). From Figure 1, and the work of Morton Grosser (1979), p. 15, it is estimated that during the period of double star observations at the Parramatta Observatory in the 1820s, the prevailing positional accuracy for single stars was approximately 5''. A steady increase in positional accuracy occurred in the following 170 years until the HIPPARCOS mission.

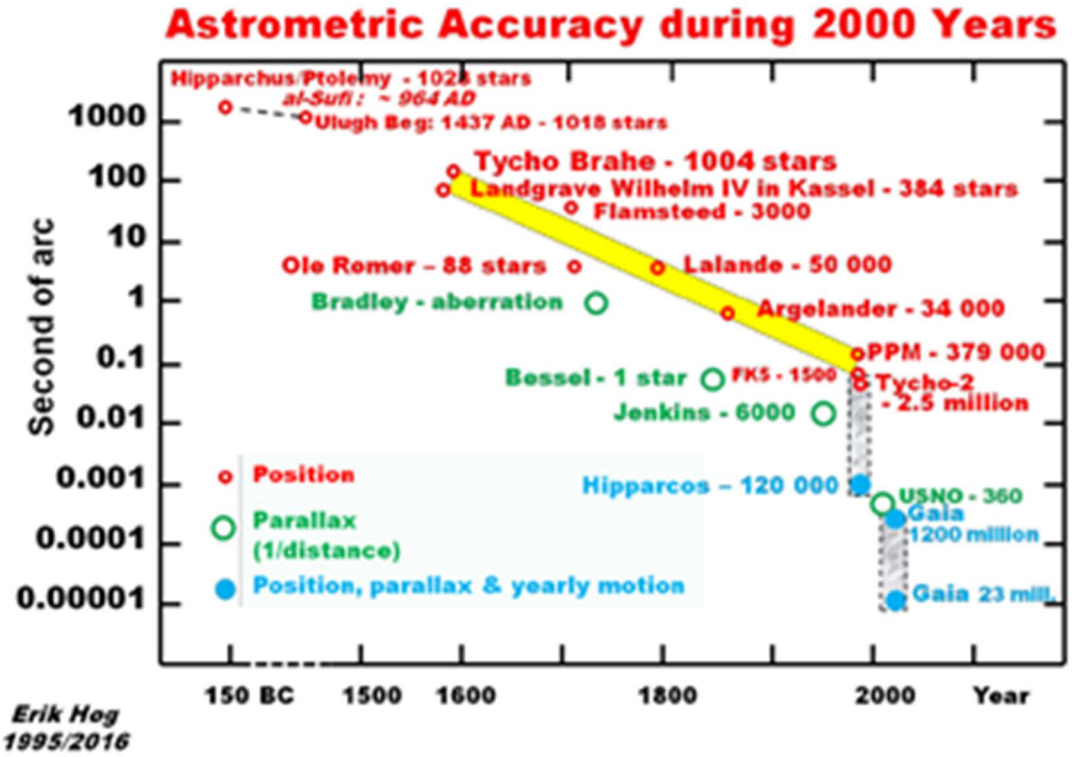


Figure 1: Evolution of astrometric accuracy during the past 2000 years (Høg, 2017).

According to Figure 1, the HIPPARCOS mission improved positional accuracy by two orders of magnitude to ~1 mas (milliarcseconds) over 1990's single-aperture ground-based positions and *Gaia* improved that again by another two orders of magnitude to ~0.01 mas (in *Gaia DR2*). HIPPARCOS mean uncertainties in right ascension at 1991.25 for the primary stars in the *Dunlop Catalogue* are ~6.1 mas and in declination the uncertainty is ~3.4 mas. Mean uncertainties both in right ascension and declination at 2015.5 from *Gaia DR2* for the primary stars in the *Dunlop Catalogue* are ~0.1 mas. Because the accuracy of *Gaia DR2* is more than three orders of magnitude better than anything expected from Dunlop, this justified neglecting the uncertainties in *Gaia DR2* when it came to comparing the measures in the *Dunlop Catalogue* with precessed *Gaia DR2* positions (see further Paper 1, Chapter 3, Section 3.4). This is

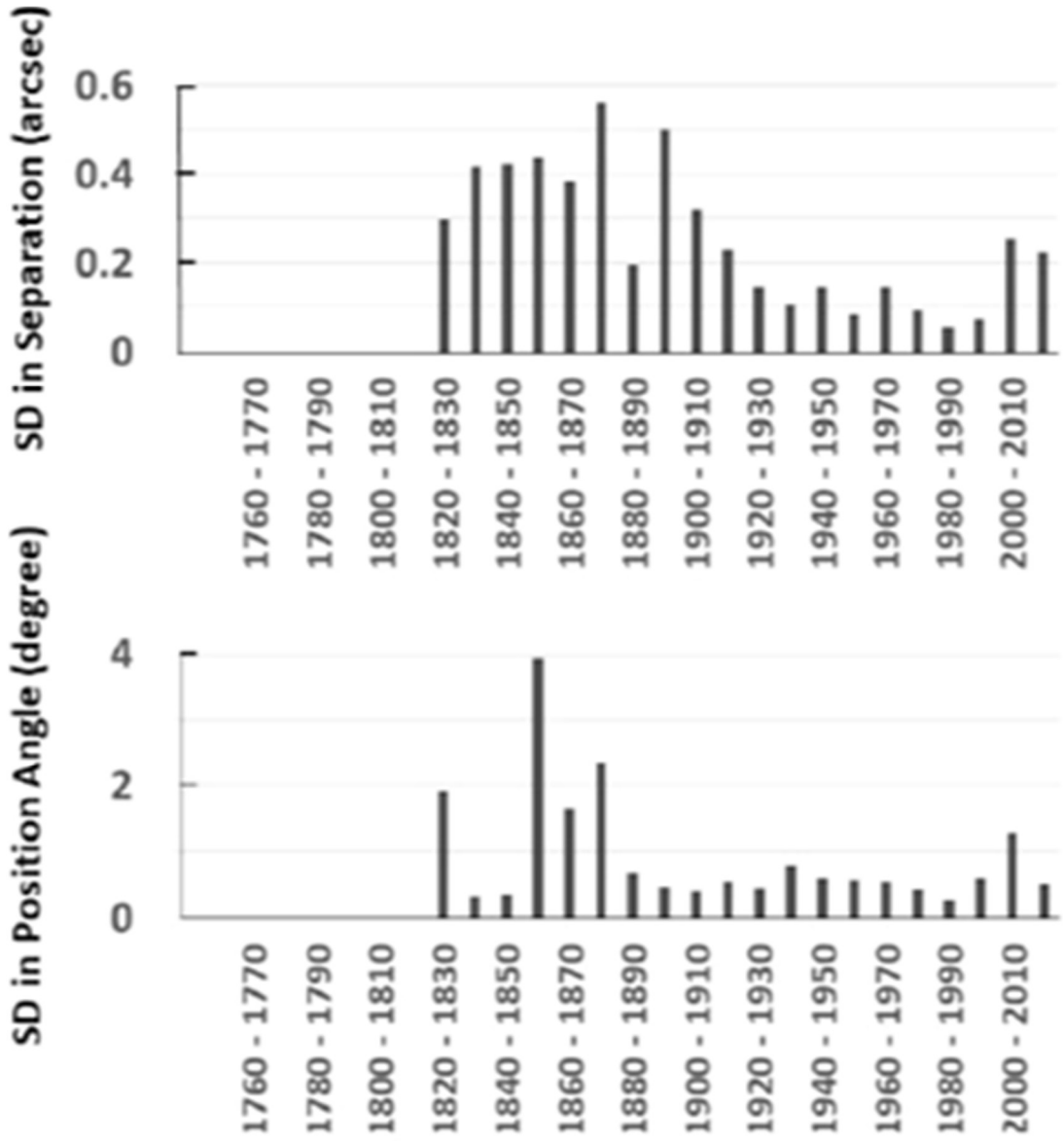


Figure 2: The standard deviation (SD) of historic measures compared to the computed orbit of α Cen AB on a decade-by-decade basis (White, Letchford, & Ernest 2018).

illustrated in Figure 2 a plot of DUN 178AC depicting rectilinear motion of the secondary compared to the primary. The error or distance of Dunlop's measure (green +) from the calculated relative position of the secondary for 1826.0 is 13.8", whereas the error

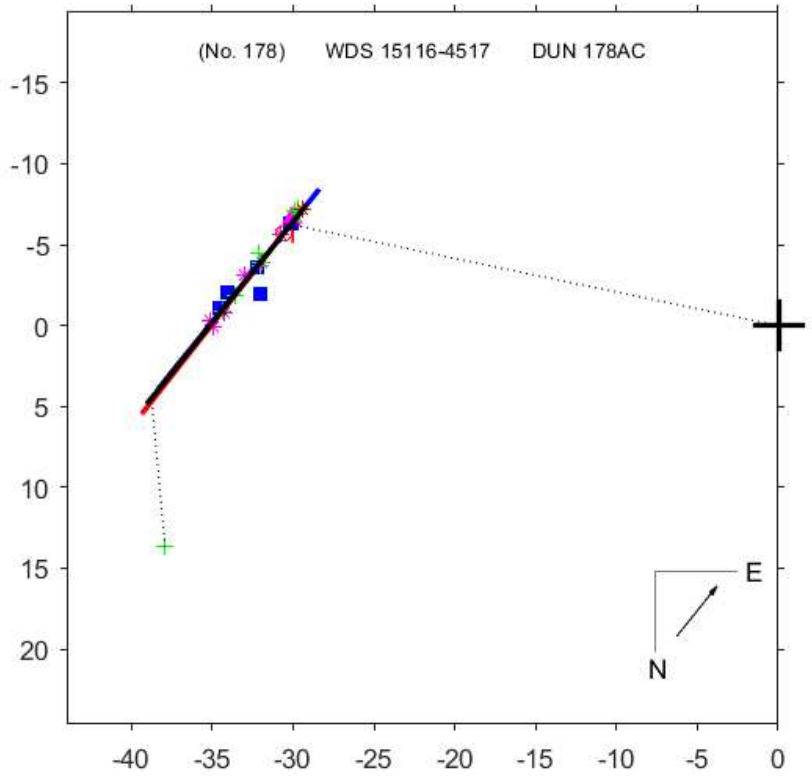


Figure 3: Rectilinear motion of DUN 178AC. The primary is represented by the large plus sign. Dunlop's 1826.0 relative position of the secondary is represented by the small green plus sign. The HIPPARCOS position at 1991.25 is represented by a red square and the Gaia DR2 position at 2015.5 by a red asterisk. For further details of the Figure see Section 4 of Paper 3 (Chapter 5).

ellipses for the HIPPARCOS (at 1991.25) and Gaia DR2 (at 2015.5) positions have an approximate radius of 0.46 mas and 0.043 mas, respectively.

With respect to uncertainties in single-aperture historic/ground-based measures, White et al. (2018), published estimates of the accuracy of double star measures (Figure 3) by comparing historic measures of α Cen AB with the published orbit from the *Sixth Catalog of Orbits of Visual Binary Stars* (Matson et al. 2020). Figure 3 shows the estimated accuracy of position angle in the decade 1820–1830 was ~4°, and that of separation measures ~0.5″. As α Cen AB is one

of the most comprehensively studied binary systems, they argued that these uncertainties in the measures represent the standard of double stars astrometry against which the historic work of others, such as Dunlop, can be related.

### 2.2.4 Visual magnitude estimation

Apart from providing positions of the primary, and measures of position angle and separation, the *Dunlop Catalogue* also gives estimates of apparent visual magnitudes.

The 1820s magnitude scales were far from uniform and were made "principally as an aid to identification" (Hearnshaw 1996, p. 16), and in the case of double stars, to distinguish the primary (brighter of the two) and the secondary. The adopted Ptolemy scale on which all magnitude scales were based at the time was not logarithmic (Dobler 2002; Grasshoff 1990; Toomer 1984; Verbunt & van Gent 2012) and this caused even greater variation when it came to classifying magnitudes of faint stars seen only in the telescope (Hearnshaw 1996).

It was not until 1905 that the modern logarithmic Pogson ratio of apparent visual magnitude became standard with the work of Edward Pickering (Fujiwara & Yamaoka 2005; Jones 1968; Pickering, Searle, & Wendell 1884; Pogson 1856). Nevertheless, from the work of Milone and Sterken (2011), where modern measures of magnitudes are directly compared with those from the last two and a half centuries, the mean difference is only ~±0.3 magnitudes (Figure 4) in the 1820s.

In comparing space-based measures of apparent visual magnitudes with those in the *Dunlop Catalogue* in Paper 1, photometry from *Gaia DR2* was employed. However, since *Gaia DR2* does not come with

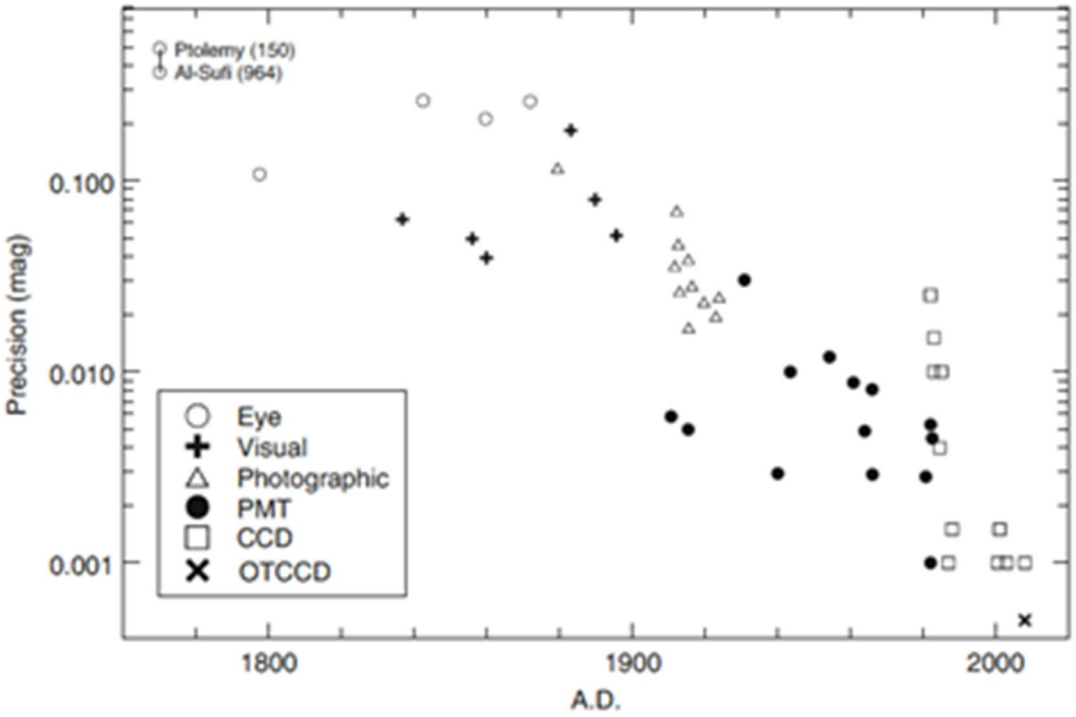


Figure 4: Evolution of precision of magnitude estimates (Milone & Sterken 2011).

apparent visual magnitudes, algorithms supplied by the European Space Agency to convert from G (G-band mean magnitude) and the BP-RP colour (Integrated BP mean magnitude - Integrated RP mean magnitude) to the Johnson-Cousins (V) system used in Paper 1 are as follows:

$$V = G - 0.01760 + 0.006860(BP - RP) + 0.1732(BP - RP)^2$$

The correction for saturation is:

$$G^{corr} = G - 0.047344 + 0.16405\mathrm{G} - 0.046799\mathrm{G}^2 + 0.0035015G^3$$

And applies when 2.0 < G < 6.5. Many Dunlop stars fall in this magnitude range.

The mean uncertainty in G for the double stars in the *Dunlop Catalogue* is ~ ±0.002 mag.

As with astrometric data (section 2.2.3), converted photometric data from *Gaia DR2* is considerably more accurate than what can be expected in the *Dunlop Catalogue*. Again, this justified neglecting the uncertainties in V magnitudes from *Gaia DR2* when comparing them to those in the *Dunlop Catalogue*.

## 2.3 CALCULATING ORBITS OF BINARY STARS

Of the over 154,000 double stars in the WDS, computed orbits are available for just over 3,300 in the *Sixth Catalog of Orbits of Visual Binary Stars*, also maintained by the USNO. Paper 2 (Chapter 4) presents a new method of estimating first order orbits which can be applied to any orbit but is especially suited to wide visual binary stars that have been measured only over a small portion of their orbit. For well-defined orbits or orbits with at least about half of their orbit populated with measures, two methods are currently employed to obtain the seven orbital elements that define the motion of the secondary about a fixed primary.

The Kowalski method derives five of the seven Orbital Elements from the constants of the Cartesian form of the general equation for the apparent relative ellipse (Aitken 1964; Glasenapp 1889; Green 1985; Kowalski 1873) and forms a part of the method presented in Paper 2 (Chapter 4). The second method is the 'Thiele-Innes-Van-den-Bos' method (Thiele 1883; van den Bos 1926, 1932, 1962) which depends on three observed positions and the areal constant, improved by using Cartesian instead of polar coordinates (Aitken 1964; Green 1985). Both methods are still used today, although the 'Thiele-Innes-Van-den-Bos' method is often modified in the way presented in Hartkopf, McAlister, and Franz (1989). The results of both methods are frequently improved with differential corrections

(Aitken 1964; Alzner 2012; Heintz 1978; Hirst 1944; van den Bos 1937).

Two attempts have been made to describe the orbits of binary stars with short arcs. First, the 'Kovole' method which is a modified version of the Kowalski method (Olević & Cvetković 2004, 2005). Second is a modified version of the 'Thiele-Innes-Van-den-Bos' method (Docobo 1985; Docobo & Hestroffer 2012; Docobo, Ling, & Prieto 1992; Docobo, Tamazian, & Campo 2018; Pearce, Wyatt, & Kennedy 2015). Prior short-arc work is also documented in Pearce, et al. (2015) and Docobo, et al. (2018). However, closer inspection of these attempts reveals that their short arcs are either at least a third of an orbit, or more than one short arc scattered over the orbit. No method to date has addressed the case of a single short arc or used space-based astrometry as the foundation of a technique to obtain orbits from short arcs, as achieved in Paper 2 (Chapter 4).

## 2.4 CALCULATING THE RECTILINEAR MOTION OF OPTICAL DOUBLE STARS

The *Second Catalog of Rectilinear Elements* (SCORE, also known as LIN2) is an online repository of Rectilinear Elements of over 1,200 double stars (Hartkopf & Mason 2020). The targets identified in this catalogue are thought to be optical double stars and therefore the motion of the secondary compared to a fixed primary is described by a straight line. The SCORE, like the WDS, is also maintained by the USNO. Paper 3 (Chapter 5) presents a new method of calculating these Rectilinear Elements which reduces the uncertainties of these Elements on average by an order of magnitude compared with those currently in the SCORE.

The first attempt to describe the relative linear motion of an optical double star was by Schlesinger and Alter (1912) (they provide no

references to earlier work), who used a least squares method on historic measures after precession to a common equinox. Debehogne and de Freitas Mourao (1977), who undertook a comparison between the least-squares method and that of mean places with differential corrections, opted for the least-squares method as the best then available. Equations for the least-squares method can be found in Torres (1988). The Rectilinear Elements in the SCORE result from the least-squares method applied to *weighted* historic measures, where the weighting system is described in Mason, Douglass, and Hartkopf (1999), Hartkopf, Mason, and Worley (2001a) and Hartkopf, McAlister, and Mason (2001b). Only 'in-house solutions' (USNO) are currently accepted into the SCORE.

Chapters 4 and 5 depend on the correct crossmatching of both the primary and secondary stars in the *Dunlop Catalogue* with HIPPARCOS (via ASCC) and *Gaia DR2* source identifiers. This crossmatching is the first step associated with Paper 1.

# CHAPTER 3: PAPER 1 - ASSESSMENT OF THE ACCURACY OF MEASURES IN THE 1829 SOUTHERN DOUBLE STAR CATALOGUE OF JAMES DUNLOP

## 3.1 INTRODUCTION

Paper 1 assesses the accuracy of measures in the 1829 double star catalogue of James Dunlop (Dunlop 1829) the *Dunlop Catalogue*. This was done by cross matching the double stars in the *Dunlop Catalogue* with source identifiers from the latest release from the Gaia space mission, *Gaia DR2*, precessing the *Gaia DR2* positions using proper motion, parallax data and nutation to the equinox date of the *Dunlop Catalogue*. Best fit regressions were then conducted to compare these calculated positions with those from the *Dunlop Catalogue*.

Seven percent of the double stars in the *Dunlop Catalogue* could not be identified, 14 were single stars, and 13 were double stars (5%) not currently listed in the WDS. The catalogue equinox was determined as B1826.0. Overall, one sigma uncertainties in right ascension were within 1 sidereal minute and declinations within 10 arcminutes. A number of quadrant errors were identified which resulted in corrected position angles with an average uncertainty of 70°”/separation”. Separations were within 7%, and apparent visual magnitudes were within 1 visual magnitude. Dunlop’s little-known catalogue remains valuable as the earliest source of over 200 double star astrometric and visual magnitude estimates.

Letchford, R. R., White, G. L., & Brown, C. J. 2022, *MNRAS*, 510, 5330-5347. https://doi.org/10.1093/mnras/stab3777.

Monthly Notices of the ROYAL ASTRONOMICAL SOCIETY

MNRAS **510,** 5330–5347 (2022) https://doi.org/10.1093/mnras/stab3777
Advance Access publication 2021 January 14

# Assessment of the accuracy of measures in the 1829 southern double star catalogue of James Dunlop

Roderick R. Letchford ,★ Graeme L. White and Carolyn J. Brown
*Centre for Astrophysics, University of Southern Queensland, Toowoomba, 4350 QLD, Australia*

Accepted 2021 December 25. Received 2021 December 23; in original form 2021 August 23

**ABSTRACT**

In 1829 James Dunlop published the first southern double star catalogue of some 253 double stars. The accuracy of this catalogue has been determined by using *Aladin* to cross-match them with *Gaia DR2* and estimate their positional (right ascension, declination, position angle, and separation) and magnitude accuracy. Seven per cent could not be identified using *Aladin* and 14 were single stars. We found 13 double stars (5 per cent) not currently listed in the *Washington Double Star Catalog*. The catalogue equinox was determined as B1826.0. Overall, 1$\sigma$ uncertainties in right ascension were within 1 sidereal minute and declinations within 10 arcmin. We also identified and corrected a number of Quadrant errors in the position angles and quantified the separations. Apparent visual magnitude estimates were generally within 1 mag. Dunlop's overall uncertainties were larger than those of his contemporaries, nevertheless the little known catalogue remains valuable as the earliest source of over 200 double star astrometric and visual magnitude estimates.

**Key words:** history and philosophy of astronomy – methods: analytical – astrometry – binaries: visual.

## 1 INTRODUCTION

Astrometric positions are the core of many astrophysical studies, and historic data often holds the key to accurately determined astrophysical parameters when incorporated with such space missions as *HIPPARCOS* and *Gaia*.

Astrometric and magnitude measures in old double star catalogues are rarely accompanied by estimates of their uncertainties. For double star studies, accurate historic positions lead to firmer distinctions between rectilinear and orbital motion, as in distinguishing binary double stars from optical double stars. Estimates of the multiplicity ratios of stellar systems, for each spectral type, and galactic environment have important ramifications for many aspects of astrophysics especially stellar formation and evolutionary models (Chanamé 2007; Guinan, Harmanec & Hartkopf 2007; Duchêne & Kraus 2013; Andrews, Chanamé & Agüeros 2017; Igoshev & Perets 2019; Moe 2019). An understanding of historic positional uncertainties can lead to tighter estimates of the orbital parameters of binary systems thus contributing to better estimates of fundamental stellar parameters such as mass.

The aims of this paper are to draw attention to and describe; as well as correct and quantify; the first published catalogue of southern double stars, by James Dunlop (Dunlop 1829) titled, *The Approximate Places of 253 Double and Triple Stars for the beginning of 1827, as observed with a 9-feet Reflecting Telescope at Paramatta, New South Wales, from the latter end of 1825 to the beginning of 1827. The Observations were made about 2$^s$ of sidereal time east of the Brisbane Observatory*. This paper is referred to here as the *Dunlop Catalogue*. The observations that contributed to it were, in part, carried out at the Parramatta Observatory. The Parramatta Observatory is well represented in the literature (e.g. Richardson & Brisbane 1835; Service 1890; Wood 1966; Bhathal & White 1991; Haynes et al. 1996; Cozens & White 2001; Saunders 2004; Rutledge 2009; Cozens, Walsh & Orchiston 2010; Schaffer 2010; Bickford 2011; Bhathal 2012), where its main goal was to produce a *single* star catalogue of the southern sky which was published in 1835 (Richardson & Brisbane 1835) and is known as the *Brisbane Catalogue*.

The *Dunlop Catalogue* was initially greeted with enthusiasm. Sir John Herschel called the catalogue 'copious and valuable' (Herschel 1828). Some years later, when he conducted his own survey of the southern sky, at the Cape of Good Hope he reversed his praise and claimed that the *Dunlop Catalogue* contained a 'great many mistakes... in the places, descriptions, or measures' (Herschel 1847).

That one comment alone meant that the *Dunlop Catalogue* was practically forgotten after 1847. It is hoped that this paper will also to some degree, restore the reputation of Dunlop and his pioneering double star work.

The first two authors of this paper have previously published material on the *Dunlop Catalogue* (Letchford, White & Ernest 2019a,b,c,d). This present paper represents a more thorough investigation of the astrometric and magnitude estimates of the *Dunlop Catalogue*. Section 2 describes the *Dunlop Catalogue* and the telescopes used. Section 3 will go on to explain the methods used to: quantify its internal consistency; identify the primary and secondary components; calculate the catalogue equinox; estimate the accuracy of the positions, position angles, separations and magnitude estimates; and discusses possible complications and solutions to the methods. The results will be presented and discussed in Section 4, along with recommendations for the observer and a note on the typographical errors in the *Dunlop Catalogue*. Finally in Section 5,

★ E-mail: rod.letchford@usq.edu.au

**Table 1.** Statistics on entries per column in the *Dunlop Catalogue*. The numbers in brackets indicate statistics for secondary and tertiary components, respectively.

| Col. | Column name | *Banks Refractor* | *Dunlop Reflector* |
|---|---|---|---|
| 1 | No. | 119 | 134 |
| 2 | Name of Star | 119 | 134 |
| 3 | Approximate AR | 119 | 134 |
| 4 | Declination | 119 | 133 |
| 5 | Angle of Pos | 98 | 73 |
| 6 | Quadrant | 112 | 101 (3) |
| 7 | Distance | 60 (3) | 77 (2) |
| 8 | Δ AR | 68 | 13 |
| 9 | Δ Declin. | 88 | 16 |
| 10 | Magnitudes | 118 (118) (1) | 131 (125) (9) |
| 11 | Remarks | 33 | 46 |

**Table 2.** Combination of columns from the *Dunlop Catalogue* that can be used to determine Dunlop's *Mean PA* and *Mean Sep*, respectively. Columns 2 and 3 indicate the number of double stars from each telescope for which a position angle and separation could be determined via each method.

| Method | *Position angle* | *Banks Refractor* | *Dunlop Reflector* |
|---|---|---|---|
| i | 5, 6 | 97 | 80 |
| ii | 4, 6, 8, 9 | 63 | 6 |
| iii | 4, 6, 7, 8 | 22 | 0 |
| iv | 4, 6, 7, 9 | 35 | 0 |
| **Method** | ***Separation*** | ***Banks Refractor*** | ***Dunlop Reflector*** |
| i | 7 | 60 | 77 |
| ii | 4, 8, 9 | 67 | 8 |
| iii | 4, 5, 8 | 55 | 3 |
| iv | 5, 9 | 70 | 4 |

we present some general conclusions. A data file accompanies this paper which digitises the *Dunlop Catalogue*, gives modern identifications, and data generated as a result of our research.

## 2 DESCRIPTION OF THE *DUNLOP CATALOGUE*

For his observations of double stars (all south of declination −23°), Dunlop used two telescopes herewith referred to as the *Dunlop Reflector* and the *Banks Refractor*. The *Dunlop Reflector* was the main telescope used for his double star work (and his survey of southern non-stellar objects) and was a 9 inch (23 cm) aperture, 9 foot (274 cm) focal length Newtonian with a speculum mirror that Dunlop himself made (Dunlop 1828, 1829). The other telescope, the *Banks Refractor*, was a 3.25 inch (8.3 cm) aperture, 46 inch (117 cm) focal length equatorial-mounted refractor made by Banks of London, equipped with micrometers and setting circles in both hour angle and declination (Dunlop 1829; Lomb 2004; Barker 2008).

The published *Dunlop Catalogue* presents various measures of 253 double stars divided into 11 columns. Statistics on what is presented in each column are given in Table 1 where the numbers in brackets indicate statistics for secondary and tertiary components, respectively. The declination for No. 50 is missing. As can be seen from Table 1, not every double star has a complete set of measures. Measures from the *Banks Refractor* are more complete than those from the *Dunlop Reflector*.

An image of the first nine entries in the original *Dunlop Catalogue* is presented in Fig. 1. A brief description of each column is given here.

*Column 1*: **No.** Number of the double, 1–253. In the *Washington Double Star Catalog* (WDS, Mason et al. 2001, the central depository for all published double star measures), the discoverer code DUN followed by a number from this column is used to designate the corresponding double from the *Dunlop Catalogue*, however, in the WDS, only 168 of the 253 double stars have DUN as the discoverer code (see Section 4.2).

*Column 2*: **Name of Star.** One of either a Bayer-style or Flamsteed-style designation (Ashbrook 1984) or 'Anonym.', as in 'Anonymous'. After each of 119 names an asterisk (*) is placed to indicate that the *Banks Refractor* was used for these measures. The lack of an asterisk indicates that the 9 inch *Dunlop Reflector* was used. We continue to use the asterisk to mark measures from the 3.25 inch *Banks Refractor*.

| No. | Name of Star. | Approximate Æ. | Declination. | Angle of Pos. | Quadrant. | Distance. | Δ Æ. | Δ Declin. | Magnitudes. | Remarks. |
|---|---|---|---|---|---|---|---|---|---|---|
| | | h m s | ° ′ | ° ′ | | ″ | s | ″ | | |
| 1 | $\beta^1\beta^2$ Toucani * | 0 23 16 | 63 56 | 84 5 | *np* | | 0,607 | 24,86 | 4,4 | Double. L. C. |
| 2 | λ Toucani * | 0 44 50 | 70 28 | | *sf* | | | 6,62 | 6,7 | |
| 3 | Anonym. | 1 19 43 | 33 31 | | | | | | 7 | A very singular star of the 7th magnitude, of an uncommon red purple colour, very dusky and ill-defined; 3 obs. on this star; a small star preceding, and another following. |
| 4 | 100 Phœnicis * | 1 32 11 | 54 18 | 17 27 | *sf* | 15,809 | | | 6,8 | |
| 5 | 6 Eridani * | 1 33 24 | 57 4 | 73 6 | *nf* | 2,5 | | | 6·7,6·7 | Very nearly equal. Pretty d. star. |
| 6 | φ Eridani | 2 10 12 | 52 20 | 50 0 | *sp* | 90 | | | 4,12 | |
| 7 | Anonym. | 2 34 57 | 60 21 | 20 0 | *np* | 35 | | | 8,8 | |
| 8 | 41 App. Chemici * | 2 50 37 | 25 40 | 49 6 | *sp* | | | | 7,7 | |
| 9 | θ Eridani * | 2 51 19 | 41 0 | 1 37 | *nf* | 10,81 | | | 4,6 | |

**Figure 1.** An image of the first nine entries in the original *Dunlop Catalogue* (Dunlop 1829).

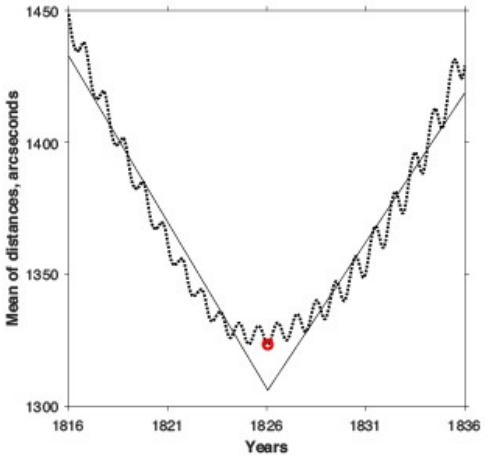


**Figure 2.** Determination of *Dunlop Catalogue* equinox. The x-axis is the possible Equinox Julian year, the y-axis is the mean distance between Dunlop primary positions and *Gaia DR2* precessed primary positions, in acrseconds. The straight lines represent the effect of precession and the dotted oscillating line represents the effect of nutation. The red circle indicates the position of the lowest net separation, at Julian year 1826.05. We adopt 1826.0 as the equinox and epoch of the *Dunlop Catalogue*.

**Table 3.** Internal consistency of columns 5, 7, 8, and 9 for the *Banks Refractor* in the *Dunlop Catalogue*, illustrated by their Gaussian bias and 1$\sigma$ values. Linear fits and associated $R^2$ are from published values versus calculated 'mean' values, again without any outliers removed, and are given to indicate the correlation between them.

| *Banks Refractor* | *Angle of Pos* (column 5) | *Distance* (column 7) |
|---|---|---|
| 1st Gaussian bias | $+51^{'} \pm 47^{'}$ | $+1.8^{''} \pm 1.2^{''}$ |
| 1st Gaussian 1$\sigma$ uncertainty | $377^{'} \pm 34^{'}$ | $7.1^{''} \pm 0.9^{''}$ |
| 1st outliers | 34* | 34* |
| 1st OLS slope | $+1.04 \pm 0.03$ | $+1.12 \pm 0.03$ |
| 1st OLS $R^2$ | 0.94 | 0.98 |
| ***Banks Refractor*** | **$\Delta$ *AR* (column 8)** | **$\Delta$ *Declin* (column 9)** |
| 1st Gaussian bias | $-0.22^{s} \pm 0.^{s}11$ | $-1.2^{''} \pm 0.7^{''}$ |
| 1st Gaussian 1$\sigma$ uncertainty | $0.78^{s} \pm 0.^{s}08$ | $5.9^{''} \pm 0.5^{''}$ |
| 1st outliers | 78*, 178* | 242* |
| 1st OLS slope | $+0.96 \pm 0.03$ | $+0.96 \pm 0.03$ |
| 1st OLS $R^2$ | 0.94 | 0.96 |

*Column 3*: **Approximate AR.** Right ascension of the primary in hours, minutes and whole seconds at the Catalogue equinox and epoch of observation (Section 4.3). The double stars are listed in order of increasing right ascension.

*Column 4*: **Declination.** Declination of the primary in degrees and whole minutes at the Catalogue equinox and epoch of observation (Section 4.3), measured south from the equator.

*Column 5*: **Angle of Pos.** The angle of the secondary relative to the primary measured from the parallel of declination of the primary into one of the Quadrants (column 6), in degrees and whole minutes. This is not the same as the present-day position angle (PA) which is the angle of the secondary with respect to the primary measured from the meridian passing through the primary, eastwards from north, in decimal degrees.

**Table 4.** Identification statistics. 'DUN in WDS' refers to double stars that are present in the *Washington Double Star Catalog* with DUN (for Dunlop) as the discoverer designation. 'Other in WDS' refers to double stars in the WDS with discoverer designations other than DUN. 'unidentified' refers to double stars in the *Dunlop Catalogue* that could not be identified. 'one' indicates that only one star was found to be associated with the Dunlop position. 'Two' indicates that a double star was found but is not currently listed in the WDS. Three, four, five indicates that a three, four, or five star system, respectively, was found at the location in the *Dunlop Catalogue*.

| Identification | *Banks Refractor* | *Dunlop Reflector* | Total | Percentage (of 253) |
|---|---|---|---|---|
| DUN in WDS | 84 | 84 | 168 | 66.4 % |
| Other in WDS | 21 | 14 | 35 | 13.8 % |
| Unidentified | 4 | 14 | 18 | 7.1 % |
| One | 3 | 11 | 14 | 5.5 % |
| Two | 7 | 3 | 10 | 4.0 % |
| Three | 0 | 5 | 5 | 2.0 % |
| Four | 0 | 2 | 2 | 0.8 % |
| Five | 0 | 1 | 1 | 0.4 % |

*Column 6*: **Quadrant.** Quadrant of the secondary relative to the primary (n = north, s = south, p = preceeding, and f = following). Thus, position angles between 0° and 90° are in Quadrant nf, between 90° and 180° in sf, between 180° and 270° in sp and between 270° and 360° in np. For Nos. 108, 194, and 211, two Quadrants are given since Dunlop recorded them as triple stars. For some double stars (all from the *Dunlop Reflector*), the Quadrant is given simply by one of the four letters, indicating a PA of either 0° (n), 90° (f), 180° (s), or 270° (p).

*Column 7*: **Distance.** Angular distance of the secondary from the primary, in arcseconds. Equivalent to separation (Sep).

*Column 8*: $\Delta AR$. Absolute difference in right ascension between the primary and secondary, in (sidereal) seconds of right ascension.

*Column 9*: $\Delta Declin$. Absolute difference in declination between the primary and secondary, in arcseconds.

*Column 10*: **Magnitudes.** Apparent visual *eyeball* magnitude estimates of the primary and secondary. The *Dunlop Catalogue* used an old form of magnitude notation where the point is read as between two magnitudes. When this occurs, we read this being the first magnitude plus 0.5.

*Column 11*: **Remarks.** Dunlop's notes on selected double stars, e.g. his remark 'Double L. C.' occurs 15 times for the 3.25 inch and 5 times for the 9 inch. This references these double stars to Nicolas-Louis de Lacaille's 1763 catalogue (Lacaille 1763).

## 3 METHODS

### 3.1 Internal consistency

Dunlop did not record the relative position of the secondary in the now familiar position angle and separation measures. Rather, columns 5–9 of the *Dunlop Catalogue* contain data such that the position angle and separation can each be calculated in up to four different ways (see Table 2). Because of this, we define Dunlop's position angle and separation for each double star as the *mean* of the results of each method (*Mean PA* and *Mean Sep*, respectively). Standard trigonometric equations were used to calculate the *Mean PA* and *Mean Sep*, and are given in Appendix B. Any effects the

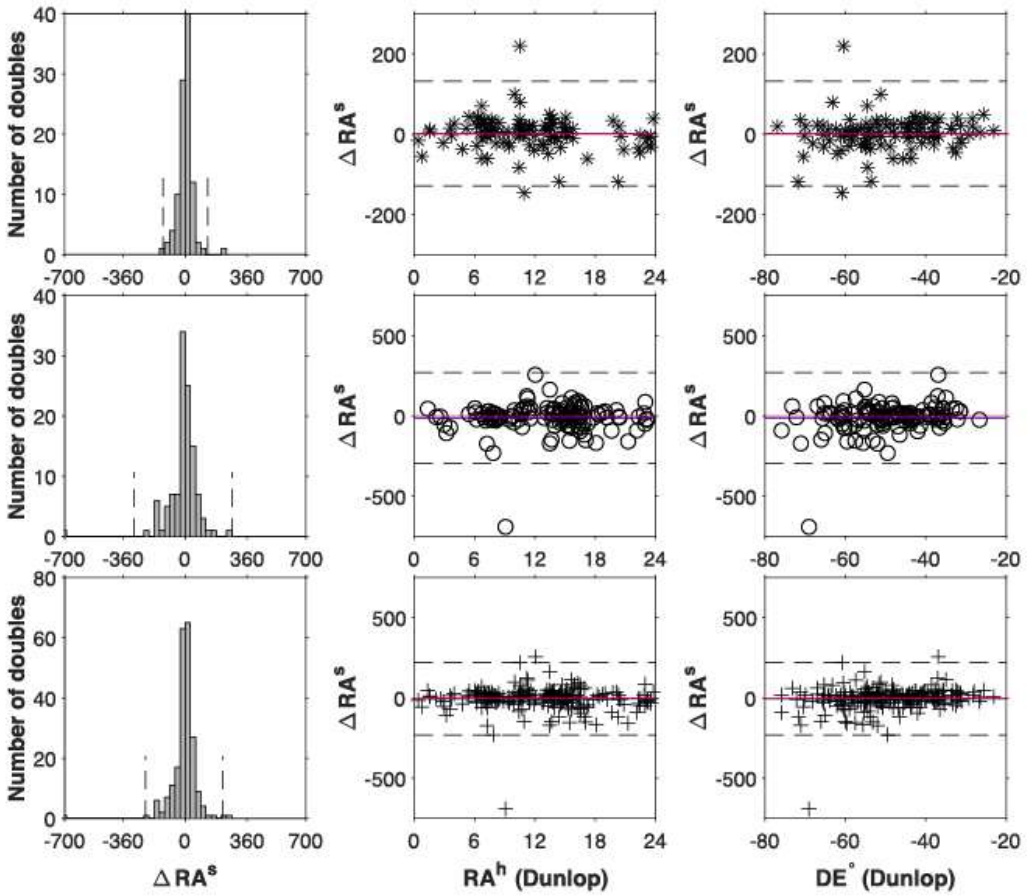


**Figure 3.** Accuracy of Dunlop's RA in sidereal seconds, without outliers removed. $\Delta RA^s$ = Difference in right ascension in sidereal seconds in the sense of equation (1). Note the relatively few but large outliers. Most are probably due to typographical errors in the published catalogue (see Section 4.4). *Left column*: Histograms of number of double stars in the *Dunlop Catalogue* versus $\Delta RA^s$. Bin widths, $30^s$ in each case, were chosen for plot clarity. The dashed black lines show the Gaussian $\pm 3\sigma$ positions, without outliers removed. *Middle* and *right columns*: Display the following overlays: a solid red line to indicate the unity line; a blue solid line to indicate the Gaussian bias; and dashed black lines to indicate the positions of the Gaussian $\pm 3\sigma$. *Top row*: Distribution of the differences in right ascension ($\Delta RA^s$) for the *Banks Refractor*. *Middle row*: Distribution of the differences in right ascension ($\Delta RA^s$) for the *Dunlop Reflector*. *Bottom row*: Distribution of the differences in right ascension ($\Delta RA^s$) for the for the catalogue as a whole. *Middle column*: Dependence of the differences in right ascension ($\Delta RA^s$) with right ascension ($RA^h$). *Right column*: Dependence of the differences in right ascension ($\Delta RA^s$) with declination (DE°).

different ways (or lack of) might have on the *Mean PA* and *Mean Sep* are discussed in in Section 4.1.

Internal consistency of columns 5–9 can be estimated by using the *Mean PA* and *Mean Sep* to calculate a 'mean' *Angle of Pos* (column 5), 'mean' *Distance* (column 7), 'mean' $\Delta AR$, and 'mean' $\Delta Declin$ for each double star. The difference between the published values (O) and the 'mean' values (C), in the sense O–C, should give a measure of consistency, by calculating the single peak Gaussian bias and $1\sigma$ uncertainties of O–C results, without any outliers removed. The bias and uncertainty of one column was not taken into account when determining the bias and uncertainty of another column. We also calculated the ordinary least-squares linear slope and $R^2$ of O versus C as a measure of the correlation between the two values.

### 3.2 Modern identification

A total of 168 double stars from the *Dunlop Catalogue* (84 each from the *Banks Refractor* and *Dunlop Reflector* already have DUN (for Dunlop) as the discoverer code in the WDS. We decided to accept these identifications. To confirm the identity of the remaining double stars in the *Dunlop Catalogue*, the position of each primary was forward precessed to equinox J2000.0. The low precision International Astronomical Union 1976 method (gives < 1 arcsec uncertainty over the required period, Lieske et al. 1977) was used as this does not depend on knowing either parallax or proper motion, and only requires the initial equinox and epoch. Because we began not knowing the catalogue equinox, we assumed an initial

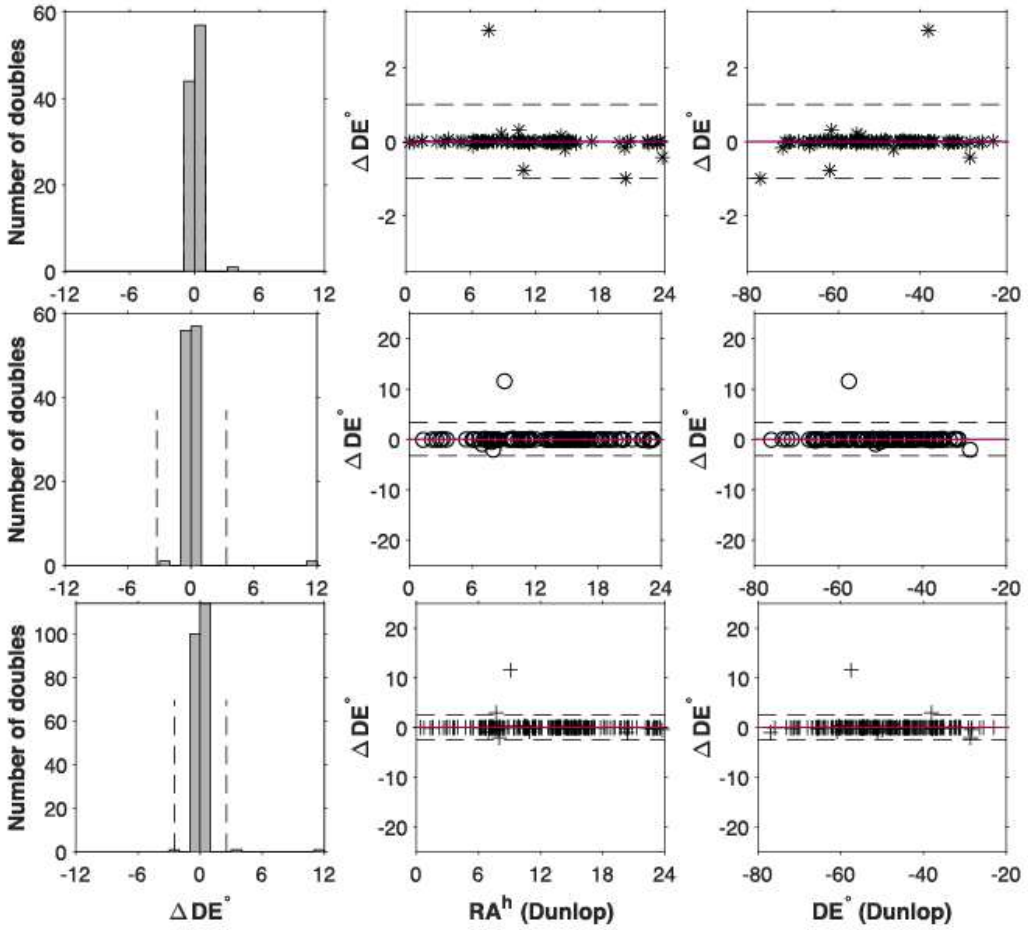


**Figure 4.** Accuracy of Dunlop's declinations without outliers removed. As per previous comments (Fig. 3). The 3$\sigma$ dashed lines in the first histogram (top left) are present but follow very closely to the bin edges. Histogram bin widths are 1° in each case, and were chosen for plot clarity. Note the relatively few but large outliers. Most are probably due to typographical errors in the published catalogue (see Section 4.4). Note also the relative accuracy of declinations from the *Banks Refractor* (first row) as contrasted with those from the *Dunlop Refractor* (second row).

temporary equinox and epoch of 1825.0, as this is the equinox of the contemporary *Brisbane Catalogue*.

Each field was examined using the *Aladin Sky Atlas* (*Aladin*, Bonnarel et al. 2000) and overlaid with SIMBAD *Astronomical Database* (Wenger et al. 2000), ASCC-2.5 V3 (Kharchenko & Roeser 2009), and *Gaia DR2* (Gaia Collaboration 2018) data. In nearly all cases, the double star in question was within 10 arcmin of the forward precessed position (for further details see Section 4.2). For the few remaining, we extended the search out to a limit of 1°. To keep to a minimum poor or false identifications and by way of confirmation, a nearest neighbour search was also conducted with positions in the WDS, imposing a narrow magnitude tolerance on the primary and secondary of ±1 mag of Dunlop's published magnitudes and excluding first separations <2 arcsec, the minimum separation recorded by Dunlop. Any poor matches may be defined as *1st outliers* and *2nd outliers* in right ascension or declination (Section 4.4) or position angle or separation (Section 4.5) or magnitudes (Section 4.6).

The SIMBAD, ASCC-2.5 V3, and *Gaia DR2* source identifiers were recorded, together with International Celestial Reference System (ICRS) and epoch 2000.0 coordinates, proper motion, parallax, and photometric data from *Gaia DR2*. For the present purposes we take ICRS as equivalent to equatorial equinox J2000.0.

This research was well underway when *Gaia Early Data Release 3* (*Gaia EDR3*; Lindegren et al. 2021) became available. The authors acknowledge that the *Gaia EDR3* catalogue is comparably more precise than the *Gaia DR2* catalogue, however, this was found not to be significant enough to result in substantial differences of the outcomes presented in this paper. Both *Gaia DR2* and *Gaia EDR3* are

**Table 5.** Accuracy of Dunlop's right ascensions and declinations after rejection of *1st outliers*. The 2nd Gaussian bias and 1$\sigma$ uncertainties do not reflect the Gaussian plots overlaying the histograms in Figs 3 and 4, which are for all available data *without* the removal of any outliers. The right ascension OLS slopes and $R^2$s are from RA (*Dunlop Catalogue*) versus RA (*Gaia DR2*) at 1826.0, after the removal of *1st outliers*. Similarly those for declination.

| ***Banks Refractor*** | **Right ascension** | **Declination** |
|---|---|---|
| 2nd Gaussian bias | $+0^s.4$ | $-32''$ |
| 2nd Gaussian 1$\sigma$ uncertainty | $35^s$ | $371''$ |
| 1st outliers | 92∗, 105∗ | 56∗, 232∗ |
| 2nd outliers | 163∗, 231∗ | 92∗,105∗, 253∗ |
| 2nd OLS slope | +0.9997 | +0.9996 |
| 2nd OLS $R^2$ | 1 | 1 |
| ***Dunlop Reflector*** | **Right ascension** | **Declination** |
| 2nd Gaussian bias | $-6^s$ | $-106''$ |
| 2nd Gaussian 1$\sigma$ uncertainty | $70^s$ | $804''$ |
| 1st outliers | 75 | 75 |
| 2nd outliers | 59, 118 | 37, 61 |
| 2nd OLS slope | +0.9999 | +0.9963 |
| 2nd OLS $R^2$ | 1 | 1 |
| **Whole catalogue** | **Right ascension** | **Declination** |
| 2nd Gaussian bias | $-4^s$ | $-88''$ |
| 2nd Gaussian 1$\sigma$ uncertainty | $56^s$ | $681''$ |
| 1st outliers | 75, 118 | 56∗, 75 |
| 2nd outliers | 59, 92∗ | 37, 61, 105∗, 232∗ |
| 2nd OLS slope | +0.9997 | 0.9990 |
| 2nd OLS $R^2$ | 1 | 1 |

known to be incomplete at the bright end (European Space Agency 2021), especially for close bright pairs. For the purpose of this paper, it is mainly the brighter end of the magnitudes that are required to compare against the *Dunlop Catalogue* (mean G of the Dunlop doubles is ∼7, with a range from ∼2.0 to ∼12.2), which are available in *Gaia DR2*.

### 3.3 The *Dunlop Catalogue* equinox

There is no published equinox or epoch for the *Dunlop Catalogue* (except for nine double stars in the introduction to the *Dunlop Catalogue* for which epochs only are given, one during 1825 and eight during 1826). Using the data from *Gaia DR2*, we conducted a high precision backwards precession to the years between 1816 and 1836 in steps of 0.01 years for each primary, using the algorithms and rotation matrices from Eckardt & Humphrey (2017) and incorporating proper motion, parallax, and nutation effects. The separations between the original catalogue coordinate and the precessed *Gaia DR2* coordinate were calculated and the mean taken for each possible equinox. The stepped year with the lowest total separation we considered to be the working equinox of the *Dunlop Catalogue*, and the working epochs of observation for each double.

### 3.4 Positional accuracy

Given the *Gaia DR2* positions of the primary at the same equinox and epoch as the positions recorded in the *Dunlop Catalogue* we compared them (and all following comparisons) in the sense:

$$\Delta = \text{Dunlop} - \textit{Gaia DR2 (backwards precessed)}. \quad (1)$$

The $\Delta$ in equation (1) should not be confused with Dunlop's limited use of $\Delta$ in columns 8 and 9 of the *Dunlop Catalogue*. We used three fitting models, Gaussian, ordinary least squares linear (OLS), and inverse power fits, and chose one of these to best reflect each set of parameters.

Two assumptions enabled us to pursue this method. The first is that both the primary and the secondary stars can be treated as independent entities with no connection between them (such as being gravitationally bound and therefore exhibiting orbital motion), and thus can be precessed separately. This assumption is reasonable as it is expected that most of the Dunlop double stars will be either optical double stars (displaying rectilinear motion of the secondary with respect to the primary) or if connected, the orbital period will be very long and the little movement of the secondary observed over the last 200 yr can be approximated by rectilinear motion. Dunlop's double stars have been observed extensively over the past 200 yr, and any detectable orbital motion may be expected to have already been reported with elements and plots in the *Sixth Catalog of Orbits of Visual Binary Stars* (Matson et al. 2020). To further support these assumptions, of the five Dunlop double stars which have entries in this catalogue, two have periods currently estimated in the thousands of centuries (Nos, 2∗ and 44), two (Nos, 5∗, 23) have 'preliminary' orbits with periods of around 500 yr, and only one (No. 165∗, $\alpha$ Cen) is a well accepted binary with a period of around 80 yr (see Appendix A).

The second assumption is that offsets (Gaussian biases and 1$\sigma$ uncertainties) describe the accuracy of the measures in the *Dunlop Catalogue* only, the contribution due to uncertainties in the *Gaia DR2* data being insignificant compared with the Dunlop data. To illustrate this, we note that the positional (astrometric) accuracy of single stars in the 1820s was ∼5 arcsec (Grosser 1979; Høg 2017). For early double star observations (of the early 19th century) the accuracy of the separations was ∼0.5 arcsec, the accuracy of the position angle was ∼4° (White, Letchford & Ernest 2018) and visual magnitudes were within 0.3 mag (Milone & Sterken 2011). On the other hand, *Gaia DR2* positional accuracy at ICRS and epoch 2015.5, is about $10^{-5}$ arcsec, with brighter stars having a slightly larger uncertainty (Gaia Collaboration2018). Even after precession, *Gaia DR2* errors are at least five orders of magnitude smaller than the 1820s uncertainties. We therefore designate the biases and uncertainties in the differences between the *Dunlop Catalogue* and precessed *Gaia DR2* astrometric positions as the bias and uncertainty in the *Dunlop Catalogue*.

### 3.5 Position angle and separation

Backwards precessing both the *Gaia DR2* primary and secondary positions using a high precision algorithm (Section 3.3), we compared Dunlop's *Mean PA* with those of precessed *Gaia DR2*, again in the sense of equation (1). Again, we applied single peak Gaussian fits, ordinary least squares linear (OLS), and inverse power fits, and chose one of these to best reflect each set of parameters.

### 3.6 Visual magnitudes

*Gaia DR2* does not directly give apparent visual magnitudes. However, these can be approximated using conversion equations (Carrasco 2020) from the *G* (*G*-band mean magnitude) and the *BP*–*RP* colour (Integrated *BP* mean magnitude – Integrated *RP* mean magnitude) to the Johnson–Cousins (*V*) system, which is assumed to approximate the spectral response of the human eye. Magnitudes determined this way are here defined as *Gaia V*.

Again, the sense of comparison is similar to equation (1):

$$\Delta v\text{mag} = \text{Dunlop} - \text{Gaia } V. \quad (2)$$

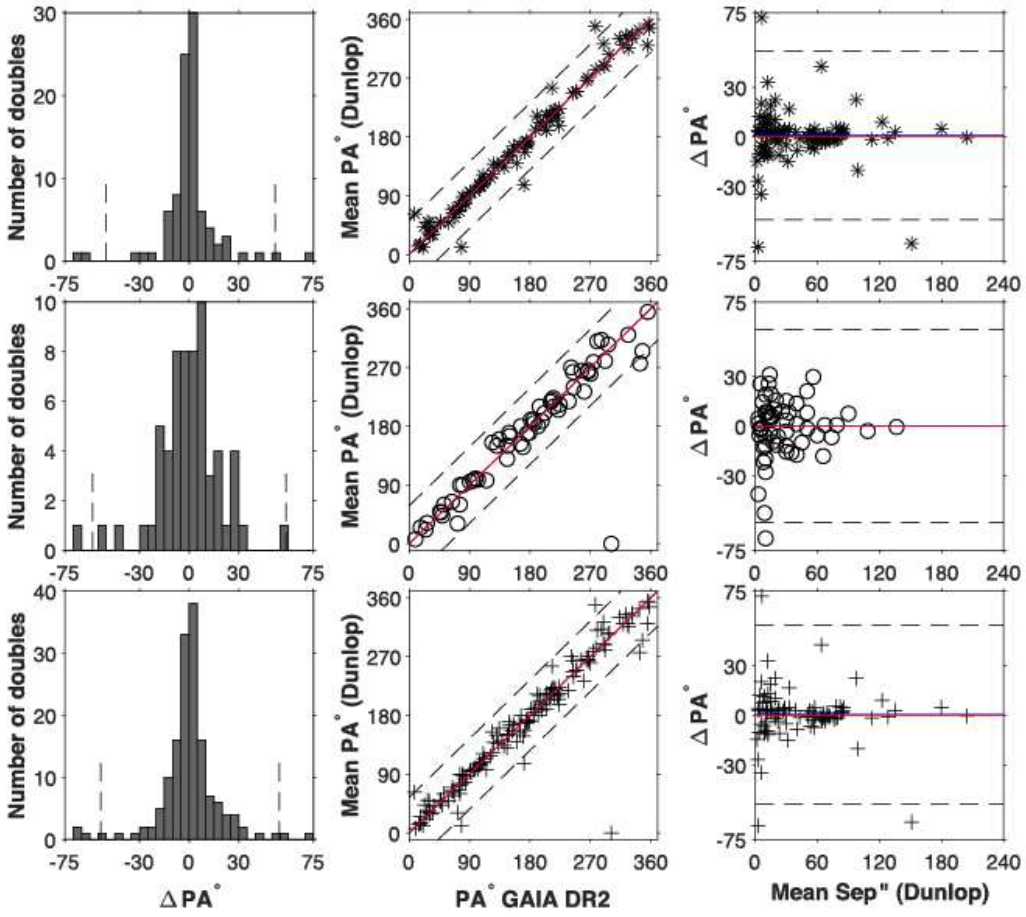


**Figure 5.** Accuracy of Dunlop's mean position angles with quadrant correction and without outliers removed. As per previous comments (Fig. 3), and histogram bin widths are 5° in each case, and were chosen for plot clarity. Note an increasing ΔPA with a decreasing *Mean Sep* (see Section 4.5).

### 3.7 Complications

There are three main complications associated with the analysis of the *Dunlop Catalogue*. The first is the fact that the *Dunlop Catalogue* is incomplete in many columns (Table 1). The second is that not all primaries and secondaries have *Gaia DR2* source identifiers and some with *Gaia DR2* source identifiers have incomplete data. Of the 253 entries in the *Dunlop Catalogue*, 221 primaries have *Gaia DR2* source identifiers, and 205 secondaries. The reasons why some stars do not have *Gaia DR2* source identifiers or have incomplete data include: they remain unidentified; they are too bright in the *G* band (*G* lower reliable limit is ≈3 mag, European Space Agency 2018); they are currently too close together (*Gaia DR2* has a lower limiting completeness separation of ≈2.2 arcsec, Gaia Collaboration2018). This means that not all double stars can be included in comparisons. In Section 4, we note the number of double stars available for comparison.

The third complication is that many of the measures in the *Dunlop Catalogue* have large outliers when equation (1) is applied to them. We define *1st outliers* as those beyond the Gaussian bias by more than three standard deviations, $3\sigma$. All plots (Figs 2–9) include all available comparisons, without any outliers removed. We then removed these *1st outliers* and recalculated the second Gaussian bias and $1\sigma$ uncertainties. We defined *2nd outliers* as those beyond this second bias by more than $3\sigma$. We further defined these second biases and $1\sigma$ uncertainties as those of the *Dunlop Catalogue* (see second assumption in Section 3.4). The OLS fits are taken from data with *1st outliers* removed.

## 4 RESULTS AND DISCUSSION

### 4.1 Internal consistency

The results of the internal consistency analysis of the measures in columns 5–9, resulting from observations made with the *Banks Re-*

**Table 6.** Accuracy of Dunlop's mean position angle and mean separation after quadrant error correction and rejection of *1st outliers*. See also comments for Table 5. C refers to the constant C in ΔPA = C/Sep and ΔSep = C/Sep (Sep = *Mean Sep*), which represent the inverse power fits for Dunlop's *Mean PA* and *Mean Sep*, respectively.

| ***BanksRefractor*** | ***Mean PA*** | ***Mean Sep*** |
|---|---|---|
| 2nd Gaussian bias | +1.1° | −1.7″ |
| 2nd Gaussian 1σ uncertainty | 10.6° | 17.8″ |
| 1st outliers | 32∗, 39∗, 109∗, 252∗ | 79∗, 102∗, 109∗ |
| 2nd outliers | 70∗, 78∗, 147∗ | 78∗, 183∗, 197∗, 216∗ |
| 2nd OLS slope | +0.9936 | +0.8722 |
| 2nd OLS $R^2$ | 0.99 | 0.82 |
| *C* (inverse power fit) | $+57''$ | $+43''2$ |
| Quadrants corrected | 1∗, 5∗, 26∗, 45∗, 78∗, 87∗, 91∗, 99∗, 105∗, 111∗, 137∗, 141∗, 216∗, 235∗, 252∗ | |
| Missing Quadrants supplied by precessed *Gaia DR2* PAs | 27∗, 29∗, 36∗, 52∗, 88∗, 89∗, 253∗ | |
| ***Dunlop Reflector*** | ***Mean PA*** | ***Mean Sep*** |
| 2nd Gaussian bias | −0.2° | −9.7″ |
| 2nd Gaussian 1σ uncertainty | 18.0° | 14.5″ |
| 1st outliers | 101, 151 | 230 |
| 2nd outliers | 181 | None |
| 2nd OLS slope | +0.9823 | +0.8254 |
| 2nd OLS $R^2$ | 0.97 | 0.75 |
| C (inverse power fit) | $+81''$ | $+58''2$ |
| Quadrants corrected | 14, 23, 59, 72, 181, 186, 188, 190, 192, 194, 200, 209, 211, 212, 224 | |
| Missing Quadrants supplied by precessed *Gaia DR2* PAs | 67, 68 | |
| **Whole catalogue** | ***Mean PA*** | ***Mean Sep*** |
| 2nd Gaussian bias | +1.2° | −4.1″ |
| 2nd Gaussian 1σ uncertainty | 10.7° | 16.6″ |
| 1st outliers | 32∗, 39∗, 101, 109∗, 151, 252∗ | 79∗, 102∗, 109∗, 183∗ |
| 2nd outliers | 23, 78∗, 181 | 78∗, 197∗, 216∗, 230 |
| 2nd OLS slope | +0.9893 | +0.8830 |
| 2nd OLS $R^2$ | 0.98 | 0.81 |
| C (inverse power fit) | $+64''$ | $+48''2$ |

*fractor*, are given in Table 3. The Gaussian bias and 1σ uncertainties were calculated as given in Section 3.1, without any outliers removed. Insufficent data was available from the *Dunlop Reflector* to provide meaningful conclusions.

Nos. 76∗, 116∗, 127∗, and 176∗ had values in column 8 (ΔAR) of the *Dunlop Catalogue* that are larger than those in column 4 (Distance), and are probably due to transcription or typographical errors. They are individually explained in Appendix A. Table 3 shows that the *Angle of Pos* (column 5) and *Distance* (column 7) biases between duplicated measures from the *Banks Refractor* are generally less than one degree, and a few arcseconds, respectively. Those for ΔAR and ΔDeclin are less than a quarter of a sidereal second and a little over 1 arcsec, respectively.

Only five *1st outliers* were detected (Table 3, and individually in Appendix A). Three of those five (34∗ (*Distance*, column 7), 78∗, and 242∗) can be satisfactorily explained as due to probable typographical errors. Any effects that may be attributable to the multiple ways of calculating Dunlop's *Mean PA* and *Mean Sep* are therefore minimal.

### 4.2 Modern identification

Aside from the 168 entries in the *Dunlop Catalogue* with DUN as the discoverer designation, we found 35 that also appear in the WDS but with other discoverer designations, for example No. 1∗ we take to be 00315-6257 LCL 119AC (the A component is only ∼102 arcsec from Dunlop's precessed position). Eighteen remain unidentified, because no suitable (Section 3.2) candidate was found within 1° (however, see No. 90 in Appendix A). Fourteen are single stars with no suitable double star candidates within 1° (however, see Nos. 92∗, 96, and 208 in Appendix A). Eight were groupings of three to five stars, again with no suitable double star candidates within 1°. Poor matches are those defined in Section 3.2.

Nos. 56∗ and 61 fell outside the strict 1° search limit (Section 3.2), but we chose to accept the identifications given here (DUN 56 and DUN 61, respectively) as they are given both in SIMBAD and the WDS. No. 75 also fell beyond 1° and is listed in SIMBAD and the WDS as RMK 10. It can be explained as typographical errors in Dunlop's RA and DE (see Appendix A).

A total of 10 double stars (marked **two** in Table 4) that are not currently listed in the WDS were found. Seven were from the *Banks Refractor* (35∗, 112∗, 119∗, 149∗, 153∗, 164∗, and 252∗), and three from the *Dunlop Reflector* (37, 107, and 198). In addition, we corrected identification errors in Letchford et al. (2019b,c) for Nos. 13, 44, 54, 96, 116∗, 118, 136, 143∗, 167, 186, and 252∗. The corrections are also noted individually in Appendix A.

### 4.3 The *Dunlop Catalogue* equinox

The fractional year with the lowest mean angular distance between Dunlop primary positions and *Gaia DR2* precessed primary positions for each fractional year was J1826.05. See Fig. 2. This was calculated from 217 of the 253 primaries because not all primaries were found and not all found primaries had sufficient *Gaia DR2* data to be able to contribute to the calculations (Section 3.7). Since J1826.05 (JD 2388010) approximates B1826.0 (JD 2387992), we fix the catalogue equinox (and epochs) at 1826.0. This is consistent with what is known of Dunlop's observational schedule (Section 1) and eight of the nine epochs published in the introduction to the *Dunlop Catalogue* (Section 3.3). Here, we correct an error made in Letchford et al. (2019c) where we determined the *Dunlop Catalogue* equinox to be 1825.0.

### 4.4 Positional accuracy

Results of the positional accuracy of the *Dunlop Catalogue* as per Section 3.4 are shown here in Figs 3 and 4 and tabulated in Table 5. Note that both figures include all data without outliers removed. Of the seven outliers from the two telescopes in right ascension, six are probably due to typographical errors (59, 75, 105∗, 118, 163∗, 231∗), and one (92∗) was identified as a single star. As for the eight outliers in declination, six may be attributed to typographical errors (37, 61, 75, 92∗, 105∗, 232∗). Each of the eight outliers are individually discussed in Appendix A.

Primaries available for comparison were 102 (out of 119) for the *Banks Refractor* and 115 (out of 134) for the *Dunlop Reflector*. Just one (102∗ = 103∗) primary from the *Banks Refractor* was within 5 arcsec (1820s accuracy, and Section 3.4) of the modern precessed right ascension (RA) and none from the *Dunlop Reflector*. In declination (DE), there were four and eight primaries, respectively, whose declination is within 5 arcsec of the modern precessed declination (Appendix C). OLS fits showed that there is no dependence of right ascension on declination or vice versa for either telescope.

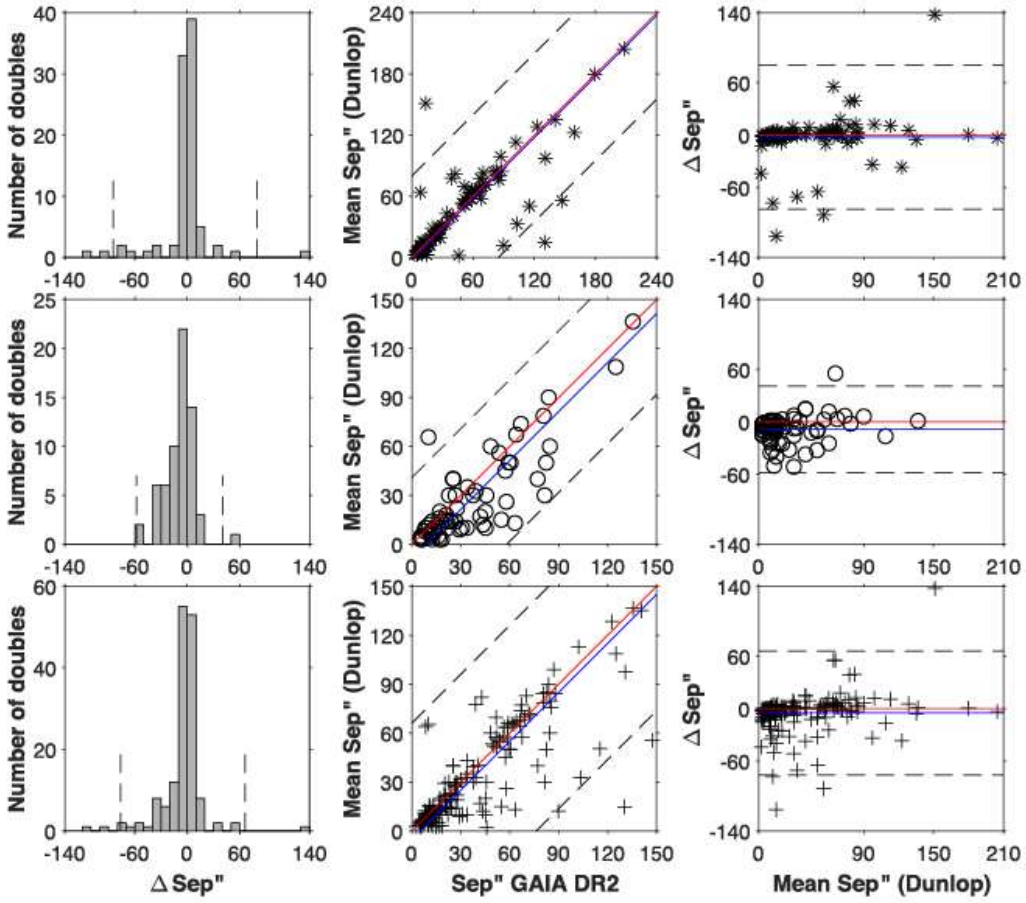


**Figure 6.** Accuracy of Dunlop's mean separations without outliers removed. As per previous comments (Fig. 3), and histogram bin widths are 10 arcsec in each case, and were chosen for plot clarity. Note a more linear relationship between ΔSep and *Mean Sep* in the third column, compared with ΔPA and *Mean Sep* in Fig. 5.

In general, the right ascensions in the *Dunlop Catalogue* are within 4 sidereal seconds of the *Gaia DR2* backwards precessed values, but with uncertainites approaching 1 sidereal minute. Right ascension biases from the *Banks Refractor* (+0.4$^s$) are 15 times better than those from the *Dunlop Reflector* (−6 ). Declinations are considerably worse from both telescopes. The *Banks Refractor* is better with a bias of $-32''$ and an uncertainty of $\pm 371''$, compared to the *Dunlop Reflector* with a bias of $-106''$ and a much larger uncertainty of $\pm 804''$.

### 4.5 Position angle and separation

Section 3.1 gave the process by which the *Mean PA* and *Mean Sep* were calculated and Quadrants identified in the *Dunlop Catalogue*. Initial results of position angle (PA) comparisons (93 and 62 double stars were available for comparison from the *Banks Refractor* and the *Dunlop Reflector*, respectively), showed that a significant number (16 from the *Banks Refractor* and 15 from the *Dunlop Reflector*), had Quadrants different from those of precessed *Gaia DR2* position angles. These differences were evenly spread such that north corrected to south (and vice versa) and following corrected to preceeding (and vice versa) occurred in about equal numbers for both telescopes. Six missing quadrants from the *Banks Refractor* and two from the *Dunlop Reflector* were supplied by precessed *Gaia DR2* position angles.

A quadrant correction was carried out on the *Dunlop Catalogue* by substituting the precessed *Gaia DR2* quadrants for those from the *Dunlop Catalogue*. After quadrant correction, the *Banks Refractor* had 44 (out of 93) double stars whose position angles fell within the expected 1820s accuracy of 4° (Section 3.4). The *Dunlop Reflector* had 14 (out of 62). These are listed in Appendix C. Fig. 5 shows the accuracy of Dunlop's *Mean PA*, *with* quadrant correction and no outliers removed. Table 6 quantifies the associated biases,

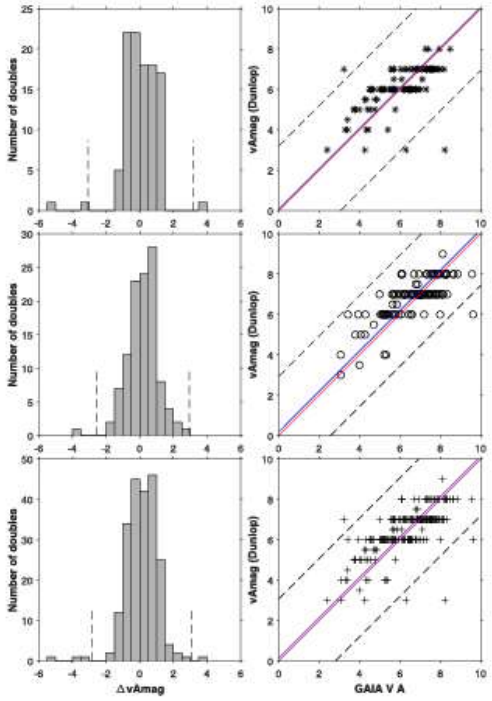


**Figure 7.** Accuracy of Dunlop's primary magnitudes without outliers removed. As per previous comments (Fig. 3), and histogram bin widths are 0.5 mag in each case, and were chosen for plot clarity. Note reasonably consistent spread of *vA* mag (Dunlop) with *Gaia V*A.

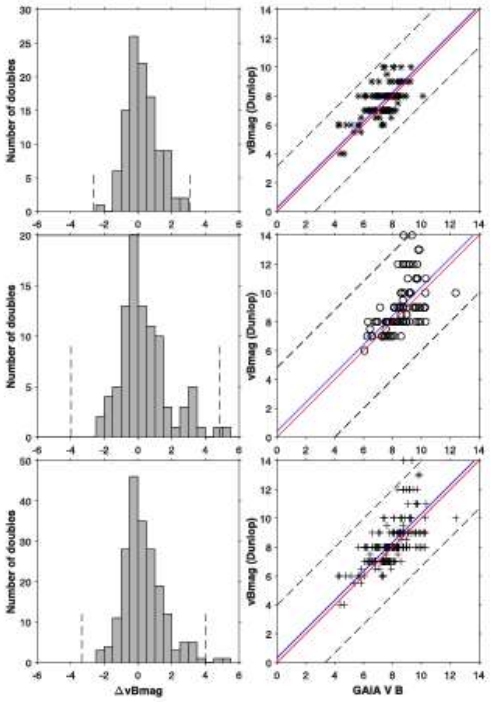


**Figure 8.** Accuracy of Dunlop's secondary magnitudes without outliers removed. As per previous comments (Fig. 3), and histogram bin widths are 0.5 mag in each case, and were chosen for plot clarity. Note increasing disparity of *vB* mag (Dunlop) with increasing *Gaia V*B.

uncertainties, OLS fits, and inverse power fits, lists the double stars whose quadrants were corrected, and lists quadrants supplied by *Gaia DR2*.

Dunlop's Mean PA bias for the *Banks Refractor*, after quadrant correction, is only a little over one degree (+1.1°). The bias from the *Dunlop Reflector* is less at −0.2°. Of the ten *Mean PA* outliers (after Quadrant correction), three (78∗, 101, 252∗) may be attributed to typographical errors, and one (151) had a quadrant improvement from n to np. All ten are noted in Appendix A.

Selecting from the fitting models applied, the Gaussian bias best reflects the overall bias in *Mean PA*. An inverse power fit to ΔPA ($\sim\pm57^{\circ\prime\prime}/$*Mean Sep*$''$ and $\sim\pm81^{\circ\prime\prime}/$*Mean Sep*$''$ for the *Banks Refractor* and *Dunlop Reflector*, respectively), best reflects the reducing range of ΔPA with increasing *Mean Sep*, and serves as an approximate measure of the uncertainty of Dunlop's *Mean PA*.

Results for separations are shown in Fig. 6 and tabulated in Table 6. With regard to separations, the *Banks Refractor* had only 8 (out of 93) and the *Dunlop Reflector* only one (No. 213 out of 62) within the contemporary accuracy of 0.5 arcsec (Section 3.4). These are noted in Appendix A.

Separation biases were −1.7 and −9.7 arcsec from the *Banks Refractor* and *Dunlop Reflector*, respectively. The smallest Mean Sep was 2.0 arcsec from Nos. 24, 33, 50, 84∗, 132∗, 152, 170, and 173. The largest at 440 arcsec was from No. 125 (DUN 125AC). The corresponding separation from the precessed *Gaia DR2* positions for DUN 125AC could not be measured because component A ($\beta$ Cru) does not have a *Gaia DR2* source identifier. Its *V* mag from SIMBAD is just 1.25.

The ΔSep range also reduces with increasing *Mean Sep*, though it is less pronounced than than of ΔPA (see Fig. 6, column 3). In a number of cases, ΔSep is larger than the *Dunlop Catalogue* separations themselves. Nevertheless, an OLS linear fit and associated uncertainty seems to be the best description of the *Mean Sep*. The slopes of the 2nd OLS linear fit of ΔSep versus *Mean Sep* with a point fixed at 0,0 is +0.05 for the *Banks Refractor* and −0.09 for the *Dunlop Refractor*. To reflect this, the Gaussian bias is the correction factor for all *Mean Sep*, and their uncertainties are ±0.05*Mean Sep*$''$ and ±0.09*Mean Sep*$''$, respectively (see Table 8).

Possible explanations for the eight separation outliers proved to be mixed. One could be a typographical error (78∗), one could be due to the high proper motion of component B (79∗), one has a complicated identification (102∗), and four are without adequate explanation (183∗, 197∗, 216∗, and 230).

The eighth separation outlier (*1st outlier*), No. 109∗, is particularly unusual. The *Dunlop Catalogue* recorded one estimate of the separation as $2'\ 49.3''$ or $169.3''$ (the other estimate was calculated to be $132.8''$). The correct quadrant is recorded, also the magnitude estimates are approximately correct, but the modern precessed separation is only 13.5 arcsec. Also Dunlop's *Mean PA* (did not need Quadrant correction) is ∼106.6°, *Gaia DR2* precessed

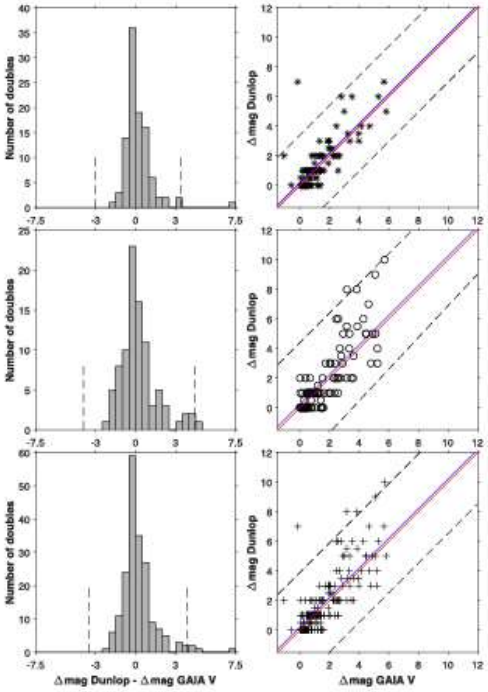


**Figure 9.** Accuracy of Dunlop's difference in magnitudes (primary–secondary) without outliers removed. As per previous comments (Fig. 3), and histogram bin widths are 0.5 mag in each case, and were chosen for plot clarity.

PA is ∼171.0°. There is no star with the right magnitude at Dunlop's separations from this primary.

### 4.6 Visual magnitudes

The results of comparing the Dunlop *eyeball* magnitude with the *Gaia V* magnitudes, for the primary star ($\Delta vA$ mag), the secondary star ($\Delta vB$ mag), in the sense of equation (2), and the differences between these two stars are shown in Figs 7, 8, and 9, respectively, and tabulated in Table 7.

The number of double stars available for comparison were 105 and 109 (out of 119) for the primary and secondary, respectively, using the *Banks Refractor*, and 112 and 94 (out of 134) for the primary and secondary, respectively, using the *Dunlop Reflector*. 16 and 32 primaries, respectively, had $\Delta vA$ mag within the contemporary accuracy of 0.3 mag (Section 3.4), and 23 and 16, respectively, had $\Delta vB$ mag within the contemporary accuracy of 0.3 mag. These are listed in Appendix C.

Dunlop's magnitude estimates had small biases but large uncertainties for both the primary and secondary components. Primary biases were +0.11 and + 0.23 mag, respectively, for the *Banks Refractor* and the *Dunlop Refractor* with uncertainties less than one magnitude at ±0.77 and ± 0.85 mag, respectively. Secondary biases were larger at +0.25 and +0.36 mag for the *Banks Refractor* and the *Dunlop Refractor*, respectively. Uncertainties were also larger at ±0.96 and ±1.39 mag, respectively. The Gaussian model seems to fit the data for both telescopes and the primaries and secondaries.

**Table 7.** Accuracy of Dunlop's magnitude estimates for the primary and secondary star, after rejection of *1st outliers*. See also comments for Table 5.

| **Primary** | ***Banks Refractor*** | ***Dunlop Reflector*** | **Whole catalogue** |
|---|---|---|---|
| 2nd Gaussian bias | +0.11 | +0.23 | +0.17 |
| 2nd Gaussian 1$\sigma$ uncertainty | 0.77 | 0.85 | 0.81 |
| 1st outliers | 92∗, 98∗, 164∗ | 25 | 25, 92∗, 98∗, 164∗ |
| 2nd outliers | None | None | None |
| 2nd OLS slope | +0.6124 | +0.12 | +0.6298 |
| 2nd OLS $R^2$ | 0.66 | 0.59 | 0.63 |
| **Secondary** | ***Banks Refractor*** | ***Dunlop Reflector*** | **Whole catalogue** |
| 2nd Gaussian bias | +0.25 | +0.36 | +0.28 |
| 2nd Gaussian 1$\sigma$ uncertainty | 0.96 | 1.39 | 1.13 |
| 1st outliers | None | 51 | 51 |
| 2nd outliers | None | 128 | 128 |
| 2nd OLS slope | +0.6639 | +0.8415 | +0.8078 |
| 2nd OLS $R^2$ | 0.40 | 0.32 | 0.46 |
| **Magnitude Differences** | ***Banks Refractor*** | ***Dunlop Reflector*** | **Whole catalogue** |
| 2nd Gaussian bias | +0.11 | +0.20 | +0.09 |
| 2nd Gaussian 1$\sigma$ uncertainty | 0.82 | 1.31 | 0.96 |
| 1st outliers | 98∗ | 166 | 6, 51, 98∗, 128, 166 |
| 2nd outliers | 9∗, 164∗ | 6, 51 | 9∗, 12, 164∗, 245 |
| 2nd OLS slope | +1.01 | +1.18 | +1.01 |
| 2nd OLS $R^2$ | 0.71 | 0.67 | 0.68 |

The outliers (25, 92∗, 98∗, 164∗ for the primary and 51 and 128 for the secondary) are difficult to explain. 98∗ and 128 may be due to variability and 164 may be due to errors in *Gaia DR2* colours, from which its visual magnitude was calculated. See Appendix A for details.

As seen in Fig. 8, we detect a clear trend of decreasing Dunlop magnitude with increasing *Gaia V* of the secondary.

We also note a near 1 to 1 relationship between Dunlop's difference in magnitude (primary–secondary) and *Gaia V* (primary–secondary) from 0 to a difference of about 2.5 mag, where Dunlop's differences increase (Fig. 9). The outliers (6, 9∗, 12, 51, 98∗, 164∗, and 166) are noted in Appendix A.

### 4.7 Recommendations

Table 8 contains the resulting recommended corrections and uncertainties from this work that should be applied to the *Dunlop Catalogue* prior to use in modern astrometry. The corrections and estimates of the uncertainties given for each measure are based on the comparison of the *Dunlop Catalogue* with the *Gaia DR2* release. Precise *Gaia DR2* identifications are given in the revised machine readable version of the *Dunlop Catalogue* (see Section 5, Data Availability).

We recommend no corrections to the right ascensions or declinations from the *Banks Refractor*. The right ascensions in the *Dunlop Catalogue* are given to whole sidereal seconds and the bias is less than half a sidereal second. Similarly the declinations are given in whole arcminutes and the bias is a little over half an

**Table 8.** Suggested corrections and uncertainties to be applied to the measures in the *Dunlop Catalogue*.

| *Banks Refractor* | Correction | 1σ Uncertainty |
|---|---|---|
| Right ascension | No correction | $\pm 35^s$ |
| Declination | No correction | $\pm 6.2'$ |
| Mean position angle | Subtract 1.1° | $\pm\sim 57^{\circ\circ}/(Mean\ Sep'')$ |
| Mean separation | Add 1.7 arcsec | $\pm 0.05 x Mean\ Sep''$ |
| Primary magnitude | No correction | ±0.8 mag |
| Secondary magnitude | No correction | ±1 mag |
| ***Dunlop Reflector*** | **Correction** | **1σ Uncertainty** |
| Right ascension | Add $6^s$ | $\pm 70^s$ |
| Declination | Move north $1.8'$ | $\pm 13.4'$ |
| Mean position angle | Add 0.2° | $\pm\sim 81^{\circ\circ}/(Mean\ Sep'')$ |
| Mean separation | Add $9.7''$ | $\pm 0.09 x Mean\ Sep''$ |
| Primary magnitude | No correction | ±0.9 mag |
| Secondary magnitude | No correction | ±1.4 mag |

arcminute. Both have large uncertainites of $35^s$ and $371''$ or $6.2'$, respectively.

We recommend corrections to the right ascensions and declinations from the *Dunlop Reflector*. Right ascension should be increased on average by $6^s$ and the declinations should be moved north by $1.8'$. Again, both have large uncertainties of $70^s$ and $13.4'$, respectively.

The *Mean PA* have biases of $+1.1°$ and $-0.2°$ for the *Banks Refractor* and the *Dunlop Reflector*, respectively. However, the uncertainties vary such that, as might be expected, the *Mean PA* has an increasing uncertainty with decreasing *Mean Sep*. This is reflected in the power fit for the *Mean PA* uncertainties. The *Mean Sep* have corresponding biases of $-1.7''$ and $-9.7''$. Again, the Gaussian $1\sigma$ uncertainties do not adequately describe the *Mean Sep* uncertainites. A better model is an OLS linear fit where the uncertainites increase linearly as a fraction of the *Sep*.

With respect to Dunlop's magnitude estimates, we recommend no correction to them as they are given in whole magnitudes (except for the occasional half magnitude) and the biases are less than about a third of a magnitude. However, the uncertainties are significant.

### 4.8 A final note on the typographical errors

During the course of our study we uncovered a number of likely typographical errors in the published *Dunlop Catalogue*. These are found in Nos. 34∗, 37, 59, 61, 70∗, 75, 76∗, 78∗, 92∗, 97, 101, 105∗, 109∗, 116∗, 118, 127∗, 163∗, 176∗, 231∗, 232∗, and 242∗, and probably account for the outlier status of many of these. We were deliberately cautious in assigning typographical errors and so there are likely to be more.

How likely are such errors? Cozens (2008) detected a number of transcription errors in Dunlop's catalogue of southern nebulae (Dunlop 1828). A few decades later, Henry Chamberlain Russell, the Director of the Sydney Observatory, Australia (1870–1904) responded to Herschel's claims against the *Dunlop Catalogue* (Section 1) by pointing out that '[T]here are a good many very stupid mistakes in Herschel's own Catalogue' (Service 1890; Saunders 2004; Cozens et al. 2010), and that '[T]here are many stars in the Cape list that cannot be found' (Russell 1882). It would appear then, that meticulous proof reading was not always of a high standard at the time of Dunlop and Herschel.

## 5 CONCLUSIONS

We have drawn attention to and described, as well as corrected and estimated, the uncertainties of the measures in the first published catalogue of southern double stars, published by James Dunlop (Dunlop 1829).

We have identified a major source of the criticism of the *Dunlop Catalogue* (see Section 1) as errors in the quadrant designation of the secondary star. In Section 4.5, we have shown that 31 double stars in the *Dunlop Catalogue* contain quadrant errors. These have been rectified for individual double stars in Appendix A and in our revised machine readable version of the *Dunlop Catalogue* (see Section 5, Data Availability). The *Mean separations* were also far from consistent in quality. We have also highlighted that in this catalogue there are missing or incomplete data, some large uncertainties, subjective comments on some double stars, and even the deliberate (No. 3) inclusion of a supposedly single star.

Despite the acknowledged shortcomings of this catalogue, there can be no question that Dunlop's publication of the **first dedicated** catalogue of southern double stars is a major achievement and should be recognized as such. It represents the earliest astrometric and visual magnitude estimates of over 200 double stars in the Southern hemisphere. Measures associated with the double stars listed in Table C1 may be used for long period baseline astrometry. Other measures from the *Dunlop Catalogue* that do not constitute *1st outliers* or *2nd outliers* may also be used provided their uncertainties are taken into account.

## ACKNOWLEDGEMENTS

We undertook this study out of respect for the pioneering work of our (albeit adopted) Australian pioneer scientist, James Dunlop. It is hoped that this study will lead to an improved recognition of his work, and that of Sir Thomas Makdougall Brisbane, Carl Rümker and the Parramatta Observatory. We acknowledge here previous work on old *single* star catalogues, especially that of Verbunt & van Gent (2010b), Verbunt & van Gent (2010a), Verbunt & van Gent (2011), Verbunt & van Gent (2012). Despite an extensive search, we are unaware of any other similar study on old *double* star catalogues. We also thank Professor Nick Lomb (Adjunct Professor, University of Southern Queensland) and Professor Tim Napier-Munn (Emeritus Professor, University of Queensland) and Allan Ernest (Adjunct Professor Charles Sturt University) for their suggestions early in the project. The authors also thank personal communications from Andrew James and Glen Cozens, and recognise the quality historic research being undertaken by both, and the web site of Andrew James (southastrodel.com). This research has made use of: NASA's Astrophysics Data System; the SIMBAD database, operated at CDS, Strasbourg, France; and the *Aladin sky atlas* developed at CDS, Strasbourg Observatory, France. The authors also wish to acknowledge and thank the anonymous reviewer for their impartial and thorough review and who supplied many helpful and insightful suggestions, all of which we have endeavoured to incorporate into the present paper.

## DATA AVAILABILITY

Machine-readable data compiled by the first author is available online *here* as one file, but can be divided into three sections:

(i) The *Dunlop Catalogue* reproduced in digital form (columns 1–16).

(ii) Cross-matched identifications of the primary and secondary with: the identifier from the WDS; the discoverer code from the

WDS; SIMBAD, ASCC-2.5 V3, and *Gaia DR2* identifiers (columns 17–24).

(iii) Data generated from this paper (columns 25–33).

## REFERENCES


Andrews J. J., Chanamé J., Agüeros M. A., 2017, MNRAS, 472, 675

Ashbrook J., 1984, in Robinson L. J., Gingerich O., eds, The Astronomical Scrapbook: Skywatchers, Pioneers and Seekers in Astronomy. Cambridge Univ. Press, Cambridge, UK, p. 411

Barker G., 2008, Technical report, Parramatta Observatory Instruments. Powerhouse Museum, Sydney

Bhathal R. S., 2012, J. Proc. R. Soc. New South Wales, 145, 111

Bhathal R. S., White G. L., 1991, Under the Southern Cross: a brief history of astronomy in Australia. Kangaroo Press, Kenthurst, Australia, p. 96

Bickford A., 2011, Technical report, Volume 1-2 FINAL, Parramatta Park Trust: Archaeological Investigation of the Parramatta Observatory Site. Parramatta Park Trust, Leichhardt, NSW

Bonnarel F. et al., 2000, A&AS, 143, 33

Carrasco J. M., 2020 Photometric Relationships with Other Photometric Systems. European Space Agency, Paris, France https://gea.esac.esa.int/archive/documentation/GDR2/Data_processing/chap_cu5pho/sec_cu5pho_calibr/ssec_cu5pho_PhotTransf.html

Chanamé J., 2007, in Hartkopf W. I., Harmanec P., Guinan E. F., eds, IAU Symp Vol. 240, Binary Stars as Critical Tools and Tests in Contemporary Astrophysics. Kluwer, Dordrecht, p. 316

Cozens G. J., 2008, PhD thesis, Townsville, Qld, http://eprints.jcu.edu.au/24051/

Cozens G., White G. L., 2001, S&T, 101, 112

Cozens G. J., Walsh A., Orchiston W., 2010, J. Astron. Hist. Heritage, 13, 59

Duchêne G., Kraus A., 2013, ARA&A, 51, 269

Dunlop J., 1828, R. Soc. Lond. Phil. Transact. (Ser. I), 118, 113

Dunlop J., 1829, MNRAS, 3, 257

Eckardt M. C., Humphrey J., 2017, Astronomical Almanac for the Year 2018. U.S. Government Publishing Office, Washington, DC

European Space Agency, 2018, Gaia Data Release 2 (GAIA DR2). European Space Agency, Paris, France, https://www.cosmos.esa.int/web/gaia/dr2

European Space Agency, 2021, Gaia Early Data Release 3 (Gaia EDR3). European Space Agency, Paris, France, https://www.cosmos.esa.int/web/gaia/earlydr3

Gaia Collaboration, 2018, A&A, 616, A1

Grosser M., 1979, The Discovery of Neptune, 2nd edn. Dover Publications, New York

Guinan E. F., Harmanec P., Hartkopf W. I., 2007, in Hartkopf W. I., Guinan E. F., Harmanec P., eds, Proc. IAU Symp. Vol. 240, Binary Stars as Critical Tools and Tests in Contemporary Astrophysics. Kluwer, Dordrecht, p. 5

Haynes R., Haynes R., Malin D., McGee R., 1996, Explorers of the Southern Sky: A History of Australian Astronomy. University Press, Cambridge

Herschel J. F. W., 1828, MNRAS, 1, 60

Herschel J. F. W., 1847, Results of Astronomical Observations made During the Years 1834, 5, 6, 7, 8, at the Cape of Good Hope; being the Completion of a Telescopic Survey of the Whole Surface of the Visible Heavens, Commenced in 1825. Smith, Elder & Co., London

Høg E., 2017, preprint (arXiv:1707.01020)

Igoshev A. P., Perets H. B., 2019, MNRAS, 486, 4098

Kharchenko N. V., Roeser S., 2001, Kinematika i Fizika Nebesnykh Tel, 17, 409

Lacaille N. L., 1763, Coelum australe stelliferum.... Hipp. Lud. Guerin and Lud. Fr., Delatour, Paris

Letchford R., White G., Ernest A., 2019a, J. Double Star Obs., 15, 350

Letchford R., White G., Ernest A., 2019b, J. Double Star Ob., 15, 361

Letchford R., White G., Ernest A., 2019c, J. Double Star Obs., 15, 378

Letchford R., White G., Ernest A., 2019d, J. Double Star Obs., 15, 394

Lieske J. H., Lederle T., Fricke W., Morando B., 1977, A&A, 58, 1

Lindegren L. et al., 2021, A&A, 649, A2

Lomb N., 2004, Hist. Rec. Aust. Sci., 15, 211

Mason B. D., Wycoff G. L., Hartkopf W. I., Douglass G. G., Worley C. E., 2001, AJ, 122, 3466

Matson R. A., Williams S. J., Hartkopf W. I., Mason B. D., 2020, Sixth Catalog of Orbits of Visual Binary Stars. United States Naval Observatory, Washington, DC

Milone E. F. F., Sterken C., 2011, Astrophysics and Space Science Library, Vol. 373, Astronomical Photometry: Past, Present, and Future. Springer-Verlag, Berlin

Moe M., 2019, Statistics of Binary and Multiple Stars, Cambridge Astrophysics. Cambridge Univ. Press, Cambridge, UK, p. 12

Richardson W., Brisbane T. M., 1835, A Catalogue of 7385 Stars Chiefly in the Southern Hemisphere, prepared from observations made in the years 1822, 1823, 1824, 1825, and 1826, at the observatory at Paramatta, New South Wales. William Clowes and Sons, London

Russell H. C., 1882, Results of double star measures made at the Sydney Observatory, New South Wales, 1871-1881. Thomas Richards, Government Printer, Sydney

Rutledge S., 2009, J. Proc. R. Soc. New South Wales, 142, 17

Saunders S. D., 2004, Hist. Rec. Aust. Sci., 15, 177

Schaffer S., 2010, in Aubin D., Bigg C., Sibum H. O., eds, The Heavens on Earth: Observatories and Astronomy in Nineteenth-century Science and Culture. Duke Univ. Press, Durham, NC, p. 118

Service J., 1890, in Thir Notandums: Being the Literary Recreations of Laird Canticarl of Mongrynen of Kittle Memory. Young J. Pentland; Angus & Robertson, Edinburgh, Sydney, p. 128

Verbunt F., van Gent R. H., 2010a, A&A, 516, A29

Verbunt F., van Gent R. H., 2010b, A&A, 516, A28

Verbunt F., van Gent R. H., 2011, A&A, 530, A93

Verbunt F., van Gent R. H., 2012, A&A, 544, A31

Wenger M. et al., 2000, A&AS, 143, 9

White G., Letchford R., Ernest A., 2018, J. Double Star Obs., 14, 432

Wood H. W., 1966, in Pike D., ed., Australian Dictionary of Biography: Volume I 1788-1850 A-H. Melbourne Univ. Press, Melbourne, VIC, p. 338


## SUPPORTING INFORMATION

Supplementary data are available at *MNRAS* online.

**Supplementary material (online).xlsx**

Please note: Oxford University Press is not responsible for the content or functionality of any supporting materials supplied by the authors. Any queries (other than missing material) should be directed to the corresponding author for the article.

## APPENDIX A: SHORT NOTES ON SOME INDIVIDUAL DOUBLE STARS

The following are short notes on some of the Dunlop double stars.

**No. 1* (LCL 119AC).** Quadrant corrected from np to sf. Dunlop uncorrected *Mean PA* is ∼352.5°. Dunlop corrected *Mean PA* is ∼172.5°. Precessed *Gaia DR2* PA is ∼177.4°.

**No. 2* (DUN 2).** Grade 5 orbit in Matson et al. 2020, with a period of 5800 centuries. A grade 5 orbit is classified as 'Indeterminate', meaning that 'the elements may not even be approximately correct'.

**No. 5* (DUN 5).** Quadrant corrected from nf to sp. Also $|\Delta \mathrm{Sep}| >$ *Mean Sep*. Dunlop uncorrected *Mean PA* is ∼16.9°. Dunlop corrected *Mean PA* is ∼196.9°. Precessed *Gaia DR2* PA is ∼223.6°. Dunlop's PA in the WDS is 343.1° (np Quadrant). *Mean Sep* = 2.5 arcsec, *Gaia DR2* precessed separation is ∼14.6 arcsec. Explanation for both is that this is a known binary with a grade 4 orbit in Matson et al. 2020, with a period of 493.3 yr. A grade 4 orbit is classified as 'Preliminary', meaning that 'individual [orbital] elements entitled to little weight, and may be subject to substantial revisions'.

**No. 6 (DUN 6AB).** *2nd outlier* in vB – vA. Component A is $\phi$ Eri and component B is CD-52 465. Dunlop's vA = 4 and vB = 12. *Gaia DR2* calculated vA is ∼5.31 and calculated vB is ∼9.15.

**No. 9∗ (PZ 2).** *2nd outlier* in vB – vA. Component A is $\theta$01 Eri and component B is $\theta$02 Eri. Dunlop's vA = 4 and vB = 6. *Gaia DR2* calculated vA is ∼5.40 and vB is ∼4.33. Both are high proper motion stars according to SIMBAD.

**No. 12 (DUN 12A,BC).** *2nd outlier* in vB – vA with respect to the whole catalogue. Component A is HD 20586 (high proper motion star) and component B is CCDM J03152−6427BC (double star). Dunlop's VA = 6 and vB = 12. *Gaia DR2* calculated vA is ∼6.56 and calculated vB is ∼9.15.

**No. 13 (unidentified).** Incorrectly identified in Letchford et al. (2019b,c) as being from the *Banks Refractor*. Position and magnitudes come from the *Dunlop Reflector*.

**No. 14 (DUN 14).** Quadrant corrected from np to sp. Dunlop uncorrected *Mean PA* is ∼280.0°. Dunlop corrected *Mean PA* is ∼260.0°. Precessed *Gaia DR2* PA is ∼269.9°.

**No. 15∗ (DUN 15).** Also |ΔSep| > *Mean Sep*. *Mean Sep* = 4 arcsec, *Gaia DR2* precessed separation is ∼10.1 arcsec.

**No. 23 (DUN 23).** Quadrant corrected from np to nf. *2nd outlier* in *Mean PA* with respect to the whole catalogue. Dunlop uncorrected *Mean PA* is ∼329.0°. Dunlop corrected *Mean PA* is ∼31.0°. Precessed *Gaia DR2* PA is ∼72.1°. However, this is a known binary with a grade 4 orbit in Matson et al. 2020 (refer to No 5∗), with a period of 552.8417 yr. Dunlop's PA in the WDS is 329° (np Quadrant).

**No. 25 (JSP 96).** *1st outlier* in vA. Component A is CD-32 2930A. Dunlop's vA = 6, *Gaia DR2* calculated vA ∼ 9.62. Not noted as a variable in SIMBAD.

**No. 26∗ (DUN 26AB).** Quadrant corrected from nf to sf. Dunlop uncorrected *Mean PA* is ∼67.8°. Dunlop corrected *Mean PA* is ∼112.2°. Precessed *Gaia DR2* PA is ∼111.6°.

**No. 27∗ (DUN 27AB).** Missing Quadrant in the *Dunlop Catalogue* and therefore no *Mean PA*. The *Gaia DR2* Quadrant is sp. Thus Dunlop's corrected *Mean PA* is 223.3°. Precessed *Gaia DR2* PA is ∼223.6°.

**No. 29∗ (DUN 29).** Missing Quadrant in the *Dunlop Catalogue* and therefore no *Mean PA*. The *Gaia DR2* Quadrant is sf. Thus Dunlop's corrected *Mean PA* is 109.1°. Precessed *Gaia DR2* PA is ∼109.9°.

**No. 32∗ (DUN 32).** *1st outlier* in corrected PA. Component A is HD 48543A, component B is HD 48543B. Dunlop's *Mean PA* (did not need Quadrant correction) is ∼349.3°, *Gaia DR2* precessed PA is ∼277.2°.

**No. 34∗ (DUN 34).** *1st outlier* in *Angle of Pos* (column 5). *Angle of Pos* is 85° 14 arcmin. The angle of position calculated from the *Distance* (column 7) and Δ *Declin* (column 9) is ∼57.5°. Dunlop's *Distance* (column 7) is an *1st outlier*. *Distance* is 2 arcmin 10.15″ (130.15″). The *Mean Sep* is 1′ 37.″4 (97.″4), where the other measure of separation can be calculated from the *Angle of Pos* and Δ *Declin* and is ∼1′ 4.″6 (64.″6). Perhaps a typographical error (2 arcmin instead of 1 arcmin).

**No. 36∗ (H 5 108A,BC).** Missing Quadrant in the *Dunlop Catalogue* and therefore no *Mean PA*. The *Gaia DR2* Quadrant is nf. Thus Dunlop's corrected *Mean PA* is 69.4°. Precessed *Gaia DR2* PA is ∼64.4°.

**No. 37 (two).** *1st outlier* in DE. Component A is HD 53142. Dunlop's DE is ∼ −51° 9 arcmin. Not noted in SIMBAD as a high proper motion star. This is the same primary as BRI 1456 in the *Brisbane catalogue* (Richardson & Brisbane 1835). There the declination is S.P.D. (South Polar Distance) 39° 46′ 55.″6 or DE ∼ −50° 13′. Could be the result of a typographical error, where −51° should be −50°.

**No. 39∗ (DUN 39).** *1st outlier* in corrected PA. Component A is HD 53921A, component B is HD 53921B. Dunlop's *Mean PA* (did not need Quadrant correction) is ∼11.23°, *Gaia DR2* precessed PA is ∼77.7°. Curiously, the *Angle of Pos* is given as 78° 48′ (78.8°), close to the *Gaia DR2* precessed PA, yet both Dunlop and *Gaia DR2* agree that the Quadrant is nf (north following).

**No. 44 (RMK 6AB).** The name of the double in the WDS is RMK 6AB, with a grade 5 orbit in Matson et al. 2020 (refer to No. 2∗), with a period of 10 000 centuries. The discoverer code 'RMK' means that the WDS attributes the discovery of the double to Carl Rümker of the Parramatta Observatory, and not to James Dunlop. Incorrectly labelled as 'unidentified' in Letchford et al. (2019b, c). The WDS system identifier is 07204-5219.

**No. 45∗ (DUN 45).** Quadrant corrected from nf to sf. Dunlop uncorrected *Mean PA* is ∼14.2°. Dunlop corrected *Mean PA* is ∼165.8°. Precessed *Gaia DR2* PA is ∼155.4°.

**No. 51 (DUN 51).** *1st outlier* in vB. *2nd outlier* in vB – vA. Component A is sig Pup and component B is sig Pup B. Dunlop's vA = 4 and vB = 14. *Gaia DR2* calculated vA is ∼3.06 and calculated vB is ∼8.77. Both noted in SIMBAD as high proper motion stars, but not as variables. *Gaia DR2* precessed Quadrant is nf. Dunlop PA remains 90°.

**No. 52∗ (H N 19).** Missing Quadrant in the *Dunlop Catalogue* and therefore no *Mean PA*. The *Gaia DR2* Quadrant is sf. Thus Dunlop's corrected *Mean PA* is 105.4°. Precessed *Gaia DR2* PA is ∼105.3°.

**No. 53∗ (H 3 27AB).** *1st outlier* in corrected PA. Component A is $\kappa$02Pup, component B is $\kappa$01Pup. Dunlop's *Mean PA* (did not need Quadrant correction) is ∼315.8°, *Gaia DR2* precessed PA is ∼326.8°.

**No. 54 (one).** Incorrectly identified in Letchford et al. (2019b, c) as being from the *Banks Refractor*. Measures come from the *Dunlop Reflector*.

**No. 56∗ (DUN 56).** *1st outlier* in DE. Component A is HD 63425. Dunlop's DE is −38° 4′, *Gaia DR2* precessed is ∼-41° 04′ 45.″71. Difference ∼ + 2.9°. In the WDS as DUN 56. Not noted as a high proper motion star in SIMBAD.

**No. 59 (DUN 59).** *2nd outlier* in RA. Quadrant corrected from sf to nf. Component A is HD 66005. Dunlop's AR (RA) = $7^h\ 50^m\ 30^s$, *Gaia DR2* precessed RA is $\sim 7^h\ 54^m\ 20^s$. Difference is ∼−0.6° (−230 ). Not noted by SIMBAD as a high proper motion star. May be a typographical error, $50^m$ should be $54^m$. Dunlop uncorrected *Mean PA* is ∼131.0°. Dunlop corrected *Mean PA* is ∼49.0°. Precessed *Gaia DR2* PA is ∼45.91°.

**No. 61 (DUN 61).** *2nd outlier* in DE. Component A is HD 67409. Dunlop's DE is −28° 39′ and the precessed *Gaia DR2* DE is ∼ −26° 37′ 9″. Probably a typographical error. −28° should be −26°. Not noted by SIMBAD as a high proper motion star.

**No. 64∗ (DUN 65AC) and 65∗ (DUN 65AB).** A group of stars associated with $\gamma$ Argus, now $\gamma$ Velorum. The identification of these pairs is made difficult by the fact that Dunlop recorded both as having the same right ascension and declination. We base our identification on his magnitude estimates: 2.3 and 8 for DUN 64∗ and 2.3 and 6 for DUN 65∗. Thus: DUN 64 AC and DUN 65 AB are the respective discoverer and component codes.

**No. 67 (DUN 67).** Missing Quadrant in the *Dunlop Catalogue* and therefore no *Mean PA*. The *Gaia DR2* Quadrant is sf. Thus Dunlop's corrected *Mean PA* is 168.6°. Precessed *Gaia DR2* PA is ∼175.3°.

**No. 68 (DUN 68).** Missing Quadrant in the *Dunlop Catalogue* and therefore no *Mean PA*. The *Gaia DR2* Quadrant is nf. Thus Dunlop's corrected *Mean PA* is ∼21.7°. Precessed *Gaia DR2* PA is ∼24.6°.

**No. 70∗ (DUN 70).** *2nd outlier* in corrected PA (did not need Quadrant correction). Component A is HD 72127A and component B is HD 72127B. Dunlop's *Mean PA* is 320.3° and the precessed *Gaia DR2* PA is ∼354.8°. Neither components are high proper motion stars according to SIMBAD. Dunlop's *Mean PA* could only be calculated one way, via *Angle of Pos* (50° 18′) and *Quadrant.* (np). Perhaps Dunlop's 50° is a typographical error and should be 54°.

**No. 72 (DUN 72A,BC).** Quadrant corrected from nf to np. Dunlop uncorrected *Mean PA* is ∼5.2°. Dunlop corrected *Mean PA* is ∼354.8°. Precessed *Gaia DR2* PA is ∼355.3°.

**No. 75 (RMK 10).** *1st outlier* in RA. *1st outlier* in DE. Component A is HD 80807. Dunlop's RA and DE are $9^h\ 4^m\ 19^s$ and −57° 30′, respectively. *Gaia DR2* precessed RA and DE are $09^h\ 15^m\ 49\overset{s}{.}25$ and −69° 04′ 11″.93, respectively. Not noted as a high proper motion star. There may be a typographical error in Dunlop's RA minutes (should be $14^m$ instead of $4^m$), and there may be a typographical error in Dunlop's DE degrees (should be −67° instead of −57°).

**No. 76∗ (DUN 76AC).** Dunlop's Δ*AR* (6.265$^s$, or 66.740″, column 8) is larger than his *Distance* (61.40″). Probably a typographical error.

**No. 78∗ (DUN 78).** *1st outlier* in Δ*AR* (column 8). *2nd outlier* in corrected PA (needed Quadrant correction). *2nd outlier* in Sep. Δ*AR* is 0.5$^s$. Δ*AR* calculated via the *Mean PA*, *Mean Sep* and declination (column 4) is ∼4.8$^s$. Dunlop's uncorrected *Mean PA* is 75.3° and the precessed *Gaia DR2* PA is ∼212.7°. Dunlop's *Quadrant.* was corrected from nf to sp. Dunlop's corrected *Mean PA* was 255.3°, or an *Angle of Pos* of 14° 42′. Dunlop's original *Angle of Pos* of 1° 7′ probably should be 14° 7′, a likely typographical error. Dunlop's *Mean Sep* is ∼63.9″. *Gaia DR2* precessed Sep is ∼8.43″. Perhaps Dunlop's *Mean Sep* should be ∼6.39″.

**No. 79∗ (DUN 79).** *1st outlier* in Sep. Also |ΔSep| > *Mean Sep*. Component A is HD 82965, component B is HD 82986. Dunlop's *Mean Sep* is ∼14.8″. *Gaia DR2* precessed Sep. is ∼130.40″. According to SIMBAD, component B is a high proper motion star. Note that Dunlop's *Mean PA* is ∼48.7°, but the calculated *Gaia DR2* precessed PA is ∼30.00°.

**No. 80 (DUN 80AB).** Also |ΔSep| > *Mean Sep*. *Mean Sep* = 3″, *Gaia DR2* precessed Sep ∼ 18.4″. Perhaps Dunlop's should have been 13″.

**No. 84∗ (HJ 4282).** Also |ΔSep| > *Mean Sep*. *Mean Sep* = 2.0″, and *Gaia DR2* precessed separation is ∼45.8″. Component A is HD 87364, component B is HD 298817. There must be an error in Dunlop's Distance (column 7). Perhaps it should read 42″.

**No. 87∗ (DUN 87).** Quadrant corrected from sp to np. Dunlop uncorrected *Mean PA* is ∼203.6°. Dunlop corrected *Mean PA* is ∼336.4°. Precessed *Gaia DR2* PA is ∼331.9°.

**No. 88∗ (PZ 3).** Missing Quadrant in the *Dunlop Catalogue* and therefore no *Mean PA*. The *Gaia DR2* Quadrant is sp. Thus Dunlop's corrected *Mean PA* is ∼221.1°. Precessed *Gaia DR2* PA is ∼217.7°.

**No. 89∗ (DUN 89AB).** Missing Quadrant in the *Dunlop Catalogue* and therefore no *Mean PA*. The *Gaia DR2* Quadrant is nf. Thus Dunlop's corrected *Mean PA* is ∼34.0°. Precessed *Gaia DR2* PA is ∼29.6°.

**No. 90 (unidentified).** The only WDS double star within 1° of Dunlop's position precessed to 2000.0 is No. 89∗. It is possible that No. 90 = No. 89∗, especially considering they were both discovered using different telescopes. At the present, we prefer to continue to classify No. 90 as unidentified.

**No. 91∗ (DUN 91).** Quadrant corrected from sp to nf. Also |ΔSep| > *Mean Sep*. Dunlop uncorrected *Mean PA* is ∼228.8°. Dunlop corrected *Mean PA* is ∼48.8°. Precessed *Gaia DR2* PA is ∼59.0°. *Mean Sep* = 3.69″ and precessed *Gaia DR2* Sep is ∼9.94″.

**No. 92∗ (one).** *1st outlier* in RA. *2nd outlier* in DE. *1st outlier* in vA. Only one star was detected in the approximate Dunlop position, namely p Car (HD 91465). Dunlop's vA = 7. The nearest suitable double star to the forward precessed Dunlop position in the WDS is DUN 87 at a distance of ∼3500″. *Gaia DR2* calculated vA ∼3.23. No. 92∗ could be the pair HD 91270 (A) and HD 91269 (B), which are in the WDS as 10307-6121, however, they are ∼22.5 arcmin (1350″) from p Car. Dunlop's Sep bias from the *Banks Refractor* is −2.4″ and his Sep uncertainty just ±27.5″. Dunlop's RA = $10^h\ 29^m\ 33^s$, *Gaia DR2* precessed RA is $\sim 10^h\ 25^m\ 53\overset{s}{.}74$. Dunlop's DE is −60° 29′ and the precessed *Gaia DR2* DE is ∼ −60° 47′ 25″. Difference is ∼ +18.4′. Could be typographical error, 49 arcmin instead of 29 arcmin.

**No. 96 (one).** Incorrectly identified in Letchford et al. (2019b,c) as being from the *Banks Refractor*. Measures come from the *Dunlop Reflector*. The nearest suitable double star in the WDS is HJ 4366 at a distance of ∼3440″. Both the forward precessed Dunlop position and HJ 4366 are in dense star fields, making it difficult to discern what Dunlop may have meant.

**No. 97 (DUN 97AB).** Also |ΔSep| > *Mean Sep*. *Mean Sep* = 3″, *Gaia DR2* precessed Sep ∼ 12.5″. Perhaps there is a typographical error here and Dunlop's *Distance* (column 7) should have been 13″ instead of 3″.

**No. 98∗ (DUN 98AH).** *1st outlier* in vA. *1st outlier* in vB - vA. Component A is $\eta$ Car, component B is HD 303308. Dunlop's vA = 3 and vB = 10. *Gaia DR2* calculated vA is ∼8.22 and calculated vB ∼8.06. According to SIMBAD component A is an emission line star, and therefore possibly variable.

**No. 99∗ (DUN 99AB).** Quadrant corrected from sp to nf. Dunlop uncorrected *Mean PA* is ∼253.6°. Dunlop corrected *Mean PA* is ∼73.6°. Precessed *Gaia DR2* PA is ∼74.4°.

**No. 101 (HJ 4378).** *1st outlier* in corrected PA. Also |ΔSep| > *Mean Sep*. Component A is HD 94173, and component B is CPD-59 2783. Dunlop's *Mean PA* = 276°, the PA from precessed *Gaia DR2* is ∼343°.8. Both in same Quadrant, so No. 101 was not Quadrant corrected. May be a typographical error. Dunlop's *Angle of Pos* is 6° 0′ and perhaps should have been 76° 0′. Neither are noted as high proper motion stars in SIMBAD. *Mean Sep* = 10″, *Gaia DR2* precessed Sep ∼ 30.8″.

**No. 102∗ (DUN 102AB).** *1st outlier* in Sep. Also |ΔSep| > *Mean Sep*. Component A is u Car, component B is HD 94491. Mean Dunlop Sep is ∼55.6″, *Gaia DR2* precessed Sep is ∼147.25″. Note component C is CPD-58 2836, which together with u Car (HD 95109) form No. 103∗. Dunlop's *Mean Sep* for AC is ∼57.5″. Our identification is based on the fact that Dunlop identified 102∗ as AB and 103∗ as AC, relying on his apparent visual magnitude estimates: vA = 5, vB = 7, and vC = 8.

**No. 105∗ (DUN 105).** *1st outlier* in RA. *2nd outlier* in DE. Quadrant corrected from sf to sp. In the WDS as DUN 105. Component A is HD 96264. Dunlop's right ascension = $10^h\ 55^m\ 21^s$, *Gaia DR2* precessed RA is $\sim 10^h\ 57^m\ 47\overset{s}{.}71$. Difference is $-146.7^s$ (−1096.6″). Dunlop's declination is −60° 53′ and the *Gaia DR2* precessed DE is −60° 6′ 43″. Right ascension and declination could be a typographical errors, right ascension should be 57′ instead of 55′, declination should be 3′ instead of 53′. Not noted by SIMBAD as a high proper motion star. Dunlop uncorrected *Mean PA* is ∼149.9°. Dunlop corrected *Mean PA* is ∼210.1°. Precessed *Gaia DR2* PA is ∼221.0°.

**No. 109● (BSO 6)**. *1st outlier* in Sep. *1st outlier* in corrected PA. Component A is HD 99803, component B is CD-41 6565B (HIP 56001). Dunlop's *Mean Sep* is ∼151.0″ and the *Gaia DR2* precessed Sep is ∼13.51″. Dunlop's *Mean Sep* is the average of two different values: 2′ 49.3″ (169.3″) given in column 5 (distance) and column 9 (Δ*Declin*) value of 42.46″ divided by the sine of the *Angle of Pos* (column 5) which yields 132.78″. Thus any typographical errors would require errors in more than one column value. Also Dunlop's *Mean PA* (did not need Quadrant correction) is ∼106.6°, *Gaia DR2* precessed PA is ∼171.0°. There is no star with the right magnitude at 169″ from the primary.

**No. 111● (H 3 96)**. Quadrant corrected from nf to sp. Dunlop uncorrected *Mean PA* is ∼23.9°. Dunlop corrected *Mean PA* is ∼203.9°. Precessed *Gaia DR2* PA is ∼210.2°.

**No. 114 (DUN 114)**. Also |ΔSep| > *Mean Sep*. *Mean Sep* = 3″, *Gaia DR2* precessed Sep ∼ 16.9″. Perhaps Dunlop's should have been 13″.

**No. 116● (DUN 116AB)**. Dunlop's Δ*AR* (1.6$^s$, or 20.50″, column 8) is larger than his *Distance* (15.2″). Probably a typographical error. ASCC and *Gaia DR2* source identifiers of components in Letchford et al. (2019b,c) swapped.

**No. 118 (HJ 4500)**. Incorrectly identified in Letchford et al. (2019b,c) as 'two'. Here we identify it as HJ 4500. *2nd outlier* in RA. Component A is HD 106132. Dunlop's RA is 12$^h$ 02$^m$ 00$^s$, *Gaia DR2* precessed RA is 12$^h$ 16$^m$ 56$^s$. Probably a typographical error. Dunlop's 02$^m$ should be 20$^m$.

**No. 122● (DUN 252AC) and 123● (DUN 252AB)**. Listed in the WDS as DUN 252AC and DUN 252AB, respectively, i.e. $\alpha$01 Cru ($\alpha$ Crucis), both with WDS 12266-6306.

**No. 127● (DUN 127)**. The *Dunlop Catalogue* Δ*AR* (1.17$^s$, or 10.08″, column 8) is larger than its *Distance* of 10″. Probably a typographical error.

**No. 128 (DUN 128)**. *1st outlier* in vB. *1st outlier* in vB – vA with respect to the whole catalogue. Component A is $\xi$02 Cen (spectroscopic binary) and component B is V1261 Cen (rotationally variable star). Dunlop's vA = 5 and vB = 14. *Gaia DR2* calculated vA is ∼4.27 and calculated vB is ∼9.35.

**No. 136 (unidentified)**. Incorrectly identified in Letchford et al. (2019b,c) as the double star SEE 179. SEE 179 or d Cen had a separation at epoch 2017 of 0.2″, well below Dunlop's resolution and that of *Gaia DR2*.

**No. 137● (DUN 137)**. Quadrant corrected from nf to np. Dunlop uncorrected *Mean PA* is ∼13.9°. Dunlop corrected *Mean PA* is ∼346.1°. Precessed *Gaia DR2* PA is ∼357.8°.

**No. 140 (DUN 140)**. *Gaia DR2* precessed Quadrant is nf. Dunlop PA remains 90°.

**No. 141● (DUN 141)**. Quadrant corrected from sp to sf. Dunlop uncorrected *Mean PA* is ∼191.6°. Dunlop corrected *Mean PA* is ∼168.4°. Precessed *Gaia DR2* PA is ∼164.3°.

**No. 143● (DUN 143)**. Incorrectly identified in Letchford et al. (2019b,c) as being from the *Dunlop Reflector*. Measures come from the *Banks Refractor*.

**No. 145 (DUN 145)**. Also |ΔSep| > *Mean Sep*. *Mean Sep* = 10″, *Gaia DR2* precessed Sep ∼ 22.1″. Perhaps Dunlop's should have been 20″.

**No. 147 (RMK 18)**. *1st outlier* in corrected PA. Dunlop's *Mean PA* did not need Quadrant correction, and is ∼322.5°. *Gaia DR2* precessed PA is ∼289.7°.

**No. 151 (DUN 151AB)**. *1st outlier* in corrected PA. Component A is HD 121504, component B is CPD-55 5793. Dunlop's *Mean PA* = 0°, as only the Angle of Pos. (90° 0′) and Quadrant (n) columns have data. *Gaia DR2* precessed PA is ∼301.14° (Quadrant np). ΔPA = 360 − 301.1° ≈ +58.9°. According to SIMBAD, HD 121504 is a high proper motion star. Dunlop PA remains 0°.

**No. 157 (HJ 4651)**. Also |ΔSep| > *Mean Sep*. *Mean Sep* = 13″, *Gaia DR2* precessed Sep ∼ 63.2″.

**No. 162 (DUN 162)**. *Gaia DR2* precessed Quadrant is sp. Dunlop PA remains 270°.

**No. 163● (DUN 163)**. *2nd outlier* in RA. Component A is HD 128291. Dunlop's RA = 14$^h$ 23$^m$ 52$^s$, *Gaia DR2* precessed RA is ∼14$^h$ 25$^m$ 50$^s$. Difference is ∼−0.3° (−120). Noted by SIMBAD as a high proper motion star. May be a typographical error, 23$^m$ should be 25$^m$.

**No. 164● (two)**. *1st outlier* in vA. *2nd outlier* in vB – vA. Component A is $\eta$ Cen, a Be star, component B is HD 127992. Dunlop's vA = 3 and vB = 9. *Gaia DR2* calculated vA is ∼6.29 (SIMBAD vA = 2.31) and calculated vB is ∼9.09 (SIMBAD vB = 9.19). Could be due to an error in *Gaia DR2* colours for this star.

**No. 165● (RHD 1AB)**. Discoverer code in the WDS is RHD 1AB ($\alpha$ Cen), with a grade 2 orbit in Matson et al. (2020), with a period of 79.91 yr. A grade 2 orbit is classified as 'Good', meaning 'most of a revolution, well observed, with sufficient curvature to give considerable confidence in the derived elements'.

**No. 166 (DUN 166AB)**. *1st outlier* in vB – vA. Dunlop's vA = 4 and vB = 12. Component A is $\alpha$ Cir A (Variable Star of $\alpha$2 CVn type) and component B is $\alpha$ Cir B. *Gaia DR2* calculated vA is ∼5.22 and calculated vB is ∼8.38.

**No. 167 (SKF 1973)**. Incorrectly identified in Letchford et al. (2019b,c) as 'two' stars not previously recorded in the WDS. It is 14410-3608 SKF 1973.

**No. 176● (DUN 176)**. Dunlop's Δ*AR* (7.385$^s$, or 69.04″, column 8) is larger than his *Distance* (68.79″). Probably a typographical error.

**No. 178● (DUN 178AC)**. Dunlop's Δ*AR* (column 8) is a *1st outlier*. Δ*AR* is 3.525$^s$. The calculated Δ*AR* [calculated via the *Mean PA*, *Mean Sep*, and declination (column 4)] is ∼7.1$^s$.

**No. 181 (DUN 181AB)**. Quadrant corrected from nf to np. *2nd outlier* in Quadrant corrected PA with respect to the whole catalogue. Also |ΔSep| > *Mean Sep*. Dunlop's uncorrected *Mean PA* = 65°. Dunlop's corrected PA = 295°. *Gaia DR2* precessed PA ∼347.5°. Perhaps Dunlop's *Angle of Pos* should be 75° 0′ and not 25° 0′. *Mean Sep* = 9″, *Gaia DR2* precessed Sep ∼ 29.2″.

**No. 183● (DUN 183AB)**. *2nd outlier* in Sep. Also |ΔSep| > *Mean Sep*. Component A is k Lup, and component B is HD 137059. Dunlop's Sep = 12″, the Sep from precessed *Gaia DR2* is ∼89.8″. There is a second Dunlop *Distance*, 15″ as Dunlop marked this as 'Three stars in a line'. Unable to explain discrepancy.

**No. 186 (DUN 186)**. Quadrant corrected from sf to np. Dunlop uncorrected *Mean PA* is ∼125.0°. Dunlop corrected *Mean PA* is ∼305.0°. Precessed *Gaia DR2* PA is ∼296.7°. ASCC and *Gaia DR2* source identifiers of components in Letchford et al. (2019b,c) swapped.

**No. 187 (DUN 187)**. Also |ΔSep| > *Mean Sep*. *Mean Sep* = 10″, *Gaia DR2* precessed Sep ∼ 33.7″.

**No. 188 (DUN 188)**. Quadrant corrected from sf to sp. Dunlop uncorrected *Mean PA* is ∼150°. Dunlop corrected *Mean PA* is ∼210.0°. Precessed *Gaia DR2* PA is ∼215.6°.

**No. 190 (DUN 190AB)**. Quadrant corrected from nf to sf. Also |ΔSep| > *Mean Sep*. Dunlop uncorrected *Mean PA* is ∼85.0°. Dunlop corrected *Mean PA* is ∼95.0°. Precessed *Gaia DR2* PA is ∼90.4°. *Mean Sep* = 3″, *Gaia DR2* precessed Sep ∼ 6.5″.

**No. 192 (DUN 192 AB,C).** Quadrant corrected from nf to sf. Dunlop uncorrected *Mean PA* is ∼50.0°. Dunlop corrected *Mean PA* is ∼130.0°. Precessed *Gaia DR2* PA is ∼145.9°.

**No. 194 (DUN 194AC).** Quadrant corrected from np to nf. Also |ΔSep| > *Mean Sep*. Dunlop uncorrected *Mean PA* is ∼317.0°. Dunlop corrected *Mean PA* is ∼43.0°. Precessed *Gaia DR2* PA is ∼49.1°. *Mean Sep* = 10″, *Gaia DR2* precessed Sep ∼ 45.2″.

**No. 195 (DUN 195AB).** Also |ΔSep| > *Mean Sep*. *Mean Sep* = 5″, *Gaia DR2* precessed Sep ∼ 11.8″.

**No. 197∗ (RMK 21AC).** *2nd outlier* in Sep. Also |ΔSep| > *Mean Sep*. Component A is $\eta$ Lup, and component B is CD-3810797B. Dunlop's *Mean Sep* ∼50.4″, and the precessed *Gaia DR2* Sep is ∼115.4″. Unable to explain discrepancy.

**No. 198 (two).** *Gaia DR2* precessed Quadrant is sp. Also |ΔSep| > *Mean Sep*. Dunlop *Mean PA* remains 180.0°. Precessed *Gaia DR2* PA is ∼192.0°. *Mean Sep* = 30″, *Gaia DR2* precessed Sep ∼ 81.3″.

**No. 199 (DUN 199AC).** Also |ΔSep| > *Mean Sep*. *Mean Sep* = 12″, *Gaia DR2* precessed Sep ∼ 43.6″.

**No. 200 (DUN 200).** Quadrant corrected from sf to sp. Also |ΔSep| > *Mean Sep*. Dunlop uncorrected *Mean PA* is ∼172.0°. Dunlop corrected *Mean PA* is ∼188.0°. Precessed *Gaia DR2* PA is ∼197.4°. *Mean Sep* = 17″, *Gaia DR2* precessed Sep ∼ 41.9″.

**No. 202 (DUN 202AC).** Also |ΔSep| > *Mean Sep*. *Mean Sep* = 26″, *Gaia DR2* precessed Sep ∼ 57.9″.

**No. 208 (one).** Nearest suitable double star from the forward precessed Dunlop position is DUN 211BC at a distance of ∼2930″.

**No. 209 (DUN 209AB).** Quadrant corrected from sp to sf. Dunlop uncorrected *Mean PA* is ∼210.0°. Dunlop corrected *Mean PA* is ∼150.0°. Precessed *Gaia DR2* PA is ∼146.4°.

**No. 211 (DUN 211BC).** Quadrant corrected from np to sp. Also |ΔSep| > *Mean Sep*. Dunlop uncorrected *Mean PA* is ∼330.0°. Dunlop corrected *Mean PA* is ∼210.0°. Precessed *Gaia DR2* PA is ∼194.2°. *Mean Sep* = 20″, *Gaia DR2* precessed Sep ∼ 45.1″.

**No. 212 (DUN 212AB).** Quadrant corrected from sp to np. Also |ΔSep| > *Mean Sep*. Dunlop uncorrected *Mean PA* is ∼228.0°. Dunlop corrected *Mean PA* is ∼312.0°. Precessed *Gaia DR2* PA is ∼286.4°. *Mean Sep* = 5″, *Gaia DR2* precessed Sep ∼ 16.2″. Perhaps Dunlop's Distance (column 7) should be 15″.

**No. 215 (DUN 215AB).** Also |ΔSep| > *Mean Sep*. *Mean Sep* = 15″, *Gaia DR2* precessed Sep ∼ 54.8″.

**No. 216∗ (DUN 216AC).** Quadrant corrected from nf to np. *2nd outlier* in Sep. Also |ΔSep| > *Mean Sep*. Dunlop uncorrected *Mean PA* is ∼30.0°. Dunlop corrected *Mean PA* is ∼330.0°. Precessed *Gaia DR2* PA is ∼313.3°. Dunlop's *Mean Sep* is ∼30.0″, the precessed *Gaia DR2* Sep is ∼103.3. Unable to explain discrepancy.

**No. 221 (DUN 211).** *Gaia DR2* precessed Quadrant is sf. Dunlop *Mean PA* remains 180.0°.

**No. 224 (DUN 224AC).** Quadrant corrected from sf to nf. Dunlop uncorrected *Mean PA* is ∼115.6°. Dunlop corrected *Mean PA* is ∼64.4°. Precessed *Gaia DR2* PA is ∼63.7°.

**No. 230 (DUN 230).** *1st outlier* in Sep. Component A is HD 192724A, component B is HD 192724B. Dunlop's Sep (by only one method) is ∼65.6″, *Gaia DR2* precessed Sep is ∼10.15″. Neither star is noted as a high proper motion star in SIMBAD. Unable to explain discrepancy.

**No. 231∗ (DUN 231).** *1st outlier* in RA. Component A is HD 195459. Dunlop's RA is $20^h\ 16^m\ 28^s$, *Gaia DR2* precessed RA is $20^h\ 18^m\ 27^s$. Probably a typographical error. Dunlop's $16^m$ should be $18^m$.

**No. 232∗ (DUN 232).** *1st outlier* in DE. Component A is mu.02 Oct. Dunlop's DE is −76° 56′, *Gaia DR2* precessed DE is −75° 56′ 15.72″. Could be due to a typographical error, as in should be −75° instead of −76°. In the WDS as 20417-7521 DUN 232.

**No. 235∗ (DUN 235AC).** Quadrant corrected from sp to sf. Dunlop uncorrected *Mean PA* is ∼236.6°. Dunlop corrected *Mean PA* is ∼123.4°. Precessed *Gaia DR2* PA is ∼124.3°.

**No. 238 (DUN 238AB).** *Gaia DR2* precessed Quadrant is nf. Dunlop *Mean PA* remains 90°.

**No. 242∗ (H 6 119AB).** *1st outlier* in Δ *Declin* (column 9). Δ *Declin* is 37.50″. The calculated Δ*Declin* [calculated from the *Mean PA*, *Mean Sep*, and declination (column 4)] is ∼75.6″. Perhaps a typographical error (as in 37 instead of 73).

**No. 245 (DUN 245).** *2nd outlier* in vB – vA with respect to the whole catalogue. Component A is HD 218392 (high proper motion star) and component B is CPD-60 7635B (high proper motion star). Dunlop's vA = 7 and vB = 13. *Gaia DR2* calculated vA is ∼7.35 and calculated vB is ∼9.79.

**No. 251∗ (DUN 251).** *Gaia DR2* precessed Quadrant is np. Dunlop PA remains 270°, *Gaia DR2* precessed PA is 291.4°.

**No. 252∗ (two).** Quadrant corrected from sf to nf. *1st outlier* in corrected PA. Dunlop uncorrected *Mean PA* is ∼117.4°. Dunlop corrected *Mean PA* is ∼62.6°. Precessed *Gaia DR2* PA is ∼8.0°. Dunlop's *Angle of Pos* is also wrong. Incorrect discoverer code (DisC) and components (Comp) in Letchford et al. (2019b,c).

**No. 253∗ (LAL 192).** Listed in the WDS as 14067-3622, but is identified here as LAL 192, WDS 23544-2703. *2nd outlier* in DE. Dunlop *Quadrant* is simply p, hence the uncorrected *Mean PA* = 270°. The *Gaia DR2* Quadrant for the secondary of LAL 192 is sp (*Gaia DR2* precessed PA ∼266.3°), but the corrected *Mean PA* remains 270°, since there is no other information to construct a more precise *Mean PA*. Component A of LAL 192 is HD 223991A. Dunlop's RA is $23^h\ 46^m\ 0^s$, DE is −28° 26′ and the *Gaia DR2* precessed RA is $23^h\ 45^m\ 22^s$ and the precessed DE is ∼−28° 00′ 43″.

## APPENDIX B: METHOD OF DETERMINING DUNLOP'S *Mean PA* AND *Mean Sep*

No. 18∗ has relevant information in all necessary columns (4–9) to serve as an example of each of the four ways of determining Dunlop's position angle for that double star.

(i) **PA method i** *Angle of Pos* (Column 5) = 30° 4′, *Quadrant* (Column 6) = nf. Therefore,
PA = 90° − 30° 4′ = 59° 56′ ≈ 59.93°

(ii) **PA method ii** *Declination* (Column 4) = −53° 46′, *Quadrant* (Column 6) = nf, Δ*AR* (Column 8) = 1ˢ.137, Δ*Declin* (Column 9) = 6.659″. Therefore,
ΔRA = 15cos(−53° 46′)1.137 ≈ 10.08″
*Angle of Pos* = arctan(Δ*Declin*/ΔRA)180/π ≈ 33.45°
PA ≈ 90° − 33.45° ≈ 56.55°

(iii) **PA method iii** *Declination* (Column 4) = −53° 46′, *Quadrant* (Column 6) = nf, *Distance* (Column 7) = 12.547″, Δ*AR* (Column 8) = 1ˢ.137. Therefore,
ΔRA = 15cos(−53° 46′)1.137 ≈ 10.08″
*Angle of Pos* = arccos(ΔRA/*Distance*)180/π ≈ 36.55°
PA ≈ 90° − 36.55° ≈ 53.45°

(iv) **PA method iv** *Declination* (Column 4) = −53° 46′, *Quadrant* (Column 6) = nf, *Distance* (Column 7) = 12.547″, Δ*Declin* (Column 9) = 6.659″. Therefore,
ΔRA = 15cos(−53° 46′)1.137 ≈ 10.08″
*Angle of Pos* = arcsin(Δ*Declin*/*Distance*) 180/π ≈ 32.05°
PA ≈ 90° − 32.05° ≈ 57.95°

The *Mean PA* for No. 18∗ is then 57.0°.

(i) **Sep method i** *Distance* (Column 7) = 12.547″. Therefore, Sep = 12.547″

(ii) **Sep method ii** *Declination* (Column 4) = −53° 46′, Δ*AR* (Column 8) = 1.137ˢ, Δ*Declin* (Column 9) = 6.659″. Therefore,
ΔRA = 15cos(−53° 46′)1.137 ≈ 10.08″
Sep = $\sqrt{(\Delta AR^2 + \Delta Declin^2)} \approx 12.082$ arcsec

(iii) **Sep method iii** *Declination* (Column 4) = −53° 46′, *Angle of Pos* (Column 5) = 30° 4′, Δ*AR* (Column 8) = 1.137ˢ. Therefore,
ΔRA = 15cos(−53° 46′)1.137 ≈ 10.08″
Sep = ΔRA/cos(*Angle of Pos*) ≈ 11.648″

(iv) **Sep method iv** *Angle of Pos* (Column 5) = 30° 4′, Δ*Declin* (Column 9) = 6.659″. Therefore,
Sep = Δ*Declin*/sin(*Angle of Pos*) ≈ 13.291″.

The *Mean Sep* for No. 18∗ is then 12.4″.

## APPENDIX C: DUNLOP DOUBLE STARS THAT FALL WITHIN CONTEMPORARY 1820S ACCURACY LIMITS

Table C1 list the Dunlop double stars from the *Dunlop Catalogue* that fall within contemporary 1820s accuracy limits for the given parameter. See Section 3.4 for the description of these contemporary astrometric and photometric standards.

**Table C1.** Dunlop double stars that fall within the contemporary 1820s accuracy limits given in column 1. For the meaning of Δ, see equations (1) and (2).

| Measure range | *Banks Refractor* | *Dunlop Reflector* |
|---|---|---|
| $-5^s < \Delta RA < +5^s$ | 102∗ = 103∗ | None |
| $-5'' < \Delta DE < +5''$ | 42∗, 109∗, 116∗, 149∗ | 60, 67, 172, 175, 188, 204, 221, 247 |
| $-4° < \Delta PA < +4°$ (Quadrant corrected) | 4∗, 26∗, 27∗, 28∗, 29∗, 31∗, 38∗, 40∗, 43∗, 52∗, 62∗, 73∗, 76∗, 88∗, 95∗, 99∗, 102∗, 103∗, 112∗, 113∗, 116∗, 117∗, 119∗, 126∗, 129∗, 131∗, 133∗, 146∗, 153∗, 163∗, 169∗, 176∗, 179∗, 182∗, 196∗, 197∗, 229∗, 231∗, 232∗, 235∗, 236∗, 241∗, 249∗, 250∗ | 59, 68, 71, 72, 114, 128, 150, 168, 195, 207, 209, 219, 224, 247 |
| $-0.5'' < \Delta Sep < +0.5''$ | 28∗, 29∗, 39∗, 66∗, 74∗, 111∗, 148∗, 149∗, 249∗ | 213 |
| $-0.3 < \Delta VmagA < +0.3$ | 6∗, 19∗, 20∗, 26∗, 39∗, 56∗, 62∗, 76∗, 78∗, 113∗, 119∗, 146∗, 163∗, 174∗, 241∗, 242∗ | 23, 58, 60, 61, 68, 71, 72, 80, 81, 82, 85, 101, 110, 115, 118, 135, 144, 157, 162, 171, 187, 192, 193, 203, 208, 212, 213, 215, 224, 225, 234, 237 |
| $-0.3 < \Delta VmagB < +0.3$ | 16∗, 17∗, 20∗, 26∗, 28∗, 32∗, 36∗, 38∗, 39∗, 73∗, 74∗, 86∗, 103∗, 109∗, 111∗, 116∗, 142∗, 143∗, 164∗, 197∗, 216∗, 229∗, 231∗ | 14, 57, 58, 67, 68, 81, 168, 175, 191, 195, 203, 212, 219, 224, 239, 247 |

This paper has been typeset from a TEX/LATEX file prepared by the author.

## 3.3 LINKS AND IMPLICATIONS FOR NEXT STUDY

Machine-readable data generated as part of Paper 1 is available online as one file and is reproduced in this thesis in Appendix A, B and C and form part of the Supplementary Online Material downloadable from the web site of Paper 1 (https://doi.org/10.1093/mnras/stab3777). Columns 20 and 21 (of Appendix B) list the ASCC source identifiers and columns 22 and 23 (of Appendix B) the *Gaia DR2* source identifiers for the primaries and secondaries, respectively, of the *Dunlop Catalogue* where available.

Positional and other parameters from the ASCC and *Gaia DR2* databases form the input data for two new techniques. One technique is used to obtain first order orbital elements of some wide visual binary stars with short and/or incomplete arcs from the *Dunlop Catalogue* (Chapter 4, Paper 2). The other technique is used to obtain Rectilinear Elements for optical double stars (Chapter 5, Paper 3) where uncertainties are at least an order of magnitude smaller than currently published in the SCORE.

# CHAPTER 4: PAPER 2 - ORBITAL ELEMENTS OF VISUAL BINARY STARS WITH VERY SHORT ARCS: WITH APPLICATION TO DOUBLE STARS FROM THE 1829 SOUTHERN DOUBLE STAR CATALOGUE OF JAMES DUNLOP

## 4.1 INTRODUCTION

Paper 2 presents a new technique for calculating first order orbits of wide slow moving binary stars making particular use of astrometric data from the HIPPARCOS (via ASCC) and *Gaia* (using *Gaia DR2*) space-based missions. Starting with the 40 double stars from the *Working Dunlop Catalogue* (consisting of double stars from the *Dunlop Catalogue* where both components have full data sets from HIPPARCOS and *Gaia Data Release 2* and are also currently listed in the *Washington Double Star Catalog)*, five were confirmed to be binary stars, based on three criteria (their binding energy must be < 0, components must be within 1pc of each other, and display common proper motion). After testing the new technique for estimating first order orbital elements on known binary stars with better defined orbits, the method was applied to the five confirmed wide binary stars in the *Working Dunlop Catalogue*.

The mean orbital period of the five binary stars is ~81,000 years, the mean semi-major axis is ~76'', and a typical uncertainty of all seven Orbital Elements is ~37%. Their Orbital Elements and associated plots are also presented.

Letchford, R. R., White, G. L., & Brown, C. J. 2022, *Astron. Nachr.*, 343, 1-13. e20210113. https://doi.org/10.1002/asna.20210113.

Received: 25 December 2021 | Revised: 3 February 2022 | Accepted: 7 February 2022 | Published on: 3 March 2022

DOI: 10.1002/asna.20210113

Astronomische Nachrichten

ORIGINAL ARTICLE

# Orbital Elements of visual binary stars with very short arcs: With application to double stars from the 1829 southern double star catalog of James Dunlop

**Roderick R. Letchford** | **Graeme L. White** | **Carolyn J. Brown**

Centre for Astrophysics, University of Southern Queensland, Toowoomba, Queensland Australia

**Correspondence**
Roderick R. Letchford, School of Mathematics, Physics and Computing, University of Southern Queensland, Toowoomba, QLD 4350, Australia.
Email: Rod.Letchford@usq.edu.au

**Abstract**

Binary double stars are those whose binding energies are less than zero. Obtaining binary star orbits from short arcs has been a long-standing problem in astrophysics. A method is presented and tested here, which addresses the problem by using space-based astrometry, photometry, and astrophysical data, together with historic measures, to generate and constrain a range of possible first-order Grade 5 orbits. After testing the method on an established binary star, we apply the method to eight double stars from the first published catalog of southern double stars, that of Dunlop (1829) and generate orbits for five. The mean orbital period is ~81,000 years, and the mean semi-major axis is ~76″ with a typical uncertainty of the Orbital Elements of ~37%. Their Orbital Elements and associated plots are also presented.

**KEYWORDS**

astrometry, binaries: visual – celestial mechanics, stars: kinematics

## 1 | INTRODUCTION

The uniqueness of two stars in abnormal astrometric proximity has been the subject of study for over 200 years and was a major area of astrophysical study from the late 18th to the early 20th centuries. The earliest measure of a double star in the United States Naval Observatory's *The Washington Double Star Catalog* (WDS, Mason et al. 2001) is $\mu$ Draconis (STFA 35), which was first measured in 1690. Now over 154,000 double stars are cataloged in the WDS. Of these, computed orbits are available for just over 3300 in the *Sixth Catalog of Orbits of Visual Binary Stars* (Matson et al. 2020). The study of orbits of binary star systems incorporating the physical laws of Newton and Kepler is the fundamental method of determining the mass of stars. The accuracy of the Orbital Elements, and subsequent physical properties of the stars, depends on the precision of the astrometric measures and the computational methodology.

Increasingly precise astrometry is now available from space-based missions such as HIPPARCOS (Perryman et al. 1997) and *Gaia DR2* (Gaia Collaboration et al. 2018), not withstanding that observational constraints in the *Gaia* instrument have resulted in a scarcity of double star measures (position angle [PA] $\theta$, and separation $\rho$) for close pairs separated by less than ~2″. The Epochs of the HIPPARCOS and *Gaia DR2* missions are similar (1991.25 and 2015.5 respectively) and therefore, for pairs that have

**TABLE 1** Statistics of the *Sixth Catalog of Orbits of Visual Binary Stars*

| Grade | Number | $P^{\text{years}}_{\text{mean}}$ | $P^{\text{years}}_{\text{median}}$ | $a''_{\text{mean}}$ | $a''_{\text{median}}$ |
|---|---|---|---|---|---|
| 1 | 89 | 17.3 | 11.4 | 18.72 | 0.33 |
| 2 | 374 | 48.0 | 27.7 | 8.52 | 0.25 |
| 3 | 697 | 106.7 | 69.4 | 6.62 | 0.26 |
| 4 | 988 | 483.5 | 218.2 | 4.57 | 0.55 |
| 5 | 660 | 18,244 | 484.2 | 813.41 | 1.57 |

long periods, it is still imperative that historic measures of lower precision, and which may extend over 200 years, are used to better define the orbit (White et al. 2018). Ultimately this work will advance through future missions with micro-arcsecond precision.

The *Sixth Catalog of Orbits of Visual Binary Stars* is divided into five Grades based on the accuracy of the orbits, where Grade 1 orbits are those with "well-distributed coverage exceeding one revolution" and Grade 5 orbits are those where "the [orbital] elements may not even be approximately correct" and the observed arc is short with little curvature (Hartkopf et al. 2001). Grades 6–9 are reserved for pairs with incomplete elements or lacking measures of relative astrometry. Therefore, they cannot be evaluated with conventional residual analysis.

Table 1 gives a statistical breakdown of the *Sixth Catalog of Orbits of Visual Binary Stars*. A superficial examination of the orbits in Grades 1–5 shows clearly the selection effects resulting from the observational precision and computational techniques. For example, the Grade 1 orbits are for pairs that have short periods (mean and median orbital period of 17.3 and 11.4 years, respectively, where the longest Grade 1 orbit is ~88.4 years) and the orbit is observed over one or more complete orbits. Such pairs have statistically smaller physical separation (mean and median semi-major axis of 18.72″ and 0.33″, respectively). These close binary star orbits are characteristically the physical size of a planetary system. Even Grade 5 orbits have a median semi-major axis of only ~1.57″. Hence all physical parameters determined from the Orbital Elements in the *Sixth Catalog of Orbits of Visual Binary Stars* are statistically biased to binaries in close orbits.

Distinguishing between optical and binary doubles has important ramifications for many aspects of astrophysics. This is especially the case for stellar formation models by contributing to multiplicity statistics (Guinan et al. 2007), the potential to distinguish between the mainstream-accepted *Weakly Interacting Massive Particles* based hypothesis of dark matter, and in Modified Newtonian Dynamics (Chanamé & Gould 2004; Longhitano & Binggeli 2010; Németh et al. 2016). The first successful estimation of the Orbital Elements of an assumed binary star was carried out by Félix Savary (Savary 1827a, 1827b). Since then numerous methods have been devised (Aitken 1964; Heintz 1978; See 1896).

The problem of estimating the Orbital Elements of wide binaries (with angular separation $\rho > 2''$) with few measures has resulted in numerous computational methods (see Docobo et al. 2018). For example, there is the so-called "Kovole" method (Ćatović & Olević 1992, 1995; Olević & Cvetković 2004, 2005), which is a modified form of the analytical Kowalski method. The Kowalski method derives five of the seven Orbital Elements from the constants of the Cartesian form of the general equation for the apparent relative ellipse (Belorizky 1949; Glasenapp 1889; Kowalski 1873; Smart 1930), and forms a part of the method presented in this paper (Section 3.2). Another is a modified form of the "Thiele-Innes-Van-den-Bos" method (Docobo 1985, 2012; Docobo et al. 2018; van den Bos 1926). However, to our knowledge, no method to date has successfully addressed the particular case of a very short arc.

This paper proposes a computational method utilizing the convergence of randomized fits (not a once off analytical method), which is now possible because of the availability of computing power for the determination of orbits of binary pairs in longer orbits: those that display short arcs in orbital plots.

Such work has been suggested to be of little value by van den Bos 1962, Worley 1990 and Dommanget 1995, who each published articles with the provocative title "Is this orbit really necessary?" The three authors criticized the publication of orbits that were unreliable because they were based on too few observations over too short an arc, or deemed useless because the quality of such recalculated orbits rarely increases with successive attempts. This paper is to show that improved first-order estimates of orbits can be now obtained using the new method coupled with space-based astrometry and photometry.

The aim of this paper is fourfold. (a) To offer an objective method of detecting binary double stars using space-based astrometric and astrophysical data from *Gaia DR2*; (b) to dispense with the traditional intellectual driver associated with orbits, which is to determine stellar mass; (c) to present a technique of determining first-order orbits of binary stars with short arcs using data from *Gaia DR2* and HIPPARCOS (via *All-sky Compiled Catalog of 2.5 million stars*; ASCC, Kharchenko 2001); and (d) to apply these aims to a subset of wide double stars.

The subset chosen for illustration of the technique is taken from the first published catalog of southern double stars by Dunlop (1829), this is referred to here and elsewhere as the *Dunlop Catalog*. A previous paper by the authors (Letchford et al. 2022) describes and analyses the *Dunlop Catalog* and gives ASCC and *Gaia DR2* source identifiers where available. For our subset used

here, all pairs from the *Dunlop Catalog* must have an entry (and therefore historic measures) in the WDS (Mason et al. 2001), and the primary and secondary must both have ASCC and *Gaia DR2* source identifiers. In total, 182 wide doubles from the original *Dunlop Catalog* satisfy this criterion. We define this subset of the original Dunlop Catalog as the *Working Dunlop Catalog*.

Previous work (Letchford et al. 2018, 2019) has presented material on the orbital motion of binary double stars. Here, we refine that work, and in Section 2 we select a sample of eight pairs from the *Working Dunlop Catalog* that satisfy the definition of a binary system. Section 3 gives a proposed new technique for determining the Orbital Elements of binary double stars, and tests the method against a set of Orbital Elements from the *Sixth Catalog of Orbits of Visual Binary Stars*. Section 4 presents and discusses the results of applying the technique to the eight double stars from Section 2.

## 2 | METHOD: DETECTING VISUAL BINARY DOUBLE STARS

By definition, binary double stars are pairs of stars whose binding energy ($E_{\text{binding}}$) is less than zero (Aarseth et al. 2008; Benacquista 2012; Kouwenhoven et al. 2010; Wiley & Rica 2015). Conversely, any double star with a binding energy greater than zero is an optical double star. The binding energy of two stars is represented by the following equation:

$$E_{\text{binding}} = \frac{1}{2}\frac{m_A m_B}{m_A + m_B}v^2 - \frac{Gm_1 m_2}{D} \tag{1}$$

where $E_{\text{binding}}$ is in $m_\odot\left(\text{km s}^{-1}\right)^2$; $m_A$ and $m_B$ are the masses of the primary and secondary in solar masses ($m_\odot$); $v$ is the galactic space speed *difference* between the two stars in km s$^{-1}$; $D$ is their physical separation, in parsec (pc); and $G$ is the gravitational constant ($4.30091 \times 10^{-3}$ $\text{pc}\left(\text{km s}^{-1}\right)^2/M_\odot$).

Reasonable estimates of the stellar masses can be obtained via luminosity data from *Gaia DR2* and using the following relationship between individual luminosity ($L$ in solar units) and individual mass ($m$ in solar masses) as given by Duric (2004):

$$m = \begin{cases} \left(\frac{L}{0.23}\right)^{1/2.3}, & \text{if } m < 0.43 \\ L^{1/4}, & \text{if } 0.43 < m < 2 \\ \left(\frac{L}{1.4}\right)^{1/3.5}, & \text{if } 2 < m < 55 \\ \frac{L}{32{,}000}, & \text{if } m > 55 \end{cases} \tag{2}$$

To calculate $D$, the physical separation of the components in pc, the cosine rule is invoked:

$$D = \sqrt{D_A^2 + D_B^2 - 2D_A D_B \cos(\rho/3{,}600)} \tag{3}$$

where $D$ is the separation distance of the two stars in pc; $D_A$ is the distance from the Sun to the primary in pc, obtained from parallax measures; $D_B$ is the distance from the Sun to the secondary in pc, and $\rho$ is the apparent separation in arcseconds ($''$).

To calculate the speed of each component ($v_1$ and $v_2$), the method of Johnson & Soderblom (1987) will be followed, except that the J2000 transformation matrix ($T$, Equation (5)) to galactic coordinates is taken from the introduction to the HIPPARCOS catalog (Perryman 1997), and the method tested by first applying it to the pair *α Cen AB,C*, making sure that the results obtained were the same as those in Kervella et al. (2017), in their Table B.1. The galactic space velocity components ($U, V, W$) are then:

$$\begin{bmatrix} U \\ V \\ W \end{bmatrix} = (\text{T.A}).\begin{bmatrix} \text{RV} \\ k.\text{pmRA/Plx} \\ k.\text{pmDE/Plx} \end{bmatrix} \tag{4}$$

where:

$$\text{T} = \begin{bmatrix} -0.0548755604 & +0.4941094279 & -0.8676661490 \\ -0.8734370902 & -0.4448296300 & -0.1980763734 \\ -0.4838350155 & +0.7469822445 & +0.4559837762 \end{bmatrix} \tag{5}$$

$$\text{A} = \begin{bmatrix} +\text{cosRA.cosDE} & -\text{sinRA} & -\text{cosRA.sinDE} \\ +\text{sinRA.cosDE} & +\text{cosRA} & -\text{sinRA.sinDE} \\ +\text{sinDE} & 0 & +\text{cosDE} \end{bmatrix} \tag{6}$$

and RV is the radial velocity of the star in km s$^{-1}$; pmRA is the proper motion in RA in mas year$^{-1}$; pmDE is the proper motion in DE in mas year$^{-1}$; Plx is the parallax in mas; and the constant $k$ = 4.74057 km s$^{-1}$ is the speed in km s$^{-1}$ required to travel 1 AU in one tropical year.

So the difference in the velocity magnitude ($v$, speed) between the primary and secondary is:

$$v = \sqrt{\left(U_1^2 - U_2^2\right)^2 + \left(V_1^2 - V_2^2\right)^2 + \left(W_1^2 - W_2^2\right)^2} \tag{7}$$

Of the 182 double stars in the *Working Dunlop Catalog* only 40 had sufficient *Gaia DR2* data to allow the calculation of binding energies (Table 2).

**TABLE 2** Catalog numbers from the *Dunlop Catalog* for the 40 double stars for which binding energies $E_{\text{binding}}$ could be calculated

| Nos. $E_{binding} < 0$ | Nos. $E_{binding} > 0$ |
|---|---|
| **2 in total** | **38 in total** |
| 38, 55 | 2, 4, 5, 23, 26, 27, 28, 29, 40, 41, 52, 57, 73, 77, 79, 80, 114, 116, 118, 146, 155, 175, 176, 178, 184, 186, 200, 215, 225, 232, 236, 238, 241, 242, 245, 246, 248, 250 |

The formal uncertainties in $E_{\text{binding}}$ will be large due to the compounding uncertainties in the observable parameters, especially from the uncertainties in stellar masses from Equation (2). Here we are assured that numbers 38 and 55 are binary systems as they have $E_{\text{binding}} < 0$. We include in our list of probable binaries numbers 5, 80, 116, 232, 242, and 245, which have binding energies <1 (thus allowing for some uncertainties in $E_{\text{binding}}$), and observables consistent with a binary system (see next paragraph). Number 5 (DUN 5) has a Grade 5 orbit in the *Sixth Catalog of Orbits of Visual Binary Stars* and clearly shows orbital motion (see Appendix).

The approximate binding energies ($E_{\text{binding}}$), physical separations ($D$, column 4) in pc, and the proper motions of the eight double stars (columns 5 and 6, where $\text{pmRA}_A$ and $\text{pmDE}_A$ are the proper motions in right ascension and declination for the primary, respectively, and similarly for the secondary, B), are presented in Table 3. Column 1 (No.) is the catalog number of the double star from the *Dunlop Catalog*. Column 2 contains the WDS system identifier, underneath which is the Discoverer code of the particular double star (from the WDS). All physical separations are less than 1 pc (Dommanget 1967 and Sinachopoulos 1991 had a separation limit of 0.01 pc, recently others have demonstrated a limit approaching 1 pc, Longhitano & Binggeli 2010, others to the galactic tidal limit of ~1.7 pc for solar type stars, Halbwachs et al. 2012; Moeckel & Bate 2010), and each of the eight also exhibit a common proper motion (following Hartkopf et al. 2013), justifying their inclusion as possible binary double stars.

## 3 | METHOD: ORBITAL MOTION

We present here a computationally-based method of determining orbits that are defined by short arcs. High precision astrometric measures are utilized as historic measures of less accuracy. Stellar mass data are incorporated and physical constraints are applied. Multiple random orbits are generated and compared with modern and historic measures, and the fit to the measures is optimized to define the orbit and its uncertainties.

The problem with dealing with short arcs is that the range of possible ellipses can be considerable with large associated uncertainties. This difficulty is overcome by introducing as many constraints on the solutions as possible.

If the double star is a binary star (the primary and secondary are gravitationally bound), the following corollaries must hold true:

1. The primary position must always be within any apparent orbit of the secondary.
2. The orbit of the secondary must cross the meridian line through the primary twice: only once to the north of the primary, and only once to the south of the primary.
3. Similarly, the orbit of the secondary must cross a line parallel to the equator and passing through the primary twice: only once to the east of the primary, and only once to the west of the primary.

By convention, binary orbit calculations are conducted in Cartesian coordinates, where the primary is fixed at the origin. Our method incorporates the Kowalski method (Section 1), which uses the Cartesian form of the apparent relative ellipse, that is, the ellipse formed on the celestial sphere of a secondary orbiting a fixed primary. The apparent relative orbit of a binary star will fit the following general form of the Cartesian equation of an ellipse:

$$Ax_i^2 + 2Hx_iy_i + By_i^2 + 2Gx_i + 2Fy_i + 1 = 0 \qquad (8)$$

where $A, H, B, G$, and $F$ are constants, and $x_i$ and $y_i$ are the Cartesian coordinates of the secondary at times $t_i$, given that the primary is fixed at the origin.

At least five positions on the Cartesian plane ($i \geq 5$) are needed to fit an ellipse to Equation (1). The normal procedure, where at least half of the orbit has been measured, is to convert the historic polar measures to Cartesian coordinates and fit a first ellipse to them using either ordinary least squares (OLS), or better, total least squares (TLS). The historic measures can be weighted before fitting (Mason et al. 1999). In the present case, a least squares approach to the historic data will not yield a suitable first ellipse because we consider the cases where much less than half an orbit has been measured. The five or more fitting points must initially be found by another method.

Four of those points can be supplied by positions described in corollaries 2 and 3, above. Two more positions can be supplied by HIPPARCOS (via ASCC) and *Gaia DR2* (Gaia Collaboration et al. 2018) at $t$ = 1991.25 and 2015.5 (both at Equinox 2000.0), respectively. In this paper,

**TABLE 3** Table of the approximate binding energies ($E_{\text{binding}}$), physical separations ($D$) in parsec (pc), and the proper motions of the eight double stars, whose binding energies <1, physical separation <1 + 1σ, and whose common proper motions (CPM) are consistent with binarity

| | | | | CPM, mas year$^{-1}$ | |
|---|---|---|---|---|---|
| | | | | $\text{pmRA}_A$ | $\text{pmRA}_B$ |
| **Nos.** | **WDS discoverer code** | $E_{\text{binding}}\, M_\odot \left(\text{km s}^{-1}\right)^2$ | **$D$, pc** | $\text{pmDE}_A$ | $\text{pmDE}_B$ |
| 5 | 01398-5612 | ~ +0.55 | 0.005 ± 0.005 | +262.378 ± 0.081 | +309.102 ± 0.080 |
| | DUN 5 | | | +15.333 ± 0.072 | +10.686 ± 0.065 |
| 38 | 07040-4337 | ~ −2.2 | 0.002 ± 0.023 | −105.060 ± 0.146 | −101.764 ± 0.043 |
| | DUN 38AB | | | +389.550 ± 0.162 | +382.276 ± 0.047 |
| 55 | 07442-5027 | ~ −0.43 | 0.009 ± 0.035 | −114.435 ± 0.047 | −111.783 ± 0.060 |
| | DUN 55AB | | | +143.459 ± 0.042 | +142.603 ± 0.053 |
| 80 | 09450-4929 | ~ +0.14 | 0.39 ± 0.18 | −21.344 ± 0.071 | −23.581 ± 0.066 |
| | DUN 80AB | | | +98.409 ± 0.062 | +97.158 ± 0.066 |
| 116 | 11567-3216 | ~ +0.26 | 0.016 ± 0.077 | −171.610 ± 0.072 | −178.910 ± 0.073 |
| | DUN 116AB | | | −8.250 ± 0.042 | −6.668 ± 0.039 |
| 232 | 20417-7521 | ~ +0.47 | 0.059 ± 0.071 | +156.596 ± 0.039 | +163.555 ± 0.048 |
| | DUN 232 | | | −162.079 ± 0.045 | −171.231 ± 0.050 |
| 242 | 22397-2820 | ~ +0.17 | 0.36 ± 0.84 | +96.822 ± 0.109 | +96.340 ± 0.106 |
| | H 6 119AB | | | −40.596 ± 0.083 | −36.578 ± 0.079 |
| 245 | 23086-5944 | ~ +0.12 | 0.40 ± 0.19 | +60.074 ± 0.043 | +62.034 ± 0.041 |
| | DUN 245 | | | −63.923 ± 0.046 | −67.227 ± 0.047 |

*Note*: Column 1 (Nos.) refers to the catalog numbers from the Dunlop Catalog.

we chose to obtain HIPPARCOS data from the ASCC (Kharchenko 2001).

Four random points are generated along the north, south, east, and west axes centering on the primary, and added to them are the two points obtained from the ASCC and *Gaia DR2*. Random iterative searches in increments of ~30″ out to 4′ locate the coordinates of these crossing points. For each increment, we generated ~$10^7$ sets of points. The search along the primary star axes is limited to a maximum of 4′, determined by the fact that all but two orbits in the *Sixth Catalog of Orbits of Visual Binary Stars* have semi-major axes less than 240″.

The algorithm of Halir & Flusser (1998) is used to find the coefficients $A, H, B, G$, and $F$ for each generated ellipse, rather than an OLS or TLS fit. The Halir and Flusser algorithm has the advantage of generating an ellipse every time, whereas the random alignment of fitting points may not always generate an ellipse using the OLS or TLS methods.

This random search domain is reduced by noting that because the secondary is slow moving, the positions obtained from the space-based HIPPARCOS (via ASCC) and *Gaia DR2* missions will define a tangent to any orbit at a mean Epoch of ~2003. Therefore the elliptical orbit will only exist on the side of this tangent containing the primary.

## 3.1 | First constraint

The first constraint is to delete obviously non-viable ellipses by discarding all generated ellipses where the origin was outside the ellipse.

## 3.2 | Orbital Elements

Next, Orbital Elements associated for each ellipse are calculated. This involves a two-step process.

First, five of the seven Orbital Elements ($a, i, \Omega, e$ and $\omega$) are calculated using the Kowalski method (Section 1).

The longitude of the ascending node of the apparent relative orbit, Ω, is:

$$\Omega^{\text{radians}} = \begin{cases} \frac{1}{2}\arctan 2(Q, R) \\ \Omega = \Omega + \pi, \text{if } \Omega < 0 \\ \Omega = \Omega - \pi, \text{if } \Omega > \pi \end{cases} \quad (9)$$

where $Q = -2(FG - H)$, $R = F^2 - G^2 + A - B$;
and,

$$\arctan 2(Q,R) = \begin{cases} \arctan(Q/R), \text{if } R > Q \\ \frac{\pi}{2} - \arctan(Q/R), \text{if } Q > 0 \\ -\frac{\pi}{2} - \arctan(Q/R), \text{if } Q < 0 \\ \arctan(Q/R) \pm \pi, \text{if } R < 0 \\ \text{undefined, if } R = 0 \text{ and } Q = 0 \end{cases} \quad (10)$$

If the ascending node is unknown, then $\Omega < \pi$.

The inclination of the plane of the true relative orbit to that of the celestial sphere, $i$, is given by either Equation (11a) or (11b):

$$i^{\text{radians}} = \arctan 2(\sqrt{|\,2Q\,|}, \sqrt{|\,S\sin(2\Omega) - Q\,|}) \quad (11a)$$

$$i^{\text{radians}} = \arctan 2(\sqrt{|\,2R\,|}, \sqrt{|\,S\cos(2\Omega) - R\,|}) \quad (11b)$$

where $S = F^2 + G^2 - A - B$ and $i = \pi - i$ if the apparent orbit is retrograde (clockwise).

The argument of periastron, $\omega$, is given by:

$$\omega^{\text{radians}} = \begin{cases} \arctan 2(-U\cos(i), -V) \\ \omega = \omega + 2\pi, \text{if } \omega < 0 \\ \omega = \omega - 2\pi, \text{if } \omega > 2\pi \end{cases} \quad (12)$$

where $U = F\cos(\Omega) - G\sin(\Omega)$ and $V = F\sin(\Omega) + G\cos(\Omega)$.

By convention, $0 \le \omega \le 2\pi$.

The eccentricity of the true relative orbit, $e$, is either Equations (13a) or (13b):

$$e = \left| \frac{-U\cos(i)}{\sin(\omega)} \sqrt{\frac{2}{S - \frac{Q}{\sin(2\Omega)}}} \right| \quad (13a)$$

$$e = \left| \frac{-V}{\sin(\omega)} \sqrt{\frac{2}{S - \frac{R}{\cos(2\Omega)}}} \right| \quad (13b)$$

For ellipses, $0 < e < 1$.

The semi-major axis of the true relative orbit, $a$, is given by Equations (14a) or (14b):

$$a'' = \frac{1}{1-e^2} \sqrt{\frac{2}{S - \frac{Q}{\sin(2\Omega)}}} \quad (14a)$$

$$a'' = \frac{1}{1-e^2} \sqrt{\frac{2}{S - \frac{R}{\cos(2\Omega)}}} \quad (14b)$$

The remaining two Orbital Elements, the orbital period ($P$) and time of periastron ($T$) are estimated using the mean anomaly ($M_A$).

To find the mean anomaly for the HIPPARCOS (via ASCC), $M_{HIPP}$, and *Gaia DR2* $M_{GaiaDR2}$, positions, the true anomaly ($V_A$) is followed by the eccentric anomaly ($E_A$), which is first found for each position:

$$V_A = \arctan 2\left[(\sin(\theta - \Omega)\sec(i), (\cos(\theta - \Omega)\right] - \omega \quad (15)$$

$$E_A = 2\arctan\left(\sqrt{\frac{1-e}{1+e}}\tan(V_A/2)\right) \quad (16)$$

$$M_A = E_A - e\sin(E_A) \quad (17)$$

where $-2\pi < V_A < 2\pi$; $-\pi < E_A < \pi$; and $-\pi < M_A < \pi$. $\theta$ is the PA of the secondary with respect to the primary at time $t$ and at Equinox 2000.0.

Continuing:

$$P = \left| 2\pi \frac{2015.5 - 1991.25}{M_{GaiaDR2} - M_{HIP}} \right| \quad (18)$$

$$T = \frac{M_{GaiaDR2}1991.25 - M_{HIP}2015.5}{M_{GaiaDR2} - M_{HIP}} \quad (19)$$

The time of periastron, $T$, is the year of closest approach normally presented as the one nearest 2000.0, and given as a decimal year. The orbital period, $P$, is measured in decimal years.

### 3.3 | Second constraint

The second constraint is to delete all orbits where the calculated total mass of the system ($M_{\text{system}}$) is greater than a preset tolerance of ±10% of the known combined masses of the primary and secondary.

In most double star work, the ultimate aim is to obtain direct measures of the stellar masses using Kepler's third law:

$$m_{\text{system}} = m_A + m_B = \frac{a^3}{\Pi^3 P^2} \quad (20)$$

where $m_A$ and $m_B$ are the masses of the primary and secondary respectively, in solar masses; $a$ is the semi-major axis of the real relative orbit in arcseconds; $\Pi$ is the parallax of the system (the primary star) in arcseconds; and $P$ is the orbital period of the secondary, in years. In this paper, we reverse the procedure and begin with good estimates of the combined masses obtained from luminosity data from *Gaia DR2* and using the mass-luminosity function, Equation (2). We set the mass constraint to ±10% of the combined masses.

The parallax of the system (Π) is deemed to be the parallax of the primary, obtained from *Gaia DR2*. Thus:

$$\frac{a^3}{P^2}\begin{cases} > \Pi^3\left(m_A + m_B - \frac{m_A+m_B}{10}\right) \\ < \Pi^3\left(m_A + m_B + \frac{m_A+m_B}{10}\right) \end{cases} \quad (21)$$

## 3.4 | Third and fourth constraints

Finally, we assumed that the best results will be obtained if the calculated positions of the secondary at 1991.25 and 2015.5 fell within the $1\sigma$ uncertainty ellipse of the HIPPARCOS (via ASCC) and *Gaia DR2* positions. HIPPARCOS positions (via ASCC) in right ascension have a $1\sigma$ uncertainty of ∼6 mas and ∼3 mas in declination. *Gaia DR2* positions in right ascension and declination have a $1\sigma$ uncertainty of ∼0.1 mas. Requiring the calculated positions at Epochs 1991.25 and 2015.5 to be within the $1\sigma$ uncertainty ellipse of the HIPPARCOS (via ASCC) and *Gaia DR2* positions proved to be the most severe constraints.

The uncertainties of the secondary position in Cartesian coordinates $(\sigma_x, \sigma_y)$ for both the HIPPARCOS (via ASCC) and *Gaia DR2* positions is approximated by:

$$\sigma_x = \pm\sqrt{\cos(\mathrm{DE1})^2\left(\sigma^2_{\mathrm{RA1}} + \sigma^2_{\mathrm{RA2}}\right) + (\mathrm{RA2} - \mathrm{RA1})^2 \sin(\mathrm{DE1})^2 \sigma^2_{\mathrm{DE1}}}$$
$$\sigma_y = \pm\sqrt{\sigma^2_{\mathrm{DE1}} + \sigma^2_{\mathrm{DE2}}} \quad (22)$$

where $x = (\mathrm{RA2} - \mathrm{RA1})\cos(\mathrm{DE1})$ and $y = \mathrm{DE2} - \mathrm{DE1}$.

RA1 and DE1 are the right ascension and declination coordinates, respectively, of the primary at Equinox 2000.0; RA2 and DE2 are the right ascension and declination coordinates, respectively, of the secondary at Equinox 2000.0; and $\sigma_{\mathrm{RA1}}$, $\sigma_{\mathrm{DE1}}$, $\sigma_{\mathrm{RA2}}$, and $\sigma_{\mathrm{DE2}}$ are their respective uncertainties (errors), obtained from ASCC and *Gaia DR2*.

To find the position at time $t$ of the secondary implied by the recalculated orbit, the following ephemeris procedure must be undertaken.

First, the true anomaly of the *calculated* position must be found via the mean and eccentric anomalies:

$$M_A = \frac{t - T}{2\pi P} \quad (23)$$

where $M_A$ is the mean anomaly of the calculated position. Next, $E$ must be calculated using Kepler's transcendental equation:

$$M_A = E_A - e\sin(E_A) \quad (24)$$

where $e$ is the eccentricity of the calculated orbit.

Now, the true anomaly of the calculated position can be determined from:

$$V_A = 2\arctan\left[\tan\left(\frac{E_A}{2}\right)\sqrt{\frac{1+e}{1-e}}\right] \quad (25)$$

And the polar coordinates of the ephemeris position can be calculated:

$$\theta^{\mathrm{radians}} = \arctan 2\left[(\sin(V_A) + \omega, \cos(V_A) + \omega\right] + \Omega \quad (26)$$

$$\rho'' = \frac{a\left(1 - e^2\right)\cos(V_A) + \omega}{(1+e)\cos(V_A)\cos(\theta - \Omega)} \quad (27)$$

where $\theta$ and $\rho$ are converted to Cartesian coordinates using:

$$x'' = \rho\cos(\theta) \quad (28)$$

$$y'' = \rho\sin(\theta) \quad (29)$$

## 3.5 | Bringing in the historic data

It is only at this point that historic measures of the double stars, as recorded in the WDS, are introduced into the computation.

The measures of PA contained in the WDS are given at Equinox of Epoch, and are converted to Equinox 2000.0 ($\theta°$). PA°s from HIPPARCOS (via ASCC) have Epochs of 1991.25 and *Gaia DR2* have Epochs of 2015.5. Both PAs are given in the WDS at Equinox 2000.0 and therefore are not converted.

The formula for conversion of $\mathrm{PA}_i$ (other than those at 1991.25 and 2015.5) at Equinox of Epoch to Equinox 2000.0 ($\theta_i$) is:

$$\theta_i^\circ = \mathrm{PA}_i^\circ + [0.00417 + \mathrm{pmRA1} + \sin(\mathrm{DE1}) + 0.00557\frac{\sin(\mathrm{RA1})}{\cos(\mathrm{DE1})}](2000.0 - t_i) \quad (30)$$

where pmRA1 is the proper motion of the primary in arcseconds, and $t_i$ is the Epoch of observation given in Besselian years.

Thus converted, $\theta_i$ together with the separation ($\rho_i$) are then converted to Cartesian coordinates via Equations (28) and (29). Using an ephemeris algorithm (Equations (23)–(29)), the positions of the historic data at times $t$ $(t_i, x_i, y_1)$, based on the Orbital Elements of each surviving orbit are calculated.

For each orbit calculated, the residuals ($R_o$) are determined by the sum of the squares of the distances between the historic positions and their predicted ephemeris positions. The orbits are then ranked in ascending order of $R_o$.

**TABLE 4** Test double star

| Orbital Elements | OLS | TLS | This paper | Sixth orbit |
|---|---|---|---|---|
| $P^{\text{years}}$ | 375.1 | 404.3 | 444.9 | 433.8 |
| $a''$ | 2.5 | 2.4 | 2.4 | 2.4 |
| $i°$ | 121.3 | 128.4 | 134.85 | 132.7 |
| $\Omega°$ | 19.1 | 27.6 | 16.4 | 13.0 |
| $T^{\text{year}}$ | 1911.7 | 1912.0 | 1905.8 | 1907.2 |
| $e$ | 0.70 | 0.80 | 0.80 | 0.81 |
| $\omega°$ | 208.6 | 215.6 | 199.2 | 193.1 |

*Note*: Orbital Elements of WDS J16160+0721 (STF 2026AB) were obtained by four different methods. See Section 3.8. Results have been truncated to one decimal place (except for eccentricity) for clarity of comparison. Columns 2 (OLS) and 3 (TLS) contain initial Orbital Elements where the ellipses were determined by ordinary least squares and total least squares, respectively, and the Orbital Elements then calculated using the Kowalski method. Column 4 contains initial Orbital Elements obtained using the method proposed in this paper. Column 5 (sixth orbit) contains the Orbital Elements currently listed in the *Sixth Catalog of Orbits of Visual Binary Stars*.

## 3.6 | Final constraint

Finally, we rejected all orbits where $R_o > R_r$, where $R_r$ is the sum of the squares of the distances between the historic positions and the ephemeris positions calculated from a rectilinear line drawn through the HIPPARCOS (via ASCC) and *Gaia DR2* positions. Clearly, if an orbit produces residuals ($R_o$) larger than those of a rectilinear motion ($R_r$) then either rectilinear motion is more likely to be present (i.e., it is a possible optical double star) or the orbital arc is still too small to distinguish between rectilinear and orbital motion.

## 3.7 | Estimating the uncertainties of the Orbital Elements

By the above method, the orbit with the lowest sum of residuals is deemed to be the best estimate of any possible orbit, provided $R_o < R_r$.

In an earlier paper, Letchford et al. (2018), we estimated the uncertainty of each Orbital Element ($\sigma_{\text{OE}}$) with the following simple equation:

$$\sigma_{\text{OE}} = \mid \text{OE} - \overline{\text{OE}} \mid \tag{31}$$

where OE is the particular Orbital Element and $\overline{\text{OE}}$ is the mean of those found, which satisfy $R_o < R_r$.

The problem with Equation (31) is that it implies that the best estimate of an Orbital Element is its mean ($\overline{\text{OE}}$). Here however the best set of Orbital Elements is *not* the mean but the set with the lowest found $R_o$, which satisfies $R_o < R_r$.

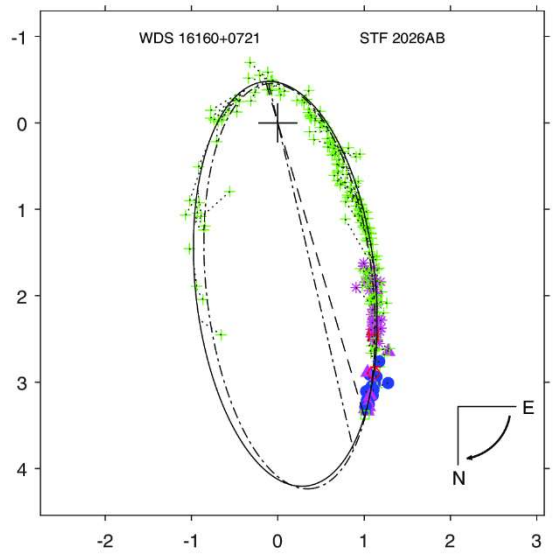


**FIGURE 1** Test double star. WDS J16160+0721 (STF 2026AB). The orbit obtained in this paper is marked by the solid black ellipse. The orbit currently in the *Sixth Catalog of Orbits of Visual Binary Stars* is the dash-dot ellipse. The primary is at 0,0 (represented by the large + sign) and the axis scales are in arcseconds. The long straight dashed line is the ascending node calculated in this paper, and the long straight dash-dot line is the ascending node from the *Sixth Catalog of Orbits of Visual Binary Stars*. Individual measures (from the *Washington Double Star Catalog* [WDS]) are color-coded: green, blue, and purple indicate micrometric, interferometric, and photographic/CCD measures, respectively, while red symbols indicate measures from space-based instruments (Hartkopf & Mason 2020). Measures are connected to their predicted locations by dotted lines

A better estimate is to use the $R_o$ for each set of Orbital Elements that satisfy $R_o < R_r$ as normalized *weights* ($w_i$), so that:

$$\sigma_{\text{OE}} = \pm\sqrt{\sum w_i\left(\text{OE}_i - \overline{\text{OE}}\right)^2} \tag{32}$$

where,

$$w_i = \frac{1}{R_{o_i}\sum \frac{1}{R_{o_i}}} \tag{33}$$

and,

$$\overline{\text{OE}} = \sum w_i \text{OE}_i \tag{34}$$

## 3.8 | Test binary double star

Any new or modified method of computing an orbit must be proven with respect to existing methods. To this end, the binary star WDS J16160+0721 (STF 2026AB) was chosen for testing as it was studied by Lobão (1994) and Sharaf et al. (2014) in their work on the Kowalski method.

**TABLE 5** Orbital Elements for five double stars from the *Working Dunlop Catalog*, at Equinox 2000.0, where $E_{binding} < 1$

| No. | WDS | Discoverer code | $P^{year}$ +/− | $a''$ +/− | $i°$ +/− | $\Omega°$ +/− | $T^{year}$ +/− | $e$ +/− | $\omega°$ +/− |
|---|---|---|---|---|---|---|---|---|---|
| 5 | 01398-5612 | DUN 5 | 620.0 | 9.9 | 120.0 | 21.0 | 1800.0 | 0.35 | 61.0 |
| | | | 750.0 | 5.7 | 4.8 | 43.0 | 210.0 | 0.15 | 63.0 |
| 38 | 07040-4337 | DUN 38AB | 55,000.0 | 110.0 | 81.0 | 170.0 | −3500.0 | 0.87 | 130.0 |
| | | | — | — | — | — | — | — | — |
| 55 | 07442-5027 | DUN 55AB | 230,000.0 | 160.0 | 95.0 | 110.0 | 91,000.0 | 0.41 | 83.0 |
| | | | 97,000.0 | 37.0 | 1.9 | 6.0 | 71,000.0 | 0.24 | 23.0 |
| 116 | 11567-3216 | DUN 116AB | 24,000.0 | 30.0 | 110.0 | 82.0 | 3600.0 | 0.69 | 100.0 |
| | | | 24,000.0 | 16.0 | 2.6 | 1.9 | 180.0 | 0.08 | 20.0 |
| 245 | 23086-5944 | DUN 245 | 37,000.0 | 23.0 | 110.0 | 110.0 | 4200.0 | 0.60 | 260.0 |
| | | | 25,000.0 | 9.3 | 2.7 | 4.0 | 500.0 | 0.13 | 22.0 |

*Note*: All results and uncertainties have been rounded to two significant figures, due to the large uncertainties. Below each Orbital Element (except for No. 38) is an estimate of its uncertainty ("+/−," Section 3.7) is given.

Both component stars of STF 2026AB have HIPPARCOS (via ASCC) and *Gaia DR2* data. It is also a Grade 3 orbit in the *Sixth Catalog of Orbits of Visual Binary Stars*, where Grade 3 orbits are described as "at least half of the orbit defined, but the lesser coverage (in number or distribution), or data consistency, leaves the possibility of larger errors than in Grade 2" (Matson et al. 2020).

Table 4 presents four sets of Orbital Elements where (a) OLS is used to obtain the ellipse coefficients, prior to determining the orbit elements by the Kowalski method (column 2); (b) TLS is used followed by the Kowalski method (column 3); (c) the method in this paper (column 4); and finally; (d) the Orbital Elements from the current *Sixth Catalog of Orbits of Visual Binary Stars* (6th orbit, source paper, Izmailov 2019) (column 5). It should be noted that the results from the method presented in this paper (column 4) and the OLS (column 2) and TLS (column 3) methods were conducted *without* weighting the historic data and *without* any outliers removed. Thus, they do not represent a final solution, but initial estimates that can be improved upon by further processing.

From Table 4 and Figure 1, it can be seen that of the three methods presented, the results obtained by the method presented in this paper are closest to the currently published values in the *Sixth Catalog of Orbits of Visual Binary Stars* in six of the seven Orbital Elements.

## 4 | RESULTS AND DISCUSSION: ORBITAL ELEMENTS

Of the 40 double stars from the *Working Dunlop Catalog* whose binding energies were calculated, eight are considered probable binaries (Table 3). Of the eight candidate binaries selected, five generated orbits (Nos. 5, 38, 55, 116, and 245). The remaining three (Nos. 80, 232, and 242) failed to generate orbits probably due either to the stringent constraints (namely: a ±10% combined mass tolerance; the requirement that the 1991.25 and 2015.5 (equinox 2000.0) calculated positions fall within the 1$\sigma$ error ellipse of the HIPPARCOS (via ASCC) and *Gaia DR2* positions; and a search limited to 4′ from the primary, see Section 3), or to the possibility that the arcs are still too short for the technique to distinguish between rectilinear and orbital motion (Section 3.6).

Sets of Orbital Elements for the five binary double stars are given in Table 5. All Orbital Elements in Table 5 are at Equinox 2000.0. Column 1 of Table 5 is the number of the pair in the *Dunlop Catalog*, column 2 is the designation of the double star system in the WDS, column 3 is the Discoverer code of the particular double star used in the WDS (Disc), and columns 4–10 are the Orbital Elements as defined in the *Sixth Catalog of Orbits of Visual Binary Stars* (Matson et al. 2020). Associated orbital plots are given in the Appendix.

Table 6 presents the mean and median values of the orbital periods ($P$) and semi-major axes ($a$) of the five orbits found from the computational technique presented above. The mean orbital period is ~81,000 years and the mean semi-major axis is ~76″. Comparing our results in Table 6 with those of the *Sixth Catalog of Orbits of Visual Binary Stars* in Table 1, it is clear that these orbits are Grade 5 orbits and extend the scope of possible orbits beyond those of "close" binaries.

As expected, the uncertainties of the Orbital Elements are large. The average percentage uncertainties of the Orbital Elements in Table 5, in $P$, $a$, $i$, $\Omega$, $e$, and $\omega$ are 83, 44, 3, 54, 34, and 40%, respectively. The average value of the uncertainty in $T$ is 3600 years, ~4% of the average period, $P$, of 81,000 years.

**TABLE 6** Statistics on orbits for Nos. 5, 38, 55, 116, and 245

| Grade | $P^{years}_{mean}$ | $P^{years}_{median}$ | $a''_{mean}$ | $a''_{median}$ |
|---|---|---|---|---|
| 5 | 81,000 | 37,000 | 76 | 30 |

*Note*: Numbers in columns 3–6 have been rounded to two significant figures, because of the large uncertainties inherent in each of the three sets of Orbital Elements.

In the case of No. 38, the proposed method did not produce uncertainties because only one orbit could be found that satisfied the curvature criteria $R_o < R_r$.

One binary double star detected in the *Working Dunlop Catalog*, DUN 5 has a Grade 4 orbit in the current *Sixth Catalog of Orbits of Visual Binary Stars*, taken from Scardia et al. (2018). Our Orbital Elements are close to those in the *Sixth Catalog of Orbits of Visual Binary Stars* (for example, our orbital period and semi-major axis of ~623 years and ~9.9″, respectively, are both only ~25% larger than the current respective measures in the *Sixth Catalog of Orbits of Visual Binary Stars*). We also include uncertainties for DUN 5, as none are given in the current *Sixth Catalog of Orbits of Visual Binary Stars*.

## 5 | CONCLUSION

Presented here is an unbiased, computationally-based method of determining orbits that are defined by short arcs. High precision astrometric measures were utilized as historic measures of less accuracy. Stellar mass data were incorporated and physical constraints were applied. Multiple random orbits were generated and compared with modern and historic measures, and the fit to the measures was optimized to define the orbit and its uncertainties. Our test binary star STF 2026AB (Section 3.8), and DUN 5, yielded results close to those in the current *Sixth Catalog of Orbits of Visual Binary Stars*.

We proposed Grade 5 Orbital Elements for five double stars from the *Working Dunlop Catalog* (Table 6), Nos. 5, 38, 55, 116, and 245. We recommend that Orbital Elements for Nos. 38 and 55 be included in the *Sixth Catalog of Orbits of Visual Binary Stars*.

## ACKNOWLEDGMENTS

This research has made use of NASA's Astrophysics Data System, operated at CDS, Strasbourg, France; the SIMBAD database, operated at CDS, Strasbourg, France; the *Aladin sky atlas* developed at CDS, Strasbourg Observatory, France; the *Sixth Catalog of Orbits of Visual Binary Stars* maintained by the United States Naval Observatory; the *Washington Double Star Catalog* (WDS) maintained by the United States Naval Observatory; We particularly wish to acknowledge the many binary orbit "computers" in the 19th and 20th centuries who labored long and hard to calculate orbits with little more than pencil and graph paper. Open access publishing facilitated by University of Southern Queensland, as part of the Wiley - University of Southern Queensland agreement via the Council of Australian University Librarians.

## ORCID

*Roderick R. Letchford* https://orcid.org/0000-0002-9753-9058
*Graeme L. White* https://orcid.org/0000-0002-4914-6292
*Carolyn J. Brown* https://orcid.org/0000-0001-6649-4531

## REFERENCES

Aarseth, S., Tout, C. A., & Mardling, R. 2008, *The Cambridge NBody Lectures*, Springer (Berlin Heidelberg).
Aitken, R. G. 1964, *The Binary Stars*, Dover Publications (New York).
Belorizky, D. 1949, *MNRAS*, *109*, 596.
Benacquista, M. 2012, *An Introduction to the Evolution of Single and Binary Stars*, Springer (New York).
van den Bos, W. H. 1926, *CiUO*, *68*, 354.
van den Bos, W. H. 1962, *PASP*, *74*, 297.
Ćatović, Z., & Olević, D. 1992, in: *IAU Colloq. 135: Complementary Approaches to Double and Multiple Star Research*, eds. H. A. McAlister & W. I. Hartkopf, Vol. *32*, Astronomical Society of the Pacific, San Francisco, CA, 217.
Ćatović, Z., & Olević, D. 1995, *Bull. Astron. Belgrade*, *152*, 65.
Chanamé, J., & Gould, A. 2004, *ApJ*, *601*, 289.
Docobo, J. A. 1985, *Celest. Mech.*, *36*, 143.
Docobo, J. A. 2012, in: *Orbital Couples: Pas de Deux in the Solar System and the Milky Way*, eds. F. Arenou & D. Hestroffer, Observatoire de Paris, Paris, 119.
Docobo, J. A., Tamazian, V. S., & Campo, P. P. 2018, *MNRAS*, *476*, 2792.
Dommanget, J. 1967, *Définition de l'objet "étoile double": Exposé Introductif*. Springer, Dordrecht, The Netherlands.
Dommanget, J. 1995, *A&A*, *301*, 919.
Dunlop, J. 1829, *MNRAS*, *3*, 257.
Duric, N. 2004, *Advanced Astrophysics*, Cambridge University Press, Cambridge, UK.
Gaia Collaboration, Brown, A. G. A., Vallenari, A., et al. 2018, *A&A*, *616*, A1.
Glasenapp, S. 1889, *MNRAS*, *49*, 276.
Guinan, E. F., Harmanec, P., & Hartkopf, W. 2007, in: *Binary Stars as Critical Tools & Tests in Contemporary Astrophysics*, eds. W. I. Hartkopf, P. Harmanec, & E. F. Guinan, Vol. *240*, Cambridge University Press, Cambridge, UK, 5.
Halbwachs, J. L., Mayor, M., & Udry, S. 2012, *MNRAS*, *422*, 14.
Halir, R., & Flusser, J. 1998, Numerically Stable Direct Least Squares Fitting of Ellipses. Retrieved from http://wscg.zcu.cz/wscg1998/wscg98.htm
Hartkopf, W. I., & Mason, B. D. 2020, Second Catalog of Rectilinear Elements. United States Naval Observatory. Retrieved from http://www.astro.gsu.edu/wds/lin2.html
Hartkopf, W. I., Mason, B. D., & Worley, C. E. 2001, *AJ*, *122*, 3472.
Hartkopf, W. I., Mason, B. D., Finch, C. T., Zacharias, N., Wycoff, G. L., & Hsu, D. 2013, *AJ*, *146*, 1.

Heintz, W. D. 1978, *Double Stars*, Vol. *15*, Reidel, Dordrecht, The Netherlands.
Izmailov, I. S. 2019, *Astron. Lett.*, *45*, 30.
Johnson, D. R. H., & Soderblom, D. R. 1987, *AJ*, *93*, 864.
Kervella, P., Thévenin, F., & Lovis, C. 2017, *A&A*, *598*, 1.
Kharchenko, N. V. 2001, *KFNT*, *17*, 409.
Kouwenhoven, M. B. N., Goodwin, S. P., Parker, R. J., Davies, M. B., Malmberg, D., & Kroupa, P. 2010, *MNRAS*, *404*, 1835.
Kowalski, M. A. 1873, *Izvestiya I Uchenye Zapiski Kazanskogo Universiteta*, *40*, 329.
Letchford, R. R., White, G. L., & Ernest, A. D. 2018, *J. Double Star Obs.*, *14*, 761.
Letchford, R. R., White, G. L., & Ernest, A. D. 2019, *J. Double Star Obs.*, *15*, 394.
Letchford, R. R., White, G. L., & Brown, C. J. 2022, *MNRAS*, *510*, 5330.
Lobão, D. C. 1994, Determination of the Orbital Elements of a Visual Binary Star, 1–15.
Longhitano, M., & Binggeli, B. 2010, in: *Binaries – Key to Comprehension of the Universe*, eds. A. Prša & M. Zejda, Vol. *435*, Astronomical Society of the Pacific (San Francisco, CA), 67.
Mason, B. D., Douglass, G. G., & Hartkopf, W. I. 1999, *AJ*, *117*, 1023.
Mason, B. D., Wycoff, G. L., Hartkopf, W. I., Douglass, G. G., & Worley, C. E. 2001, *AJ*, *122*, 3466.
Matson, R. A., Williams, S. J., Hartkopf, W. I., & Mason, B. D. 2020, Sixth Catalog of Orbits of Visual Binary Stars. United States Naval Observatory. Retrieved from http://www.astro.gsu.edu/wds/orb6.html
Moeckel, N., & Bate, M. R. 2010, *MNRAS*, *404*, 721.
Németh, P., Ziegerer, E., Irrgang, A., Geier, S., Fürst, F., Kupfer, T., & Heber, U. 2016, *ApJ*, *821*, L13.
Olević, D., & Cvetković, Z. 2004, *A&A*, *415*, 259.
Olević, D., & Cvetković, Z. 2005, *ASRB*, *5*, 237.
Perryman, M. A. C. 1997, *Transformation of Astrometric Data and Associated Error Propagation*, Vol. *1*, European Space Agency (Noordwijk).
Perryman, M. A. C., Lindegren, L., Kovalevsky, J., et al. 1997, *A&A*, *500*, 501.
Savary, F. 1827a, *CDT pour*, *1830*, 163.
Savary, F. 1827b, *CDT pour*, *1830*, 56.
Scardia, M., Prieur, J. L., Pansecchi, L., Argyle, R. W., Zanutta, A., & Aristidi, E. 2018, *Astron. Nach.*, *339*, 571.
See, T. J. J. 1896, *Researches on the Evolution of Stellar Systems*, Vol. *I*, T. P. Nichols (Lynn, MA), 41.
Sharaf, M. A., Saad, A. S., & Alshaery, A. A. 2014, *Aust. J. Basic Appl. Sci.*, *8*, 640.
Sinachopoulos, D. 1991, *Astron. Astrophys. Suppl. Ser.*, *87*, 453.
Smart, W. M. 1930, *MNRAS*, *90*, 534.
White, G., Letchford, R., & Ernest, A. 2018, *J. Double Star Obs.*, *14*, 432.
Wiley, E. O., & Rica, F. M. 2015, *J. Double Star Obs.*, *11*, 2.
Worley, C. E. 1990, in: Errors, Bias and Uncertainties in Astronomy, Proceedings of a Meeting held in Strasbourg, September 1989, eds. C. Jaschek, & F. Murtagh, Cambridge UK: Cambridge University Press, 419.

## AUTHOR BIOGRAPHY

The first author is currently completing his Ph.D. in Astrophysics at the University of Southern Queensland. He teaches at Vianney College Seminary, Wagga Wagga NSW Australia.

**How to cite this article:** Letchford, R. R., White, G. L., & Brown, C. J. 2022, *Astron. Nachr.*, *343*, e210113. https://doi.org/10.1002/asna.20210113

## APPENDIX: PLOTS OF BINARY DOUBLE STARS

A total of 40 double stars from the *Working Dunlop Catalog* had sufficient *Gaia DR2* data for their binding energies to the calculated. Of those 40, just two had binding energies $< 0$ (Nos. 38, and 55), indicating that they are most probably binary double stars.

Plots of the two probable binary double stars and No. 5 are presented here, and their Orbital Elements (rounded to two significant figures) are listed in Table 6. Refer to Figure 1 for an explanation of the contents of each Figure. Plots of two other orbits are displayed; No. 116 and 245. Double stars Nos. 5, 116, and 245 returned $0 < E_{\text{binding}} < 1$. No. 5 is currently in the *Sixth Catalog of Orbits of Visual Binary Stars*.

Note that the orbital plots rely on the non-rounded Orbital Elements to ensure that each orbit passes through the $1\sigma$ uncertainty ellipses of the HIPPARCOS (via ASCC) and *Gaia DR2* positions.

The orbit plot of DUN 5 (Section 4), a double star for which there are currently Orbital Elements in the *Sixth Catalog of Orbits of Visual Binary Stars*, includes a comparison plot of the Orbital Elements in the *Sixth Catalog of Orbits of Visual Binary Stars*, marked by a dash-dot line. It is discussed in Section 4 (Figures A1–A5).

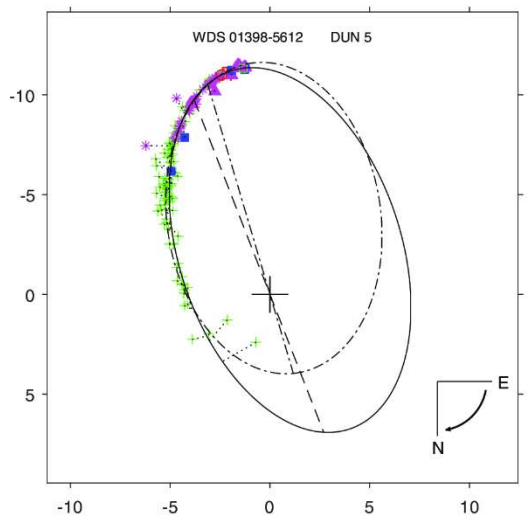


FIGURE A1 No. 5 01398-5612 DUN 5

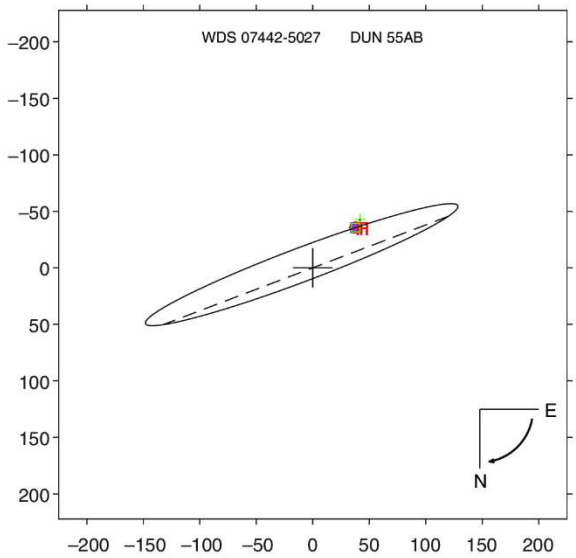


FIGURE A3 No. 55 07442-5027 DUN 55AB

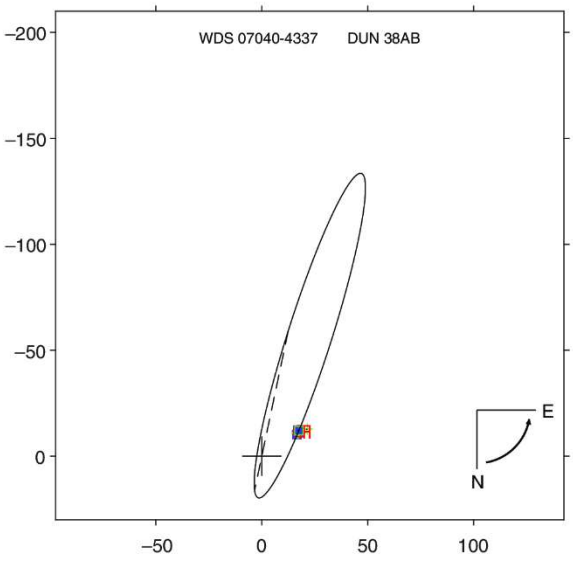


FIGURE A2 No. 38 07040-4337 DUN 38AB

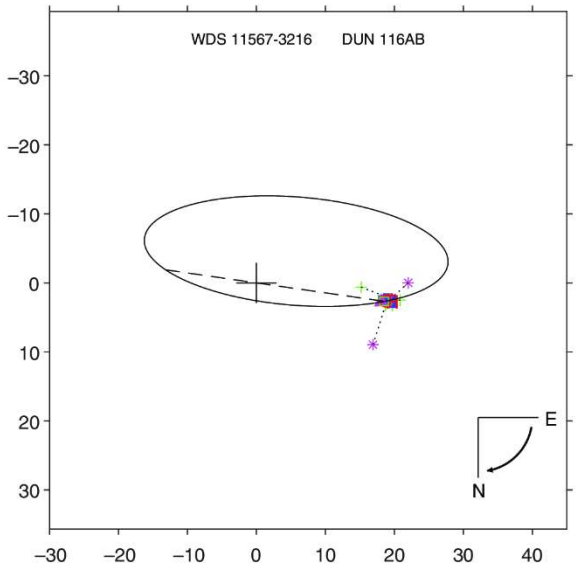


FIGURE A4 No. 116 11567-3216 DUN 116AB

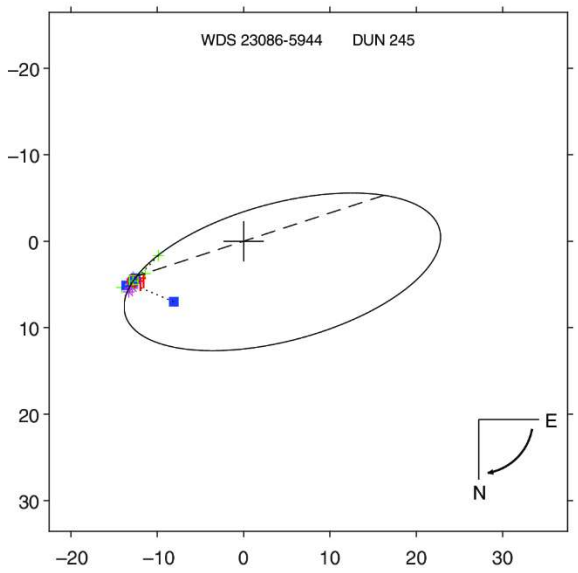


**FIGURE A5** No. 245 23086-5944 DUN 245

## 4.3 LINKS AND IMPLICATIONS FOR NEXT STUDY

The method used in Paper 2 to detect confirmed binary double stars was modified and then applied in Paper 3 to detect confirmed optical double stars from the *Working Dunlop Catalogue*. Binary double stars are here defined as double stars whose binding energy is less than zero. Therefore, any double star which is not a binary star, that is, whose binding energy is greater than zero, is unbound and therefore must be considered as an optical double star. A new technique was developed to describe their relative motion in a straight (rectilinear) line.

# CHAPTER 5: PAPER 3 - RECTILINEAR ELEMENTS OF VISUAL OPTICAL DOUBLE STARS: WITH APPLICATION TO THE 1829 SOUTHERN DOUBLE STAR CATALOGUE OF JAMES DUNLOP

## 5.1 INTRODUCTION

Paper 3 proposes a new technique for characterising the rectilinear motion of the secondary of a confirmed optical star with that of a fixed primary. A similar method employed in Paper 2 used to confirm the presence of a binary star was modified to confirm the presence of an optical double star. The new technique to characterise rectilinear motion is then presented, tested on a select set of double stars from the SCORE, and then applied to the 14 confirmed optical double stars in the *Working Dunlop Catalogue*. The resultant uncertainties are, on average, an order of magnitude smaller than the method currently accepted in this field.

Letchford, R. R., White, G. L., & Brown, C. J. 2022, *Astron. Nachr.*, 343, 1-14, e20220018. https://doi.org/10.1002/asna.20220018.

# 5.2 PAPER 3 AS PUBLISHED



Received: 11 March 2022 | Revised: 28 April 2022 | Accepted: 5 May 2022

DOI: 10.1002/asna.20220018

Astronomische Nachrichten

REVIEW ARTICLE

# Rectilinear elements of visual optical double stars: With application to the 1829 southern double star catalogue of James Dunlop

**Roderick R. Letchford** | **Graeme L. White** | **Carolyn J. Brown**

Centre for Astrophysics, University of Southern Queensland, Toowoomba, Queensland, Australia

**Correspondence**
Roderick R. Letchford, Centre for Astrophysics, University of Southern Queensland, Toowoomba 4350, QLD, Australia.
Email: rod.letchford@usq.edu.au

**Abstract**

The relative Rectilinear motion of optical double stars provides an important clue to the relationship of the components. We provide an objective method of confirming the optical status of double stars, and of obtaining unbiased rectilinear elements solely on data obtained from the HIPPARCOS and *Gaia DR2* space missions. We apply this technique to determine the rectilinear elements of 14 optical double stars from the southern double star catalogue of James Dunlop. The resultant uncertainties are, on average, an order of magnitude smaller than the method currently used.

**KEYWORDS**

astrometry, binaries: visual, celestial mechanics, stars: kinematics

## 1 | INTRODUCTION

Distinguishing between optical and binary double stars has important ramifications for many aspects of astrophysics (Letchford et al. 2022b, paper II). The rectilinear elements of optical double stars describe the on-sky projection of the linear motion of the secondary star compared with the primary. The *United States Naval Observatory* (USNO) maintains the *Second Catalogue of Rectilinear Elements* (Hartkopf & Mason 2020), hereafter referred to as the SCORE, which contains the rectilinear elements of over 1,200 double stars, determined from historic astrometric measures with typical uncertainties of ∼0.2 arcseconds (″), and uncertainties in average relative proper motion of ∼3 milli-arcseconds per year (mas year$^{-1}$).

The first attempt to describe the relative linear motion of an optical double star was by Schlesinger & Alter (1912) (they provide no references to earlier work), who used a least squares method on historic measures after precession to a common equinox. This method was later adopted by Torres (1985, 1988a, 1988b). Debehogne & de Freitas Mourao (1977) who undertook a comparison between the least squares method and that of mean places with differential corrections, opted for the least squares method as the best. Equations for the least squares method can be found in Torres (1988b). The SCORE rectilinear elements result from the least squares method applied to *weighted* historic measures, where weighting is described in Hartkopf et al. (2001) and Mason et al. (1999).

Rectilinear plot visualization (and rectilinear elements) has a number of important benefits. Any erroneous, or poor measures, are readily identified and non-linear motion resulting from orbital motion of a binary system is easily visualized by curvature in the linear path of the companion, as are nonlinear sub-motions due

to close additional components such as astrometric binaries (Hartkopf & Mason 2020). In addition, well-defined linear elements provide scale calibration for imaging systems and proper motions comparable in precision with those of HIPPARCOS (Perryman et al. 1997) and *Gaia DR2* (Gaia Collaboration et al. 2018).

The aim of this paper is to present a modified method of obtaining the rectilinear elements of confirmed optical double stars from the space-based astrometry of HIPPARCOS (via ASCC, Kharchenko 2001) and *Gaia DR2* alone, and which relegates historic measures to a secondary role of confirmation of curvature or other nonlinear motion, in the Rectilinear plots. We then apply this method to a set of confirmed optical double stars.

The set of double stars from which we extract a subset of confirmed optical double stars we call the *Working Dunlop Catalogue*, which itself is a subset from the first published catalogue of southern double stars by James Dunlop (Dunlop 1829). This original 1829 catalogue will hereafter be referred to as the *Dunlop Catalogue*. A previous paper by the authors (Letchford et al. 2022a, paper I) described and analyzed the accuracy of the original 1829 *Dunlop Catalogue* based on ASCC and *Gaia DR2* source identifiers (where available). A digitized version is available on the website of paper I under supplementary data.[1] The *Working Dunlop Catalogue* is defined in paper II and is a subset of 40 pairs from the original *Dunlop Catalogue* (of 253 pairs), which have entries in the *The Washington Double Star Catalogue* (WDS, Mason et al. 2001) and for which accurate astrometry is available, both in ASCC and *Gaia DR2*. The *Working Dunlop Catalogue* is thus a reliable and accurate catalogue of pairs with observational histories of ~200 years.

The first two authors of this paper have earlier published material on the Rectilinear motion of optical double stars (Letchford et al. 2018, 2019). This present paper is a more thorough investigation of Rectilinear motion and presents a modified technique.

Section 2 of this paper summarizes the method used in paper II for the separation of binary and optical double stars, and presents a conservative list of "confirmed" optical double stars from the *Working Dunlop Catalogue*. Section 3 proposes our technique for determining the rectilinear elements of optical double stars and compares the results with rectilinear elements from the SCORE. Section 4 presents and discusses the results of applying our technique to the confirmed optical double stars from the *Working Dunlop Catalogue*.

[1] https://doi.org/10.1093/mnras/stab3777.

**TABLE 1** Catalogue numbers from the *Dunlop Catalogue* for the 40 double stars for which binding energies $E_{\text{binding}}$ could be calculated

| Nos. | Nos. |
|---|---|
| $E_{\text{binding}}$ <0 | $E_{\text{binding}}$ >0 |
| 2 in total | 38 in total |
| 38, 55 | 2, 4, 5, 23, 26, 27, 28, 29, 40, 41, 52, 57, 73, 77, 79, 80, 114, 116, 118, 146, 155, 175, 176, 178, 184, 186, 200, 215, 225, 232, 236, 238, 241, 242, 245, 246, 248, 250 |

## 2 | METHOD: DETECTING OPTICAL DOUBLE STARS

By definition, binary double stars are double stars whose binding energy ($E_{\text{binding}}$) is less than zero (paper II). Therefore, any double star that is not a binary star, that is, whose binding energy is greater than zero, is unbound and therefore must be an optical double star.

In paper II, we selected a subset of double stars from the *Working Dunlop Catalogue* where binding energies were able to be calculated using data from *Gaia DR2*. On the available data, only two double stars had binding energies <0 and 38 had binding energies > 0. These are reiterated here in Table 1. However, large uncertainties are expected in the estimation of binding energies for individual double stars (paper II, equation 1), due to the inexact nature of calculating stellar masses from luminosity estimates (paper II, equation 2) and estimating physical distances from parallaxes (paper II, equation 3) where even a small inaccuracy in a parallax measure can lead to a large uncertainty in physical separations.

Because of the expected large uncertainties in the calculated $E_{\text{binding}}$, paper II placed a conservative criteria for "confirmed" binary double stars of (a) $E_{\text{binding}} < +1$, (b) a physical separation ($D$) such that $D - 1\sigma < 1pc$, and (c) which displayed common proper motion (CPM). With these constraints, there are eight "confirmed" binary stars (no. 5, 38, 55, 80, 116, 232, 242, and 245) in the *Working Dunlop Catalogue*.

Conversely, 14 of the 38 double stars with $E_{\text{binding}} > +1$ in Table 1 are now suggested as "confirmed" *optical* double stars since $D - 1\sigma > 1pc$ and since they displayed no CPM (paper II). These 14 double stars are given in Table 2 where Column 1 is the catalogue number of the double star from the original *Dunlop Catalogue* retained in the *Working Dunlop Catalogue* and column 2 is the system identifier from the WDS, underneath which is the Discoverer Code identifying the particular double star within the system, also from the WDS. Columns 3–5 give

**TABLE 2** Table of 14 "confirmed" optical double stars from the *Working Dunlop Catalogue*

| No. | WDS<br>Discoverer code | $E_{binding}$<br>$M_\odot$ km$^{-2}$ s$^{-2}$ | $D$<br>*pc* | No CPM |
|---|---|---|---|---|
| 4 | 01388-5327<br>DUN 4 | ~2.5 | 1.83 ± 0.56 | ✓ |
| 28 | 06240-3642<br>DUN 28AC | ~2,700 | 47.89 ± 0.83 | ✓ |
| 29 | 06291-4022<br>DUN 29 | ~8,600 | 160.5 ± 5.9 | ✓ |
| 40 | 07092-5622<br>DUN 40 | ~670 | 146.2 ± 2.4 | ✓ |
| 73 | 08562-5532<br>DUN 73AB | 3,400 | 190 ± 11 | ✓ |
| 79 | 09336-4945<br>DUN 79 | ~4,400 | 8.0 ± 2.2 | ✓ |
| 146 | 13493-4031<br>DUN 146 | ~360 | 480 ± 21 | ✓ |
| 155 | 14077-5341<br>DUN 155 | ~36 | 1200 ± 84 | ✓ |
| 178 | 15116-4517<br>DUN 178AC | ~3,000 | 10.5 ± 1.8 | ✓ |
| 184 | 15263-4252<br>DUN 184 | ~50 | 440 ± 9 | ✓ |
| 200 | 16225-4355<br>DUN 200 | ~550 | 280 ± 14 | ✓ |
| 225 | 19124-5148<br>DUN 225AB | ~1,500 | 510 ± 60 | ✓ |
| 241 | 22366-3140<br>DUN 241 | ~400 | 255.9 ± 6.5 | ✓ |
| 250 | 23272-5017<br>DUN 250 | ~37,000 | 890 ± 53 | ✓ |

*Note*: The estimated binding energies ($E_{binding}$) have been rounded to two significant figures.
Abbreviations: CPM, common proper motion; WDS, *Washington Double Star Catalogue*.

the binding energy ($E_{binding}$) in $M_\odot$ km$^{-2}$ s$^{-2}$, the physical separation of the two components of the optical double star in parsecs (*pc*), and an indication that no CPM is found (no CPM, following the methodology of Hartkopf et al. 2013).

The remaining 18 double stars could not be confirmed as either binary or optical double stars because they failed one or two of the three tests necessary for classification as either a binary *or* an optical double star; they are listed in Table 3.

## 3 | RECTILINEAR MOTION AND RECTILINEAR ELEMENTS

As mentioned in Section 1, we here determine the rectilinear elements in a relatively simple way. We take advantage of space-based astrometry where the uncertainties in the positions of the two stars are measured in milli-arcseconds (mas) and simply describe the straight line running through the HIPPARCOS and *Gaia DR2* positions. This straight line is better determined, by orders

**TABLE 3** List of 18 double stars from the *Working Dunlop Catalogue* which cannot be confirmed as either binary or optical double stars

| | Indicators for binary double stars | | | Indicators for optical double stars | | |
|---|---|---|---|---|---|---|
| **No.** | $E_{\text{binding}}$ **<1** | $D-1\sigma<1$ | **CPM** | $E_{\text{binding}}$ **>1** | $D-1\sigma>1$ | **No CPM** |
| 2 | | ✓ | ✓ | ✓ | | |
| 23 | | ✓ | ✓ | ✓ | | |
| 26 | | ✓ | ✓ | ✓ | | |
| 27 | | | ✓ | ✓ | ✓ | |
| 41 | ✓ | ✓ | | | | ✓ |
| 52 | | ✓ | ✓ | ✓ | | |
| 57 | | ✓ | | ✓ | | ✓ |
| 77 | | ✓ | ✓ | ✓ | | |
| 114 | | ✓ | ✓ | ✓ | | |
| 118 | ✓ | ✓ | | | | ✓ |
| 175 | ✓ | ✓ | | | | ✓ |
| 176 | | ✓ | ✓ | ✓ | | |
| 186 | | | ✓ | ✓ | ✓ | |
| 215 | | | ✓ | ✓ | ✓ | |
| 236 | | | ✓ | ✓ | ✓ | |
| 238 | | ✓ | | ✓ | | ✓ |
| 246 | ✓ | ✓ | | | | ✓ |
| 248 | | ✓ | ✓ | ✓ | | |

*Note*: For these pairs there is sufficient *Gaia DR2* data to calculate each of the three parameters ($E_{\text{binding}}$, $D$ and common proper motion [CPM]—see text), but they do not pass all three tests necessary for confirmation as either a binary or optical double star.

of magnitude, than a similar projection through historic measures. The rectilinear elements are derived from this straight line. The HIPPARCOS (via ASCC) mission has an epoch of observation of 1991.25 and the *Gaia DR2* mission an epoch of 2015.25, and both are at ICRS (≡ equinox 2000.0).

The formal uncertainty in this definition of the Rectilinear proper-motion vector of the secondary, determined from the HIPPARCOS and *Gaia DR2* astrometry, is dominated by the combination (in quadratic form) of the HIPPARCOS and *Gaia DR2* uncertainties in the positions of both the primary and secondary stars, and the uncertainty in the epochs of the observations (considered here to be of little consequence). These are reflected in the rectilinear elements as listed in Table 6.

Historic measures are not used in this calculation of the rectilinear elements as the uncertainties are orders of magnitude larger than those of the space-based measures. Historic measures, either weighted or unweighted, can be placed into the calculation, and onto the Rectilinear plots, not to strengthen the calculations but rather to confirm the values of the rectilinear elements determined without them. Misalignment of the historic data with the Rectilinear plots, or any other variation from the straight line projection of HIPPARCOS and *Gaia DR2*, will be evidence of orbital motion or some form of third body in the system, assuming of course, that the HIPPARCOS and *Gaia DR2* positions and their proper motions are consistent within their uncertainties.

In addition, we adopt the conventional form of conversion from polar to Cartesian coordinates ($x = \rho\cos(\theta)$, $y = \rho\sin(\theta)$, and define $t0$ ($T0$ in the SCORE) to be precisely 2000.0 in every case.

The seven rectilinear elements, with our definitions, are given in Table 4 along with their uncertainties. Derivations of the Cartesian coordinates of the HIPPARCOS and *Gaia DR2* positions and their uncertainties are given in Appendix A (together with the definition of arctan2) and Appendix B, respectively. Formulae for an ephemeris are given in Table 5.

## 3.1 | Test optical double stars

Any modified method of computing rectilinear elements must be proven with respect to existing methods. A total

**TABLE 4** Definition of the rectilinear elements proposed in this paper

| Element | Units | Description | Definition | Uncertainty |
|---|---|---|---|---|
| $x0$ | as | Difference in declination (primary – secondary) at time $t0$ | $xg - xa(2015.5 - t0)$ | $\sigma_{x0} = \pm\sqrt{[(2015.5 - t0)\sigma_{xa}]^2 + \sigma_{xg}^2}$ |
| $xa$ | as year$^{-1}$ | Rate of change of declination | $(xg - xh)/(2015.5 - 1991.25)$ | $\sigma_{xa} = \pm\sqrt{\frac{\sigma_{xg}^2 + \sigma_{xh}^2}{(2015.5-1991.25)^2}}$ |
| $y0$ | as | Difference in right ascension (primary – secondary) at time $t0$ | $yg - ya(2015.5 - t0)$ | $\sigma_{y0} = \pm\sqrt{[(2015.5 - t0)\sigma_{ya}]^2 + \sigma_{yg}^2}$ |
| $ya$ | as year$^{-1}$ | Rate of change of right ascension | $(yg - yh)/(2015.5 - 1991.25)$ | $\sigma_{ya} = \pm\sqrt{\frac{\sigma_{yg}^2 + \sigma_{yh}^2}{(2015.5-1991.25)^2}}$ |
| $t0$ | year | Time $t0$ | 2000.0 | $\sigma_{t0} = 0$ |
| $\theta 0$ | deg | Position angle of secondary relative to primary at time $t0$ | $\frac{180}{\pi}\arctan 2(y0, x0)$ | $\sigma_{\theta 0} = \pm\frac{180}{\pi}\sqrt{\frac{(x0\sigma_{y0})^2 + (y0\sigma_{x0})^2}{(x0^2 + y0^2)^2}}$ |
| $\rho 0$ | as | Separation of primary and secondary at time $t0$ | $\sqrt{x0^2 + y0^2}$ | $\sigma_{\rho 0} = \pm\sqrt{\frac{(x0\sigma_{x0})^2 + (y0\sigma_{y0})^2}{x0^2 + y0^2}}$ |

*Note*: Definitions and mathematical derivations of the Cartesian coordinates of the HIPPARCOS and *Gaia DR2* positions ($xh$,$yh$ and $xg$,$yg$, respectively) and their uncertainties ($\sigma_{xh}$,$\sigma_{yh}$ and $\sigma_{xg}$,$\sigma_{yg}$), respectively, are given in Appendices A and B, respectively.

**TABLE 5** Formulae for calculating an ephemeris

| Position | Units | Description | Definition | Uncertainty |
|---|---|---|---|---|
| $x_{\mathrm{Eph}}$ | as | Difference in declination (primary – secondary) at time $t_{\mathrm{Eph}}$ | $xa(t_{\mathrm{Eph}} - t0) + x0$ | $\sigma_{x\mathrm{Eph}} = \pm\sqrt{\left[\left(t_{\mathrm{Eph}} - t0\right)\sigma_{xa}\right]^2 + \sigma_{x0}^2}$ |
| $y_{\mathrm{Eph}}$ | as | Difference in right ascension (primary – secondary) at time $t_{\mathrm{Eph}}$ | $ya(t_{\mathrm{Eph}} - t0) + y0$ | $\sigma_{y\mathrm{Eph}} = \pm\sqrt{\left[\left(t_{\mathrm{Eph}} - t0\right)\sigma_{ya}\right]^2 + \sigma_{y0}^2}$ |
| $\theta_{\mathrm{Eph}}$ | deg | Position angle of secondary relative to primary at time $t_{\mathrm{Eph}}$ | $\frac{180}{\pi}\arctan 2\left(y_{\mathrm{Eph}}, x_{\mathrm{Eph}}\right)$ | $\sigma_{\theta\mathrm{Eph}} = \pm\frac{180}{\pi}\sqrt{\frac{\left(x_{\mathrm{Eph}}\sigma_{y_{\mathrm{Eph}}}\right)^2 + \left(y_{\mathrm{Eph}}\sigma_{x_{\mathrm{Eph}}}\right)^2}{\left(x_{\mathrm{Eph}}^2 + y_{\mathrm{Eph}}^2\right)^2}}$ |
| $\rho_{\mathrm{Eph}}$ | as | Separation of primary and secondary at time $t_{\mathrm{Eph}}$ | $\sqrt{x_{\mathrm{Eph}}^2 + y_{\mathrm{Eph}}^2}$ | $\sigma_{\rho\mathrm{Eph}} = \pm\sqrt{\frac{\left(x_{\mathrm{Eph}}\sigma_{x_{\mathrm{Eph}}}\right)^2 + \left(y_{\mathrm{Eph}}\sigma_{y_{\mathrm{Eph}}}\right)^2}{x_{\mathrm{Eph}}^2 + y_{\mathrm{Eph}}^2}}$ |

*Note*: $t_{\mathrm{Eph}}$ is the time in decimal years for which an ephemeris is required.

of 11 double stars in the *Working Dunlop Catalogue* also have entries in the SCORE (some of which could not be confirmed here as optical double stars), from which a comparison of rectilinear elements can be made, after the rectilinear elements from the SCORE have been converted to $T0 = 2000.0$. Table 6 lists the rectilinear elements taken directly from the SCORE (without conversion), and the rectilinear elements derived from the method proposed in this paper. Column 1 gives the catalogue number from the original *Dunlop Catalogue*, and column 2 gives the WDS system name and underneath the Discoverer Code. Columns 3–9 give the rectilinear elements from this paper and the corresponding ones from the SCORE.

The results of our comparison between our rectilinear elements and those from the SCORE on the test sample of 11 double stars in Table 6 are summarized in Table 7. Column 1 of Table 7 lists our rectilinear elements with the SCORE equivalents in brackets. Columns 2–5 give the number of each of our Rectilinear Element's uncertainty that falls within $1\sigma$, $2\sigma$, and $3\sigma$, and greater than $3\sigma$ of the corresponding uncertainty from the SCORE, respectively.

We compared the rectilinear elements generated with those in the SCORE by:

- using the rectilinear elements of the 11 double stars in the SCORE to generate an ephemeris for $t_{\mathrm{Eph}} = 2000.0$ (necessary as our $\theta 0$ and $\rho 0$ are all at 2000.0 and the corresponding elements from the SCORE, THETA0 and RHO0 respectively, are at different epochs);
- recalling that our $xa$ and $ya$ are equivalent to $YA$ and $XA$ from the SCORE, respectively; and

**TABLE 6** Test sample of rectilinear elements of 11 double stars from the *Working Dunlop Catalogue* that also have entries in the SCORE

| No. | WDS<br>Discoverer code | *x*0 (DE)″<br>+/−<br>*Y*0 (DE)″<br>+/− | *xa*″/year<br>+/−<br>*YA*″/year<br>+/− | *y*0 (RA)″<br>+/−<br>*X*0 (RA)″<br>+/− | *ya*″/year<br>+/−<br>*XA*″/year<br>+/− | *t*0 year<br><br>*T*0 year | *θ*0°<br>+/−<br>THETA0°<br>+/− | *ρ*0″<br>+/−<br>RHO0″<br>+/− |
|---|---|---|---|---|---|---|---|---|
| 27 | 06163-5913 | −20.723058 | 0.107208 | −27.500542 | 0.072198 | 2000.000 | 233.000 | 34.434 |
| | DUN 27AB | 0.000105 | 0.000006 | 0.000257 | 0.000017 | | 0.000 | 0.000 |
| | | −22.026257 | 0.109352 | −28.366165 | 0.071572 | 1987.755 | 232.170 | 35.914 |
| | | 0.060615 | 0.002781 | 0.030768 | 0.001412 | | 0.080 | 0.044 |
| 29 | 06291-4022 | −30.146026 | −0.026564 | 57.018287 | −0.055537 | 2000.000 | 117.866 | 64.497 |
| | DUN 29 | 0.000102 | 0.000006 | 0.000382 | 0.000025 | | 0.000 | 0.000 |
| | | −29.801716 | −0.027721 | 57.704216 | −0.056859 | 1988.246 | 117.310 | 64.946 |
| | | 0.054306 | 0.000944 | 0.037148 | 0.000646 | | 0.050 | 0.041 |
| 151 | 13573-5602 | 21.095364 | 0.083706 | 29.543929 | 0.234760 | 2000.000 | 54.472 | 36.302 |
| | DUN 151AB | 0.000426 | 0.000016 | 0.000518 | 0.000032 | | 0.001 | 0.000 |
| | | 19.707088 | 0.083942 | 25.497437 | 0.234590 | 1982.651 | 52.300 | 32.226 |
| | | 0.082986 | 0.001178 | 0.035395 | 0.000503 | | 0.120 | 0.058 |
| 163 | 14380-5431 | −14.686554 | 0.027036 | 62.645700 | 0.071106 | 2000.000 | 103.194 | 64.344 |
| | DUN 163 | 0.000115 | 0.000006 | 0.000372 | 0.000024 | | 0.000 | 0.000 |
| | | −15.076161 | 0.024868 | 61.561581 | 0.070268 | 1984.638 | 103.760 | 63.381 |
| | | 0.057987 | 0.001004 | 0.037107 | 0.000643 | | 0.050 | 0.039 |
| 178 | 15116-4517 | −6.249198 | −0.061738 | −30.141038 | 0.049520 | 2000.000 | 258.287 | 30.782 |
| | DUN 178AC | 0.000104 | 0.000006 | 0.000453 | 0.000029 | | 0.000 | 0.000 |
| | | −5.657417 | −0.060943 | −30.675056 | 0.048137 | 1989.454 | 259.550 | 31.192 |
| | | 0.054860 | 0.001079 | 0.061269 | 0.001205 | | 0.100 | 0.061 |
| 187 | 15336-4732 | −19.271781 | 0.021731 | −15.064421 | 0.064620 | 2000.000 | 218.014 | 24.461 |
| | DUN 187 | 0.010378 | 0.000670 | 0.006532 | 0.000421 | | 0.019 | 0.009 |
| | | −18.898331 | −0.000165 | −15.465071 | 0.074130 | 1996.419 | 219.290 | 24.420 |
| | | 0.106683 | 0.002485 | 0.051082 | 0.001190 | | 0.180 | 0.089 |
| 203 | 16331-6054 | 2.729017 | 0.103470 | −22.019539 | 0.073548 | 2000.000 | 277.065 | 22.188 |
| | DUN 203 | 0.000100 | 0.000006 | 0.009531 | 0.000615 | | 0.003 | 0.009 |
| | | 1.002347 | 0.101794 | −23.280334 | 0.071153 | 1983.182 | 272.470 | 23.302 |
| | | 0.053328 | 0.001080 | 0.065672 | 0.001330 | | 0.130 | 0.066 |
| 214 | 17133-6712 | 36.329818 | 0.080494 | 8.998040 | 0.146916 | 2000.000 | 13.911 | 37.428 |
| | DUN 214AB | 0.003453 | 0.000223 | 0.002306 | 0.000149 | | 0.004 | 0.003 |
| | | 35.404930 | 0.079604 | 7.425738 | 0.151083 | 1988.470 | 11.850 | 36.175 |
| | | 0.118374 | 0.002824 | 0.116790 | 0.002786 | | 0.190 | 0.118 |
| 219 | 17589-3652 | −14.413043 | −0.057786 | −51.139547 | −0.035364 | 2000.000 | 254.260 | 53.132 |
| | DUN 219AB | 0.004029 | 0.000260 | 0.002339 | 0.000151 | | 0.004 | 0.003 |
| | | −13.562767 | −0.063280 | −50.699947 | −0.034422 | 1985.265 | 255.020 | 52.483 |
| | | 0.106047 | 0.002934 | 0.053613 | 0.001483 | | 0.110 | 0.059 |

**TABLE 6** (Continued)

| No. | WDS Discoverer code | $x0$ (DE)″ +/− $Y0$ (DE)″ +/− | $xa$″/year +/− $YA$″/year +/− | $y0$ (RA)″ +/− $X0$ (RA)″ +/− | $ya$″/year +/− $XA$″/year +/− | $t0$ year $T0$ year | $\theta 0$° +/− THETA0° | $\rho 0$″ +/− RHO0″ +/− |
|---|---|---|---|---|---|---|---|---|
| 247 | 23180-6100 | 19.979530 | 0.099800 | −45.932176 | −0.056297 | 2000.000 | 293.508 | 50.089 |
| | DUN 247 | 0.000099 | 0.000006 | 0.000243 | 0.000016 | | 0.000 | 0.000 |
| | | 19.307772 | 0.094191 | −45.642963 | −0.057577 | 1993.129 | 292.930 | 49.559 |
| | | 0.064555 | 0.001424 | 0.088271 | 0.001947 | | 0.080 | 0.085 |
| 250 | 23272-5017 | 3.564678 | 0.029713 | 28.124534 | −0.128381 | 2000.000 | 82.776 | 28.350 |
| | DUN 250 | 0.000102 | 0.000006 | 0.001902 | 0.000123 | | 0.001 | 0.002 |
| | | 3.304039 | 0.029910 | 29.239500 | −0.127354 | 1991.423 | 83.550 | 29.426 |
| | | 0.042141 | 0.000840 | 0.034182 | 0.000681 | | 0.080 | 0.034 |

*Note*: The first set of elements ($x0$, $xa$, $y0$, $ya$, $t0$, $\theta 0$, $\rho 0$) are the result of the method proposed in this paper. For their definitions, see Table 4. The second set of elements ($Y0$, $YA$, $X0$, $XA$, $T0$, THETA0, RHO0) are those from the SCORE. Following the SCORE, the first four rectilinear elements are given to six decimal places.

**TABLE 7** Comparison of rectilinear elements from Table 6 with those from SCORE at $t0 = 2000.0$

| Rectilinear elements | <1σ | <2 σ | <3σ | >3σ |
|---|---|---|---|---|
| $x0$ (≡ $Y0$ of SCORE at 2000.0) | 10 | 10 | 10 | 1 |
| $xa$ (≡ $YA$ of SCORE at 2000.0) | 5 | 8 | 9 | 2 |
| $y0$ (≡ $X0$ of SCORE at 2000.0) | 7 | 10 | 11 | 0 |
| $ya$ (≡ $XA$ of SCORE at 2000.0) | 4 | 9 | 10 | 1 |
| $\theta 0$ (≡$\theta 0$ of SCORE at 2000.0) | 9 | 10 | 10 | 1 |
| $\rho 0$ (≡$\rho 0$ of SCORE at 2000.0) | 7 | 103 | 11 | 0 |
| Overall | 42 (64%) | 57 (86%) | 61 (92%) | 5 (8%) |

*Note*: See Section 3.1.

- then noting if our Rectilinear Element falls within $1\sigma$, $2\sigma$, $3\sigma$, or beyond $3\sigma$, of the Rectilinear Element generated by the SCORE at $t_{\mathrm{Eph}} = 2000.0$.

From Table 7, 86% of the comparison rectilinear elements fall within $2\sigma$ of the SCORE uncertainties, and our uncertainties are, on average, at least one order of magnitude smaller than those in the SCORE. In particular, our uncertainties for $\theta 0$ and $\rho 0$—the two most important parameters for a given epoch—are as little as 2 and 4%, respectively, of those from the SCORE. In addition, 4 out of 11 (36%) of our residuals (sum of distances between observed and calculated positions) are smaller than those generated from the SCORE (on residuals, see paper II). Assuming the sample of 11 is representative, then an order of 80–90% of our rectilinear elements would also fall within $2\sigma$ of the uncertainties of any Rectilinear Element generated from the SCORE.

## 4 | RESULTS AND DISCUSSION: RECTILINEAR ELEMENTS

The 14 sets of rectilinear elements of confirmed optical double stars from the *Working Dunlop Catalogue* (Table 1) are given in Table 8, and are recommended for inclusion in the SCORE. Column 1 (No.) contains the catalogue numbers from the original *Dunlop Catalogue*, and column 2 is the WDS identifier for the star system, underneath which is the Discoverer Code for the particular double star within that system. Columns 3–9 contain the rectilinear elements, underneath which are given the uncertainties from the method presented in this paper (Section 3).

Plots of the 14 optical double stars are given in Appendix C: rectilinear plots (Figures C1–C14). The primary is at 0.0 (represented by the large + sign) and the units on both axes are arcseconds. The thick black line represents the Rectilinear motion of the secondary

**TABLE 8** Rectilinear elements of the 14 "confirmed" optical double stars from the *Working Dunlop Catalogue*

| No. | WDS<br>Discoverer code | $x0''$ (≡*YO*)<br>+/− | $xa''$/yr (≡*YA*)<br>+/− | $y0''$ (≡*XO*)<br>+/− | $ya''$/year (≡*XA*)<br>+/− | $t0$ year (≡*TO*)<br>+/− | $\theta 0°$ (≡THETAO)<br>+/− | $\rho 0''$ (≡RHO0)<br>+/− |
|---|---|---|---|---|---|---|---|---|
| 4 | 01388-5327 | −2.587946 | 0.001093 | 10.006183 | −0.001618 | 2000.000 | 104.501 | 10.335 |
| | DUN 4 | 0.000098 | 0.000006 | 0.002479 | 0.000160 | | 0.003 | 0.002 |
| 28 | 06240-3642 | 17.208936 | −0.060040 | 61.278826 | −0.012771 | 2000.000 | 74.314 | 63.649 |
| | DUN 28AC | 0.000123 | 0.000007 | 0.000366 | 0.000023 | | 0.000 | 0.000 |
| 29 | 06291-4022 | −30.146026 | −0.026564 | 57.018287 | −0.055537 | 2000.000 | 117.866 | 64.497 |
| | DUN 29 | 0.000102 | 0.000006 | 0.000382 | 0.000025 | | 0.000 | 0.000 |
| 40 | 07092-5622 | −29.204218 | −0.000046 | 22.335882 | −0.009278 | 2000.000 | 142.591 | 36.767 |
| | DUN 40 | 0.005786 | 0.000373 | 0.003331 | 0.000215 | | 0.007 | 0.005 |
| 73 | 08562-5532 | 65.861664 | 0.000468 | 0.286351 | 0.022489 | 2000.000 | 0.249 | 65.862 |
| | DUN 73AB | 0.005306 | 0.000342 | 0.002650 | 0.000171 | | 0.002 | 0.005 |
| 79 | 09336-4945 | 117.722013 | 0.033202 | 76.462160 | 0.054654 | 2000.000 | 33.004 | 140.374 |
| | DUN 79 | 0.003389 | 0.000219 | 0.002040 | 0.000132 | | 0.001 | 0.003 |
| 146 | 13493-4031 | 4.056898 | −0.003984 | 66.703532 | 0.089333 | 2000.000 | 86.520 | 66.827 |
| | DUN 146 | 0.003837 | 0.000247 | 0.002593 | 0.000167 | | 0.003 | 0.003 |
| 155 | 14077-5341 | 18.360533 | −0.015981 | 1.973034 | −0.050425 | 2000.000 | 6.134 | 18.466 |
| | DUN 155 | 0.000119 | 0.000006 | 0.004866 | 0.000314 | | 0.015 | 0.001 |
| 178 | 15116-4517 | −6.249198 | −0.061738 | −30.141038 | 0.049520 | 2000.000 | 258.287 | 30.782 |
| | DUN 178AC | 0.000104 | 0.000006 | 0.000453 | 0.000029 | | 0.000 | 0.000 |
| 184 | 15263-4252 | −2.705922 | 0.023630 | 20.961041 | 0.061352 | 2000.000 | 97.356 | 21.135 |
| | DUN 184 | 0.000098 | 0.000006 | 0.007905 | 0.000510 | | 0.003 | 0.008 |
| 200 | 16225-4355 | −37.888038 | 0.014447 | −10.111217 | 0.009853 | 2000.000 | 194.942 | 39.214 |
| | DUN 200 | 0.013870 | 0.000895 | 0.012942 | 0.000835 | | 0.019 | 0.014 |
| 225 | 19124-5148 | −23.713882 | −0.009434 | −66.085579 | 0.000528 | 2000.000 | 250.260 | 70.211 |
| | DUN 225AB | 0.000124 | 0.000007 | 0.000509 | 0.000033 | | 0.000 | 0.000 |
| 241 | 22366-3140 | 79.481567 | 0.036499 | 48.658853 | 0.033682 | 2000.000 | 31.475 | 93.193 |
| | DUN 241 | 0.000140 | 0.000007 | 0.000470 | 0.000030 | | 0.000 | 0.000 |
| 250 | 23272-5017 | 3.564678 | 0.029713 | 28.124534 | −0.128381 | 2000.000 | 82.776 | 28.350 |
| | DUN 250 | 0.000102 | 0.000006 | 0.001902 | 0.000123 | | 0.001 | 0.002 |

*Note*: Following the practice of the SCORE, the first four rectilinear elements are given to six decimal places. $t0$ is exactly 2000.0. An explanation of the columns is given in Section 4.

compared with the primary as calculated in this paper. The line represents the relative proper motion of the secondary compared with the primary according to HIPPARCOS (via ASCC). The blue line represents the relative proper motion of the secondary compared with the primary according to *Gaia DR2*. In most of the plots, these three lines cannot be easily distinguished because of their similarity in magnitude and direction.

Individual unweighted historic measures for the period 1820–2020 are now plotted onto the HIPPARCOS/Gaia Rectilinear plot after precession to equinox 2000.0 and are color-coded, following Hartkopf & Mason (2020): green, blue, and purple, which indicate micrometric, interferometric, and photographic/CCD measures, respectively. A red "H" and "T" indicate HIPPARCOS and Tycho positions, respectively. A green "G" indicates the *Gaia DR2* position. Measures are connected to their predicted locations by dotted lines. A dotted line runs from the origin to the predicted relative position of the secondary at epoch 2000.0.

Overall, the mean uncertainty of the 14 positions at 2000.0 ($x0$,$y0$) is ∼3 mas and the mean uncertainty of the

calculated proper motions (*xa*,*ya*) is ∼2 mas year$^{-1}$. This compares with the SCORE (Section 1) of ∼200 mas and ∼3 mas year$^{-1}$, respectively.

## 5 | SUMMARY

We propose here a variant on the method of calculating rectilinear elements that differs from the currently accepted method by using (a) standard polar to Cartesian conversion; (b) only two high-precision space-based astrometric measures, that of HIPPARCOS (via ASCC) and *Gaia DR2*; and (c) fixing the *t*0 (*T*0) at precisely 2000.0 in every set of rectilinear elements.

With our test of rectilinear elements, the uncertainties were, on average, an order of magnitude smaller than those in the SCORE, and we expect ∼80% or higher of any rectilinear elements generated by our technique to fall within 2$\sigma$ of the uncertainties of any rectilinear elements generated using the current method.

We stress that these results were obtained *without* the inclusion of historic non-space-based measures, and suggest that the inclusion of these measures (weighed or unweighted) adds little to the computation of rectilinear elements for optical double stars. However, ongoing follow-up with terrestrial-based high-precision measures to detect both the presence of perturbers and as a check on space-based astrometry may continue to be vital.

## ACKNOWLEDGMENTS

This research has made use of: NASA's Astrophysics Data System, operated at CDS, Strasbourg, France. the SIMBAD database, operated at CDS, Strasbourg, France. The *Aladin sky atlas* developed at CDS, Strasbourg Observatory, France. The *Sixth Catalogue of Orbits of Visual Binary Stars* maintained by the United States Naval Observatory. The *Washington Double Star Catalogue* (WDS) maintained by the United States Naval Observatory. The *Second Catalogue of Rectilinear Elements* maintained by the United States Naval Observatory (SCORE). Open access publishing facilitated by University of Southern Queensland, as part of the Wiley - University of Southern Queensland agreement via the Council of Australian University Librarians.

## ORCID

*Roderick R. Letchford* https://orcid.org/0000-0002-9753-9058
*Graeme L. White* https://orcid.org/0000-0002-4914-6292
*Carolyn J. Brown* https://orcid.org/0000-0001-6649-4531

## REFERENCES

Debehogne, H., & de Freitas Mourao, R. R. 1977, *A&A*, *61*(4), 453.
Dunlop, J. 1829, *MNRAS*, *3*(1), 257.
Gaia Collaboration,Brown, A. G. A., Vallenari, A., et al. 2018, *A&A*, *616*, A1.
Hartkopf, W. I., & Mason, B. D. 2020, Second Catalog of Rectilinear Elements. Retrieved from http://www.astro.gsu.edu/wds/lin2.html.
Hartkopf, W. I., Mason, B. D., Finch, C. T., Zacharias, N., Wycoff, G. L., & Hsu, D. 2013, *AJ*, *146*(76), 1.
Hartkopf, W. I., Mason, B. D., & Worley, C. E. 2001, *AJ*, *122*(6), 3472.
Kharchenko, N. V. 2001, *KFNT*, *17*(5), 409.
Letchford, R. R., White, G. L., & Brown, C. J. 2022a, *MNRAS*, *510*, 5330.
Letchford, R. R., White, G. L., & Brown, C. J. 2022b, *Astron. Nachr*, *342*(3), 13.
Letchford, R. R., White, G. L., & Ernest, A. D. 2018, *JDSO*, *14*, 208.
Letchford, R. R., White, G. L., & Ernest, A. D. 2019, *JDSO*, *15*, 393.
Mason, B. D., Douglass, G. G., & Hartkopf, W. I. 1999, *AJ*, *117*(2), 1023.
Mason, B. D., Wycoff, G. L., Hartkopf, W. I., Douglass, G. G., & Worley, C. E. 2001, *AJ*, *122*(6), 3466.
Perryman, M. A. C., Lindegren, L., Kovalevsky, J., et al. 1997, *A&A*, *500*, 501.
Schlesinger, F., & Alter, D. 1912, *PAllO*, *2*, 13.
Torres, G. 1985, *A&AS*, *62*, 191.
Torres, G. 1988a, *A&AS*, *72*, 209.
Torres, G. 1988b, *Ap&SS*, *141*(2), 271.

## AUTHOR BIOGRAPHY

**Roderick R. Letchford** is currently completing his Ph.D. in Astrophysics at the University of Southern Queensland. He teaches at Vianney College Seminary, Wagga Wagga NSW Australia.

**How to cite this article:** Letchford, R. R., White, G. L., & Brown, C. J. 2022, *Astron. Nachr.*, e20220018. https://doi.org/10.1002/asna.20220018

## APPENDIX A. CARTESIAN COORDINATES OF HIPPARCOS AND *GAIA DR2* POSITIONS

Here we present the following coordinates:

- $xh = x$ Cartesian coordinate of the HIPPARCOS position relative to the primary, in arcseconds.
- $yh = y$ Cartesian coordinate of the HIPPARCOS position relative to the primary, in arcseconds.
- $\theta h$ = Polar coordinate of the HIPPARCOS position angle of the secondary relative the the primary, in degrees.

- $\rho h$ = Polar coordinate of the HIPPARCOS angular separation of the secondary from the primary, in arcseconds.

The procedure is the same for *Gaia DR2* coordinates, $xg$, $yg$, and $\theta g$, $\rho g$, respectively.
Let:

- RA1h = Right ascension of primary from HIPPARCOS at equinox 2000.0 (≡ ICRS) and epoch 1991.25, measured in degrees.
- DE1h = Declination of primary from HIPPARCOS at equinox 2000.0 and epoch 1991.25, measured in degrees.
- RA2h = Right ascension of secondary from HIPPARCOS at equinox 2000.0 and epoch 1991.25, measured in degrees.
- DE2h = Declination of secondary from HIPPARCOS at equinox 2000.0 and epoch 1991.25, measured in degrees.

Therefore:

$$yh'' = 3600(\mathrm{RA2h} - \mathrm{RA1h})\cos(\mathrm{DE1h})$$
$$xh'' = 3600(\mathrm{DE2h} - \mathrm{DE1h}).$$

And so:

$$\theta h^{\circ} = \begin{cases} \frac{180}{\pi}\arctan 2(yh, xh) \\ \theta h + 360, \text{if } \theta h < 0 \\ \theta h - 360, \text{if } \theta h > 360 \end{cases}$$
$$\rho h'' = \sqrt{xh^2 + yh^2}.$$

The definition of arctan2 (from paper II) is:

$$\arctan 2(Q,R) = \begin{cases} \arctan(Q/R), \text{if } R > Q \\ \frac{\pi}{2} - \arctan(Q/R), \text{if } Q > 0 \\ -\frac{\pi}{2} - \arctan(Q/R), \text{if } Q < 0 \\ \arctan(Q/R) \pm \pi, \text{if } R < 0 \\ \text{undefined, if } R = 0 \text{ and } Q = 0 \end{cases} . \quad \text{(A1)}$$

## APPENDIX B. UNCERTAINTIES OF THE CARTESIAN COORDINATES OF HIPPARCOS AND *GAIA DR2* POSITIONS

Here we derive the following uncertainties:

- $\sigma_{xh}$ = uncertainty in $xh$, in arcseconds.
- $\sigma_{yh}$ = uncertainty in $yh$, in arcseconds.

Again the procedure is the same for *Gaia DR2* uncertainties, $\sigma_{xg}$ and $\sigma_{yg}$.

Throughout, the definition of uncertainties is that of:

$$\sigma_{f(x_i)} = \pm\sqrt{\sum\left(\frac{\partial f(x_i)}{\partial x_i}\sigma_{x_i}\right)^2}, \quad \text{(B2)}$$

where $\sigma_{xi}$ is the uncertainty of an individual $x_i$.

Let:

- RAh1e = uncertainty (error) in right ascension of the primary from HIPPARCOS at equinox 2000.0 (≡ ICRS) and epoch 1991.25, measured in arcseconds.
- RAh2e = uncertainty (error) in right ascension of the secondary from HIPPARCOS at equinox 2000.0 and epoch 1991.25, measured in arcseconds.
- DEh1e = uncertainty (error) in declination of the primary from HIPPARCOS at equinox 2000.0 and epoch 1991.25, measured in arcseconds.
- DEh2e = uncertainty (error) in declination of the secondary from HIPPARCOS at equinox 2000.0 and epoch 1991.25, measured in arcseconds.

Therefore:

$$\sigma_{yh} = \pm\sqrt{\begin{array}{c}\cos(\mathrm{DEh1})^2\left(\mathrm{RAh1}e^2 + \mathrm{RAh2}e^2\right) \\ +\sin(\mathrm{DEh1})^2(\mathrm{RAh2} - \mathrm{RAh1})^2\mathrm{DEh1}e^2\end{array}}$$
$$\sigma_{xh} = \pm\sqrt{\mathrm{DEh2}e^2 + \mathrm{DEh1}e^2}.$$

The uncertainties of the polar coordinates:

$$\sigma^{\circ}_{\theta h} = \pm\frac{180}{\pi}\sqrt{\frac{(yh\sigma_{xh})^2 + (xh\sigma_{yh})^2}{(xh^2 + yh^2)^2}}$$
$$\sigma''_{\rho h} = \pm\sqrt{\frac{(xh\sigma_{xh})^2 + (yh\sigma_{yh})^2}{xh^2 + yh^2}}.$$

## APPENDIX C. RECTILINEAR PLOTS

A total of 40 double stars from the *Working Dunlop Catalogue* had sufficient *Gaia DR2* data for their binding energies to be calculated. Of those 40, a total of 14 were confirmed as optical double stars. For an explanation of the plots, see Section 4.

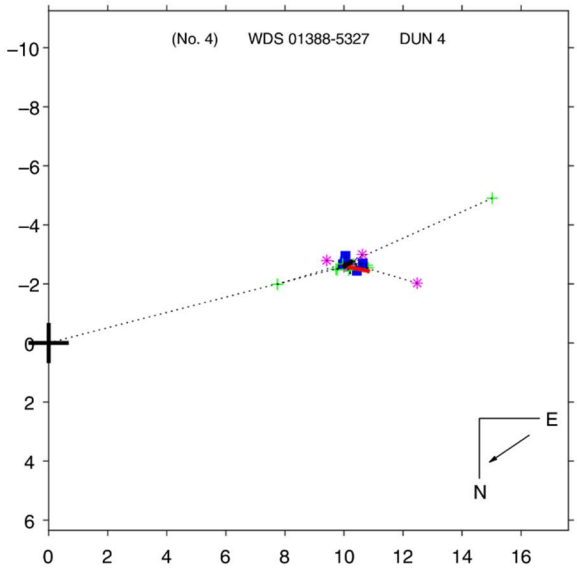


FIGURE C1 01388-5327 DUN 4

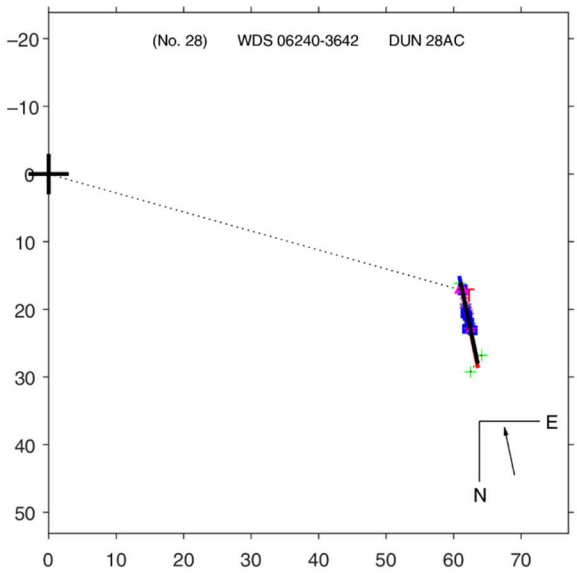


FIGURE C2 06240-3642 DUN 28AC

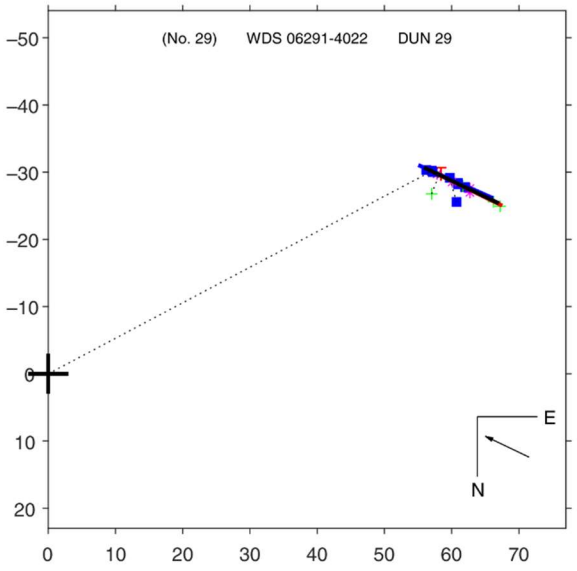


FIGURE C3 06291-4022 DUN 29

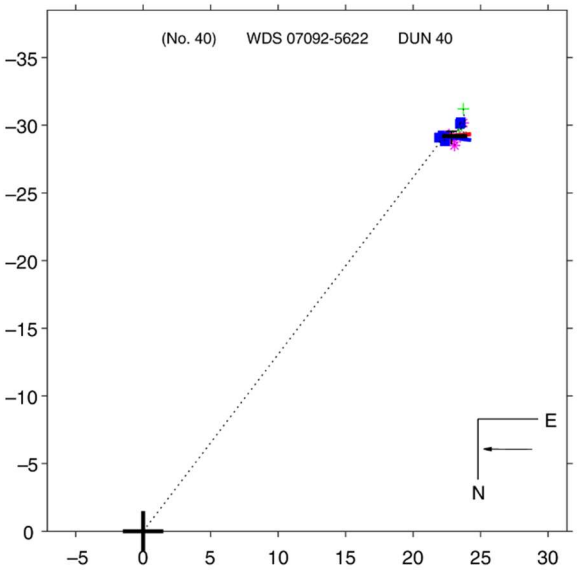


FIGURE C4 07092-5622 DUN 40

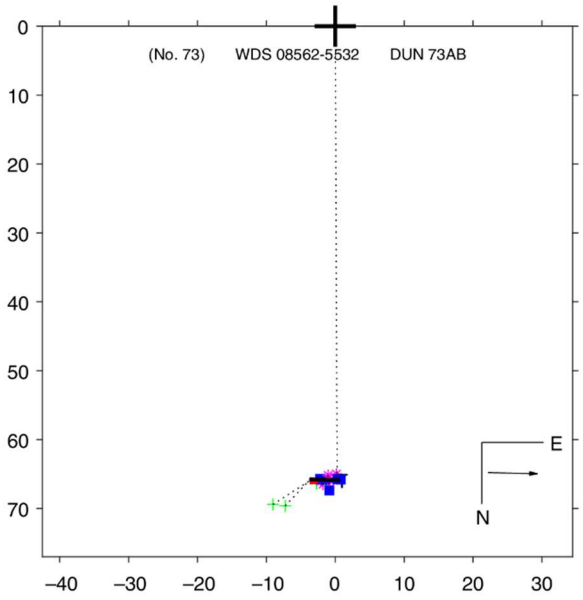


FIGURE C5 08562-5532 DUN 73AB

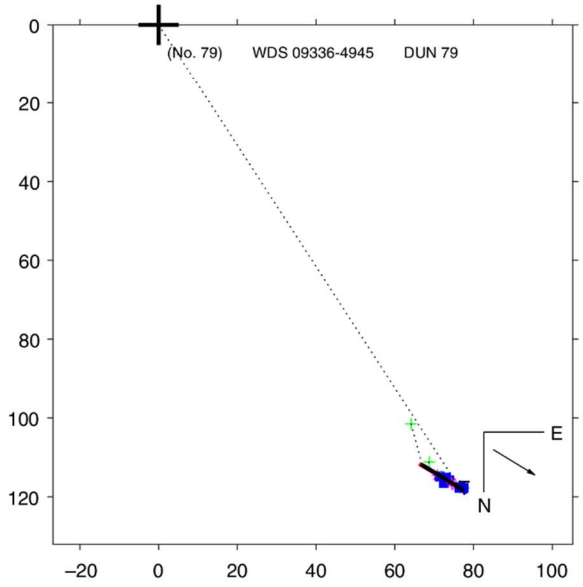


FIGURE C6 09336-4945 DUN 79

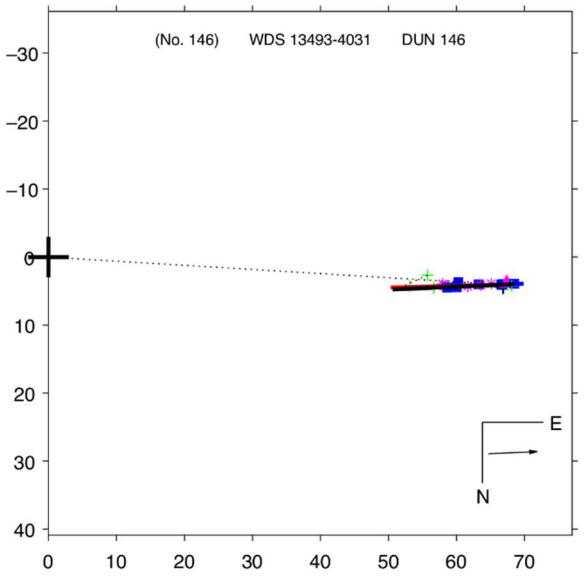


FIGURE C7 13493-4031 DUN 146

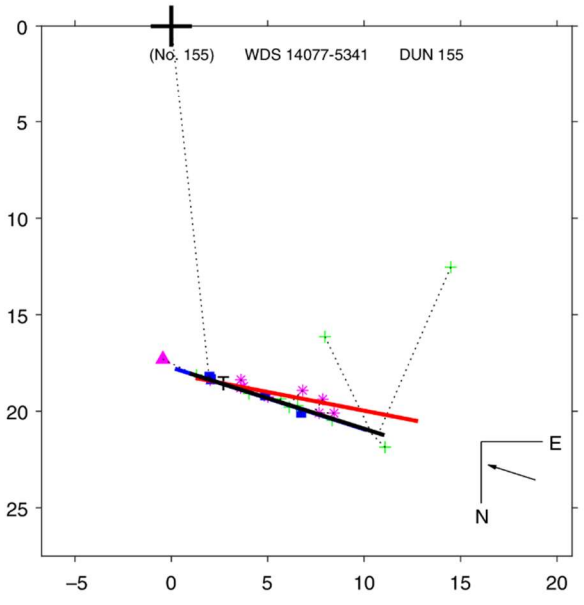


FIGURE C8 14077-5341 DUN 155

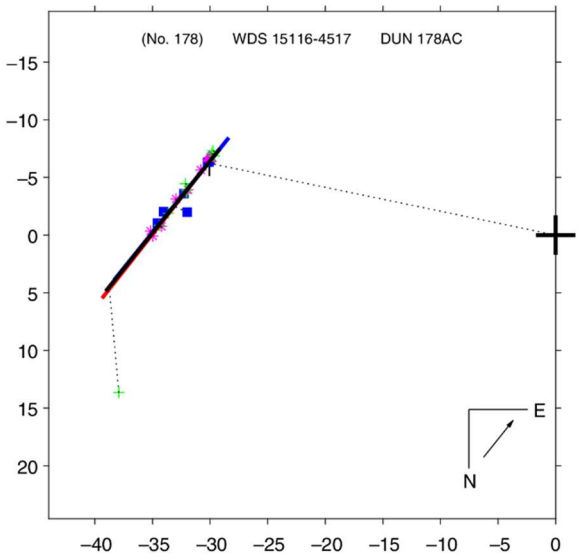


FIGURE C9 15116-4517 DUN 178AC

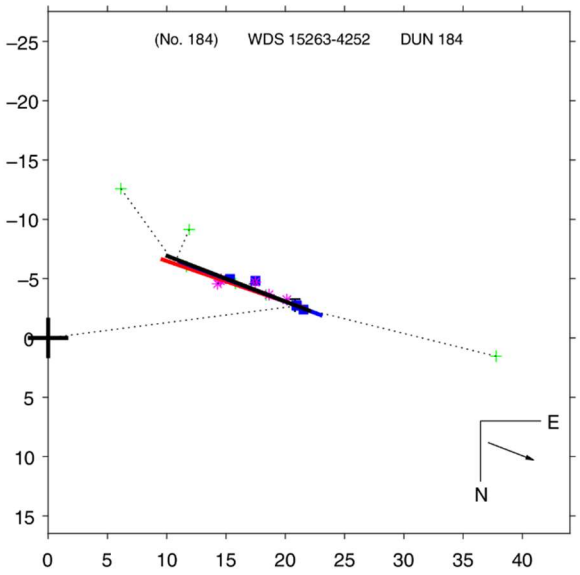


FIGURE C10 15263-4252 DUN 184

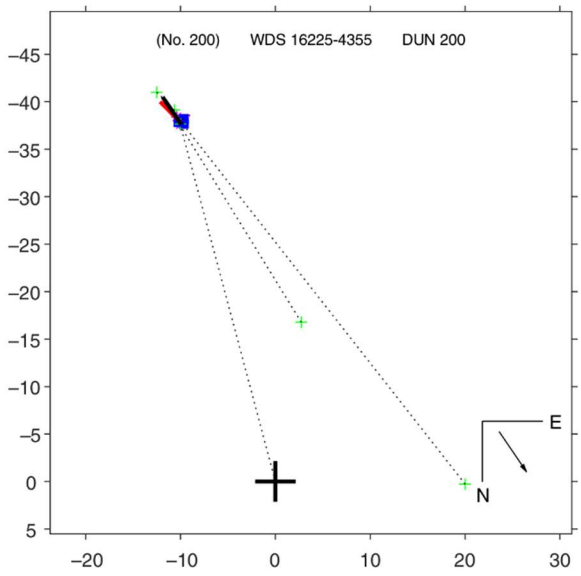


FIGURE C11 16225-4355 DUN 200

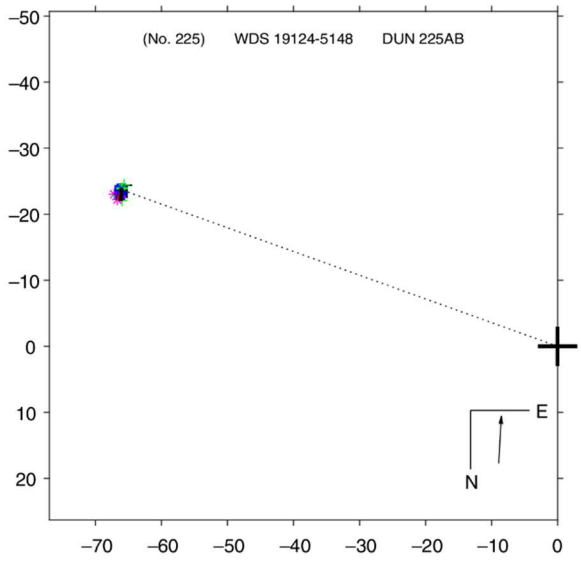


FIGURE C12 19124-5148 DUN 225AB

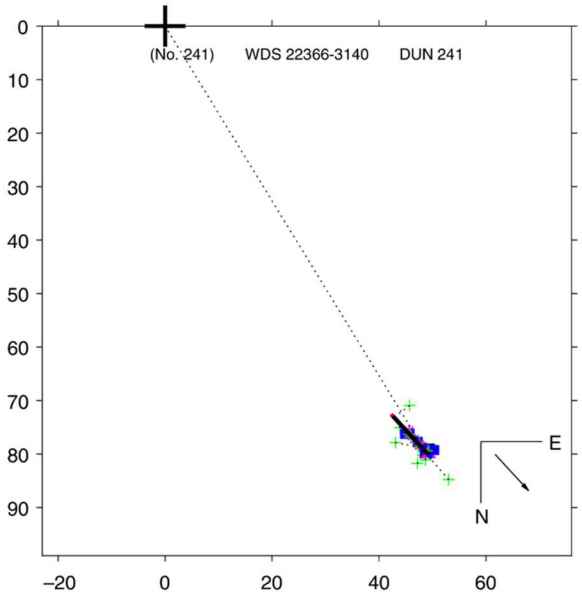


FIGURE C13 22366-3140 DUN 241

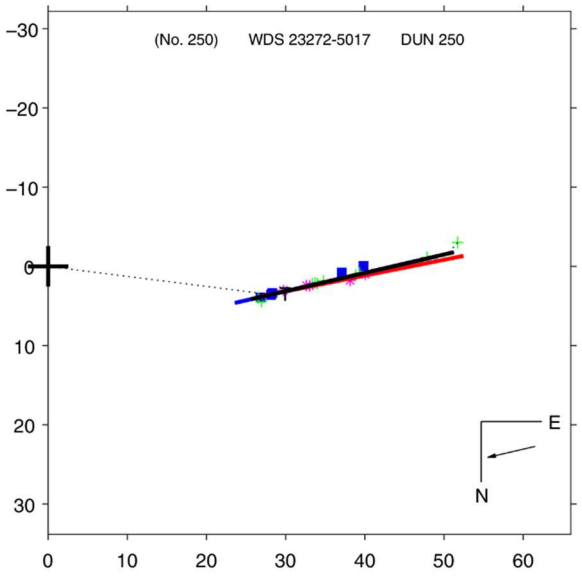


FIGURE C14 23272-5017 DUN 250

# CHAPTER 6: DISCUSSION AND CONCLUSION

This thesis explored the use of space-based astrometry from the HIPPARCOS (via ASCC) and *Gaia* (via *Gaia DR2*) missions together with historic data to advance double star studies. Firstly, the accuracy of the measures contained in the 1829 double star catalogue of James Dunlop was investigated and a subset of the catalogue, the *Working Dunlop Catalogue*, delineated. Computational techniques were then developed which extend the current ability to calculate first order orbits of wide slow moving binary stars and applied to the confirmed binary stars in the *Working Dunlop Catalogue*. Further computational techniques were proposed which described the rectilinear (straight line) relative motion of optical double stars and applied to confirmed optical double stars in the *Working Dunlop Catalogue*.

The three published papers introduced in this thesis were, in the opinion of the author, pioneering in double star astronomy, and the techniques introduced in these papers are directly applicable to historic data and space-based data. This work can pioneer a better understanding of this fundamental research area, and the astrophysical work that follows.

## 6.1 DISCUSSION

### 6.1.1 Paper 1 - Accuracy of measures in the Dunlop Catalogue

Paper 1 (Chapter 3) aimed at answering the research question, "How accurate are the historic non-space-based measures?". The double star catalogue of James Dunlop, the *Dunlop Catalogue* (Dunlop 1829), was chosen as a case study for a variety of reasons. It is the

first published catalogue of southern double stars, and because of the limits of resolution in the telescopes available to Dunlop, was likely to contain a high number of wide double stars which are suitable candidates for the analyses in Papers 2 and 3.

The results from the *Dunlop Catalogue* as a whole (not separated according to the telescope used) were that the mean position angles are within 70°"/separation" (i.e., 1 degree at a separation of 70 arcseconds, and increasing with decreasing separations), separations within 7%, and apparent visual magnitudes were/are within 1 mag.

Although there were numerous exceptions, many of the measures in the *Dunlop Catalogue* compare well with similar contemporary measures in the 1820s. This, despite being equipped with less than state of the art equipment.

Two aspects that degraded the usability of the *Dunlop Catalogue* were a number of typographical errors and the incomplete nature of the catalogue itself. In addition, the research highlighted the large number of "quadrant errors" made by Dunlop, most of which were able to be corrected after comparison with precessed *Gaia DR2* positions.

In the wider context of double star catalogues in general, the Paper establishes a methodology for assessing the accuracy of double star catalogues, something that has not be undertaken to date. It highlighted the need to distinguish not only between observers, but between the instruments used. More importantly, the paper provides a method of objectively quantifying these uncertainties.

If Paper 1 is followed by similar accuracy assessments on other double star catalogues, a more useful set of measures, with improved uncertainties can be obtained, and thus to more accurate determinations of orbital motion (or rectilinear motion). This will, in

turn, give better estimates of the astrophysical parameters of stars and stellar systems.

### 6.1.2 Paper 2 - Orbital Elements of visual binary stars with very short arcs

In Section 1.2 the second research question posed was, "How can the inclusion of space-based astrometry lead to better estimates of orbits of wide slow-moving binaries?".

A preliminary issue to be addressed was the validity of the binary or rectilinear motion of the stars. In Paper 2, and again in Paper 3, this question is answered using various tests for validation of gravitational binding, the most definitive of which is the "binding energy test".

Two problems are present in current techniques for calculating the orbits of wide binary stars.

i. Binaries with orbital periods ~<100 years, i.e., with around half or more of the orbit mapped. The procedure is to use historic measures, assign weights to the measures using subjective criteria (Hartkopf, et al. 2001b; Mason, et al. 1999) and then use either the Kowalski or the Thiele-Innes-Van-den-Bos (or a combination of both) method to obtain orbits, and then perhaps, use differential corrections to improve the orbital parameters. The problem here is the use of subjective weighting which is neither published nor repeatable.
ii. Binaries with orbital periods ~>1000 years, i.e., where measures cover only a small section of the orbit. There is no current technique, other than the one presented in Paper 2. There have been attempts to calculate orbits where there are a few measures scattered over the orbit, or a few short arc sections similarly scattered (see Section 2.3), however no

method, except for Paper 2, has addressed the case of a single short arc or used space-based astrometry as the technique to obtain orbits from short arcs.

Orbital elements of type ii pairs are found the *Sixth Catalog of Orbits of Visual Binary Stars* maintained by the USNO (United States Naval Observatory) and given a grade 5 orbit. Grade 5 orbits are those with orbital elements that "may not even be approximately correct", the arc of measures being "short with little curvature" (http://www.astro.gsu.edu/wds/orb6/orb6text.html).

The technique presented in Paper 2 addressed both issues (weighting and short arcs) by relying on two space-based positions, that of HIPPARCOS and *Gaia*, and the raw values of the historic measures. Following this, the five confirmed binary stars in the *Working Dunlop Catalogue* have a mean period of ~81,000 years (extending the current mean period of grade 5 orbits from ~18,000 years), a mean semi-major axis of ~76", and a mean uncertainty of the orbital elements of ~37%. These orbital elements are offered for inclusion in the *Sixth Catalog of Orbits of Visual Binary Stars*.

The technique published in Paper 2 used a number of constraints to reduce the inevitably large family of possible orbits. Two of the most important constraints were the following:

- Any calculated positions at the HIPPARCOS and *Gaia DR2* epochs (1991.25 and 2015.5, respectively) must be within the 1-sigma uncertainty ellipses of their space-based positions.
- Any orbit must have the total residuals from the historic data greater than the residuals generated by the historic data from a rectilinear line drawn through the HIPPARCOS and *Gaia DR2* positions.

The resulting technique was tested against a grade 3 orbit (that of STF 2026AB), the parameters for which are published in the *Sixth*

*Catalog of Orbits of Visual Binary Stars.* The two orbits compared well, and the technique was applied to determine grade 5 orbits for five confirmed binary stars in the *Working Dunlop Catalogue*.

The success of the technique depends on the veracity of the constraints and the criteria for choosing the best set of elements from the resulting family of orbits. Relaxing the constraints does result in orbits with smaller historic data residuals but produces a larger family of possible orbits with a larger set of uncertainties for the orbital elements.

The criteria for choosing the best set of elements from the resulting family of orbits was to select the orbit with the lowest total residuals from the historic data, with the uncertainties of each element taken from a weighted standard deviation of the elements of all orbits whose residuals were less than those produced by a straight line through the HIPPARCOS and *Gaia DR2* positions.

While the method for estimating the uncertainties for each orbital element seems reasonable, it should be noted that the best orbit is not necessarily the one with the lowest residuals. While this is likely, the problem here is again the probable large uncertainties in early measures, for which Paper 1 provides a possible solution.

The computation of the orbital elements in Paper 2 can also generate orbital elements for optical pairs (non-orbiting pairs) where the curvature of the rectilinear plot is found only with the inclusion of large uncertainties in the historic measures. Hence the important preliminary step in Paper 2 was to provide criteria for confirming that a given double star is in fact a binary star. Confirmation of binarity, or otherwise, does not appear to be always undertaken, as 23 individual double stars have elements in both the *Sixth Catalog of Orbits of Visual Binary Stars* and the *Second Catalog of Rectilinear Elements* (They are, in order of right ascension: J 868, STF 315, STF

326AB, STF 360, RMK 4, STU 2051AB, CHR 153, STF, 572AB, D 5AB, J 47, BU 1008, JSP 132AB, J 703, A 2762, J 1011, STF 1608AB, STF 1619AB, I 425, BU 346, STF 1890, STF 2135AB, MAD 7AC, STF 2804AB).

I propose this method of computation of the elements of wide binary stars to the astrometric community.

### 6.1.3 Paper 3 - Rectilinear Elements of visual optical double stars

Paper 3 attempted to answer the third research question (Section 1.2), "How can the inclusion of space-based astrometry lead to better estimates of the rectilinear motion of optical double stars?" Rectilinear motion characterises the relative motion of the secondary companion of an optical star compared to a fixed primary. Currently, this motion is described using a least squares method applied to subjectively weighted historic data (Hartkopf, et al. 2001b; Mason, et al. 1999). The USNO which maintains the *Second Catalog of Rectilinear Elements*, currently uses this method.

In contrast, the technique proposed in Paper 3 mathematically described such motion using the two high-precision points from HIPPARCOS and *Gaia DR2*. This resulted in the reduction of uncertainties of at least an order of magnitude without the use of subjective weighting. The historic measures can be added to the resulting rectilinear plot to confirm the rectilinear motion of the secondary companion.

In Paper 3, 14 confirmed optical double stars from the *Working Dunlop Catalogue* had their Rectilinear Elements calculated, and motions plotted using this technique. This technique will produce elements with significantly smaller uncertainties because it only uses

two positions, and those positions have inherently small uncertainties due to their space-based origins.

I propose that the method of Paper 3 is superior to the current method in that it:

- removes the necessity for assessment of weights to historic measures, but allows an inspection of deviation from rectilinear motion, that can be assessed (and corrected in retrospect if warranted); and
- fixes the equinox of the rectilinear elements to precisely 2000.0 and does not move with the inclusion of new measures.

As stated, the resulting uncertainties in the elements are smaller, being dominated by the precision of the space-based measures.

## 6.2 AVENUES FOR FUTURE RESEARCH

During this research, many avenues of possible research suggested themselves. Presented here are the most important.

Many nineteenth and early twentieth century southern hemisphere double star catalogues would benefit from a similar analysis to that in Paper 1. Of particular interest to the author would be the catalogues that have come out of Australia such as:

- The southern double star catalogue of Carl Rümker (Rümker 1832), who also worked at the Parramatta Observatory alongside James Dunlop;
- The double stars noted in the *Brisbane Catalogue* (Richardson 1835), which also came out of the Parramatta Observatory;
- A catalogue of double stars produced by Henry C. Russell of the Sydney Observatory (Russell 1882);
- A catalogue of double stars produced by Robert Ellery of the Melbourne Observatory (Ellery 1877); and

- The many measures of double stars made by John Tebbutt and published in 17 papers in the *Monthly Notices of the Royal Astronomical Society* between 1885 and 1915 (Tebbutt 1885, 1915).

These catalogues and the measures of John Tebbutt represent the most important double star work undertaken in Australia in the nineteenth and early twentieth centuries. Their contributions provide long-base line measures, where their usefulness can only be enhanced with estimates of their uncertainties.

One of the necessary steps prior to presenting the new technique of estimating first order orbits of binary stars in Paper 2 and 3 was to confirm that the double stars undergoing the technique were in fact (or not) binary stars. This was done by taking the definition of a binary star (binding energies less than zero) and imposing two other conditions for binarity: their physical separations must be less than 1 pc, and they must exhibit common proper motion.

A desirable series of future projects would be to calculate these three parameters (binding energy, physical separation, and proper motions) for each of the binary stars in the *Sixth Catalog of Orbits of Visual Binary Stars*, and to further characterise the parameters in terms of their orbital grades. This would provide valuable feedback on the use of these parameters to confirm the presence of binary stars and provide a measure of the reliability of the measured parameters.

The technique of calculating first order orbits of wide slow-moving binaries can also provide first order orbits for many binary stars whose orbits have not yet been determined or whose orbital elements are incomplete. It can also determine improved first order orbits for already published grade 5 orbits in the *Sixth Catalog of Orbits of Visual Binary Stars.*

Another project stemming from Paper 2 would be a comprehensive examination of the different methods of determining the orbital parameters of binary stars that have been proposed since that of Félix Savary in 1827. See (1896) gave a sketch of such attempts at his time, but there are no known other accounts since. Aitken (1964) does however, provide a similar historical overview to that of See (1896) and a thorough presentation of the Kowalski and Thiele-Innes-van den Bos methods. These techniques should be revised and reviewed now that space-based data is available and computing tools are more powerful.

The technique of determining Rectilinear Elements for confirmed optical double stars as given in Paper 3, has the potential to provide many sets of Rectilinear Elements of confirmed optical stars, including those with few historic measures, and reduce the uncertainties of others. Again, calculating the binding energies, physical separations and comparing proper motions with the double stars in the *Second Catalog of Rectilinear Elements* would enable the characteristics of the three parameters in optical double stars to be determined. This would likely result in the detection of some binary stars in the *Second Catalog of Rectilinear Elements*.

In addition, because of the low resulting uncertainties and completely objective nature of the proposed technique to describe the rectilinear motion of optical double stars, this would also be an ideal environment to retrospectively measure the uncertainties of individual observers over all measured optical double stars. These uncertainties could then be applied particularly to the binary star measures of the individual observers which in turn would contribute to improved Orbital Elements. This would be achievable in collaboration with the *United States Naval Observatory* and the full digital data set that is stored by this organisation.

## 6.3 CONCLUSION

The Aims of this thesis (Section 1.2) emphasised that modern space-based astronomy has opened a new sophisticated avenue of double star studies with precisions that are 3 - 4 orders of magnitude more precise than has been available to-date from single-aperture ground observations (aside from speckle interferometry on close pairs).

The Aims also suggested three questions which were addressed in the thesis:

- How accurate are the historic non-space-based measures?
- How can the inclusion of space-based astrometry lead to better estimates of orbits of wide slow-moving binaries?
- How can the inclusion of space-based astrometry lead to better estimates of the rectilinear motion of optical double stars?

This thesis addressed these questions in three published papers, Papers 1, 2 and 3, reproduced in Chapters 3, 4 and 5, respectively, of this thesis.

The conclusion of the thesis is therefore that:

- the accuracy of historic data can be assessed and improved by comparing the historic data against space-based data, and
- that the inclusion of space-based data (together with historic data sets), and the use of power-based computational techniques, opens the possibility of the better determination of the orbital and rectilinear elements of long period binary stars and optical double stars, respectively.

# REFERENCES


Aarseth, S., Tout, C. A., & Mardling, R. 2008, The Cambridge N-Body Lectures (Berlin Heidelberg: Springer)

Aitken, R. G. 1964, The binary stars (New York: Dover Publications)

Alzner, A. 2012, in Observing and Measuring Visual Double Stars, ed. R. W. Argyle (New York, NY: Springer New York), 81

Andersen, J. 1991, Astronomy and Astrophysics Review, 3, 91

Andrews, J. J., Chanamé, J., & Agüeros, M. A. 2017, Monthly Notices of the Royal Astronomical Society, 472, 675

Argyle, B., Swan, M., & James, A. 2019, An Anthology of Double Stars (Cambridge, UK: Cambridge University Press)

Benacquista, M. 2012, An Introduction to the Evolution of Single and Binary Stars (New York: Springer)

Chanamé, J., & Gould, A. 2004, The Astrophysical Journal, 601, 289

Chanamé, J., Harmanec, P., & Guinan, E. F. 2007. in IAU Symposium 240: Binary Stars as Critical Tools and Tests in Contemporary Astrophysics, Catalogs of Wide Binaries: Impact on Galactic Astronomy, eds. W. I. Hartkopf, E. F. Guinan, & P. Harmanec (Cambridge, UK: Cambridge University Press), 316

Collaboration, G., et al. 2018, Astronomy and Astrophysics, 616, A1

Debehogne, H., & de Freitas Mourao, R. R. 1977, Astronomy and Astrophysics, 61, 453

Dobler, H. R. 2002, Journal for the History of Astronomy, 33, 265

Docobo, J. A. 1985, Celestial Mechanics, 36, 143

Docobo, J. A., & Hestroffer, D. 2012, in Orbital Couples: Pas de Deux in the Solar System and the Milky Way, 119

Docobo, J. A., Ling, J. F., & Prieto, C. A. 1992. in Complementary Approaches to Double and Multiple Star Research, ASP Conference Series, Adaptation of Docobo's Method for the Calculation of Orbits of Spectroscopic-Interferometric Binaries with Mixed Data, 220

Docobo, J. A., Tamazian, V. S., & Campo, P. P. 2018, Monthly Notices of the Royal Astronomical Society, 476, 2792

Dunlop, J. 1829, Memoirs of the Royal Astronomical Society, 3, 257

Ellery, R. L. J. 1877, Nature, 15, 470

Fujiwara, T., & Yamaoka, H. 2005, Journal of Astronomical History and Heritage, 8, 39

Glasenapp, S. 1889, Monthly Notices of the Royal Astronomical Society, 49, 276

Grasshoff, G. 1990, The History of Ptolemy's Star Catalogue (Springer)

Green, R. M. 1985, Spherical Astronomy (Cambridge University Press)

Grosser, M. 1979, The Discovery of Neptune (2nd ed.; New York: Dover Publications)

Guinan, E. F., Harmanec, P., & Hartkopf, W. I. 2007. in IAU Symposium 240: Binary Stars as Critical Tools and Tests in Contemporary Astrophysics, Introduction & Overview to Symposium 240: Binary Stars as Critical Tools and Tests in Contemporary Astrophysics, eds. W. I. Hartkopf, E. F. Guinan, & P. Harmanec (Cambridge, UK: Cambridge University Press), 5

Hartkopf, W. I., Harmanec, P., & Guinan, E. F. 2007, Binary Stars as Critical Tools and Tests in Contemporary Astrophysics (IAU S240)

Hartkopf, W. I., & Mason, B. D. 2020, Second Catalog of Rectilinear Elements

Hartkopf, W. I., Mason, B. D., & Worley, C. E. 2001a, The Astronomical Journal, 122, 3472

Hartkopf, W. I., McAlister, H. A., & Franz, O. G. 1989, The Astronomical Journal, 98, 1014

Hartkopf, W. I., McAlister, H. A., & Mason, B. D. 2001b, The Astronomical Journal, 122, 3480

Haynes, R., Haynes, R., Malin, D., & McGee, R. 1996, Explorers of the Southern Sky: A History of Australian Astronomy (Cambridge: University Press)

Hearnshaw, J. B. 1996, The Measurement of Starlight: Two Centuries of Astronomical Photometry (Cambridge University Press)

Heintz, W. D. 1978, Double stars (Springer)

Herschel, F. W. 1803, Royal Society of London Philosophical Transactions Series I, 93, 339

Hirst, W. P. 1944, Monthly Notices of the Royal Astronomical Society, 103, 337

Høg, E. 2017, in eprint arXiv, arXiv:1707.01020

Igoshev, A. P., & Perets, H. B. 2019, Monthly Notices of the Royal Astronomical Society, 486, 4098

Jones, D. 1968, Astronomical Society of the Pacific Leaflets, 10, 145

Kouwenhoven, M. B. N., Goodwin, S. P., Parker, R. J., Davies, M. B., Malmberg, D., & Kroupa, P. 2010, Monthly Notices of the Royal Astronomical Society, 404, 1835

Kowalski, M. A. 1873, Izvestiya I Uchenye Zapiski Kazanskogo Universiteta, 40, 329

LeBlanc, F. 2011, An Introduction to Stellar Astrophysics (Chichester: Wiley)

Letchford, R. R., White, G. L., & Ernest, A. D. 2017, Journal of Double Star Observations, 13, 220

---. 2018a, Journal of Double Star Observations, 14, 208

---. 2018b, Journal of Double Star Observations, 14, 761

---. 2019a, Journal of Double Star Observations, 15, 350

---. 2019b, Journal of Double Star Observations, 15, 361

---. 2019c, Journal of Double Star Observations, 15, 378

---. 2019d, Journal of Double Star Observations, 15, 393

Maceroni, C., & Sterken, C. 2006. in ASP Conference Proceedings 349: Astrophysics of Variable Stars, Binaries as Astrophysical Laboratories: an Overview, eds. C. Sterken, & C. Aerts, 41

Mason, B. D., Douglass, G. G., & Hartkopf, W. I. 1999, The Astronomical Journal, 117, 1023

Matson, R. A., Williams, S. J., Hartkopf, W. I., & Mason, B. D. 2020, in (Washington DC: United States Naval Observatory)

Milone, E. F., & Sterken, C. 2011, Astronomical Photometry: Past, Present, and Future, Vol. 373 (Edited by ed.; Berlin: Springer)

Moe, M. 2019, in The Impact of Binary Stars on Stellar Evolution, eds. G. Beccari, & H. M. J. Boffin (Cambridge, UK: Cambridge University Press), 12

Olević, D., & Cvetković, Z. 2004, Astronomy and Astrophysics, 415, 259

---. 2005, Publications of the Astronomical Society "Rudjer Boskovic", 5, 237

Pearce, T. D., Wyatt, M. C., & Kennedy, G. M. 2015, Monthly Notices of the Royal Astronomical Society, 448, 3679

Penoyre, Z., Belokurov, V., & Evans, N. W. 2022, Monthly Notices of the Royal Astronomical Society, 513, 2437

Perryman, M. A. C., et al. 1997, Astronomy and Astrophysics, 500, 501

Pickering, E. C., Searle, A., & Wendell, O. C. 1884, Annals of Harvard College Observatory, 14, 1

Pogson, N. 1856, Monthly Notices of the Royal Astronomical Societyp, 17, 12

Richardson, W. 1835, A Catalogue of 7385 Stars: Chiefly in the Southern Hemisphere, Prepared from Observations Made in the Years 1822, 1823, 1824, 1825, and 1826, at the Observatory at Paramatta, New South Wales, Founded by Lieutenant General Sir Thomas Makdougall Brisbane (London: William Clowes and Sons)

Rümker, C. 1832, Preliminary Catalogue of Fixed Stars: Intended for a Prospectus of a Catalogue of the Stars of the Southern Hemisphere Included Within the Tropic of Capricorn : Now Reducing from the Observations Made in the Observatory at Paramatta (Hamburg: Perthes and Besser)

Russell, H. C. 1882, Results of double star measures made at the Sydney Observatory, New South Wales, 1871-1881 (Sydney: Thomas Richards, Government Printer)

Saunders, S. D. 1990, in

---. 2004, Historical Records of Australian Science, 15, 177

Savary, F. 1827a, in Connaissance des Temps pour 1830 (Paris: Bureau des Longitudes), 163

---. 1827b, Connaissance des Temps pour 1830, 56

Schaffer, S. 2010, in The heavens on earth : observatories and astronomy in nineteenth-century science and culture, eds. D. Aubin, C. Bigg, & H. O. Sibum (Durham NC: Duke University Press), 118

Schlesinger, F., & Alter, D. 1912, Publications of the Allegheny Observatory of the University of Pittsburgh ; v II, 13

See, T. J. J. 1896, in Researches on the evolution of stellar systems, Volume I (Lynn, Mass.: T. P. Nichols), 41

Struve, F. G. W. 1822, Catalogus 795 stellarum duplicium ex diversis astronomorum observationibus congestus in specula (Dorpat: J. C. Schuenmannus)

---. 1827, Catalogus novus stellarum duplicium et multiplicium maxima ex parte in Specula Universitatis caesareae dorpatensis per magnum telescopium achromaticum Fraunhoferi detectarum (typis J.C. Schuenmanni, typographi academici)

---. 1837, Astronomische Nachrichten, 14, 249

Struve, F. G. W., & Struve, O. W. 1840, in (Petropoli: Typis Academicis), 30 p.

Tebbutt, J. 1885, Monthly Notices of the Royal Astronomical Society, 46, 50

---. 1915, Monthly Notices of the Royal Astronomical Society, 76, 36

Thiele, T. N. 1883, Astronomische Nachrichten, 104, 245

Toomer, G. J. 1984, Ptolemy's Almagest (New York: Springer)

Torres, G. 1988, Astronomy and Astrophysics Supplement Series (ISSN 0365-0138), 72, 209

Torres, G., Andersen, J., & Giménez, A. 2010, Astronomy and Astrophysics Review, 18, 67

van de Kamp, P. 1966, Transactions of the International Astronomical Union, Series B, 12B, 267

van den Bos, W. H. 1926, Circular of the Union Observatory Johannesburg, 68, 354

---. 1932, Circular of the Union Observatory Johannesburg, 86, 261

---. 1962, in Astronomical Techniques, ed. W. A. Hiltner (Chicago and London: U. Chicago), 537

van den Bos, W. H. 1937, Circular of the Union Observatory Johannesburg, 98

Verbunt, F., & van Gent, R. H. 2010a, Astronomy and Astrophysics, 516, 1

---. 2010b, Astronomy and Astrophysics, 516, 1

---. 2011, Astronomy and Astrophysics, 530, 1

---. 2012, Astronomy and Astrophysics, 544, 1

White, G. L., Letchford, R. R., & Ernest, A. D. 2018, Journal of Double Star Observations, 14, 432

Wiley, E. O., & Rica, F. M. 2015, JDSO, 11, 2

Yoo, J., Chanamé, J., & Gould, A. 2004, The Astrophysical Journal, 601, 311

# APPENDIX

Supporting information in the form of machine-readable data compiled by the first author forms the online supplementary information for Paper 1, available at:

https://doi.org/10.1093/mnras/stab3777.

Although one file, it can be divided into three sections. These sections are reprinted here under Appendix A, B and C.

# APPENDIX A

Table 1: Digitised version of the *Dunlop Catalogue*.

| 1 | 2 | 3 | 4 | 5 | 6 | 7 | 8 | 9 | 10 | 11 | 12 | 13 | 14 | 15 |
|---|---|---|---|---|---|---|---|---|---|---|---|---|---|---|
| **No.** | **Name** | **RA_DUN** | **DE_DUN** | **Angle_ of_Pos** | **Quad1** | **Quad2** | **Dist1** | **Dist2** | **delta_RA** | **delta_DE** | **vA** | **vB** | **vC** | **Remarks** |
| | | **(h:m:s)** | **(d:m:s)** | **(d:m)** | | | **('')** | **('')** | **(s)** | **('')** | **(mag)** | **(mag)** | **(mag)** | |
| 1 | β1 β2 Toucani* | 00 23 16 | -63 56 | 84 5 | np | | | | 0.607 | 24.860 | 4 | 4 | | Double L. C. |
| 2 | λ Toucani* | 00 44 50 | -70 28 | | sf | | | | | 6.620 | 6 | 7 | | |
| 3 | Anonym. | 01 19 43 | -33 31 | | | | | | | | 7 | | | A very singular star of the 7th magnitude, of an uncommon red purple colour, very dusky and ill defined; 3 obs, on this star; a small star preceding, and another following. |
| 4 | 100 Phoenicis* | 01 32 11 | -54 18 | 17 27 | sf | | 15.809 | | | | 6 | 8 | | |
| 5 | δ Eridani* | 01 33 24 | -57 04 | 73 6 | nf | | 2.5 | | | | 6.5 | 6.5 | | Very nearly equal. Pretty d. Star. |
| 6 | φ Eridani | 02 10 12 | -52 20 | 50 0 | sp | | 90 | | | | 4 | 12 | | |
| 7 | Anonym. | 02 34 57 | -60 21 | 20 0 | np | | 35 | | | | 8 | 8 | | |
| 8 | 41 App. Chemici* | 02 50 37 | -25 40 | 49 6 | sp | | | | | | 7 | 7 | | |

| 1 | 2 | 3 | 4 | 5 | 6 | 7 | 8 | 9 | 10 | 11 | 12 | 13 | 14 | 15 |
|---|---|---|---|---|---|---|---|---|---|---|---|---|---|---|
| **No.** | **Name** | **RA_DUN** | **DE_DUN** | **Angle_ of_Pos** | **Quad1** | **Quad2** | **Dist1** | **Dist2** | **delta_RA** | **delta_DE** | **vA** | **vB** | **vC** | **Remarks** |
| | | **(h:m:s)** | **(d:m:s)** | **(d:m)** | | | **('')** | **('')** | **(s)** | **('')** | **(mag)** | **(mag)** | **(mag)** | |
| 9 | θ Eridani* | 02 51 19 | -41 00 | 1 37 | nf | | 10.81 | | | | 4 | 6 | | |
| 10 | Anonym. | 02 58 14 | -52 01 | 15 0 | nf | | 30 | | | | 8 | 9 | | |
| 11 | Anonym. | 03 03 14 | -59 03 | | s | | 10 | | | | 8 | 12 | | A triangle of stars. The following a double star. |
| 12 | Anonym. | 03 10 42 | -65 01 | 8 0 | sf | | 14 | | | | 6 | 12 | | |
| 13 | 172 Eridani | 03 31 24 | -40 41 | | | | | | | | 5 | 8 | 9 | A triangle of stars. Large star fine yellow. |
| 14 | Anonym. | 03 33 32 | -60 22 | 10 0 | np | | 45 | | | | 7.5 | 8 | | |
| 15 | 184 Eridani* | 03 33 49 | -40 55 | 64 55 | np | | 4 | | | | 6 | 7 | | |
| 16 | 207 Eridani* | 03 42 09 | -38 10 | 67 48 | sp | | 7 | | | | 5 | 5.5 | | |
| 17 | Anonym* | 03 57 16 | -54 49 | 49 23 | sf | | 63 | 41 | | 38.820 | 7 | 8 | 8 | A triangle of stars. |
| 18 | ι Pictoris* | 04 46 28 | -53 46 | 30 4 | nf | | 12.547 | | 1.137 | 6.659 | 6 | 7 | | |
| 19 | κ Columbae* | 05 10 17 | -33 44 | 48 12 | sp | | | | | | 7 | 7 | | |
| 20 | θ Pictoris* | 05 20 00 | -52 28 | 14 4 | np | | 38.516 | | 4.190 | 9.055 | 6 | 7 | | |
| 21 | 25 Pictoris | 05 25 37 | -47 12 | | | | | | | 19.000 | 6 | 7 | | |
| 22 | 26 Pictoris* | 05 26 31 | -42 26 | 80 7 | sf | | 5.534 | | | | 6.5 | 7 | | |
| 23 | 53 Pictoris | 06 01 07 | -48 26 | 59 0 | np | | 3 | | | | 7 | 7 | | Very pretty d. Star. |
| 24 | 58 Pictoris | 06 07 21 | -54 55 | | | | 2 | | | | 6 | 10 | | A close double star. |
| 25 | Anonym. | 06 12 05 | -32 06 | | | | | | | | 6 | 8 | | |
| 26 | Anonym* | 06 12 11 | -65 36 | 22 5 | nf | | | | 3.183 | 8.130 | 7 | 8 | | |
| 27 | Anonym* | 06 13 27 | -59 06 | | | | | | 5.175 | 42.230 | 6 | 7 | | |
| 28 | 11 Argûs* | 06 18 40 | -36 37 | 25 33 | nf | | | | 5.142 | 30.620 | 7 | 7 | | Double L. C. |

| 1 | 2 | 3 | 4 | 5 | 6 | 7 | 8 | 9 | 10 | 11 | 12 | 13 | 14 | 15 |
|---|---|---|---|---|---|---|---|---|---|---|---|---|---|---|
| No. | Name | RA_DUN (h:m:s) | DE_DUN (d:m:s) | Angle_of_Pos (d:m) | Quad1 | Quad2 | Dist1 ('') | Dist2 ('') | delta_RA (s) | delta_DE ('') | vA (mag) | vB (mag) | vC (mag) | Remarks |
| 29 | 21 Argûs* | 06 24 12 | -40 16 | | | | | | 5.920 | 23.460 | 7 | 7 | | |
| 30 | 24 Argûs | 06 25 58 | -50 07 | 40 0 | np | | 14 | | | | 6 | 10 | | |
| 31 | 45 Argûs* | 06 34 26 | -48 03 | 48 36 | np | | 12.32 | | 0.675 | 8.630 | 6 | 10 | | |
| 32 | 48 Argûs* | 06 36 30 | -38 14 | 79 20 | np | | 6.24 | | | | 6 | 8 | | Beautiful d. Star. |
| 33 | 53 Argûs | 06 40 31 | -39 21 | 50 0 | sf | | 2 | | | | 6 | 8 | | |
| 34 | 55 Argûs* | 06 41 53 | -54 33 | 85 14 | sp | | 130.15 | | | 64.400 | 6 | 7 | | Double L. C. |
| 35 | 57 Argûs* | 06 42 28 | -43 37 | | | | | | | 8.150 | 6 | 6 | | |
| 36 | 95 Canis Majoris* | 06 43 39 | -31 30 | 20 36 | | | | | | 28.870 | 6 | 8 | | |
| 37 | 79 Argûs | 06 56 48 | -51 09 | | | | | | | | 6 | 8 | | |
| 38 | 83 Argûs* | 06 59 08 | -43 22 | 29 12 | sf | | 21.5 | | 1.788 | 10.320 | 6 | 7 | | Double L. C. |
| 39 | 89 Argûs* | 07 01 13 | -58 55 | 78 48 | nf | | 2.83 | | | | 6 | 7 | | |
| 40 | 100 Argûs* | 07 06 09 | -56 04 | | sf | | | | 2.940 | 30.520 | 7 | 8 | | Double L. C. |
| 41 | Anonym. | 07 06 26 | -55 17 | | | | | | | | 7 | 7 | | |
| 42 | γ Pis. Volantis* | 07 10 10 | -70 13 | 32 8 | np | | 15.68 | | 2.287 | 8.720 | 5 | 8 | | Large star yellow. S. star greenish. |
| 43 | π Argûs* | 07 10 57 | -36 47 | 56 24 | sp | | | | | 69.060 | 3 | 10 | | Large star yellow. Small star dusky. |
| 44 | Anonym. | 07 13 20 | -51 50 | 65 0 | nf | | 12 | | | | 7 | 7 | | Nearly equal. |
| 45 | Anonym.* | 07 15 35 | -48 12 | 70 12 | nf | | | | 0.350 | 22.950 | 6 | 6.5 | | |
| 46 | Anonym. | 07 16 18 | -48 02 | 3 0 | np | | | | 3.416 | | 6 | 10 | | |
| 47 | 137 Argûs | 07 18 34 | -31 27 | | | | | | | | 6 | 8 | | |
| 48 | 144 Argûs* | 07 22 20 | -61 55 | 60 30 | sf | | | | | | 7 | 9 | | Double L. C. |
| 49 | 145 Argûs | 07 22 43 | -31 28 | | | | | | 0.560 | | | | | |

| 1 | 2 | 3 | 4 | 5 | 6 | 7 | 8 | 9 | 10 | 11 | 12 | 13 | 14 | 15 |
|---|---|---|---|---|---|---|---|---|---|---|---|---|---|---|
| **No.** | **Name** | **RA_DUN (h:m:s)** | **DE_DUN (d:m:s)** | **Angle_of_Pos (d:m)** | **Quad1** | **Quad2** | **Dist1 ('')** | **Dist2 ('')** | **delta_RA (s)** | **delta_DE ('')** | **vA (mag)** | **vB (mag)** | **vC (mag)** | **Remarks** |
| 50 | 146 Argûs | 07 22 47 | | | | | 2 | | | | 5 | 8 | | Very close d. Star |
| 51 | σ Argûs | 07 23 38 | -42 57 | | f | | 18 | | | | 4 | 14 | | |
| 52 | 153 Argûs* | 07 27 08 | -23 05 | 15 23 | | | | | | | 5 | 5.5 | | |
| 53 | κ Argûs* | 07 31 48 | -26 26 | 45 48 | np | | 8.765 | | | | 4 | 4 | | Both stars of the small 4th magn. |
| 54 | 195 Argûs | 07 38 44 | -37 46 | | | | 3 | | | | 6 | 9 | | Beautiful close d. Star. |
| 55 | 209 Argûs* | 07 40 11 | -50 02 | 43 40 | sf | | | | 3.810 | 44.400 | 6 | 7 | | |
| 56 | 215 Argûs* | 07 41 46 | -38 04 | | sf | | | | 0.830 | 52.400 | 7 | 7 | | |
| 57 | ζ Pis. Volantis | 07 43 50 | -72 10 | | sf | | | | 3.040 | | 6 | 9 | | Very unequal. L. Star yellow. S star blue. |
| 58 | 258 Argûs | 07 49 32 | -43 54 | | | | | | | | 7 | 8 | 8 | A triangle of small stars. |
| 59 | Anonym. | 07 50 30 | -50 00 | 41 0 | sf | | | | | | 7 | 8 | | |
| 60 | Anonym. | 07 57 24 | -54 02 | | | | | | 1.830 | | 6 | 9 | | |
| 61 | 285 Argûs | 07 59 17 | -28 39 | | sf | | | | 3.050 | | 7 | 8 | | |
| 62 | 299 Argûs* | 08 02 30 | -62 19 | | sp | | | | 12.097 | 5.580 | 6 | 7 | | |
| 63 | k1 Argûs* | 08 04 00 | -42 07 | 12 5 | nf | | | | | | 6 | 8 | | Large star blue. S. star dusky red. |
| 64 | γ Argûs* | 08 04 05 | -46 50 | 34 48 | nf | | | | 3.000 | 46.150 | 2.5 | 8 | | Four small stars accompany γ Argûs. |
| 65 | γ Argûs* | 08 04 05 | -46 50 | 47 50 | sp | | | | 2.930 | 30.800 | 2.5 | 6 | | Four small stars accompany γ Argûs. |
| 66 | ε Pis. Volantis* | 08 07 00 | -68 06 | 46 0 | nf | | 6 | | 0.715 | | 5 | 10 | | Large star white. Small star blue. |

| 1 | 2 | 3 | 4 | 5 | 6 | 7 | 8 | 9 | 10 | 11 | 12 | 13 | 14 | 15 |
|---|---|---|---|---|---|---|---|---|---|---|---|---|---|---|
| No. | Name | RA_DUN (h:m:s) | DE_DUN (d:m:s) | Angle_ of_Pos (d:m) | Quad1 | Quad2 | Dist1 ('') | Dist2 ('') | delta_RA (s) | delta_DE ('') | vA (mag) | vB (mag) | vC (mag) | Remarks |
| 67 | 320 Argûs | 08 07 00 | -35 48 | | | | | | 1.200 | 72.300 | 6 | 6 | | Four stars forming a parallelogram. L. C. |
| 68 | 320 Argûs | 08 07 00 | -35 48 | | | | | | 3.300 | 101.000 | 7 | 7 | | Four stars forming a parallelogram. L. C. |
| 69 | Anonym. | 08 20 21 | -51 16 | 65 0 | sp | | 40 | | | | 6 | 12 | | |
| 70 | 359 Argûs* | 08 24 07 | -44 08 | 50 18 | np | | 5.49 | | | | 6 | 9 | | Large star yellow. S. star pale green. |
| 71 | 363 Argûs | 08 24 14 | -39 55 | | nf | | | | 4.330 | 45.100 | 7 | 7 | | Double. L. C. |
| 72 | 383 Argûs | 08 34 10 | -41 51 | | nf | | | | 1.100 | 136.000 | 7 | 8 | | Double. L. C. |
| 73 | Anonym* | 08 51 02 | -54 39 | 82 46 | np | | | | 0.920 | 69.500 | 7 | 8 | | |
| 74 | 426 Argûs* | 08 52 50 | -58 33 | | nf | | 38.98 | | 4.805 | 19.040 | 5.5 | 7 | | |
| 75 | Anonym. | 09 04 19 | -57 30 | | | | | | | | 9 | 9 | | |
| 76 | 484 Argûs* | 09 22 14 | -44 45 | 7 2 | sf | | 61.4 | | 6.265 | 8.090 | 7 | 7 | | |
| 77 | Anonym. | 09 22 27 | -43 47 | | sp | | | | | 24.650 | 8 | 8 | | |
| 78 | ζ1 Antl. pneum.* | 09 23 00 | -31 08 | 1 7 | nf | | | | 0.500 | 3.470 | 6 | 8 | | Double. L. C. |
| 79 | 494 Argûs* | 09 27 00 | -48 57 | 58 34 | nf | | 20.03 | | | 8.150 | 7 | 7 | | Double. L. C. |
| 80 | Anonym. | 09 38 39 | -48 41 | | | | 3 | | | | 8 | 9 | | |
| 81 | 524 Argûs | 09 47 31 | -44 27 | 30 34 | sp | | 4 | | | | 6 | 8 | | |
| 82 | Anonym. | 09 52 26 | -85 00 | 2 0 | sp | | | | | | 7 | 8 | | |
| 83 | Anonym. | 09 56 32 | -54 09 | | | | | | | | 7 | 7 | | Double. |
| 84 | Anonym.* | 09 58 25 | -51 14 | 79 52 | sp | | 2 | | | | 7 | 7.5 | | |
| 85 | Anonym. | 10 22 31 | -61 48 | | | | | | | | 8 | 8 | | |

| 1 | 2 | 3 | 4 | 5 | 6 | 7 | 8 | 9 | 10 | 11 | 12 | 13 | 14 | 15 |
|---|---|---|---|---|---|---|---|---|---|---|---|---|---|---|
| No. | Name | RA_DUN (h:m:s) | DE_DUN (d:m:s) | Angle_of_Pos (d:m) | Quad1 | Quad2 | Dist1 ('') | Dist2 ('') | delta_RA (s) | delta_DE ('') | vA (mag) | vB (mag) | vC (mag) | Remarks |
| 86 | 557 Argûs* | 10 24 08 | -41 21 | | np | | | | | 34.180 | 7 | 8 | | Double. L. C. |
| 87 | Anonym.* | 10 24 26 | -60 26 | 66 25 | sp | | | | 4.600 | 78.180 | 7 | 8 | | |
| 88 | 558 Argûs* | 10 24 49 | -44 08 | 47 15 | | | 14.92 | | 0.930 | 11.610 | 7 | 7 | | |
| 89 | Anonym.* | 10 25 07 | -54 29 | | | | | | 1.800 | 23.230 | 7 | 7 | | |
| 90 | Anonym. | 10 27 24 | -53 34 | | nf | | | | | | 7 | 8 | | |
| 91 | Anonym.* | 10 28 09 | -71 13 | 41 11 | sp | | 3.69 | | | | 8 | 8 | | |
| 92 | Anonym.* | 10 29 33 | -60 29 | | nf | | | | 3.000 | 5.500 | 7 | 8 | | |
| 93 | Anonym.* | 10 30 20 | -63 13 | 49 34 | nf | | 23.66 | | 2.183 | 17.100 | 7 | 8 | | |
| 94 | 34 Rob. Caroli* | 10 32 20 | -58 16 | 78 54 | nf | | 10.13 | | | | 6 | 9 | | |
| 95 | 35 Rob. Caroli* | 10 32 27 | -54 41 | 15 21 | sf | | | | 6.050 | 11.950 | 5.5 | 8 | | |
| 96 | 40 Rob. Caroli | 10 36 11 | -58 19 | | sf | | | | | | 6 | 10 | | Very pretty d. Star. |
| 97 | Anonym. | 10 37 15 | -60 16 | | | | 3 | | | | 7 | 7 | | Pretty double star. |
| 98 | η Rob. Caroli* | 10 38 27 | -58 43 | 79 2 | nf | | | | | 60.200 | 3 | 10 | | |
| 99 | Anonym.* | 10 39 28 | -69 57 | | sp | | | | 12.250 | 18.550 | 7 | 7 | | |
| 100 | 562 Argûs | 10 40 29 | -59 41 | | | | | | | 2.000 | 6.5 | 6.5 | | Very nearly equal. |
| 101 | Anonym. | 10 43 00 | -58 58 | 6 0 | np | | 10 | | | | 7 | 9 | | |
| 102 | κ Rob. Caroli* | 10 46 29 | -57 56 | 68 51 | sp | | | | 1.650 | 62.300 | 5 | 7 | | Triple star. Very nearly in a line. |
| 103 | κ Rob. Caroli* | 10 46 29 | -57 56 | 77 2 | nf | | | | | 56.000 | 5 | 8 | | Triple star. Very nearly in a line. |
| 104 | Anonym. | 10 53 26 | -51 03 | | | | | | | | 8 | 8 | 8 | Three stars nearly equidistant. Very pretty. |

| 1 | 2 | 3 | 4 | 5 | 6 | 7 | 8 | 9 | 10 | 11 | 12 | 13 | 14 | 15 |
|---|---|---|---|---|---|---|---|---|---|---|---|---|---|---|
| No. | Name | RA_DUN (h:m:s) | DE_DUN (d:m:s) | Angle_ of_Pos (d:m) | Quad1 | Quad2 | Dist1 ('') | Dist2 ('') | delta_RA (s) | delta_DE ('') | vA (mag) | vB (mag) | vC (mag) | Remarks |
| 105 | Anonym.* | 10 55 21 | -60 53 | 59 57 | sf | | 23.1 | | 1.600 | 20.030 | 7 | 8 | | |
| 106 | Anonym. | 11 11 00 | -37 03 | 30 0 | nf | | | | | | 7 | 8 | | A beautiful line of pretty bright stars. |
| 107 | Anonym. | 11 13 23 | -73 13 | | np | | | | | 58.000 | 8 | 9 | | |
| 108 | Anonym. | 11 16 19 | -57 23 | | sp | nf | | | | | 7 | | | Four stars in a line. |
| 109 | 25 Centauri* | 11 20 19 | -41 43 | 18 39 | sf | | 169.3 | | | 42.460 | 6 | 8 | | |
| 110 | Anonym. | 11 22 15 | -54 22 | | | | | | | | 8 | | | Three pretty bright stars in a line. |
| 111 | 275 Hydrae* | 11 24 00 | -28 19 | 61 25 | nf | | 9.965 | | 0.200 | 8.252 | 6 | 6 | | |
| 112 | 32 Centauri* | 11 28 00 | -49 50 | 19 0 | np | | | | 19.733 | 68.200 | 7 | 7 | | Double L. C. |
| 113 | 35 Centauri* | 11 28 00 | -38 02 | 66 12 | sf | | 143 | | 4.300 | 125.000 | 7 | 7 | | Double L. C. |
| 114 | Anonym. | 11 31 10 | -37 15 | 7 0 | sf | | 3 | | | | 7 | 10 | | |
| 115 | Anonym. | 11 32 09 | -32 20 | | np | | | | 3.000 | 3.400 | 7 | 8 | | |
| 116 | Anonym.* | 11 48 17 | -31 18 | 2 26 | nf | | 15.2 | | 1.600 | 2.560 | 7 | 8 | | |
| 117 | Anonym.* | 11 55 13 | -61 01 | 63 27 | sf | | 22.72 | | 1.394 | 19.290 | 7 | 8 | | |
| 118 | 82 Centauri | 12 02 00 | -36 53 | | | | | | | | 7 | 8 | | |
| 119 | 1 Muscae* | 12 05 00 | -65 34 | | nf | | | | 9.150 | 97.600 | 7 | 7 | | Double L. C. |
| 120 | Anonym.* | 12 10 26 | -65 52 | | nf | | | | 0.925 | 96.200 | 6 | 8 | | |
| 121 | Anonym. | 12 14 35 | -54 33 | | np | | | | | | 7 | 8 | | |
| 122 | α Crucis* | 12 16 50 | -62 07 | 70 0 | sp | | | | 4.450 | 81.956 | 2 | 6 | | |
| 123 | α Crucis* | 12 16 50 | -62 07 | 24 24 | sf | | 5.421 | | | | 2 | 2.5 | | |
| 124 | γ Crucis* | 12 21 30 | -56 07 | 46 42 | nf | | | | 7.216 | 70.854 | 2 | 7 | | |
| 125 | β Crucis* | 12 37 33 | -58 43 | | nf | | | | 19.030 | 414.300 | 2 | 8 | | |

| 1 | 2 | 3 | 4 | 5 | 6 | 7 | 8 | 9 | 10 | 11 | 12 | 13 | 14 | 15 |
|---|---|---|---|---|---|---|---|---|---|---|---|---|---|---|
| **No.** | **Name** | **RA_DUN** | **DE_DUN** | **Angle_ of_Pos** | **Quad1** | **Quad2** | **Dist1** | **Dist2** | **delta_RA** | **delta_DE** | **vA** | **vB** | **vC** | **Remarks** |
| | | **(h:m:s)** | **(d:m:s)** | **(d:m)** | | | **('')** | **('')** | **(s)** | **('')** | **(mag)** | **(mag)** | **(mag)** | |
| 126 | o Crucis* | 12 44 00 | -56 13 | 79 48 | nf | | 35.91 | | 1.375 | 34.510 | 5 | 6 | | |
| 127 | Anonym.* | 12 49 09 | -54 57 | 51 0 | sf | | 10 | | 1.170 | 8.260 | 7 | 8 | | |
| 128 | ξ2 Centauri | 12 56 37 | -48 58 | 10 0 | sf | | 40 | | | | 5 | 14 | | |
| 129 | Anonym* | 12 57 11 | -64 22 | 79 0 | sp | | 3.31 | | | | 7 | 9.5 | | |
| 130 | Anonym. | 13 02 07 | -52 48 | | nf | | | | | | 8 | 8 | | |
| 131 | η Muscae* | 13 03 58 | -66 59 | 63 48 | np | | | | 5.340 | 52.640 | 6 | 8 | | |
| 132 | Anonym.* | 13 11 09 | -66 53 | 85 0 | nf | | 2 | | | | 8 | 8 | | Very pretty. |
| 133 | 165 Centauri* | 13 11 40 | -60 05 | 76 12 | np | | | | 2.557 | 56.680 | 6 | 8 | | |
| 134 | ι Centauri | 13 11 41 | -35 48 | 50 0 | sf | | | | | | | | | Very unequal. |
| 135 | Anonym. | 13 12 00 | -61 08 | | | | | | | | 8 | | | A curious group of five pretty bright stars. |
| 136 | Anonym. | 13 19 11 | -38 30 | | nf | | | | | 3.200 | 7 | 8 | | |
| 137 | Anonym.* | 13 19 36 | -62 06 | 72 50 | nf | | 12.4 | | | 12.190 | 8 | 9 | | |
| 138 | 369 Hydrae* | 13 28 00 | -25 37 | | sp | | | | | 9.630 | 6 | 8 | | |
| 139 | Anonym. | 13 28 35 | -55 17 | | nf | | | | | | 6 | 7 | 8 | Triple star. |
| 140 | Anonym. | 13 29 12 | -71 04 | | f | | 7 | | | | 8 | 9 | | |
| 141 | 195 Centauri* | 13 30 56 | -53 41 | 78 24 | sp | | 3 | 4 | | | 6 | 9 | | |
| 142 | Anonym.* | 13 32 09 | -58 24 | 5 23 | sf | | 32.376 | | 4.100 | 3.130 | 7 | 8 | | With two stars of the 14th magnitude between them. |
| 143 | Anonym.* | 13 37 08 | -61 13 | 60 32 | nf | | 11.183 | | 0.675 | 8.720 | 7 | 8 | | |
| 144 | Anonym. | 13 39 04 | -46 26 | 5 0 | sp | | 10 | | | | 8 | 8 | | |
| 145 | Anonym. | 13 39 14 | -66 01 | 30 0 | nf | | 10 | | | | 7 | 8.5 | | |

| 1 | 2 | 3 | 4 | 5 | 6 | 7 | 8 | 9 | 10 | 11 | 12 | 13 | 14 | 15 |
|---|---|---|---|---|---|---|---|---|---|---|---|---|---|---|
| No. | Name | RA_DUN (h:m:s) | DE_DUN (d:m:s) | Angle_ of_Pos (d:m) | Quad1 | Quad2 | Dist1 ('') | Dist2 ('') | delta_RA (s) | delta_DE ('') | vA (mag) | vB (mag) | vC (mag) | Remarks |
| 146 | 208 Centauri* | 13 39 36 | -39 39 | 2 12 | nf | | | | 4.832 | 3.730 | 7 | 7 | | Double L. C. |
| 147 | 215 Centauri* | 13 41 23 | -51 56 | 60 0 | np | | 13.2 | | | 9.340 | 6 | 8 | | |
| 148 | k Centauri* | 13 42 28 | -32 09 | 30 10 | sf | | 9.232 | | 0.570 | 4.254 | 6 | 8 | | |
| 149 | 222 Centauri* | 13 43 45 | -37 24 | 50 0 | sp | | | | 9.800 | 136.600 | 7 | 7 | | Double L. C. |
| 150 | Anonym. | 13 45 20 | -56 46 | 6 0 | sp | | | | 7.300 | 3.140 | 8 | 8 | | |
| 151 | Anonym. | 13 46 30 | -55 14 | 90 0 | n | | | | | | 7 | 10 | | |
| 152 | υ2 Centauri | 13 51 09 | -44 43 | | nf | | 2 | | | | 6 | 13 | | |
| 153 | χ Centauri* | 13 55 22 | -40 20 | 14 32 | nf | | | | 6.700 | 17.540 | 5.5 | 9 | | |
| 154 | Anonym. | 13 55 57 | -35 39 | 60 0 | sf | | 15 | | | | 7 | 8 | | |
| 155 | Anonym.* | 13 56 07 | -52 53 | 40 0 | nf | | 19.16 | | | | 7 | 8 | | |
| 156 | θ Centauri | 13 56 20 | -35 30 | 50 0 | sf | | 3 | | | | 3 | 14 | | Large star yellow. Small star blue. |
| 157 | Anonym. | 13 57 12 | -50 36 | 70 0 | sf | | 13 | | | | 6 | 9.5 | | |
| 158 | Anonym. | 14 00 12 | -45 07 | 14 0 | nf | | 6 | | | | 7 | 9 | | Large star white. Small star greenish. |
| 159 | Y Centauri* | 14 10 27 | -57 40 | 70 55 | sf | | 12.789 | | 0.150 | 9.580 | 5.5 | 8 | | |
| 160 | τ1 Centauri* | 14 14 51 | -44 25 | | sp | | | | 6.300 | 102.370 | 5 | 9 | | |
| 161 | Anonym. | 14 16 30 | -53 51 | 58 3 | nf | | | | 2.860 | 40.360 | 8 | 8 | | |
| 162 | 295 Centauri | 14 22 50 | -45 41 | | p | | | | | | 7 | 10 | | Very minute double stars. |
| 163 | Anonym.* | 14 23 52 | -53 35 | 23 48 | sf | | | | 5.500 | 23.040 | 8 | 8 | | |
| 164 | η Centauri* | 14 24 20 | -41 24 | | sf | | | | | 99.150 | 3 | 9 | | |
| 165 | α Centauri* | 14 28 00 | -60 06 | 56 49 | sp | | | | 1.783 | 18.788 | 1 | 4 | | Double L. C. |

| 1 | 2 | 3 | 4 | 5 | 6 | 7 | 8 | 9 | 10 | 11 | 12 | 13 | 14 | 15 |
|---|---|---|---|---|---|---|---|---|---|---|---|---|---|---|
| **No.** | **Name** | **RA_DUN (h:m:s)** | **DE_DUN (d:m:s)** | **Angle_ of_Pos (d:m)** | **Quad1** | **Quad2** | **Dist1 ('')** | **Dist2 ('')** | **delta_RA (s)** | **delta_DE ('')** | **vA (mag)** | **vB (mag)** | **vC (mag)** | **Remarks** |
| 166 | α Circini | 14 28 50 | -64 12 | 7 0 | sp | | 10 | | | | 4 | 12 | | |
| 167 | Anonym. | 14 29 40 | -35 12 | 80 0 | sf | | 50 | | | | 6.5 | 10 | | Large star white. Small star pale. |
| 168 | Anonym. | 14 30 57 | -54 31 | 70 0 | sp | | 5 | | | | 8 | 8.5 | | |
| 169 | Anonym.* | 14 32 09 | -54 50 | 13 54 | sf | | | | 8.120 | 20.760 | 7 | 8 | | |
| 170 | Anonym. | 14 32 16 | -55 30 | 90 0 | n | | 2 | | | | 8 | 8 | | Very nearly equal. |
| 171 | Anonym. | 14 41 22 | -45 10 | 57 0 | sp | | 20 | | | | 7 | 9 | | |
| 172 | ζ Circini | 14 41 27 | -65 16 | | | | 3 | | | | | | | A close double star. |
| 173 | 328 Centauri | 14 42 07 | -37 05 | 60 0 | sf | | 2 | | | | 7 | 10 | | |
| 174 | Anonym.* | 14 44 06 | -46 07 | 20 44 | np | | 3 | | | | 7 | 8 | | Large star dusky. Small star greenish. Very pretty. |
| 175 | Anonym. | 14 49 22 | -51 13 | | np | | | | | | 7 | 10 | | |
| 176 | ζ Lupi* | 14 59 54 | -51 25 | 20 48 | sp | | 68.79 | | 7.380 | 24.470 | 4.5 | 8 | | |
| 177 | κ Lupi* | 15 00 00 | -48 01 | 55 40 | sf | | 28.88 | | 1.397 | 25.558 | | | | |
| 178 | 25 Lupi* | 15 00 09 | -44 36 | 5 19 | np | | | | 3.525 | 14.350 | 6 | 7 | | |
| 179 | Anonym.* | 15 03 39 | -42 44 | 40 36 | nf | | 11 | | | | 8 | 9 | | |
| 180 | μ Lupi* | 15 06 23 | -47 13 | 64 36 | sf | | | | 1.500 | 14.613 | 5 | 8 | | |
| 181 | Anonym. | 15 09 56 | -37 46 | 25 0 | nf | | 9 | 10 | | | 8 | 9 | 9 | Three stars in a line nearly equidistant. |
| 182 | ε Lupi* | 15 10 48 | -44 03 | 83 38 | sf | | 19.12 | | | | 4 | 10 | | |
| 183 | 51 Lupi* | 15 14 07 | -38 07 | | sp | | 12 | 15 | | | 6 | 10 | | A star of the 6th magn. With two |

| 1 | 2 | 3 | 4 | 5 | 6 | 7 | 8 | 9 | 10 | 11 | 12 | 13 | 14 | 15 |
|---|---|---|---|---|---|---|---|---|---|---|---|---|---|---|
| No. | Name | RA_DUN (h:m:s) | DE_DUN (d:m:s) | Angle_of_Pos (d:m) | Quad1 | Quad2 | Dist1 ('') | Dist2 ('') | delta_RA (s) | delta_DE ('') | vA (mag) | vB (mag) | vC (mag) | Remarks |
| | | | | | | | | | | | | | | stars of the 10th. |
| 184 | Anonym. | 15 14 32 | -42 12 | 65 0 | sf | | 14 | | | | 7 | 8 | 12 | |
| 185 | Anonym. | 15 15 20 | -50 59 | | f | | 3 | | | | 7 | 11 | | |
| 186 | Anonym. | 15 18 30 | -57 30 | 35 0 | sf | | | | | 18.670 | 8 | 8 | | |
| 187 | Anonym. | 15 20 17 | -46 57 | 52 0 | sp | | 10 | | | | 7 | 9 | | |
| 188 | ε Trianguli Aust. | 15 20 40 | -65 43 | 60 0 | sf | | 60 | | | | 5 | 10 | | |
| 189 | π Normae | 15 26 13 | -51 47 | 40 0 | np | | 56 | | | | 6 | 11 | | |
| 190 | Anonym. | 15 26 30 | -57 38 | 5 0 | nf | | 3 | | | | 7 | 8 | | |
| 191 | Anonym. | 15 31 55 | -57 59 | 55 0 | np | | 12 | | | | 8 | 8 | | |
| 192 | Anonym. | 15 37 48 | -35 03 | 40 0 | nf | | 35 | | | | 7 | 7 | | |
| 193 | υ Normae | 15 38 00 | -54 31 | | nf | | | | | | 6 | 11 | | |
| 194 | Anonym. | 15 39 00 | -60 10 | 47 0 | np | f | 10 | | | | 7 | 9 | 10 | Triple star. |
| 195 | Anonym. | 15 41 56 | -49 38 | 83 0 | nf | | 5 | | | | 7.5 | 7.5 | | Very pretty d. Star. |
| 196 | ξ Lupi* | 15 46 01 | -33 30 | 40 43 | nf | | | | 0.700 | 7.095 | 6 | 6 | | Beautiful d. Star. |
| 197 | η Lupi* | 15 48 26 | -37 53 | 25 0 | sp | | 60 | | | 17.270 | 4 | 9 | | |
| 198 | Anonym. | 15 52 00 | -53 09 | 90 0 | s | | 30 | | | | 7 | 11 | | |
| 199 | Anonym. | 15 58 19 | -38 35 | 80 0 | sp | | 12 | | | | 7 | 7 | | |
| 200 | Anonym. | 16 09 48 | -43 31 | 82 0 | sf | | 17 | | | | 6.5 | 12 | | |
| 201 | ι Trianguli Aust. | 16 12 10 | -63 39 | 58 0 | nf | | 14 | | | | 6 | 13 | | |
| 202 | Anonym. | 16 18 36 | -41 25 | 80 0 | sp | | 26 | | | | 6 | 11 | | |
| 203 | Anonym. | 16 19 23 | -60 35 | | | | | | | | 8 | 8 | | |
| 204 | 57 Normae | 16 23 40 | -35 21 | | | | | | | | 6 | 7 | | |

| 1 | 2 | 3 | 4 | 5 | 6 | 7 | 8 | 9 | 10 | 11 | 12 | 13 | 14 | 15 |
|---|---|---|---|---|---|---|---|---|---|---|---|---|---|---|
| No. | Name | RA_DUN | DE_DUN | Angle_ of_Pos | Quad1 | Quad2 | Dist1 | Dist2 | delta_RA | delta_DE | vA | vB | vC | Remarks |
| | | (h:m:s) | (d:m:s) | (d:m) | | | ('') | ('') | (s) | ('') | (mag) | (mag) | (mag) | |
| 205 | Anonym. | 16 24 32 | -49 01 | 50 0 | nf | | 16 | | | | 8 | 8 | | |
| 206 | Anonym. | 16 29 40 | -48 17 | | | | | | | | 7 | 8 | | |
| 207 | Anonym. | 16 30 38 | -42 05 | 85 0 | sp | | 6 | | | | 8 | 9 | | |
| 208 | Anonym. | 16 31 00 | -46 48 | | nf | | | | | | 7 | 8 | | |
| 209 | Anonym. | 16 35 21 | -36 35 | 60 0 | sp | | 14 | | | | 7 | 8 | | |
| 210 | Anonym. | 16 35 30 | -55 08 | | | | | | | | 7 | 7 | | Very nearly equal. |
| 211 | Anonym. | 16 35 30 | -48 05 | 60 0 | np | f | 20 | | | | 7 | 9 | 9 | Triangle of stars. |
| 212 | Anonym. | 16 49 43 | -50 51 | 42 0 | sp | | 5 | | | | 8 | 9 | | Not certain; but the declination should be -49 05 00. |
| 213 | Anonym. | 16 55 30 | -46 27 | 63 0 | sf | | 8 | | | | 7 | 9 | | |
| 214 | Anonym. | 16 56 34 | -66 59 | 50 0 | np | | 22 | | | | 7 | 12 | | |
| 215 | Anonym. | 17 02 49 | -53 06 | | | | 15 | 18 | | | 8 | | | Triangle; p. b. stars. The southernmost star is double. 8th and 12th magnitudes. |
| 216 | 48 Arae* | 17 13 00 | -45 40 | 59 56 | nf | | 33.07 | | 1.550 | 28.400 | 7 | 7 | | |
| 217 | Anonym. | 17 15 40 | -43 49 | 58 0 | sf | | 8 | | | | 7 | 10 | | |
| 218 | λ Scorpii | 17 21 44 | -36 58 | 56 0 | nf | | 60 | | | | 3 | 12 | | |
| 219 | Anonym. | 17 46 54 | -36 54 | 7 0 | sp | | 30 | | | | 7 | 8 | | |
| 220 | Anonym. | 18 04 46 | -55 31 | 80 0 | sf | | | | | | 7 | 8 | | |
| 221 | σ Telescopii | 18 11 56 | -44 11 | 90 0 | s | | 40 | | | | 6 | 11 | | |
| 222 | κ Coronae Aust. | 18 21 30 | -38 51 | | | | 14 | | | | 6 | 7 | | Double L. C. |

| 1 | 2 | 3 | 4 | 5 | 6 | 7 | 8 | 9 | 10 | 11 | 12 | 13 | 14 | 15 |
|---|---|---|---|---|---|---|---|---|---|---|---|---|---|---|
| **No.** | **Name** | **RA_DUN** | **DE_DUN** | **Angle_ of_Pos** | **Quad1** | **Quad2** | **Dist1** | **Dist2** | **delta_RA** | **delta_DE** | **vA** | **vB** | **vC** | **Remarks** |
| | | **(h:m:s)** | **(d:m:s)** | **(d:m)** | | | **('')** | **('')** | **(s)** | **('')** | **(mag)** | **(mag)** | **(mag)** | |
| 223 | Anonym. | 18 27 08 | -42 21 | 50 0 | nf | | 8 | | | | 6 | 7 | 7 | |
| 224 | Anonym. | 18 41 20 | -47 28 | | sf | | | | 7.000 | 34.000 | 7 | 7 | | |
| 225 | Anonym. | 18 59 13 | -52 05 | | sp | | | | | 20.900 | 7 | 8 | | |
| 226 | β1 Sagittarii | 19 09 57 | -44 47 | 30 0 | nf | | 30 | | | | 3.5 | 9 | | |
| 227 | Anonym. | 19 37 11 | -55 26 | 75 0 | sf | | 30 | | | | 7 | 7.5 | | Large star yellow. Small star blue. |
| 228 | Anonym.* | 19 38 45 | -64 19 | 62 8 | sf | | | | 1.850 | 20.750 | 6 | 7 | | |
| 229 | Anonym.* | 19 45 28 | -52 22 | 23 22 | sp | | | | | 33.400 | 7 | 8 | | |
| 230 | Anonym. | 20 06 44 | -40 39 | 7 0 | sf | | | | | 8.000 | 8 | 8 | | |
| 231 | 74 Pavonis* | 20 16 28 | -71 49 | 18 15 | np | | 64.37 | | | 20.200 | 6 | 9 | | |
| 232 | Anonym.* | 20 21 00 | -76 56 | 76 18 | nf | | 18.47 | | 1.410 | 17.780 | 6 | 6.5 | | |
| 233 | φ Pavonis | 20 21 00 | -61 10 | 12 0 | nf | | 40 | | | | 5.5 | 12 | | Exceedingly unequal. |
| 234 | α Indi | 20 25 08 | -47 54 | 85 0 | sp | | 5 | | | | 3 | 14 | | Large star yellow. Small star blue. |
| 235 | Anonym.* | 20 32 17 | -51 07 | 33 25 | sp | | | | | 70.700 | 7 | 7 | | |
| 236 | Anonym.* | 20 50 00 | -43 39 | 14 33 | nf | | 67.23 | | 5.650 | 15.370 | 6 | 6.5 | | |
| 237 | Anonym. | 21 16 23 | -59 34 | | | | | | | | 8 | | | Four pretty bright stars in a straight line. |
| 238 | Anonym. | 22 08 56 | -75 58 | | f | | 14 | | | | 8 | 12 | | |
| 239 | δ2 Gruis | 22 19 15 | -44 39 | 47 0 | sp | | 50 | | | | 5 | 9 | | |
| 240 | β Piscis Aust.* | 22 21 00 | -33 14 | 82 46 | sf | | 35.31 | | | 27.680 | 3 | 9 | | |
| 241 | σ Piscis Aust.* | 22 26 00 | -32 34 | 56 48 | nf | | | | 2.860 | 75.300 | 6 | 7 | | |

| 1 | 2 | 3 | 4 | 5 | 6 | 7 | 8 | 9 | 10 | 11 | 12 | 13 | 14 | 15 |
|---|---|---|---|---|---|---|---|---|---|---|---|---|---|---|
| **No.** | **Name** | **RA_DUN (h:m:s)** | **DE_DUN (d:m:s)** | **Angle_of_Pos (d:m)** | **Quad1** | **Quad2** | **Dist1 ('')** | **Dist2 ('')** | **delta_RA (s)** | **delta_DE ('')** | **vA (mag)** | **vB (mag)** | **vC (mag)** | **Remarks** |
| 242 | 50 Piscis Aust.* | 22 30 00 | -29 17 | 69 17 | sf | | | | 4.930 | 37.500 | 6 | 7 | | |
| 243 | β Gruis | 22 32 05 | -47 48 | | f | | | | | | 3 | 14 | | Triple. Two very minute stars in a line following the large star. |
| 244 | σ Toucani | 22 51 22 | -65 29 | | sf | | 60 | | | | 7 | 9 | | σ is a small pale star of the 7.8th magnitude. |
| 245 | Anonym. | 22 57 12 | -60 40 | 10 0 | np | | 10 | | | | 7 | 13 | | Large star white. Small star blue. |
| 246 | Anonym. | 22 58 36 | -51 38 | 37 0 | sp | | 10 | | | | 7 | 8 | | |
| 247 | Anonym. | 23 07 20 | -61 57 | 8 0 | np | | 30 | | | | 8 | 8 | | |
| 248 | Anonym. | 23 10 36 | -51 19 | 53 0 | sp | | 16 | | | | 8 | 10 | | |
| 249 | ψ Gruis* | 23 13 50 | -54 49 | 58 24 | sp | | 27.09 | | | 22.730 | 6.5 | 8 | | |
| 250 | Anonym.* | 23 17 00 | -51 14 | 3 38 | sf | | 51.8 | | 5.460 | 3.450 | 7 | 8 | | |
| 251 | θ Phoenicis* | 23 30 00 | -47 36 | | p | | | | | | 6 | 6 | | |
| 252 | 29 Toucani * | 23 34 00 | -65 22 | 27 24 | sf | | | | | | 6 | 8 | | |
| 253 | φ Sculptoris* | 23 46 00 | -28 26 | | p | | 5.031 | | | | 6 | 6 | | |

# APPENDIX B

Table 2: Cross-matched source identifiers of the primary and secondary with, the identifier from the WDS, the discoverer code from the WDS, SIMBAD, ASCC and Gaia DR2 identifiers.

| 1 | 16 | 17 | 18 | 19 | 20 | 21 | 22 | 23 |
|---|---|---|---|---|---|---|---|---|
| **No.** | **WDS** | **Disc** | **SIMBAD_A** | **SIMBAD_B** | **ASCC_A** | **ASCC_B** | **GAIA_DR2_A** | **GAIA_DR2_B** |
| 1 | 00315-6257 | LCL 119AC | *bet01 Tuc | *bet02 Tuc | 2292377 | 2292378 | 4900927434176620160 | 4900926678262376704 |
| 2 | 00524-6930 | DUN 2 | *lam01 Tuc | HD 5208 | 2373287 | 2373289 | 4691995692046507520 | 4691996001284152576 |
| 3 | 01270-3233 | LDS2199 | V* R Scl | CCDM J01270-3233B | 1716249 | | 5016138145186249088 | |
| 4 | 01388-5327 | DUN 4 | HD 10241 | CPD-54 358B | 2103580 | 2103581 | 4912810337375316992 | 4912810337375317632 |
| 5 | 01398-5612 | DUN 5 | *p Eri A | *p Eri B | 2199057 | 2199056 | 4911306239828325632 | 4911306239828325760 |
| 6 | 02165-5131 | DUN 6AB | *phi Eri | CD-52 465 | 2104402 | 2104399 | 4936685751335824896 | 4936685716976087552 |
| 7 | 02397-5934 | DUN 7A,BC | HD 16852 | HD 16853 | 2200322 | 2200329 | 4726060211542143616 | 4726066018337928192 |
| 8 | 02572-2458 | S 423AB,C | HD 18455A | HD 18445 | 1525490 | 1525486 | | 5076269164798852864 |
| 9 | 02583-4018 | PZ 2 | *tet01 Eri | *tet02 Eri | 1909803 | 1909804 | 5044368071869592832 | 5044368071868204160 |
| 10 | 03046-5119 | DUN 10AB | HD 19330 | CD-51 706 | 2105363 | 2105365 | 4747692278185293312 | 4747693686934567040 |
| 11 | unidentified | | | | | | | |
| 12 | 03152-6427 | DUN 12A,BC | HD 20586 | CCDM J03152-6427BC | 2295352 | 2295353 | 4672336699019592320 | 4672336694724418560 |
| 13 | unidentified | | | | | | | |
| 14 | 03382-5947 | DUN 14 | HD 22989 | HD 22960 | 2201630 | 2201628 | 4728825002249947904 | 4728825036609672576 |
| 15 | 03398-4022 | DUN 15 | HD 22986A | HD 22986B | 1910857 | 1910855 | 4849246401941883264 | 4849246397645456000 |
| 16 | 03486-3737 | DUN 16 | HD 24072 | HD 24071 | 1817423 | 1817421 | 4856719713756945664 | 4856719713756946176 |

| 1<br>No. | 16<br>WDS | 17<br>Disc | 18<br>SIMBAD_A | 19<br>SIMBAD_B | 20<br>ASCC_A | 21<br>ASCC_B | 22<br>GAIA_DR2_A | 23<br>GAIA_DR2_B |
|---|---|---|---|---|---|---|---|---|
| 17 | 04010-5424 | DUN 17AB | HD 25590 | HD 25591 | 2106767 | 2106768 | 4779816503255644672 | 4779816297097214336 |
| 18 | 04509-5328 | DUN 18AB | *iot Pic A | *iot Pic B | 2108254 | 2108256 | 4777112872882315648 | 4777112872882315264 |
| 19 | one | | HD 34496 | | 1724040 | | 4826073060516094080 | |
| 20 | 05248-5219 | DUN 20AB,C | * tet Pic | HD 35859 | 2109422 | 2109419 | 4771835629385988992 | 4771835595026248832 |
| 21 | 05302-4705 | DUN 21AD | HD 36553 | HD 36520 | 2012117 | 2012100 | 4798709239757160320 | 4798709067958473216 |
| 22 | 05312-4219 | DUN 22 | HD 36648A | HD 36648B | 1915226 | 1915228 | 4806195676992118784 | 4806195299034996864 |
| 23 | 06048-4828 | DUN 23 | V* V575 Pup | TYC 8105-1651-2 | 2013728 | 2013729 | 5554191685020871424 | 5554191685019290368 |
| 24 | one | | *del Pic | | 2111224 | | 5499415974230271488 | |
| 25 | 06189-3212 | JSP 96 | CD-32 2930A | CD-32 2930B | 1728092 | 1728093 | 2892904187481797504 | 2892904187482208128 |
| 26 | 06122-6532 | DUN 26AB | HD 43618 | HD 43639 | 2379551 | 2379552 | 5476519984615508224 | 5476521251625953152 |
| 27 | 06163-5913 | DUN 27AB | HD 44120 | HD 44105 | 2206307 | 2206304 | 5482551183847322752 | 5482551183847322496 |
| 28 | 06240-3642 | DUN 28AC | HD 45145 | HD 45158 | 1824828 | 1824835 | 5575351648860045312 | 5575351545780828032 |
| 29 | 06291-4022 | DUN 29 | HD 46039 | HD 46040 | 1918620 | 1918630 | 5570747993673945984 | 5570747890594733568 |
| 30 | 06298-5014 | DUN 30AB,CD | HR 2384 | TYC 8111-2008-2 | 2112078 | 2112074 | | |
| 31 | 06386-4813 | DUN 31 | HD 47973 | HD 47973B | 2015711 | 2015708 | 5551248086235237248 | 5551248292393667200 |
| 32 | 06423-3824 | DUN 32 | HD 48543A | HD 48543B | 1826228 | 1826223 | 5576835955197352192 | 5576836023916828288 |
| 33 | one | | HD 49319 | | 1826535 | | 5575933531029392896 | |
| 34 | 06442-5442 | DUN 34 | HD 49219 | HD 49192 | 2112826 | 2112821 | 5497185992850609152 | 5497185133857153920 |
| 35 | two | | HD 49942 | HD 49850 | 1920145 | 1920113 | 5562241106570387584 | 5562253407356693120 |
| 36 | 06504-3142 | H 5 108A,BC | V* HZC Ma | CD-31 3719 | 1730756 | 1730759 | 5583324035874959360 | 5583323314320455936 |
| 37 | two | | HD 53142 | HD 53348 | 2113773 | 2113809 | 5505040697762533760 | 5505041728554364928 |
| 38 | 07040-4337 | DUN 38AB | HD 53705 | HD 53706 | 1921369 | 1921372 | 5559265690666326016 | 5559265690666327168 |

| 1<br>No. | 16<br>WDS | 17<br>Disc | 18<br>SIMBAD_A | 19<br>SIMBAD_B | 20<br>ASCC_A | 21<br>ASCC_B | 22<br>GAIA_DR2_A | 23<br>GAIA_DR2_B |
|---|---|---|---|---|---|---|---|---|
| 39 | 07033-5911 | DUN 39 | HD 53921A | HD 53921B | 2208454 | 2208456 | 5480486644608749696 | 5480486640313882880 |
| 40 | 07092-5622 | DUN 40 | HD 55327 | HD 55352 | 2208793 | 2208795 | 5490000787442758144 | 5490000787442760576 |
| 41 | 07104-5536 | RMK 5 | HD 55598 | CD-55 1708 | 2208862 | 2208857 | 5490328648067150720 | 5490328648067151104 |
| 42 | 07087-7030 | DUN 42 | *gam02 Vol | *gam01 Vol | 2445952 | 2445949 | 5267405895348357120 | 5267405964069463680 |
| 43 | 07171-3706 | DUN 43AB | *pi. Pup Aa | HD 56856 | 1829087 | 1829080 | 5589311357724458368 | 5589305477912168192 |
| 44 | 07204-5219 | RMK 6AB | HD 57852 | HD 57853 | 2114933 | 2114936 | 5492026740697659648 | 5492026740697659264 |
| 45 | 07214-4832 | DUN 45 | HD 58017 | HD 58018 | 2018751 | 2018756 | 5506905297684851584 | 5506905228965376768 |
| 46 | unidentified | | | | | | | |
| 47 | 07247-3149 | DUN 47A,CD | HD 58535 | HD 58534 | 1734969 | 1734962 | 5592885801315568768 | 5592886110552963968 |
| 48 | unidentified | | | | | | | |
| 49 | 07289-3151 | DUN 49 | HD 59499 | HD 59500 | 1735664 | 1735667 | 5593011729755869696 | 5593011832835083008 |
| 50 | unidentified | | | | | | | |
| 51 | 07292-4318 | DUN 51 | *sig Pup | *sig Pup B | 1923547 | 1923553 | 5512070906388269568 | 5512071009471894912 |
| 52 | 07343-2328 | H N 19 | *n Pup A | *n Pup B | 1550714 | 1550719 | 5618420137803147008 | 5618420137803146240 |
| 53 | 07388-2648 | H 3 27AB | *k02 Pup | *k01 Pup | 1645677 | 1645672 | 5612323414549657728 | 5612323414549657984 |
| 54 | one | | * c Pup | | 1831780 | | 5538814190271704960 | |
| 55 | 07442-5027 | DUN 55AB | HD 63008 | CD-50 2948 | 2116430 | 2116437 | 5493209501673364736 | 5493209437253410432 |
| 56 | 07471-4130 | DUN 56 | HD 63425 | V* V394 Pup | 1925301 | 1925303 | 5535916496103849088 | 5535916393024640896 |
| 57 | 07418-7236 | DUN 57 | *zet Vol | *zet Vol B | 2447249 | 2447251 | 5263150888430032256 | 5263150888430032384 |
| 58 | three | | HD 65013 | HD 65037 | 1926351 | 1926359 | 5531438838080560384 | 5531438558901143680 |
| 59 | 07592-4959 | DUN 59 | HD 66005 | HD 66006 | 2022196 | 2022202 | 5514090400016110976 | 5514090434376720512 |
| 60 | 08014-5431 | DUN 60 | V* V461 Car | CD-54 2029 | 2117504 | 2117508 | 5320234267972369152 | 5320234057513080320 |

| 1<br>No. | 16<br>WDS | 17<br>Disc | 18<br>SIMBAD_A | 19<br>SIMBAD_B | 20<br>ASCC_A | 21<br>ASCC_B | 22<br>GAIA_DR2_A | 23<br>GAIA_DR2_B |
|---|---|---|---|---|---|---|---|---|
| 61 | 08069-2707 | DUN 61 | HD 67409 | CD-26 5531 | 1652760 | 1652767 | 5694066331642125824 | 5694066709599229568 |
| 62 | 08047-6250 | DUN 62 | HD 67536 | CD-62 329 | 2304263 | 2304251 | 5289522090708710656 | 5289516936747952768 |
| 63 | 08098-4238 | DUN 63 | HD 68242A | HD 68242B | 1928607 | 1928610 | 5533290621824556672 | 5533290621824555264 |
| 64 | 08095-4720 | DUN 65AC | *gam02 Vel | CD-46 3848 | 2023562 | 2023566 | | 5519219999721187968 |
| 65 | 08095-4720 | DUN 65AB | *gam02 Vel | *gam01 Vel | 2023562 | 2023557 | | 5519266900766220800 |
| 66 | 08079-6837 | RMK 7 | *eps Vol A | *eps Vol B | 2383172 | 2383174 | 5270986008289935232 | 5270986008289935488 |
| 67 | 08140-3619 | DUN 67 | HD 69081 | HD 69082 | 1835488 | 1835490 | 5541637564345383808 | 5541624335846120192 |
| 68 | 08136-3621 | DUN 68 | HD 68944 | HD 68962 | 1835397 | 1835404 | 5541636739711787264 | 5541636945870181632 |
| 69 | 08255-5144 | DUN 69AB | HD 71510 | CD-51 3003 | 2118943 | 2118941 | 5322244690627583104 | 5322244690627585280 |
| 70 | 08295-4443 | DUN 70 | HD 72127A | HD 72127B | 1931221 | 1931220 | 5522979294390810752 | 5522979294390810624 |
| 71 | 08306-4031 | DUN 71 | HD 72318 | HD 72317 | 1931403 | 1931411 | 5527782446519946880 | 5527782480879666816 |
| 72 | 08404-4223 | DUN 72A,BC | HD 74105 | HD 74104 | 1932766 | 1932764 | 5525075856907721216 | 5525076548400146688 |
| 73 | 08562-5532 | DUN 73AB | HD 76824 | HD 76823 | 2215700 | 2215701 | 5305072895992630784 | 5305073136510805760 |
| 74 | 08570-5914 | DUN 74 | *b01 Car | CD-58 2350 | 2215750 | 2215754 | 5303286052150068352 | 5303286017790332416 |
| 75 | 09179-6948 | RMK 10 | HD 80807 | CPD-691035B | 2386328 | 2386329 | 5222647212228907136 | 5222650171466372480 |
| 76 | 09286-4530 | DUN 76AC | HD 82109 | HD 82121 | 2032680 | 2032690 | 5423001668454182656 | 5423001462295754368 |
| 77 | 09293-4432 | DUN 77AB | HD 82207 | HD 82241 | 1938548 | 1938560 | 5423340970868485504 | 5423346674585062144 |
| 78 | 09308-3153 | DUN 78 | *zet01 Ant A | *zet01 Ant B | 1753443 | 1753440 | 5632038276500794496 | 5632038276500795648 |
| 79 | 09336-4945 | DUN 79 | HD 82965 | HD 82986 | 2033099 | 2033117 | 5409197334336573056 | 5409197437415809024 |
| 80 | 09450-4929 | DUN 80AB | HD 84627 | HD 84612 | 2034180 | 2034174 | 5409029212137818368 | 5409029212137815808 |
| 81 | 09543-4517 | DUN 81 | HD 85980 | HD 85980B | 2035254 | 2035252 | 5411771119252271872 | 5411771119252271360 |
| 82 | 09333-8601 | DUN 82 | HD 85300 | CPD-85 210B | 2453141 | 2453130 | 5189985016733501440 | 5189985021031273472 |

| 1 | 16 | 17 | 18 | 19 | 20 | 21 | 22 | 23 |
|---|---|---|---|---|---|---|---|---|
| No. | WDS | Disc | SIMBAD_A | SIMBAD_B | ASCC_A | ASCC_B | GAIA_DR2_A | GAIA_DR2_B |
| 83 | 10021-5459 | DUN 83 | HD 87254 | HD 87221 | 2130673 | 2224417 | 5260124688857959040 | 5260124345260563200 |
| 84 | 10032-5203 | HJ 4282 | HD 87364 | HD 298817 | 2130814 | 2130810 | 5404964317652126336 | 5404964283292384384 |
| 85 | 10288-6235 | DUN 85 | HD 91027 | HD 91026 | 2316921 | 2316914 | 5252242702326780160 | 5252242667967046016 |
| 86 | 10312-4214 | DUN 86AB | HD 91239 | HD 91223 | 1945198 | 1945183 | 5368269388368281600 | 5368269285289064832 |
| 87 | 10307-6121 | DUN 87 | HD 91270 | HD 91269 | 2317155 | 2317146 | 5253945227372557312 | 5253948354108765696 |
| 88 | 10320-4504 | PZ 3 | HD 91355 | HD 91356 | 2039586 | 2039582 | 5367389229311297280 | 5367389229311295872 |
| 89 | 10333-5523 | DUN 89AB | HD 300791 | HD 91593 | 2230402 | 2230408 | 5352404294598481920 | 5352404397648913152 |
| 90 | unidentified | | | | | | | |
| 91 | 10319-7207 | DUN 91 | HD 91601 | CPD-71 1045B | 2456738 | 2456739 | 5229628256374245248 | 5229628256374246528 |
| 92 | one | | *p Car | | 2317331 | | 5253796346588022656 | |
| 93 | 10349-6408 | DUN 93AB | HD 91906 | HD 307860 | 2317750 | 2317757 | 5251822104760873344 | 5251822139120626432 |
| 94 | 10387-5911 | DUN 94 | HD 92397 | HD 92398 | 2231436 | 2231442 | 5350588691654540544 | 5350588691654545792 |
| 95 | 10393-5536 | DUN 95AB | *x Vel | HD 92463 | 2231547 | 2231572 | 5352174702825907840 | 5352174805905137920 |
| 96 | one | | HD 92964 | | 2232192 | | 5350406619413548032 | |
| 97 | 10432-6110 | DUN 97AB | HD 93010 | CPD-60 2203B | 2318912 | 2318913 | 5254068613204875264 | 5254068613204866432 |
| 98 | 10451-5941 | DUN 98AH | *eta Car | HD 303308 | 2232700 | 2232708 | 5350358580171706624 | 5350358683250920704 |
| 99 | 10443-7052 | DUN 99AB | HD 93344 | HD 93359 | 2457524 | 2457533 | 5231271579581900800 | 5231271476495341952 |
| 100 | unidentified | | | | | | | |
| 101 | 10510-5957 | HJ 4378 | HD 94173 | CPD-59 2783 | 2233856 | 2233851 | 5338305738062716544 | 5338305841141942272 |
| 102 | 10535-5851 | DUN 102AB | *u Car | HD 94491 | 2234363 | 2234336 | 5338833263115792512 | 5338832919518362752 |
| 103 | 10535-5851 | DUN 103AC | *u Car | CPD-58 2836 | 2234363 | 2234366 | 5338833263115792512 | 5338833297475543936 |
| 104 | three | | HD 95429 | | 2138437 | | 5359955053246566144 | |

| 1<br>No. | 16<br>WDS | 17<br>Disc | 18<br>SIMBAD_A | 19<br>SIMBAD_B | 20<br>ASCC_A | 21<br>ASCC_B | 22<br>GAIA_DR2_A | 23<br>GAIA_DR2_B |
|---|---|---|---|---|---|---|---|---|
| 105 | 11049-6103 | DUN 105 | HD 96264 | HIP 54171 | 2321918 | 2321912 | 5337284326102045568 | 5337283948144897664 |
| 106 | one | | HD 98161 | | 1855147 | | 5397046115926029056 | |
| 107 | two | | HD 98537 | HD 98486 | 2459375 | 2459352 | 5226029103836945280 | 5226076112259827968 |
| 108 | four | | HD 98897 | | 2239471 | | 5339606563379239040 | |
| 109 | 11286-4240 | BSO 6 | HD 99803 | HIP 56001 | 1949977 | 1949980 | 5382258371728407680 | 5382258371728407040 |
| 110 | three | | HD 100015 | | 2240660 | | 5343376445138829824 | |
| 111 | 11323-2916 | H 3 96 | *17 Crt A | *17 Crt B | 1670309 | 1670306 | 3482326708703712896 | 3482326708703712640 |
| 112 | two | | HD 100838 | HD 100786 | 2143041 | 2142996 | 5369911474631774080 | 5369911058009191424 |
| 113 | 11370-3858 | DUN 113 | HD 100954 | HD 100965 | 1856216 | 1856220 | 5384606275726561792 | 5384603045914957952 |
| 114 | 11400-3806 | DUN 114 | HD 101406 | SAO 202691 | 1856371 | 1856373 | 5385035016545554560 | 5385035016545554688 |
| 115 | 11400-3327 | I 232 | | | 1762657 | 1762658 | 3477249370166290048 | |
| 116 | 11567-3216 | DUN 116AB | HD 103742 | HD 103743 | 1763490 | 1763493 | 3466924200065405184 | 3466924200065405824 |
| 117 | 12048-6200 | DUN 117AB | HD 104901 | V* BY Cru | 2330777 | 2330783 | 6057680496326765184 | 6057680423278480512 |
| 118 | 12066-3752 | HJ 4500 | HD 105173 | CD-37 7665 | 1857859 | 1857862 | 3459806786421605120 | 3459806786421611136 |
| 119 | two | | HD 106344 | HD 106362 | 2397544 | 2397555 | 5860530296185991552 | 5860530399265248512 |
| 120 | unidentified | | | | | | | |
| 121 | unidentified | | | | | | | |
| 122 | 12266-6306 | DUN 252AC | *alf01 Cru | HD 108250 | 2333718 | 2333711 | | 6053807844582485248 |
| 123 | 12266-6306 | DUN 252AB | *alf01 Cru | *alf02 Cru | 2333718 | 2333721 | | |
| 124 | 12312-5707 | DUN 124AB | *gam Cru | HD 108925 | 2248482 | 2248502 | | 6071671369457586688 |
| 125 | 12477-5941 | DUN 125AC | *bet Cru | HD 111160 | 2250231 | 2250260 | | 6056724299185776512 |
| 126 | 12546-5711 | DUN 126AB | *mu.01 Cru | *mu.02 Cru | 2250896 | 2250898 | 6060547163653418112 | 6060547331128876928 |

| 1 | 16 | 17 | 18 | 19 | 20 | 21 | 22 | 23 |
|---|---|---|---|---|---|---|---|---|
| No. | WDS | Disc | SIMBAD_A | SIMBAD_B | ASCC_A | ASCC_B | GAIA_DR2_A | GAIA_DR2_B |
| 127 | 12598-5555 | DUN 127 | HD 112764 | HD 112781 | 2251414 | 2251416 | 6061478965373623680 | 6061478209476557696 |
| 128 | 13069-4954 | DUN 128 | *ksi02 Cen | V* V1261 Cen | 2052802 | 2052804 | 6081542475600377472 | 6081530720270030208 |
| 129 | 13081-6518 | RMK 16AB | *tet Mus A | *tet Mus B | 2401910 | 2401908 | 5858915766471945984 | 5858915766471941248 |
| 130 | unidentified | | | | | | | |
| 131 | 13152-6754 | DUN 131AC | *eta Mus A | *eta Mus C | 2402372 | 2402368 | 5845487808865581568 | 5845487911944804864 |
| 132 | unidentified | | | | | | | |
| 133 | 13226-6059 | DUN 133AB,C | *J Cen | HD 116072 | 2339008 | 2339002 | 5869474548409857024 | 5869474617129630976 |
| 134 | one | | *iot Cen | | 1862167 | | 6165699748415726848 | |
| 135 | five | | HD 116119 | | 2339037 | | 5868514605999645696 | |
| 136 | unidentified | | | | | | | |
| 137 | 13321-6303 | DUN 137 | HD 117460 | CD-62 732B | 2340319 | 2340318 | 5865249812400697472 | 5865249812400694272 |
| 138 | 13368-2630 | H N 69AB | HD 118349A | HD 118349B | 1675685 | 1675683 | 6188997162858447360 | 6188994207920947328 |
| 139 | three | | HD 118258 | | 2255294 | | 6064406277664894208 | |
| 140 | 13458-7159 | DUN 140 | CPD-71 1507 | CPD-71 1507B | 2468095 | 2468099 | 5839923627169745664 | 5839923622864522112 |
| 141 | 13417-5434 | DUN 141 | *Q Cen A | *Q Cen B | 2154813 | 2154815 | 6065381024758288128 | 6065381029065308416 |
| 142 | 13440-5914 | DUN 142 | HD 119283 | HD 119312 | 2256060 | 2256069 | 5870795061866221952 | 5870795096225959808 |
| 143 | 13492-6206 | DUN 143 | HD 120112 | HD 120113 | 2342940 | 2342944 | 5865546577434035712 | 5865546680492798976 |
| 144 | 13496-4722 | DUN 144 | HD 120275A | HD 120275B | 2056192 | 2056190 | 6095002662584749056 | 6095002623922974080 |
| 145 | 13546-6654 | DUN 145 | HD 120891 | CD-66 1486 | 2404962 | 2404966 | 5850667092761177856 | 5850667092761180416 |
| 146 | 13493-4031 | DUN 146 | HD 120272 | HD 120287 | 1959103 | 1959109 | 6113942884244624384 | 6113945804822385408 |
| 147 | 13521-5249 | RMK 18 | HD 120642 | HD 120641 | 2155481 | 2155477 | 6065984557860591360 | 6065984179910876032 |
| 148 | 13518-3300 | H 3 101 | * 3 Cen A | * 3 Cen B | 1769687 | 1769689 | 6170485544575679104 | 6170485544575678592 |

| 1 | 16 | 17 | 18 | 19 | 20 | 21 | 22 | 23 |
|---|---|---|---|---|---|---|---|---|
| No. | WDS | Disc | SIMBAD_A | SIMBAD_B | ASCC_A | ASCC_B | GAIA_DR2_A | GAIA_DR2_B |
| 149 | two | | HD 120974 | HD 120957 | 1864369 | 1864353 | 6115338095775994880 | 6115337546020644480 |
| 150 | 13575-5743 | DUN 150AB | V* V412 Cen | HD 121506 | 2257485 | 2257470 | 5871308465073102720 | 5871311316931389312 |
| 151 | 13573-5602 | DUN 151AB | HD 121504 | CPD-55 5793 | 2257462 | 2257469 | 5872266689452551552 | 5872266723812297216 |
| 152 | one | | *ups02 Cen | | 2057267 | | 6097035006747824768 | |
| 153 | 14060-4111 | WFC 145AB | *chi Cen | HD 123021 | 1960483 | 1960490 | 6110115278109271808 | 6110115621706655616 |
| 154 | 14055-3633 | DUN 154 | HD 122917 | CD-35 9249B | 1865200 | 1865203 | 6120853555338661888 | 6120853555338661248 |
| 155 | 14077-5341 | DUN 155 | CPD-53 5879 | HD 123186 | 2156705 | 2156706 | 5896839777864869120 | 5896839846584347264 |
| 156 | 14067-3622 | DUN 253AB | *tet Cen | | 1865291 | | | |
| 157 | 14096-5130 | HJ 4651 | V* V869 Cen | HD 123530 | 2156835 | 2156844 | 6089748096519831296 | 6089747340605583616 |
| 158 | unidentified | | | | | | | |
| 159 | 14226-5828 | DUN 159AB | HD 125628A | HD 125628B | 2260099 | 2260102 | 5891112112577938816 | 5891112112577932800 |
| 160 | 14261-4513 | DUN 160AB | *tau01 Lup | CD-44 9321 | 2059445 | 2059437 | 6099307559838681216 | 6099307181888632960 |
| 161 | unidentified | | | | | | | |
| 162 | 14339-4628 | DUN 162 | HD 127629 | | 2060207 | | 6098217909463037440 | 6098217836443755776 |
| 163 | 14380-5431 | DUN 163 | HD 128291 | HD 128306 | 2159018 | 2159023 | 5894221187876054656 | 5894221119156564352 |
| 164 | two | | *eta Cen | HD 127992 | 1962822 | 1962835 | 6103094140452223872 | 6103093865574313216 |
| 165 | 14396-6050 | RHD 1AB | *alf Cen A | *alf Cen B | 2348879 | 2348875 | | |
| 166 | 14425-6459 | DUN 166AB | *alf Cir | *alf Cir B | 2349085 | | 5849837854817580672 | 5849837820492182272 |
| 167 | 14410-3608 | SKF 1973 | HD 128974 | HD 128975 | 1867812 | 1867814 | 6202874511432521600 | 6202873686798792704 |
| 168 | 14428-5511 | DUN 168 | HD 129107 | CPD-54 6120B | 2262002 | 2262001 | 5893460978673615104 | 5893460978673614336 |
| 169 | 14452-5536 | DUN 169 | V* BU Cir | HD 129578 | 2262258 | 2262269 | 5893392327911628928 | 5893392362271368192 |
| 170 | unidentified | | | | | | | |

| 1<br>No. | 16<br>WDS | 17<br>Disc | 18<br>SIMBAD_A | 19<br>SIMBAD_B | 20<br>ASCC_A | 21<br>ASCC_B | 22<br>GAIA_DR2_A | 23<br>GAIA_DR2_B |
|---|---|---|---|---|---|---|---|---|
| 171 | 14534-4551 | DUN 171AB | HD 131168 | CD-45 9492B | 2062279 | 2062275 | 5907676972474481920 | 5907676976779709312 |
| 172 | one | | *zet Cir | | 2408966 | | 5848760573954755968 | |
| 173 | 14529-3748 | SHT 57 | HR 5543 | | 1868661 | | 6198599507144514432 | |
| 174 | one | | HD 131464 | | 2062468 | | 5906831108744751616 | |
| 175 | 15019-5155 | HJ 4723AB | HD 132606A | HD 132606B | 2161181 | 2161182 | 5900200263369385728 | 5900200263369382272 |
| 176 | 15123-5206 | DUN 176 | *zet Lup | HD 134483 | 2162355 | 2162342 | 5888394463418285312 | 5888394257280681856 |
| 177 | 15119-4844 | DUN 177 | *kap Lup | *kap02 Lup | 2064147 | 2064151 | 5902489309143933056 | 5902489102985502208 |
| 178 | 15116-4517 | DUN 178AC | HD 134444 | HD 134443 | 2064113 | 2064106 | 5904208906640444928 | 5904209082753017600 |
| 179 | 15145-4323 | DUN 179 | HD 135034 | HD 135034B | 1966427 | 1966431 | 6003544598199761408 | 6003544632559500288 |
| 180 | 15185-4753 | DUN 180AC | *mu.02 Lup | HD 135748 | 2064815 | 2064822 | | 5902970620350884736 |
| 181 | 15202-3823 | DUN 181AB | HD 136125 | CPD-37 6455 | 1870909 | 1870908 | 6006932605834289792 | 6006932635892069248 |
| 182 | 15227-4441 | DUN 182AC | *eps Lup | *eps Lup C | 1967246 | | 6000130236633865856 | 6000130236647036288 |
| 183 | 15253-3844 | DUN 183AB | *k Lup | HD 137059 | 1871257 | 1871250 | 6006429373106563712 | 6006429235667604096 |
| 184 | 15263-4252 | DUN 184 | HD 137214 | CD-42 10392 | 1967615 | 1967618 | 6000758641901550720 | 6000758573181780736 |
| 185 | 15285-5136 | SEE 234 | HD 137465 | | 2164420 | | 5888999332297729024 | |
| 186 | 15331-5812 | DUN 186 | HD 138181 | HD 138168 | 2266209 | 2266206 | 5882204934544118528 | 5882204934544123264 |
| 187 | 15336-4732 | DUN 187 | HD 138362 | CPD-47 7206 | 2066357 | 2066352 | 5986870951058297728 | 5986870916698555136 |
| 188 | 15367-6619 | DUN 188 | *eps Tr A | HD 138510 | 2412057 | 2412046 | 5823955832118781184 | 5823955694698562816 |
| 189 | 15388-5222 | DUN 189AB | HD 139129 | CD-51 9323 | 2165954 | 2165944 | 5886050373367262080 | 5886050437749100800 |
| 190 | 15430-5807 | DUN 190AB | V* V359 Nor | TYC 8704-2534-1 | 2266975 | 2266976 | 5882323574372973952 | 5882323578753114624 |
| 191 | 15453-5841 | DUN 191AB,C | HIP 77160 | HD 140177 | 2267183 | 2267181 | | 5834232658151618304 |
| 192 | 15471-3531 | DUN 192AB,C | HD 140817 | HD 140840 | 1872803 | 1872805 | 6011560759514133760 | 6011549008483608192 |

| 1 | 16 | 17 | 18 | 19 | 20 | 21 | 22 | 23 |
|---|---|---|---|---|---|---|---|---|
| No. | WDS | Disc | SIMBAD_A | SIMBAD_B | ASCC_A | ASCC_B | GAIA_DR2_A | GAIA_DR2_B |
| 193 | 15511-5503 | DUN 193AB | HD 141318 | SAO 243045 | 2267782 | 2267783 | 5884607985911748224 | 5884608088990966528 |
| 194 | 15549-6045 | DUN 194AC | HD 141913 | CD-60 5919 | 2354178 | 2354188 | 5832716255424187392 | 5832716362853215104 |
| 195 | 15548-5020 | DUN 195AB | HD 142080 | CD-49 10123 | 2168121 | 2168122 | 5982530525830998016 | 5982530525831001344 |
| 196 | 15569-3358 | PZ 4 | * ksi01 Lup | * ksi02 Lup | 1777138 | 1777140 | 6012174802400278016 | 6012174836760016512 |
| 197 | 16001-3824 | RMK 21AC | *eta Lup | CD-3810797B | 1873533 | 1873521 | 5998019895872140800 | 5998065285088239360 |
| 198 | two | | V* QY Nor | CD-53 6383 | 2169105 | 2169101 | 5932866131031997696 | 5932864657931055744 |
| 199 | 16086-3906 | DUN 199AC | V * V1027 Sco | V * V856 Sco | 1874042 | 1874040 | 5997082115537645696 | 5997082081177906048 |
| 200 | 16225-4355 | DUN 200 | HD 147225 | CD-43 10723 | 1972315 | 1972313 | 5992149225369945344 | 5992149191010199168 |
| 201 | 16280-6403 | DUN 201 | *iot Tr A | TYC9 045-2914-1 | 2357385 | 2357386 | 5828317422956035072 | 5828317422956037376 |
| 202 | 16317-4149 | DUN 202AC | HD 148688 | CPD-41 7500C | 1973070 | 1973071 | 5968761680983851776 | 5968761582230644992 |
| 203 | 16331-6054 | DUN 203 | V* NP Tr A | HD 148628 | 2357806 | 2357801 | 5830447000863289344 | 5830447005197478400 |
| 204 | one | | HD 149274 | | 1874980 | | 6020514769906985728 | |
| 205 | unidentified | | | | | | | |
| 206 | 16413-4846 | DUN 206AC | HD 150136 | HD 150135 | 2073934 | 2073931 | 5940954177259978880 | 5940954898814487168 |
| 207 | 16444-4224 | DUN 207 | HD 150674 | HD 150673 | 1973850 | 1973849 | 5967756491149042304 | 5967756491149041024 |
| 208 | one | | HD 150500 | | 2074201 | | 5942647283393791232 | |
| 209 | 16482-3653 | DUN 209AB | HD 151315 | HD 151316 | 1875678 | 1875680 | 5971596329361239808 | 5971596260664472704 |
| 210 | 16487-5526 | DUN 210AB | HD 151163 | HD 151162 | 2274180 | 2274176 | 5929426381963737344 | 5929426416323498112 |
| 211 | 16475-4819 | DUN 211BC | HD 151115 | HD 151116 | 2074679 | 2074676 | 5939444375994517376 | 5939444272915289216 |
| 212 | 17040-5105 | DUN 212AB | HD 153772 | HD 153771 | 2176845 | 2176843 | 5937998243333786112 | 5937998243333788416 |
| 213 | 17103-4644 | DUN 213 | CCDM J17103-4644AB | CD-46 11258B | 2076679 | 2076681 | 5950941488064653056 | 5950941488064651136 |
| 214 | 17133-6712 | DUN 214AB | HD 154903 | TYC 9064-3629-1 | 2418812 | 2418813 | 5814757008599356928 | 5814757008599360896 |

| 1<br>No. | 16<br>WDS | 17<br>Disc | 18<br>SIMBAD_A | 19<br>SIMBAD_B | 20<br>ASCC_A | 21<br>ASCC_B | 22<br>GAIA_DR2_A | 23<br>GAIA_DR2_B |
|---|---|---|---|---|---|---|---|---|
| 215 | 17193-5323 | DUN 215AB | HD 156239 | HD 156260 | 2178088 | 2178095 | 5923327700182691840 | 5923327356584965760 |
| 216 | 17269-4551 | DUN 216AC | HD 157661A | HD 157649 | 2078475 | 2078460 | 5951986642593137408 | 5951987398507431808 |
| 217 | 17290-4358 | DUN 217 | HD 158042 | CD-43 11741B | 1978893 | 1978895 | 5958561447264080768 | 5958561447264078208 |
| 218 | 17336-3706 | DUN 218AC | *lam Sco | CD-36 11635 | 1880898 | 1880889 | | 5962581880247644288 |
| 219 | 17589-3652 | DUN 219AB | HD 163652 | HD 163651 | 1884115 | 1884101 | 4037358426191922688 | 4037358597990619264 |
| 220 | 18222-5534 | DUN 220 | V* QW Tel | CD-55 7677 | 2280785 | 2280786 | 6649398690418063232 | 6649398690418059392 |
| 221 | 18243-4407 | DUN 221 | HD 168905 | CD-44 12570 | 1986993 | 1986998 | 6721718444965335936 | 6721718170088625664 |
| 222 | 18334-3844 | DUN 222 | *kap02 Cr A | *kap01 Cr A | 1889607 | 1889606 | 6726876327040339712 | 6726876327040344576 |
| 223 | unidentified | | | | | | | |
| 224 | 18540-4716 | DUN 224AC | HD 174691 | HD 174713 | 2088578 | 2088587 | 6710469826831780736 | 6710469655033078016 |
| 225 | 19124-5148 | DUN 225AB | HD 178734 | HD 178710 | 2187130 | 2187123 | 6656986282721029120 | 6656985939123649920 |
| 226 | 19226-4428 | DUN 226 | *bet01 Sgr | HD 181484 | 1992514 | 1992517 | 6664464851575462016 | 6664464851575461120 |
| 227 | 19526-5458 | DUN 227 | HD 187420 | HD 187421 | 2189330 | 2189331 | 6641186850384256896 | 6641186850384254848 |
| 228 | unidentified | | | | | | | |
| 229 | 19583-5154 | DUN 229 | HD 188557 | HD 188534 | 2189635 | 2189627 | 6666516540271227904 | 6666516505911492224 |
| 230 | 20178-4011 | DUN 230 | HD 192724A | HD 192724B | 1995385 | 1995387 | 6692595444253828480 | 6692595547333043456 |
| 231 | 20366-7104 | DUN 231 | HD 195459 | CD-71 1627 | 2494845 | 2494836 | 6374497315769911296 | 6374497384489388800 |
| 232 | 20417-7521 | DUN 232 | *mu.02 Oct | HD 196068 | 2495054 | 2495055 | 6369544118965772416 | 6369544118966055296 |
| 233 | one | | *phi01 Pav | | 2367957 | | 6454999399628150016 | |
| 234 | 20376-4717 | HJ 5209AB | *alf Ind | | 2094623 | | 6674382927491854848 | |
| 235 | 20450-5029 | DUN 235AC | CCDM J20451-5030AB | HD 197341 | 2191473 | 2191478 | 6480764633558584704 | 6480763877644331904 |
| 236 | 21022-4300 | DUN 236 | HD 200011 | HD 200026 | 1997452 | 1997457 | 6484888042680733824 | 6484888008320993152 |

| 1<br>No. | 16<br>WDS | 17<br>Disc | 18<br>SIMBAD_A | 19<br>SIMBAD_B | 20<br>ASCC_A | 21<br>ASCC_B | 22<br>GAIA_DR2_A | 23<br>GAIA_DR2_B |
|---|---|---|---|---|---|---|---|---|
| 237 | four | | V* BT Ind | | 2288078 | | 6458506566841143040 | |
| 238 | 22259-7501 | DUN 238AB | HD 212168 | CPD-75 1748B | 2498785 | 2498787 | 6357835694518769408 | 6357835488360338560 |
| 239 | 22298-4345 | DUN 239 | *del02 Gru | CD-44 14934 | 2000590 | 2000587 | 6520955322607576320 | 6520953845138827264 |
| 240 | 22315-3221 | PZ 7AC | *bet Ps A | CD-32 17127 | 1808438 | 1808439 | 6601750220152445440 | 6601750151432831104 |
| 241 | 22366-3140 | DUN 241 | HD 214122 | HD 214121 | 1808592 | 1808596 | 6601132054099267456 | 6601736899415399680 |
| 242 | 22397-2820 | H 6 119AB | HD 214599 | CD-28 17874B | 1711391 | 1711392 | 6608821179430481408 | 6608821076351265024 |
| 243 | three | | *bet Gru | | 2099216 | | | |
| 244 | 23023-6418 | DUN 244 | HD 217488 | CPD-64 4310 | 2371330 | 2371332 | 6393362255241691648 | 6393362358320906368 |
| 245 | 23086-5944 | DUN 245 | HD 218392 | CPD-60 7635B | 2290627 | 2290626 | 6490761943032664960 | 6490761943032665344 |
| 246 | 23072-5041 | DUN 246 | HD 218269 | HD 218268 | 2195694 | 2195691 | 6502570319958250496 | 6502570319958250624 |
| 247 | 23180-6100 | DUN 247 | HD 219631 | HD 219621 | 2371641 | 2371639 | 6490359006380772480 | 6490359075100249856 |
| 248 | 23208-5018 | DUN 248AB,C | HD 220003A | CD-50 13947 | 2196066 | 2196064 | 6502030631546224512 | 6502030631547502720 |
| 249 | 23239-5349 | DUN 249 | V* DQ Gru | HD 220391 | 2196130 | 2196129 | 6499534465274954496 | 6499534465274949376 |
| 250 | 23272-5017 | DUN 250 | HD 220803 | HD 220815 | 2196210 | 2196212 | 6525816229153083776 | 6525816332232298112 |
| 251 | 23395-4638 | DUN 251 | *tet Phe A | *tet Phe B | 2100751 | 2100750 | 6525488231089676800 | 6525488226794240256 |
| 252 | two | | HR 8996 | HD 222830 | 2372143 | 2372146 | 6485678866417832704 | 6485685051170731648 |
| 253 | 23544-2703 | LAL 192 | HD 223991A | HD 223991B | 1713655 | 1713654 | 2334419836112293120 | 2334419797455932160 |

# APPENDIX C

Table 3: Data generated from the research for Paper 1.

| 1 No. | 24 RA_A_GAIA_ DR2 (d, 1826.0) | 25 DE_A_GAIA_ DR2 (d, 1826.0) | 26 Mean_PA_ DUN (d, 1826.0) | 27 Mean_PA_DUN_ CORRECTED (d, 1826.0, quadrant corrected) | 28 PA_GAIA_ DR2 (d, 1826.0) | 29 Mean_Sep_ DUN ('', 1826.0) | 30 Sep_GAIA_ DR2 ('', 1826.0) | 31 vA_GAIA_ DR2 (mag) | 32 vB_GAIA_ DR2 (mag) |
|---|---|---|---|---|---|---|---|---|---|
| 1 | 5.883 | -63.921 | 352.5 | 172.5 | 177.4 | 29.7 | 27.7 | 4.34 | 4.37 |
| 2 | 11.440 | -70.451 | | | 74.2 | | 19.7 | 6.60 | 7.33 |
| 3 | 19.742 | -33.450 | | | | | | 7.79 | |
| 4 | 23.016 | -54.326 | 107.5 | 107.5 | 104.5 | 15.8 | 10.7 | 7.04 | 8.41 |
| 5 | 23.304 | -57.082 | 16.9 | 196.9 | 223.6 | 2.5 | 14.6 | 5.69 | 5.82 |
| 6 | 32.578 | -52.324 | 220.0 | 220.0 | 212.4 | 90.0 | 83.8 | 5.31 | 9.15 |
| 7 | 38.754 | -60.321 | 290.0 | 75.0 | | 35.0 | | 7.58 | 7.69 |
| 8 | | | 220.9 | 180.0 | | | | | 7.74 |
| 9 | 42.923 | -41.009 | 88.4 | 88.4 | 80.2 | 10.8 | 7.9 | 5.40 | 4.33 |
| 10 | 44.784 | -52.009 | 75.0 | 75.0 | | 30.0 | | 7.50 | 8.54 |
| 11 | | | 180.0 | 180.0 | | 10.0 | | | |
| 12 | 48.118 | -65.088 | 98.0 | 98.0 | 102.5 | 14.0 | 18.3 | 6.56 | 9.15 |
| 13 | | | | | | | | | |
| 14 | 53.684 | -60.350 | 280.0 | 260.0 | 269.9 | 45.0 | 57.3 | 6.89 | 8.29 |
| 15 | 53.393 | -40.923 | 334.9 | 334.9 | 322.6 | 4.0 | 10.1 | 6.90 | 7.82 |
| 16 | 55.552 | -38.159 | 202.2 | 202.2 | 194.6 | 7.0 | 6.3 | 4.76 | 5.35 |
| 17 | 59.207 | -54.885 | 133.7 | 133.7 | 140.9 | 57.1 | 58.7 | 7.66 | 8.14 |
| 18 | 71.773 | -53.763 | 57.0 | 57.0 | 66.8 | 12.4 | 7.9 | 5.58 | 6.35 |

| 1 No. | 24 RA_A_GAIA_ DR2 (d, 1826.0) | 25 DE_A_GAIA_ DR2 (d, 1826.0) | 26 Mean_PA_ DUN (d, 1826.0) | 27 Mean_PA_DUN_ CORRECTED (d, 1826.0, quadrant corrected) | 28 PA_GAIA_ DR2 (d, 1826.0) | 29 Mean_Sep_ DUN ('', 1826.0) | 30 Sep_GAIA_ DR2 ('', 1826.0) | 31 vA_GAIA_ DR2 (mag) | 32 vB_GAIA_ DR2 (mag) |
|---|---|---|---|---|---|---|---|---|---|
| 19 | 77.513 | -33.736 | 221.8 | 221.8 | | | | 6.90 | |
| 20 | | | 281.8 | 281.8 | | 38.6 | | 6.23 | 6.74 |
| 21 | 81.354 | -47.209 | | | 263.3 | | 199.8 | 5.41 | 6.59 |
| 22 | 81.449 | -42.438 | 170.1 | 170.1 | 175.5 | 5.5 | 8.4 | 7.11 | 7.80 |
| 23 | 90.078 | -48.448 | 329.0 | 31.0 | 72.1 | 3.0 | 5.4 | 7.17 | 7.54 |
| 24 | 91.739 | -54.934 | | | | 2.0 | | 5.12 | |
| 25 | 93.111 | -32.138 | | | 355.9 | | 2.2 | 9.62 | 10.30 |
| 26 | 92.955 | -65.490 | 67.8 | 112.2 | 111.6 | 21.4 | 20.5 | 6.75 | 8.17 |
| 27 | 93.487 | -59.136 | | 223.3 | 223.6 | 58.1 | 56.2 | 6.37 | 7.69 |
| 28 | 94.505 | -36.623 | 64.1 | 64.1 | 65.3 | 69.6 | 69.3 | 5.58 | 6.79 |
| 29 | 95.876 | -40.264 | | 109.1 | 109.9 | 71.7 | 71.5 | 7.51 | 7.84 |
| 30 | | | 310.0 | | | 14.0 | | | |
| 31 | 98.508 | -48.070 | 320.4 | 320.4 | 319.0 | 11.3 | 13.2 | 5.00 | 7.46 |
| 32 | 99.106 | -38.235 | 349.3 | 349.3 | 277.2 | 6.2 | 8.2 | 6.51 | 7.81 |
| 33 | 100.080 | -39.361 | 140.0 | 140.0 | | 2.0 | | 6.43 | |
| 34 | 100.179 | -54.519 | 212.6 | 212.6 | 190.0 | 97.4 | 130.9 | 6.43 | 6.64 |
| 35 | 100.870 | -43.610 | | | 268.1 | | 268.9 | 7.30 | 7.37 |
| 36 | 100.963 | -31.511 | | 69.4 | 64.4 | 82.1 | 42.7 | 5.61 | 7.83 |
| 37 | 104.240 | -50.221 | | | 72.6 | | 483.5 | 7.20 | 7.57 |
| 38 | 104.665 | -43.372 | 117.7 | 117.7 | 121.1 | 21.8 | 20.0 | 5.50 | 6.79 |
| 39 | 105.156 | -58.921 | 11.2 | 11.2 | 77.7 | 2.8 | 2.7 | 5.81 | 6.78 |

| 1<br>No. | 24<br>RA_A_GAIA_<br>DR2<br>(d, 1826.0) | 25<br>DE_A_GAIA_<br>DR2<br>(d, 1826.0) | 26<br>Mean_PA_<br>DUN<br>(d, 1826.0) | 27<br>Mean_PA_DUN_<br>CORRECTED<br>(d, 1826.0, quadrant corrected) | 28<br>PA_GAIA_<br>DR2<br>(d, 1826.0) | 29<br>Mean_Sep_<br>DUN<br>('', 1826.0) | 30<br>Sep_GAIA_<br>DR2<br>('', 1826.0) | 31<br>vA_GAIA_<br>DR2<br>(mag) | 32<br>vB_GAIA_<br>DR2<br>(mag) |
|---|---|---|---|---|---|---|---|---|---|
| 40 | 106.478 | -56.080 | 141.1 | 141.1 | 138.1 | 39.2 | 37.8 | 7.98 | 8.47 |
| 41 | 106.730 | -55.302 | | | 224.5 | | 7.0 | 7.56 | 7.73 |
| 42 | 107.564 | -70.216 | 306.3 | 306.3 | 297.9 | 15.1 | 10.7 | 3.74 | 5.64 |
| 43 | 107.760 | -36.791 | 213.6 | 213.6 | 212.2 | 82.9 | 70.1 | 2.40 | 8.08 |
| 44 | 109.051 | -51.995 | 25.0 | 25.0 | 17.1 | 12.0 | 10.6 | 5.94 | 6.54 |
| 45 | 109.152 | -48.202 | 14.2 | 165.8 | 155.4 | 19.3 | 23.0 | 6.78 | 7.92 |
| 46 | | | 273.0 | 273.0 | | 34.3 | | | |
| 47 | 109.526 | -31.474 | | | 340.7 | | 100.0 | 5.30 | 7.59 |
| 48 | | | 150.5 | 150.5 | | | | | |
| 49 | 110.552 | -31.497 | | | 54.0 | | 8.9 | 6.36 | 7.08 |
| 50 | | | | | | 2.0 | | | |
| 51 | 110.939 | -42.954 | 90.0 | 90.0 | 79.7 | 18.0 | 21.0 | 3.06 | 8.77 |
| 52 | 111.749 | -23.102 | | 105.4 | 105.3 | | 9.0 | 5.77 | 5.81 |
| 53 | 112.935 | -26.415 | 315.8 | 315.8 | 326.8 | 8.8 | 10.6 | 4.43 | 4.64 |
| 54 | 114.774 | -37.552 | | | | 3.0 | | 3.42 | |
| 55 | 114.896 | -50.048 | 137.0 | 137.0 | 132.1 | 57.6 | 51.5 | 6.57 | 7.51 |
| 56 | 115.327 | -41.079 | 169.4 | 169.4 | 175.8 | 53.3 | 49.4 | 6.88 | 7.65 |
| 57 | 115.992 | -72.187 | | | 119.2 | | 18.4 | 3.93 | 8.73 |
| 58 | 117.299 | -43.902 | | | 158.4 | | 84.7 | 7.13 | 7.80 |
| 59 | 118.584 | -49.505 | 131.0 | 49.0 | 45.9 | | 16.5 | 6.29 | 6.31 |
| 60 | 119.299 | -54.034 | | | 161.3 | | 39.8 | 6.06 | 8.12 |

| 1 No. | 24 RA_A_GAIA_ DR2 (d, 1826.0) | 25 DE_A_GAIA_ DR2 (d, 1826.0) | 26 Mean_PA_ DUN (d, 1826.0) | 27 Mean_PA_DUN_ CORRECTED (d, 1826.0, quadrant corrected) | 28 PA_GAIA_ DR2 (d, 1826.0) | 29 Mean_Sep_ DUN ('', 1826.0) | 30 Sep_GAIA_ DR2 ('', 1826.0) | 31 vA_GAIA_ DR2 (mag) | 32 vB_GAIA_ DR2 (mag) |
|---|---|---|---|---|---|---|---|---|---|
| 61 | 119.918 | -26.619 | | | 34.7 | | 71.9 | 7.01 | 8.97 |
| 62 | 120.569 | -62.340 | 266.2 | 266.2 | 264.2 | 84.5 | 87.9 | 6.18 | 7.62 |
| 63 | 120.984 | -42.132 | 77.9 | 77.9 | 83.4 | | 5.4 | 6.55 | 7.67 |
| 64 | | | 44.5 | 44.5 | | 57.9 | | | 7.62 |
| 65 | | | 223.2 | 223.2 | | 43.1 | | | 4.24 |
| 66 | 121.848 | -68.106 | 42.9 | 42.9 | 22.7 | 5.9 | 6.1 | 4.39 | 7.38 |
| 67 | 121.869 | -35.800 | | 168.6 | 175.3 | 73.8 | 66.8 | 5.03 | 6.06 |
| 68 | 121.704 | -35.822 | | 21.7 | 24.6 | 108.7 | 125.0 | 7.27 | 7.28 |
| 69 | 125.152 | -51.162 | 205.0 | 205.0 | 222.3 | 40.0 | 25.3 | 5.16 | 9.44 |
| 70 | 125.910 | -44.147 | 320.3 | 320.3 | 354.8 | 5.5 | 4.7 | 5.14 | 7.05 |
| 71 | 126.082 | -39.931 | 47.8 | 47.8 | 47.2 | 67.2 | 63.9 | 7.00 | 7.46 |
| 72 | 128.550 | -41.777 | 5.2 | 354.8 | 355.3 | 136.6 | 135.5 | 6.84 | 7.65 |
| 73 | 132.844 | -54.862 | 353.1 | 353.1 | 356.4 | 67.8 | 66.1 | 7.66 | 8.11 |
| 74 | 133.189 | -58.560 | 66.2 | 66.2 | 74.4 | 40.6 | 40.5 | 4.87 | 6.78 |
| 75 | 138.955 | -69.070 | | | 16.6 | | 10.4 | 8.12 | 8.48 |
| 76 | 140.533 | -44.741 | 97.2 | 97.2 | 98.4 | 65.5 | 61.2 | 7.09 | 7.58 |
| 77 | 140.702 | -43.781 | | | 77.5 | | 110.5 | 6.93 | 6.91 |
| 78 | 140.840 | -31.127 | 75.2 | 255.2 | 212.7 | 63.9 | 8.4 | 6.15 | 6.94 |
| 79 | 141.879 | -48.985 | 48.7 | 48.7 | 30.0 | 14.8 | 130.4 | 7.31 | 7.49 |
| 80 | 144.683 | -48.691 | | | 249.3 | 3.0 | 18.4 | 7.96 | 8.13 |
| 81 | 146.871 | -44.464 | 239.4 | 239.4 | 244.9 | 4.0 | 5.3 | 5.78 | 8.30 |

| 1 No. | 24 RA_A_GAIA_ DR2 (d, 1826.0) | 25 DE_A_GAIA_ DR2 (d, 1826.0) | 26 Mean_PA_ DUN (d, 1826.0) | 27 Mean_PA_DUN_ CORRECTED (d, 1826.0, quadrant corrected) | 28 PA_GAIA_ DR2 (d, 1826.0) | 29 Mean_Sep_ DUN ('', 1826.0) | 30 Sep_GAIA_ DR2 ('', 1826.0) | 31 vA_GAIA_ DR2 (mag) | 32 vB_GAIA_ DR2 (mag) |
|---|---|---|---|---|---|---|---|---|---|
| 82 | 148.276 | -85.204 | 268.0 | 268.0 | | | | 7.05 | 7.58 |
| 83 | 148.988 | -54.143 | | | 221.0 | | 107.6 | 7.71 | 7.86 |
| 84 | 149.192 | -51.208 | 190.1 | 190.1 | 204.6 | 2.0 | 45.8 | 7.31 | 8.37 |
| 85 | 155.719 | -61.694 | | | 219.3 | | 21.9 | 8.28 | 8.71 |
| 86 | 155.927 | -41.337 | | | 290.6 | | 83.7 | 7.32 | 8.01 |
| 87 | 156.130 | -60.464 | 203.6 | 336.4 | 331.9 | 85.2 | 82.8 | 6.33 | 7.44 |
| 88 | 156.144 | -44.173 | | 221.1 | 217.7 | 15.2 | 13.1 | 5.70 | 6.06 |
| 89 | 156.625 | -54.490 | | 34.0 | 29.6 | 28.0 | 26.2 | 6.65 | 7.82 |
| 90 | | | | | | | | | |
| 91 | 156.890 | -71.214 | 228.8 | 48.8 | 59.0 | 3.7 | 9.9 | 8.49 | 8.78 |
| 92 | 156.474 | -60.790 | 76.1 | 76.1 | | 22.8 | | 3.23 | |
| 93 | 157.255 | -63.234 | 40.9 | 40.9 | 36.5 | 22.9 | 25.8 | 7.43 | 8.34 |
| 94 | 158.046 | -58.277 | 11.1 | 11.1 | 20.4 | 10.1 | 14.6 | 4.62 | 7.99 |
| 95 | 158.109 | -54.697 | 104.1 | 104.1 | 105.0 | 51.1 | 51.9 | 4.26 | 6.19 |
| 96 | 159.003 | -58.304 | | | | | | 5.31 | |
| 97 | 159.165 | -60.256 | | | 174.2 | 3.0 | 12.5 | 6.55 | 8.13 |
| 98 | | | 11.0 | 11.0 | | 61.3 | | 8.22 | 8.06 |
| 99 | 159.787 | -69.944 | 253.6 | 73.6 | 74.4 | 65.7 | 62.9 | 6.20 | 6.46 |
| 100 | | | | | | | | | |
| 101 | 161.039 | -59.034 | 276.0 | 276.0 | 343.8 | 10.0 | 30.8 | 6.75 | 10.21 |
| 102 | 161.622 | -57.929 | 196.5 | 196.5 | 199.2 | 55.6 | 147.3 | 3.75 | 6.22 |

| 1 No. | 24 RA_A_GAIA_ DR2 (d, 1826.0) | 25 DE_A_GAIA_ DR2 (d, 1826.0) | 26 Mean_PA_ DUN (d, 1826.0) | 27 Mean_PA_DUN_ CORRECTED (d, 1826.0, quadrant corrected) | 28 PA_GAIA_ DR2 (d, 1826.0) | 29 Mean_Sep_ DUN ('', 1826.0) | 30 Sep_GAIA_ DR2 ('', 1826.0) | 31 vA_GAIA_ DR2 (mag) | 32 vB_GAIA_ DR2 (mag) |
|---|---|---|---|---|---|---|---|---|---|
| 103 | 161.622 | -57.929 | 13.0 | 13.0 | 14.0 | 57.5 | 67.6 | 3.75 | 7.74 |
| 104 | 163.152 | -50.884 | | | | | | 6.12 | |
| 105 | 164.449 | -60.112 | 149.9 | 210.1 | 221.0 | 23.2 | 23.9 | 7.54 | 10.11 |
| 106 | 167.235 | -37.065 | 60.0 | 60.0 | | | | 6.21 | |
| 107 | 168.093 | -73.236 | | | 299.8 | | 114.4 | 7.66 | 8.53 |
| 108 | 168.623 | -57.428 | | | | | | 6.59 | |
| 109 | 170.064 | -41.716 | 106.6 | 106.6 | 171.0 | 151.0 | 13.5 | 5.10 | 7.77 |
| 110 | 170.464 | -54.358 | | | | | | 7.72 | |
| 111 | 170.922 | -28.308 | 23.9 | 203.9 | 210.2 | 8.4 | 8.6 | 5.60 | 5.70 |
| 112 | 171.919 | -49.779 | 289.3 | 289.3 | 289.6 | 204.7 | 208.0 | 7.75 | 8.09 |
| 113 | 172.114 | -37.996 | 156.1 | 156.1 | 153.1 | 135.1 | 140.6 | 6.90 | 7.41 |
| 114 | 172.855 | -37.143 | 97.0 | 97.0 | 95.4 | 3.0 | 16.9 | 6.60 | 8.60 |
| 115 | 172.836 | -32.484 | 275.1 | 97.0 | | 38.2 | | 6.86 | |
| 116 | 176.984 | -31.299 | 83.6 | 83.6 | 83.1 | 29.2 | 20.0 | 7.59 | 7.75 |
| 117 | 178.974 | -61.025 | 151.8 | 151.8 | 149.1 | 22.2 | 22.9 | 7.32 | 7.64 |
| 118 | 179.431 | -36.890 | | | 30.7 | | 49.9 | 6.58 | 9.16 |
| 119 | 181.261 | -65.577 | 30.2 | 30.2 | 31.8 | 112.9 | 102.1 | 7.06 | 7.37 |
| 120 | | | 3.4 | 3.4 | | 96.4 | | | |
| 121 | | | | | | | | | |
| 122 | | | 200.4 | 200.4 | | 88.7 | | | 4.80 |
| 123 | | | 114.4 | 114.4 | | 5.4 | | | |

| 1 No. | 24 RA_A_GAIA_ DR2 (d, 1826.0) | 25 DE_A_GAIA_ DR2 (d, 1826.0) | 26 Mean_PA_ DUN (d, 1826.0) | 27 Mean_PA_DUN_ CORRECTED (d, 1826.0, quadrant corrected) | 28 PA_GAIA_ DR2 (d, 1826.0) | 29 Mean_Sep_ DUN ('', 1826.0) | 30 Sep_GAIA_ DR2 ('', 1826.0) | 31 vA_GAIA_ DR2 (mag) | 32 vB_GAIA_ DR2 (mag) |
|---|---|---|---|---|---|---|---|---|---|
| 124 | | | 41.9 | 41.9 | | 92.8 | | | 6.39 |
| 125 | | | 19.7 | 19.7 | | 440.0 | | | 7.12 |
| 126 | 191.113 | -56.228 | 15.8 | 15.8 | 17.0 | 43.0 | 34.0 | 3.99 | 5.13 |
| 127 | 192.398 | -54.968 | 138.7 | 138.7 | 125.6 | 12.4 | 16.9 | 8.19 | 8.95 |
| 128 | 194.205 | -48.969 | 100.0 | 100.0 | 98.7 | 40.0 | 25.2 | 4.27 | 9.35 |
| 129 | 194.252 | -64.369 | 191.0 | 191.0 | 188.0 | 3.3 | 5.3 | 5.58 | 7.61 |
| 130 | | | | | | | | | |
| 131 | 195.898 | -66.966 | 331.5 | 331.5 | 332.3 | 63.6 | 58.4 | 4.73 | 7.29 |
| 132 | | | 5.0 | 5.0 | | 2.0 | | | |
| 133 | 197.872 | -60.069 | 343.8 | 343.8 | 342.5 | 66.1 | 59.1 | 4.51 | 6.15 |
| 134 | 197.715 | -35.790 | 140.0 | 140.0 | | | | 2.87 | |
| 135 | 197.918 | -61.094 | | | | | | 7.83 | |
| 136 | | | | | | | | | |
| 137 | 200.107 | -62.137 | 13.9 | 346.1 | 357.8 | 12.6 | 16.2 | 7.42 | 8.49 |
| 138 | 201.797 | -25.603 | | | 193.0 | | 9.8 | 5.70 | 6.63 |
| 139 | 201.461 | -55.259 | | | | | | 7.99 | |
| 140 | 203.011 | -71.100 | 90.0 | 90.0 | 75.5 | 7.0 | 10.8 | 8.65 | 9.64 |
| 141 | 202.670 | -53.670 | 191.6 | 168.4 | 164.3 | 3.0 | 4.9 | 5.24 | 6.57 |
| 142 | 203.103 | -58.351 | 95.5 | 95.5 | 90.7 | 32.6 | 33.2 | 6.45 | 7.80 |
| 143 | 204.304 | -61.227 | 30.8 | 30.8 | 34.9 | 10.3 | 11.7 | 7.46 | 7.93 |
| 144 | 204.710 | -46.497 | 265.0 | 265.0 | 256.6 | 10.0 | 9.1 | 8.15 | 8.93 |

| 1 No. | 24 RA_A_GAIA_ DR2 (d, 1826.0) | 25 DE_A_GAIA_ DR2 (d, 1826.0) | 26 Mean_PA_ DUN (d, 1826.0) | 27 Mean_PA_DUN_ CORRECTED (d, 1826.0, quadrant corrected) | 28 PA_GAIA_ DR2 (d, 1826.0) | 29 Mean_Sep_ DUN ('', 1826.0) | 30 Sep_GAIA_ DR2 ('', 1826.0) | 31 vA_GAIA_ DR2 (mag) | 32 vB_GAIA_ DR2 (mag) |
|---|---|---|---|---|---|---|---|---|---|
| 145 | 205.423 | -66.033 | 60.0 | 60.0 | 51.8 | 10.0 | 22.1 | 7.79 | 8.98 |
| 146 | 204.742 | -39.644 | 87.0 | 87.0 | 85.3 | 69.6 | 51.5 | 6.88 | 7.31 |
| 147 | 205.236 | -51.941 | 322.5 | 322.5 | 289.7 | 12.0 | 17.9 | 5.25 | 7.51 |
| 148 | 205.456 | -32.126 | 121.6 | 121.6 | 110.1 | 8.6 | 8.4 | 4.53 | 6.02 |
| 149 | 205.822 | -37.400 | 220.3 | 220.3 | 215.4 | 179.9 | 179.4 | 7.60 | 8.23 |
| 150 | 206.437 | -56.851 | 265.5 | 265.5 | 267.0 | 50.2 | 59.2 | 7.34 | 8.77 |
| 151 | 206.457 | -55.176 | 0.0 | 0.0 | 301.1 |  | 12.8 | 7.48 | 9.20 |
| 152 | 207.732 | -44.753 |  |  |  | 2.0 |  | 4.29 |  |
| 153 | 208.868 | -40.339 | 76.3 | 76.3 | 78.4 | 75.9 | 85.2 | 4.32 | 8.29 |
| 154 | 208.798 | -35.705 | 150.0 | 150.0 | 130.5 | 15.0 | 20.6 | 8.13 | 9.79 |
| 155 | 209.052 | -52.853 | 50.0 | 50.0 | 27.5 | 19.2 | 23.6 | 7.82 | 8.36 |
| 156 |  |  | 140.0 | 140.0 |  | 3.0 |  |  |  |
| 157 | 209.556 | -50.670 | 160.0 | 160.0 | 134.3 | 13.0 | 63.2 | 5.94 | 8.72 |
| 158 |  |  | 76.0 | 76.0 |  | 6.0 |  |  |  |
| 159 |  |  | 161.7 | 161.7 |  | 9.1 |  | 4.75 | 6.95 |
| 160 | 213.755 | -44.426 | 213.4 | 213.4 | 204.3 | 122.6 | 159.2 | 4.54 | 8.68 |
| 161 |  |  | 32.0 | 32.0 |  | 47.7 |  |  |  |
| 162 | 215.636 | -45.687 | 270.0 | 270.0 | 241.3 |  | 76.2 | 7.14 | 12.38 |
| 163 | 216.458 | -53.743 | 114.5 | 114.5 | 112.2 | 54.9 | 53.9 | 7.94 | 8.31 |
| 164 |  |  |  |  |  |  |  | 6.29 | 9.09 |
| 165 |  |  | 214.3 |  |  | 23.3 |  |  |  |

| 1 No. | 24 RA_A_GAIA_ DR2 (d, 1826.0) | 25 DE_A_GAIA_ DR2 (d, 1826.0) | 26 Mean_PA_ DUN (d, 1826.0) | 27 Mean_PA_DUN_ CORRECTED (d, 1826.0, quadrant corrected) | 28 PA_GAIA_ DR2 (d, 1826.0) | 29 Mean_Sep_ DUN ('', 1826.0) | 30 Sep_GAIA_ DR2 ('', 1826.0) | 31 vA_GAIA_ DR2 (mag) | 32 vB_GAIA_ DR2 (mag) |
|---|---|---|---|---|---|---|---|---|---|
| 166 | 217.142 | -64.206 | 263.0 | 263.0 | 244.0 | 10.0 | 16.5 | 5.22 | 8.38 |
| 167 | 217.593 | -35.379 | 170.0 | 170.0 | 148.9 | 50.0 | 82.3 | 5.64 | 9.26 |
| 168 | 217.600 | -54.427 | 200.0 | 200.0 | 201.3 | 5.0 | 5.7 | 8.33 | 8.60 |
| 169 | 218.178 | -54.853 | 105.2 | 105.2 | 106.9 | 77.3 | 67.3 | 6.04 | 7.45 |
| 170 | | | 0.0 | 0.0 | | 2.0 | | | |
| 171 | 220.458 | -45.132 | 213.0 | 213.0 | 224.3 | 20.0 | 17.1 | 7.02 | 9.58 |
| 172 | 220.025 | -65.265 | | | | 3.0 | | 6.03 | |
| 173 | 220.493 | -37.079 | 150.0 | 150.0 | | 2.0 | | 4.99 | |
| 174 | 220.919 | -45.912 | 290.7 | 290.7 | | 3.0 | | 7.25 | |
| 175 | 222.416 | -51.217 | | | 168.9 | | 5.5 | 7.41 | 10.29 |
| 176 | 224.961 | -51.426 | 249.6 | 249.6 | 249.7 | 71.2 | 72.4 | 3.41 | 6.63 |
| 177 | 224.973 | -48.065 | 150.0 | 150.0 | 146.0 | 28.5 | 27.5 | 3.84 | 5.68 |
| 178 | 224.969 | -44.608 | 283.1 | 283.1 | 277.6 | 77.7 | 39.1 | 6.43 | 7.32 |
| 179 | 225.739 | -42.725 | 49.4 | 49.4 | 47.2 | 11.0 | 10.4 | 7.27 | 8.47 |
| 180 | | | 144.2 | 144.2 | | 24.3 | | | 6.84 |
| 181 | 227.263 | -37.736 | 65.0 | 295.0 | 347.5 | 9.0 | 29.2 | 9.57 | 10.20 |
| 182 | 227.727 | -44.053 | 173.6 | 173.6 | 173.9 | 19.1 | 27.7 | 3.29 | 8.59 |
| 183 | 228.522 | -38.107 | | | 205.8 | 12.0 | 89.8 | 4.58 | 9.28 |
| 184 | 228.659 | -42.237 | 155.0 | 155.0 | 123.8 | 14.0 | 12.4 | 8.35 | 9.61 |
| 185 | 228.953 | -50.979 | 90.0 | | | 3.0 | | 6.05 | |
| 186 | 229.855 | -57.590 | 125.0 | 305.0 | 296.7 | 32.6 | 39.2 | 8.64 | 8.72 |

| 1 No. | 24 RA_A_GAIA_ DR2 (d, 1826.0) | 25 DE_A_GAIA_ DR2 (d, 1826.0) | 26 Mean_PA_ DUN (d, 1826.0) | 27 Mean_PA_DUN_ CORRECTED (d, 1826.0, quadrant corrected) | 28 PA_GAIA_ DR2 (d, 1826.0) | 29 Mean_Sep_ DUN ('', 1826.0) | 30 Sep_GAIA_ DR2 ('', 1826.0) | 31 vA_GAIA_ DR2 (mag) | 32 vB_GAIA_ DR2 (mag) |
|---|---|---|---|---|---|---|---|---|---|
| 187 | 230.341 | -46.934 | 218.0 | 218.0 | 237.5 | 10.0 | 33.7 | 7.08 | 10.23 |
| 188 | 230.228 | -65.717 | 150.0 | 210.0 | 215.6 | 60.0 | 84.6 | 4.07 | 9.17 |
| 189 | 231.487 | -51.787 | 310.0 | 310.0 | 280.2 | 56.0 | 53.5 | 5.41 | 10.31 |
| 190 | 232.268 | -57.542 | 85.0 | 95.0 | 90.4 | 3.0 | 6.5 | 7.88 | 9.92 |
| 191 | | | 325.0 | 325.0 | | 12.0 | | | 8.06 |
| 192 | 233.980 | -34.957 | 50.0 | 130.0 | 145.9 | 35.0 | 34.0 | 6.93 | 7.32 |
| 193 | 234.411 | -54.512 | | | 21.1 | | 23.1 | 5.71 | 9.05 |
| 194 | 235.057 | -60.211 | 317.0 | 43.0 | 49.4 | 10.0 | 45.2 | 6.27 | 9.85 |
| 195 | 235.513 | -49.808 | 7.0 | 7.0 | 9.2 | 5.0 | 11.8 | 6.78 | 7.53 |
| 196 | 236.448 | -33.447 | 50.1 | 50.1 | 46.6 | 11.2 | 10.4 | 5.08 | 5.59 |
| 197 | 237.155 | -37.888 | 249.1 | 249.1 | 248.7 | 50.4 | 115.4 | 3.42 | 9.25 |
| 198 | 237.735 | -53.214 | 180.0 | 180.0 | 192.0 | 30.0 | 81.3 | 6.41 | 9.75 |
| 199 | 239.236 | -38.616 | 190.0 | 190.0 | 185.0 | 12.0 | 43.6 | 6.59 | 7.98 |
| 200 | 242.560 | -43.486 | 172.0 | 188.0 | 197.4 | 17.0 | 41.9 | 5.84 | 9.72 |
| 201 | 242.964 | -63.646 | 32.0 | 32.0 | 26.5 | 14.0 | 24.1 | 5.24 | 9.87 |
| 202 | 244.907 | -41.427 | 190.0 | 190.0 | 181.0 | 26.0 | 57.9 | 5.21 | 9.69 |
| 203 | 244.461 | -60.511 | | | 248.2 | | 37.7 | 7.86 | 8.12 |
| 204 | 245.941 | -35.349 | | | | | | 6.60 | |
| 205 | | | 40.0 | 40.0 | | 16.0 | | | |
| 206 | 247.082 | -48.409 | | | 265.5 | | 9.5 | 5.60 | 6.79 |
| 207 | 248.055 | -42.051 | 185.0 | 185.0 | 186.3 | 6.0 | 11.3 | 8.86 | 9.44 |

| 1 | 24 | 25 | 26 | 27 | 28 | 29 | 30 | 31 | 32 |
|---|---|---|---|---|---|---|---|---|---|
| No. | RA_A_GAIA_DR2 (d, 1826.0) | DE_A_GAIA_DR2 (d, 1826.0) | Mean_PA_DUN (d, 1826.0) | Mean_PA_DUN_CORRECTED (d, 1826.0, quadrant corrected) | PA_GAIA_DR2 (d, 1826.0) | Mean_Sep_DUN ('', 1826.0) | Sep_GAIA_DR2 ('', 1826.0) | vA_GAIA_DR2 (mag) | vB_GAIA_DR2 (mag) |
| 208 | 247.736 | -46.761 | | | | | | 6.99 | |
| 209 | 249.137 | -36.560 | 210.0 | 150.0 | 146.4 | 14.0 | 23.7 | 7.44 | 8.36 |
| 210 | 248.632 | -55.106 | | | 352.6 | | 74.6 | 8.09 | 8.59 |
| 211 | 248.656 | -48.006 | 330.0 | 210.0 | 194.2 | 20.0 | 45.1 | 8.12 | 8.13 |
| 212 | 252.626 | -50.819 | 228.0 | 312.0 | 286.4 | 5.0 | 16.2 | 8.27 | 8.74 |
| 213 | 254.362 | -46.502 | 153.0 | 153.0 | 165.7 | 8.0 | 7.9 | 6.85 | 8.37 |
| 214 | 253.887 | -66.957 | 320.0 | 320.0 | 326.2 | 22.0 | 27.7 | 5.81 | 8.73 |
| 215 | 256.332 | -53.175 | | | 62.5 | 15.0 | 54.8 | 8.28 | 8.86 |
| 216 | 258.507 | -45.674 | 30.0 | 330.0 | 313.3 | 32.8 | 103.3 | 5.68 | 7.07 |
| 217 | 259.104 | -43.815 | 148.0 | 148.0 | 169.7 | 8.0 | 13.9 | 6.24 | 8.60 |
| 218 | | | 34.0 | 34.0 | | 60.0 | | | 8.93 |
| 219 | 266.776 | -36.828 | 263.0 | 263.0 | 266.2 | 30.0 | 45.6 | 5.69 | 8.01 |
| 220 | 271.891 | -55.626 | 170.0 | 170.0 | 179.3 | | 31.2 | 7.94 | 8.38 |
| 221 | 272.908 | -44.184 | 180.0 | 180.0 | 166.3 | 40.0 | 77.1 | 5.20 | 9.64 |
| 222 | 275.344 | -38.839 | | | 358.6 | 14.0 | 21.6 | 5.59 | 6.25 |
| 223 | | | 40.0 | 40.0 | | 8.0 | | | |
| 224 | 280.247 | -47.471 | 115.6 | 64.4 | 63.7 | 78.7 | 80.7 | 7.00 | 7.28 |
| 225 | 284.682 | -52.077 | | | 252.9 | | 69.6 | 7.01 | 8.38 |
| 226 | 287.525 | -44.775 | 60.0 | 60.0 | 75.5 | 30.0 | 26.7 | 3.99 | 7.15 |
| 227 | 294.676 | -55.402 | 165.0 | 165.0 | 149.7 | 30.0 | 22.7 | 5.69 | 6.44 |
| 228 | | | 151.0 | 151.0 | | 24.4 | | | |

| 1 No. | 24 RA_A_GAIA_ DR2 (d, 1826.0) | 25 DE_A_GAIA_ DR2 (d, 1826.0) | 26 Mean_PA_ DUN (d, 1826.0) | 27 Mean_PA_DUN_ CORRECTED (d, 1826.0, quadrant corrected) | 28 PA_GAIA_ DR2 (d, 1826.0) | 29 Mean_Sep_ DUN ('', 1826.0) | 30 Sep_GAIA_ DR2 ('', 1826.0) | 31 vA_GAIA_ DR2 (mag) | 32 vB_GAIA_ DR2 (mag) |
|---|---|---|---|---|---|---|---|---|---|
| 229 | 296.228 | -52.347 | 246.6 | 246.6 | 243.7 | 84.2 | 80.5 | 7.57 | 8.15 |
| 230 | 301.531 | -40.713 | 97.0 | 97.0 | 115.1 | 65.6 | 10.1 | 7.30 | 7.58 |
| 231 | 304.614 | -71.653 | 288.3 | 288.3 | 291.5 | 64.4 | 66.1 | 6.80 | 8.78 |
| 232 | 305.171 | -75.938 | 14.9 | 14.9 | 16.6 | 18.8 | 17.9 | 6.42 | 7.09 |
| 233 | 305.269 | -61.158 | 78.0 | 78.0 | | 40.0 | | 4.71 | |
| 234 | 306.320 | -47.890 | 185.0 | 185.0 | | 5.0 | | 3.07 | |
| 235 | 308.094 | -51.107 | 236.6 | 123.4 | 124.3 | 128.4 | 122.8 | 7.96 | 7.37 |
| 236 | 312.662 | -43.671 | 73.5 | 73.5 | 75.5 | 63.7 | 56.4 | 6.59 | 6.85 |
| 237 | 319.757 | -59.573 | | | | | | 8.28 | |
| 238 | 332.609 | -75.894 | 90.0 | | 75.0 | 14.0 | 26.8 | 6.06 | 8.76 |
| 239 | 334.831 | -44.637 | 223.0 | 223.0 | 214.8 | 50.0 | 60.5 | 3.80 | 9.03 |
| 240 | 335.398 | -33.236 | 157.2 | 157.2 | 172.0 | 31.6 | 29.8 | 4.27 | 7.78 |
| 241 | 336.694 | -32.561 | 29.4 | 29.4 | 30.8 | 79.8 | 84.7 | 5.78 | 7.40 |
| 242 | 337.508 | -29.227 | 139.7 | 139.7 | 159.9 | 99.0 | 87.0 | 6.27 | 7.40 |
| 243 | | | 90.0 | 90.0 | | | | | |
| 244 | 342.772 | -65.231 | | | 100.4 | 60.0 | 48.3 | 7.60 | 9.91 |
| 245 | 344.507 | -60.676 | 280.0 | 280.0 | 291.9 | 10.0 | 14.1 | 7.35 | 9.79 |
| 246 | 344.286 | -51.626 | 233.0 | 233.0 | 260.7 | 10.0 | 8.2 | 6.18 | 6.99 |
| 247 | 346.904 | -61.951 | 278.0 | 278.0 | 274.4 | 30.0 | 37.5 | 6.69 | 8.20 |
| 248 | 347.751 | -51.257 | 217.0 | 217.0 | 210.9 | 16.0 | 16.8 | 6.10 | 8.82 |
| 249 | 348.503 | -54.763 | 212.3 | 212.3 | 209.7 | 26.9 | 27.2 | 6.08 | 7.06 |

| 1 | 24 | 25 | 26 | 27 | 28 | 29 | 30 | 31 | 32 |
|---|---|---|---|---|---|---|---|---|---|
| No. | RA_A_GAIA_ DR2 (d, 1826.0) | DE_A_GAIA_ DR2 (d, 1826.0) | Mean_PA_ DUN (d, 1826.0) | Mean_PA_DUN_ CORRECTED (d, 1826.0, quadrant corrected) | PA_GAIA_ DR2 (d, 1826.0) | Mean_Sep_ DUN ('', 1826.0) | Sep_GAIA_ DR2 ('', 1826.0) | vA_GAIA_ DR2 (mag) | vB_GAIA_ DR2 (mag) |
| 250 | 349.366 | -51.236 | 94.9 | 94.9 | 92.0 | 52.3 | 50.4 | 7.49 | 8.42 |
| 251 | 352.523 | -47.605 | 270.0 | | 291.4 | | 4.9 | 6.46 | 7.24 |
| 252 | 353.633 | -65.374 | 117.4 | 62.6 | 8.0 | | 241.9 | 5.66 | 7.04 |
| 253 | 356.340 | -28.012 | 270.0 | 270.0 | 266.3 | 5.0 | 7.0 | 6.78 | 7.38 |